Structural and behavioural signatures of enhanced plasticity resulting from a single dose of the psychedelic drug DOI



Merima Šabanović

Green Templeton College
University of Oxford

A thesis submitted for the degree of
Doctor of Philosophy

Michaelmas 2022

Progress is impossible without change, and those who cannot change their minds cannot change anything.

George Bernard Shaw

Structural and behavioural signatures of enhanced plasticity resulting from a single dose of the psychedelic drug DOI

Merima Šabanović
Green Templeton College
University of Oxford

A thesis submitted for the degree of
Doctor of Philosophy
Michaelmas 2022

Abstract

Psychedelic drugs can aid fast and lasting remission from various neuropsychiatric disorders, presumably by increasing neuroplasticity. Growing evidence shows enhanced neuronal plasticity in the first week post-treatment, but it is unclear if these changes are integrated across higher levels of analysis to explain the long-term shifts in behaviour. We searched for signatures of enhanced plasticity at behavioural, cognitive, and structural levels to determine if a single dose of the psychedelic drug DOI induces a comprehensive and lasting high-plasticity state in young adult C57BL/6 male mice.

On a behavioural level, high-plasticity states are environmentally sensitive, so we tested whether the acute psychedelic state in mice is context-dependent. We compared DOI's dose-response curves in a familiar and novel context and found that novelty modulated the frequency of psychedelic-like behaviours without modulating the drug's effects on exploration.

On a cognitive level, high plasticity implies better cognitive flexibility, so we tested reversal learning in a two-step decision-making task in the weeks after a single moderate dose of DOI. Adaptability to a novel reversal one day after DOI was comparable to the controls. But when we initiated a novel reversal one week after treatment, allowing for consolidation of putative neuronal plasticity, DOI-treated mice adapted faster and developed a richer choice strategy.

On a structural level, high and extensive neuronal plasticity would lead to regional changes in grey matter volume. Using *ex vivo* magnetic resonance imaging, we showed increased volumes of several sensory and association cortices 24h, but not three weeks, after one moderate dose of DOI.

In conclusion, we found signs of DOI-induced higher brain plasticity at several levels of analysis that are correlated but not necessarily coincidental with known neuronal plasticity. We suggest that while DOI's neuronal plasticity can initiate higher-level plasticity, its consolidation might be required for any enduring cognitive and behavioural change.

I carried out the work in this thesis at the Department of Experimental Psychology, University of Oxford between September 2019 and December 2022 under the supervision of David M. Bannerman, Mark E. Walton, Jason P. Lerch, and Vladyslav Vyazovskiy. My research was funded by the Wellcome Trust 1+3 PhD and Clarendon Fund studentships. No part of this thesis has been submitted in support of another degree, diploma, or other qualification at the University of Oxford or any other university. Except where otherwise stated, the work in this thesis is all mine.

Table of contents

Acknowledgements **2**
Frequently used abbreviations **3**
1 | Introduction **5**
1.1 The psychedelic renaissance 5
1.2 The promise of psychedelic-assisted psychotherapy 8
1.3 A brief introduction to the pharmacology of psychedelics 13
1.4 The window of plasticity 18
1.5 An integrative model of neuroplasticity 26
1.6 Reviewing the evidence for plasticity effects of psychedelics 29
1.7 Research aims 50
2 | Approach **55**
2.1 Animal model 55
2.2 Drug 60
2.3 Studying cognitive flexibility 63
2.4 Studying brain structure 71
3 | The behavioural level: Environmental sensitivity under DOI **78**
3.1 Introduction 78
3.2 Methods 80
3.3 Results 95
3.4 Discussion 103
4 | The cognitive level: Flexibility in the weeks after DOI **116**
4.1 Introduction 116
4.2 Methods 118
4.3 Results 136
4.4 Discussion 155
5 | The structural level: Regional brain volumes after DOI **163**
5.1 Introduction 163
5.2 Methods 165
5.3 Results 172
5.4 Discussion 179
6 | Discussion **195**
6.1 Summary of main results 195
6.2 Integrative model – a reappraisal 201
6.3 Experience-dependent plasticity 204
6.4 The generalizability of our findings and their translational significance 207
6.5 The importance of psychedelic experience 211
7 | Conclusions **216**
8 | A note on the impact of the COVID-19 pandemic on the experiments reported in this thesis **218**
9 | Statistics appendix **221**
10 | References **243**

Acknowledgements

Major thanks to my team of supervisors – David Bannerman, Mark Walton, Jason Lerch, and Vladyslav Vyazovskiy – who had the trust in me to generously grant me the freedom and independence to explore a field of research new to us all. Throughout my DPhil, the feedback of my examiners Trevor Sharp and Heidi Johansen-Berg has allowed me to develop my experimental design with greater nuance and has continuously improved the writing and communication for this thesis and my scientific career in general.

My sincere thanks are extended to the various members of the Bannerman, Walton, and Vyazovskiy labs, with special mention to Marta Blanco-Pozo, Raquel Pinacho, Beatriz Godinho, Yi-ge Huang, and the “watering crew” (I am convinced that having that one day off in a week when running the two-step task preserved my sanity). I am extremely grateful to the Lerch lab who have graciously gone out of their way to help with the magnetic resonance imaging and analysis – without them a whole chapter of this thesis would not have been possible. Katie Hewitt, Debbie Cobley, Angela Curran and the supporting staff of Biomedical Sciences are warranted their thanks for their mark in my project. I am also grateful to my friends Ilma Jahović, Alex Vourvoukelis and Basile Confavreux for their editing help, feedback sessions, and invaluable moral support.

I am indebted to the Wellcome Trust and Clarendon Fund who have provided the generous financial support required, not only for this research project, but for my education and life in the UK as well. The availability of such funding packages was the main limiting factor determining my academic and scientific career and that of many other international students faced with the same challenge.

Appreciation is also due to the animals without whom the science as we know it would not be possible.

I would be remiss in not mentioning my parents whose kindness and steadfastness remains incomparable to anyone I have ever met all across the world. Their belief in me and their support has been the only constant that has kept my spirits and motivation during this process.

Last but not least, I would like to end with an unlikely quote by the rap icon Snoop Dog in saying that I want to thank me. I want to thank me for believing in me, for doing all this hard work, never quitting, for trying to give more than I receive, and just being me at all times. To young Mima who was always made fun of in school for being the nerd who knows the answer to everything – this one is for you.

Frequently used abbreviations

5-HT	5-hydroxytryptamine, serotonin
5-HT_{2A}R	serotonin 2A receptor
ACC	anterior cingulate cortex
AICc	Akaike Information Criterion corrected for small sample sizes
AMPA	α-amino-3-hydroxy-5-methyl-4-isoxazolepropionic acid
ASR	acoustic startle response
AuV	ventral secondary auditory cortex
BDNF	brain-derived neurotrophic factor
BF	Bayes factor
BOLD	blood oxygen level dependent signal
CBT	cognitive behavioural therapy
CI	confidence interval
CNR	contrast-to-noise ratio
CSF	cerebrospinal fluid
DBM	deformation-based morphometry
DMN	default mode network
DMT	dimethyltryptamine
DOI	2,5-dimethoxy-4-iodoamphetamine
DOM	1-(2,5-dimethoxy-4-methylphenyl)-2-aminopropane
DWI	diffusion-weighted imaging
ECN	executive control network
ENT	entorhinal cortex
EPSC	excitatory post-synaptic current
ESR	ear-scratch response
FDA	Food and Drug Administration
FDR	false discovery rate
H_0	null hypothesis
H_1	alternative hypothesis
HTR	head-twitch response
IEG	immediate early gene
IL	infralimbic area
IP	intraperitoneal injection
JD	Jacobian determinant
LPtA	lateral parietal association cortex
LSD	lysergic acid diethylamide
M1	primary motor cortex

M2	secondary motor cortex
MDMA	3,4-methylenedioxy metamphetamine
MRI	magnetic resonance imaging
NAc	nucleus accumbens
NMDA	N-methyl-D-aspartate
OCD	obsessive compulsive disorder
OFC	orbitofrontal cortex
PCC	posterior cingulate cortex
PET	positron emission tomography
PFC	prefrontal cortex
PiMS	pivotal mental state
PnC	caudal pontine reticular nucleus
PrL	prelimbic area
PTSD	post-traumatic stress disorder
QSM	quantitative susceptibility mapping
RAAD	rapid-acting antidepressant
RCT	randomized control trial
RE	roaming entropy
RL	reinforcement learning
(RM) ANOVA	(repeated measures) analysis of variance
ROI	region of interest
RSA	retrosplenial agranular area
(rs)fMRI	(resting state) functional magnetic resonance imaging
S1	primary sensory cortex
SC	subcutaneous injection
SD	standard deviation
SNR	signal-to-noise ratio
SSRI	selective serotonin reuptake inhibitor
TeA	temporal association area
TR	transition reversal
V1	primary visual cortex
V2L	lateral secondary visual cortex
VBM	voxel-based morphometry
VEH	vehicle

1 | Introduction

1.1 The psychedelic renaissance

Psychedelic drugs are psychoactive substances that cause a non-ordinary state of consciousness characterized by changes in: (i) the perception of environment, self, and time, (ii) mood, and (iii) cognition (Carhart-Harris et al., 2016c). These profound alterations in perception and affect can result in a mystical-like experience (Griffiths et al., 2006). The subjective effects of these drugs are less a psychotic-like state of delirium, and more of a non-ordinary state of consciousness that can be challenging yet perceived as deeply meaningful.

The term *psychedelic* is a derivation of Greek words with the intended meaning “mind manifesting”, implying psychedelics can reveal the hidden potentials of the mind. The terms *hallucinogen* and *psychedelic* are often used interchangeably, although describing psychedelic effects as true hallucinations is considered inaccurate. Compared to hallucinations and psychoses seen in, for example, schizophrenia spectrum disorders, psychedelics have distinct pharmacology and phenomenology (Leptourgos et al., 2020). Schizophrenic hallucinations are dopamine-based (Kesby et al., 2018; Schmack et al., 2021), mostly in the auditory domain, with rare geometric hallucinations and synaesthesia. Psychedelic states are serotonin-based (see section 1.3 for further details on the pharmacology of psychedelics), mostly in the visual domain, with common geometric hallucinations and synaesthesia. Most notably, in contrast to schizophrenic psychoses, reality monitoring is often preserved under psychedelics. While some brain-imaging markers are shared between the two

states, such as impaired thalamocortical connectivity and reduced internal integration of functional networks (see section 1.6.c for discussion on how psychedelics affect brain network function), psychedelics induce overactivation of the primary sensory cortex, while schizophrenic hallucinations are associated with an overactive association cortex (Leptourgos et al., 2020).

Most psychedelic drugs fall into two main groups of chemical compounds: tryptamines and phenethylamines. Tryptamines include plant-derived indoleamines, such as dimethyltryptamine (DMT, a component of ayahuasca), psilocybin (derived from *Psilocybe* magic mushrooms), and its active metabolite psilocin (4-hydroxy-DMT). A sub-class of tryptamines are ergolines, such as lysergic acid diethylamide (LSD). Phenethylamines include 3,4,5-trimethoxyphenethylamine, better known as mescaline (derived from the peyote cactus), and synthetic substituted amphetamines, such as 2,5-dimethoxy-4-iodoamphetamine (DOI).

After the discovery of LSD in 1943 (Hofmann, 1980), characterization of other psychedelics unleashed a period of extensive research done on psychedelic-assisted psychotherapy as treatment for various forms of depression and neuroses, anxiety disorders, alcohol dependence, and personality disorders (reviewed in Fadiman et al., 2003). By today's research standards, much of that literature has serious limitations, and some findings were based only on case reports, but the potential for using psychedelics to treat some of the most complex and intractable mental health problems was becoming discernible. The apparent uniqueness of psychedelics was that their therapeutic effects significantly

outlasted their metabolism in brain and body since behavioural changes were visible long after the drug has cleared from the system.

However, illicit use of psychedelics became popular over time, and most psychedelics were placed in the Schedule I category by the Controlled Substances Act in 1971 in the United States, and in an equivalent restricted category in other countries soon after. Schedule I is a category for compounds with high potential for abuse and no current medical use. Another important factor to consider was that the Federal and Drug Administration (FDA) was changing its definitions of what a “quality drug” is. A quality of a drug was defined not only as its suitability for an intended use, but also as the consistency and the predictability of drug performance, meant to ensure clinical efficacy and safety. Psychedelics induce highly individualistic experiences that are inherently unpredictable and different depending on how and when they are used, so psychedelics cannot satisfy the requirement for predictability.

Following the Controlled Substances Act, human research on psychedelics became severely limited, and only a few preclinical research findings trickled in. However, with the development of modern neuroimaging techniques in the 1990s, interest for psychedelics was renewed. There were efforts to redefine the safety guidelines for the use of psychedelics in human research (Johnson et al., 2008) that allowed for the first studies of the neural correlates of psychedelic experiences under psilocybin (Carhart-Harris et al., 2012) and LSD (Carhart-Harris et al., 2016a). Research efforts then extended to pilot clinical trials with psilocybin for the treatment of cancer-related anxiety and

depression (Grob et al., 2011; Griffiths et al., 2016; Ross et al., 2016), and for major depressive disorder in treatment-resistant patients, where at least two types of classic antidepressants failed to achieve any effect (Carhart-Harris et al., 2016b). Psilocybin's antidepressant effects were also detectable at a six-month follow-up (Carhart-Harris et al., 2018a). These initial studies were based on small sample sizes (30-50 participants for cancer-related anxiety and only 12 for treatment-resistant depression) and had inadequate control groups (only Ross et al. included a placebo control, but blinding was still limited). Nonetheless, the results drove a surge of scientific interest in the clinical use of psychedelics, despite their highly controlled status.

1.2 The promise of psychedelic-assisted psychotherapy

The therapeutic potential of psychedelics for a variety of psychiatric disorders has been reinforced by the results of multiple independent small clinical trials with different types of psychedelic drugs. A single dose of ayahuasca or psilocybin was found to induce rapid relief from depression with the effects lasting at least three weeks (Osório et al., 2015; Sanches et al., 2016; Palhano-Fontes et al., 2019; Goodwin et al., 2022). 3,4-methylenedioxymethamphetamine (MDMA, known as "ecstasy") has shown therapeutic efficacy for post-traumatic stress disorder (PTSD) remarkable enough to warrant a "breakthrough therapy" designation by the FDA (Mithoefer et al., 2011, 2013). Preliminary evidence for treatment efficacy is also available for obsessive compulsive disorder (OCD) (Moreno et al., 2006), addiction to nicotine (Johnson et al., 2017) and alcohol (Bogenschutz et al., 2015, 2022). Healthy volunteers also report lasting positive

psychological effects, measured as increased openness (MacLean et al., 2011) and positive affect (Barrett et al., 2020), convergent thinking (Uthaug et al., 2018), increased psychological wellbeing and higher life satisfaction (Kettner et al., 2021), with subjects often describing the psychedelic experiences as some of the most meaningful experiences of their lives (Schmid and Liechti, 2018).

Searching www.ClinicalTrials.gov in October of 2022 using the term *psychedelics* for intervention resulted in 122 active trials on psychedelic treatment for a wide range of conditions, including: depression, anxiety and distress in Parkinson's or cancer patients, burnout in caregivers and COVID-19 response staff, addictions (nicotine, alcohol, cocaine, opioids), PTSD, OCD, attention deficit disorder (ADHD), bipolar disorder, eating disorders (anorexia nervosa, binge eating), migraines or cluster headaches, phantom limb pain, chronic pain, and fibromyalgia. The most frequent psychedelics being tested are psilocybin/psilocin, followed by MDMA (the most frequent psychedelic in trials involving PTSD), LSD, DMT, and ibogaine (a natural psychedelic found in the roots of the Tabernanthe iboga plant).

The acute psychedelic experience mimics aspects of a psychotic episode and could therefore exacerbate existing risks of psychoses or induce the first episode in a vulnerable subject. Therefore, when recruiting participants for psychedelic research, anyone with a personal or family history of psychotic episodes is excluded. Often, previous experience with a psychedelic drug is also required. Requiring prior psychedelic experience is motivated by safety, to minimize the likelihood of an adverse drug response. However, the consequence

is that we cannot know if the observed effects on mood and behaviour are confounded by previous drug use, not only of psychedelics but of other recreational drugs too, as resultant population samples often also report previous use of other stimulants. Whether a single psychedelic treatment would be sufficient to produce comparable effects is yet to be shown with adequately powered studies. The exclusion criteria do not only limit the generalizability of findings, but also the availability of psychedelic-assisted therapy. Ideally, a safe psychedelic therapy should be available to any patient that may benefit from it, regardless of their previous experience with such drugs and comorbid disorders.

Importantly, psychedelics are not considered addictive, as rates of self-administration are suggestive of only transient weak reinforcing effects (Fantegrossi et al., 2004). This may be in part due to rapid pharmacological tolerance developed with frequent use (Heal et al., 2018). However, like any treatment, psychedelic-assisted therapy still does not come without any risks. While most acute physical side effects, such as nausea or headaches, dissipate within one day of treatment, there exists a rare but documented risk of a Hallucinogen Persisting Perception Disorder (HPPD) that refers to flashbacks of the psychedelic effects, most commonly the visual imagery and the synaesthesia (Martinotti et al., 2018). Rates of HPPD are higher with illicit use and in the presence of existing comorbidities with severe mental illness, so its risk in the clinic is judged to be extremely rare due to the beforementioned exclusion criteria.

The value of psychedelic therapeutic findings is notable considering the limitations of available pharmacological treatments of neuropsychiatric disorders.

Despite advances in research methods and our understanding of mental disorders, contemporary psychiatry still lacks effective treatments. Traditional pharmacotherapies are associated with a great number of adverse effects and withdrawal symptoms, require chronic administration for long-term remission, and most often only partially mask the symptoms of mental disorders. In addition to, or instead of, pharmacological interventions, treatments such as psychotherapy and cognitive behavioural therapy (CBT) are used, but they are labour-intensive and expensive, limiting their availability for less privileged clinical populations. In contrast, clinical studies of psychedelic drugs suggest therapeutic efficacy without chronic treatment and across different symptomatologies (dos Santos et al., 2016b; Carhart-Harris and Goodwin, 2017; Nichols et al., 2017) with a good safety profile *if* administered in controlled settings (dos Santos et al., 2018).

When evaluating what aspects of the psychedelic neurobiology are responsible for the lasting effects on mood and behaviour, some consider the acute alterations in consciousness as secondary to the more fundamental alterations in brain structure and function (Olson, 2020), while others argue that the characteristic psychedelic experience is necessary for and is the main determinant of any lasting benefits (Yaden and Griffiths, 2020). There is evidence to support both sides of the debate, so the field remains divided on the matter, although finding a non-psychedelic analogue with plasticity and therapeutic effects comparable to those of classic psychedelics has become an ardent goal of several labs (Cameron et al., 2021; Dong et al., 2021; Kaplan et al., 2022). However, the behavioural effects of such drugs were so far only investigated in the first week after treatment, so whether non-psychedelic analogues have any

long-term effects on behaviour, as their psychedelic counterparts do, remains an open question.

1.2.a The trouble with over-promising

The FDA has designated psilocybin as a “breakthrough therapy” for depression. This designation is meant to expedite the development and review of drugs that are either intended for treatment of serious conditions or are supported by preliminary clinical evidence to have a clear advantage over available therapies. Psilocybin’s designation belongs to the latter category as psilocybin-assisted psychotherapy is *potentially* better, in terms of its safety and efficacy, at treating depression than all the other available options.

The FDA’s reference to psilocybin’s “potential” is critical, as higher efficacy has not yet been proven. While it is true that the therapeutic potential of psychedelics for depression is no longer hypothetical, as it has been demonstrated by numerous, albeit small, independent clinical trials and supported by growing preclinical research, psychedelic-assisted psychotherapy is unlikely to replace current gold standard treatments for depression, such as selective serotonin reuptake inhibitors (SSRIs). Efficacies of SSRIs and psilocybin have so far been compared mainly through systematic reviews. The only direct comparison with an SSRI escitalopram suggested no clinically meaningful difference between the efficacy of psilocybin and escitalopram (Carhart-Harris et al., 2021; Nayak et al., 2022). Psilocybin, and psychedelics in general, do not necessarily need to work better than standard pharmacotherapies – they just need to work as well. A more relevant advantage of psilocybin is that

it can be effective in treatment-resistant populations, where standard antidepressants have failed to produce any effect. Psychedelics show great promise for bettering mental health, but these are not miracle drugs, and they are not a blanket solution.

1.3 A brief introduction to the pharmacology of psychedelics

Before we explore current theories on the mechanisms of action underlying psychedelics, this section aims to provide a summary of psychedelic pharmacology. All the psychedelics introduced in the previous sections have a mechanism of action reliant on the neurotransmitter serotonin (5-hydroxytryptamine, 5-HT), except for MDMA which, in addition to affecting 5-HT release and re-uptake, also affects the release of dopamine and norepinephrine (de la Torre et al., 2004). Therefore, the psychedelic pharmacology discussed in this section excludes MDMA.

Based on converging evidence from pharmacological (Glennon et al., 1984), electrophysiological (Aghajanian and Marek, 1999), and behavioural (Wing et al., 1990) studies in animals, such as mice or rats[1], acute psychedelic effects are believed to be mainly mediated by activating the 5-HT 2A receptor (5-HT_{2A}R). Blocking or ablating 5-HT_{2A}Rs completely abolishes the non-ordinary consciousness state in humans (Vollenweider and Kometer, 2010) and the

[1] This chapter will discuss research done on both humans and animals. Pharmacology and neurobiology of psychedelics has been studied extensively in preclinical models. The question of how to investigate psychedelics in an animal model is discussed in detail in section 2.1.

psychedelic-like effects in animals[2] (Schreiber et al., 1995; González-Maeso et al., 2007; Halberstadt and Geyer, 2011). The first evidence for 5-HT_{2A}R involvement was the report that the potency of 19 5-HT antagonists to block the psychedelic response to mescaline and DOI is highly correlated with their 5-HT_{2A} binding affinity (Leysen et al., 1982; Schreiber et al., 1995; Dursun and Handley, 1996). The ability of psychedelics to elicit a psychedelic-like response in rodents is blocked by 5-HT_{2A} antagonists M100907 and MDL11939 (Vickers et al., 2001; Fantegrossi et al., 2006, 2008b, 2010; Carbonaro et al., 2015), and is completely abolished in mice lacking the 5-HT_{2A}R gene (González-Maeso et al., 2007; Halberstadt et al., 2011). Importantly, however, the psychedelic responses can be rescued in 5-HT_{2A} knockout mice by selectively restoring 5-HT_{2A}Rs in the forebrain (González-Maeso et al., 2007). Notably, 5-HT_{2A}R occupancy has been found to closely correlate with the psychedelic effects of psilocybin (Madsen et al., 2019).

Psychedelics stimulate postsynaptic 5-HT_{2A}Rs across the brain, especially where 5-HT_{2A}R density is particularly high, like in layer 5 cortical pyramidal neurons in the prefrontal cortex (PFC) (González-Maeso et al., 2007; Andrade and Weber, 2010) (Fig.1.1). However, psychedelics are *not* specific agonists. They have varying affinities to a wide range of other 5-HT receptors (Nichols, 2016) (Fig.1.1 right insert). Different classes of psychedelics have

[2] The animal model of acute psychedelic state is the head twitch, also referred to as head shake/bob, or whole-body "wet dog" shake. These have been described across species, in mice, rats, rabbits, pigs, the least shrew, and the elephant (Siegel, 1984; Darmani et al., 1994; Canal and Morgan, 2012; Halberstadt and Geyer, 2013). The utility of head twitches as a model of psychedelic activity will also be discussed in greater detail in section 2.1.

different receptor affinity profiles (Table 1.1). Phenethylamines are relatively selective for 5-HT_2R subtypes, whereas tryptamines bind to a larger set of 5-HT receptors, including 5-HT_1, 5-HT_6, and 5-HT_7 receptors. Ergolines are less selective for 5-HT receptors in general, interacting with dopaminergic, adrenergic, and histaminergic receptors as well.

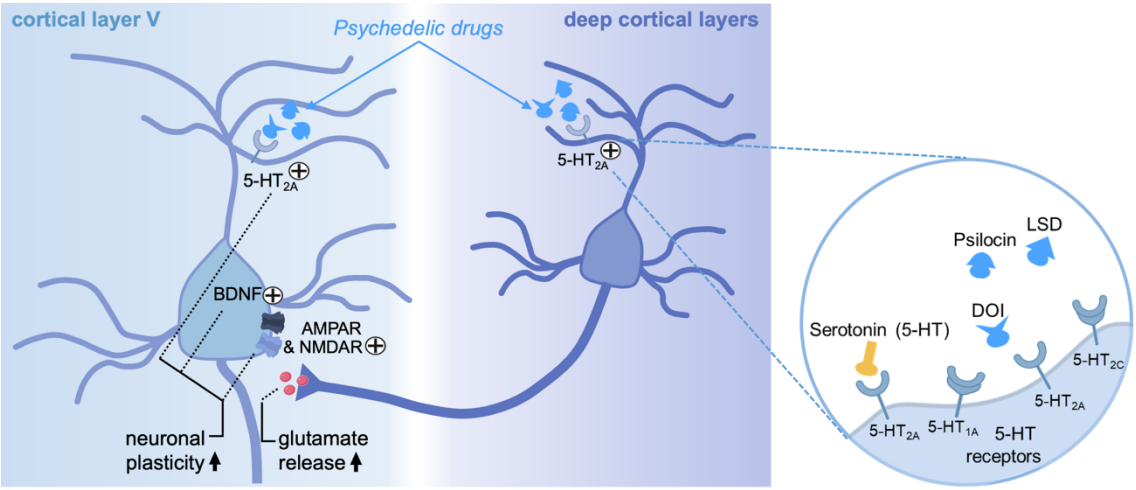


Fig.1.1 The proposed model of action of psychedelic drugs. Serotonergic psychedelics such as psilocin, lysergic acid diethylamide (LSD) and 2,5-dimethoxy-4-iodoamphetamine (DOI) stimulate postsynaptic serotonin 2A (5-HT_{2A}) receptors across the brain. Some of the highest densities of 5-HT_{2A} receptors are in layer 5 cortical pyramidal neurons. Psychedelics also have varying affinities for other 5-HT receptors, especially 5-$HT_{1A/B}$ and 5-HT_{2C} receptors. Classic psychedelics also induce a glutamate-dependent increase in the activity of the prefrontal cortex (PFC), preferentially its layer 5 pyramidal cells. Increased extracellular glutamate in the PFC is suggested to result from 5-HT_{2A} receptor activation of glutamatergic pyramidal cells in deep cortical layers (5 and 6) projecting to layer 5 pyramidal neurons. The resulting glutamate release activates α-amino-3-hydroxy-5-methyl-4-isoxazolepropionic acid (AMPA) and N-methyl-D-aspartate (NMDA) receptors and ion channels on layer 5 neurons. Activation of 5-HT_{2A}, AMPA, and NMDA ultimately leads to increased expression of brain-derived neurotrophic factor (BDNF) and further plasticity-related changes. *Adapted from:* Vollenweider F. X. & Kometer M. (2010) and Stahl's Essential Psychopharmacology (2013). Note that one post-synaptic neuron would not express as many receptors as shown in the illustration – two or three 5-HT receptor subtypes at most would be expressed.

Table 1.1 Measures of affinity with which some psychedelic drugs bind to a different 5-HT receptor subtypes. Inhibitory constant, K_i, reflects the binding affinity of the psychedelic to the receptor, with smaller values signaling greater binding affinity. K_i values quoted are sourced from the PDSP K_i database freely available at https://pdsp.unc.edu/databases/kidb.php (Roth et al., 2000). We reported the values from the rodent species if available. If the same hot ligand was used to determine K_i of several psychedelic ligands of interest, those values were reported over other hot ligands. If several sources reported different K_i values measured in the same species and using the same hot ligand, we reported the average K_i. *value reported for psilocin.

Psychedelic drug	Receptor K_i [nM]										
	5-HT$_{1A}$	5-HT$_{1B}$	5-HT$_{1D}$	5-HT$_{1E}$	5-HT$_{2A}$	5-HT$_{2B}$	5-HT$_{2C}$	5-HT$_3$	5-HT$_5$	5-HT$_6$	5-HT$_7$
DOI	2,355.00	1,261.00	1,241.38	2,970.00	1.65	26.84	3.01		1,000.00	>10,000	
ligand	*3H-8-OH-DPAT*	*3H-5HT*	*3H-5HT*	*3H-5HT*	*125I-DOI*	*3H-5HT*	*125I-DOI*		*125I-LSD*	*3H-5HT*	
species	*rat*	*rat*	*cow*	*human*	*rat*	*rat*	*rat*		*rat*	*mouse*	
Psilocybin	>10,000	>10,000	2,119.00	194.80	13.00	98.7	10.00*	>10,000	6,181.00	413.50	597.90
ligand	*3H-8-OH-DPAT*	*3H-GR-125743*	*3H-GR-125743*	*3H-5HT*	*125I-DOI*	*3H-LSD*	*125I-DOI*	*3H-LY 278584*	*3H-LSD*	*3H-LSD*	*3H-LSD*
species	*human*	*human*	*human*	*human*	*rat*	*human*	*rat*	*human*	*human*	*human*	*human*
LSD	2.34	3.90	8.85	93.00	4.69	30.00	5.50	>10,000	9.00	2.82	6.60
ligand	*3H-8-OH-DPAT*	*3H-GR-125743*	*3H-5HT*	*3H-5HT*	*125I-DOI*	*3H-LSD*	*125I-DOI*	*3H-Quipazine*	*3H-LSD*	*3H-LSD*	*3H-LSD*
species	*rat*	*rat*	*rat*	*rat*	*rat*	*rat*	*rat*	*rat*	*rat*	*mouse*	*rat*
DMT	245.00	2,200.00	270.00	455.70	42.00	107.60	166.00	>10,000	611.00	277.70	87.50
ligand	*3H-8-OH-DPAT*	*125I-CYP*	*3H-5HT*	*3H-5HT*	*125I-DOI*	*3H-LSD*	*125I-DOI*	*3H-GR-65630*	*3H-LSD*	*3H-LSD*	*3H-LSD*
species	*rat*	*rat*	*human*	*human*	*rat*	*human*	*human*	*human*	*human*	*human*	*human*
Serotonin	2.06	23.67	2.10	7.53	3.87	13.98	9.90	269.15	251.18	95.50	6.00
ligand	*3H-8-OH-DPAT*	*125I-CYP*	*3H-5HT*	*3H-5HT*	*125I-DOI*	*3H-5HT*	*125I-DOI*	*3H-GR-65630*	*125I-LSD*	*3H-LSD*	*3H-LSD*
species	*rat*	*rat*	*rat*	*human*	*rat*	*rat*	*human*	*mouse*	*mouse*	*mouse*	*human*

Different psychedelics can activate different signalling pathways downstream of the same receptor (Fantegrossi et al., 2008a; Sharp and Barnes, 2020). This property, called *biased agonism*, refers to functional selectivity of 5-HT$_{2A}$R agonists such that different agonists interact with the same receptor but preferentially activate different intracellular signalling pathways (Sharp and Barnes, 2020). For example, psilocybin preferentially activates the phospholipase C (PLC) pathway, while LSD prefers the phospholipase A2 (PLA2) pathway (Fantegrossi et al., 2008a). Simultaneous activation of different 5-HT receptors can also alter functions of other receptor subtypes (Darmani et al., 1990b, 1990c). Therefore, while 5-HT$_{2A}$Rs may be necessary for the most apparent acute psychedelic experience, they are likely not sufficient to produce the full range of diverse effects of psychedelics on brain and behaviour. Other 5-HT receptors, such as 1A or 2C (Nichols, 2016), as well as other receptors, such as dopamine

(Vollenweider and Kometer, 2010) and sigma-1 (Szabo, 2015), play accompanying roles. It remains unknown how activation of different intracellular signalling events relates to the subjective experiences induced by the drug, or the post-acute changes in mood and behaviour. Therefore, 5-HT_{2A} activation cannot be thought of as the sole neurochemical cause of either the acute or the long-term effects.

Not all 5-HT_{2A}Rs exhibit strong psychedelic-like effects. For example, lisuride and ergotamine were reported to not induce a head-twitch response, a rodent psychedelic-like behaviour (González-Maeso et al., 2007). The difference in behavioural effects is believed to be due to biased agonism of G-protein coupled 5-HT_{2A}Rs. Lisuride targets the same population of 5-HT_{2A}Rs like LSD does, but it induces distinct effects on intracellular signalling, electrophysiology, and behaviour (González-Maeso et al., 2007). However, the branding of lisuride as a non-psychedelic 5-HT_{2A}R agonist is controversial. There is some generalization of the subjective effects of lisuride and LSD in lab animals as lisuride substituted for LSD in rats trained to differentiate between LSD and saline (Appel et al., 1999). In humans, high doses of lisuride were able to induce hallucination-like responses in humans (Lees and Bannister, 1981; Critchley et al., 1986), although these effects have only been observed in patients with Parkinson's disease.

Psychedelics also produce a net excitatory effect on most pyramidal neurons, making them more likely to fire action potentials (Marek, 2017), an effect that is also produced by endogenous 5-HT activation of 5-HT_{2A}Rs (Aghajanian

and Marek, 1999). Neuronal activity effects in layer 5 PFC were shown to be mediated by an increase in concentrations of extracellular glutamate which activates α-amino-3-hydroxy-5-methyl-4-isoxazolepropionic acid (AMPA) and N-methyl-D-aspartate (NMDA) receptors on layer 5 pyramidal neurons (Béïque et al., 2007; Zhang and Marek, 2008; Marek, 2017). The additional extracellular glutamate is released by the terminals of layer-5-projecting neurons in deeper cortical layers which are triggered by activation of their postsynaptic 5-HT_{2A}Rs (Béïque et al., 2007). Activation of presynaptic 5-HT_{2A}Rs on thalamocortical afferents also sends excitatory glutamatergic input to prefrontal layer 5 neurons (Marek, 2017).

The findings that psychedelics increase levels of glutamate and brain-derived neurotrophic factor (BDNF) has led to the hypothesis that psychedelic therapeutic effects are driven by neuroplastic adaptations via glutamate-driven increased AMPA receptor activation (Vollenweider and Kometer, 2010; Catlow et al., 2013; Ly et al., 2018). In the next section, we will discuss the theory that the benefits of psychedelics that are promoted and solidified in the weeks after of the therapy are the result of increased neuroplasticity which enables the brain to alter its structure and function more easily.

1.4 The window of plasticity

A sudden benevolent and enduring experience of a psychological transformation affecting emotions, cognition, behaviour, and personality is referred to as a *quantum change* (Miller, 2004). Quantum change can occur in

pivotal mental states (PiMSs) that have been defined as “transient, intense hyper-plastic mind and brain states” that can aid quicker and deeper learning (Brouwer and Carhart-Harris, 2021). PiMSs do not imply a positive outcome – context, both immediate and past, shapes the outcome. For example, chronic stress can lead to a PiMS that will shift deeply held beliefs about self and the world to a negative bias. Psychedelic states are also PiMSs as psychedelics induce transient, intense neuroplasticity (Ly et al., 2018, 2020; Shao et al., 2021) and can catalyse changes in associative learning and perspectives (Harvey, 2003; Griffiths et al., 2006; Carhart-Harris and Friston, 2019) in a context-dependent fashion (Carhart-Harris et al., 2018b; Roseman et al., 2018b).

The proposed molecular gateway for a PiMS is the 5-HT_{2A} receptor. Robin Carhart-Harris and David Nutt (2017) suggest psychedelic 5-HT signalling, particularly at the 2A receptor, as the inception of a hyper-plastic brain state, or a *window of plasticity*, that can lead to enduring changes in mood and learning *if* mediated by psychological support and a positive environment. They suggested that enhanced plasticity, which they define as the “capacity for change,” may be one of the ways in which psychedelics, potent 5-HT_{2A}R agonists, act as such an effective and widely applicable therapy. Serotonergic psychedelics have been described as *psychoplastogens* (Olson, 2018) – compounds capable of rapidly promoting structural and functional neuroplasticity within days of a single administration, similar to ketamine, another rapid-acting antidepressant (RAAD) (Lee et al., 2015) (see section 1.6.e for the comparison of psychedelics with classic antidepressants and RAADs).

The window of plasticity hypothesis builds on earlier work positing that one of the key roles of 5-HT is in enabling plasticity for greater adaptability, due to 5-HT's effects on increasing the influence of environmental factors (Branchi, 2011). Thus, psychedelic 5-HT signalling opens a window of plasticity during which increased environmental sensitivity allows for more efficient and effective therapeutic work to be accomplished. Therefore, psychedelics offer an opportunity to study rapid heightened neuroplasticity as a pre-requisite of lasting behavioural change.

1.4.a The importance of context

Enhanced neuroplasticity has been described as a "double-edged sword" (Branchi, 2011). Plasticity enhances the effects of environment to manipulate and direct structural and functional change to both a beneficial and a detrimental effect. Plasticity-enhancing psychedelic therapy is therefore "biopsychosocial" (Deacon, 2013) – outcomes are bidirectionally modulated by social, psychological, and biological factors. Since the environment can be either supportive or unfavourable, its effects can be either beneficial or damaging. In an unfavourable environment, high plasticity is disadvantageous to a highly plastic system that will be more liable to negative effects, but in a favourable environment, high responsivity will allow the same system to benefit more readily. On the other hand, less responsive lower-plasticity systems will be less susceptible to negative environments, but they are also less likely to be enriched by positive environments. This is why plasticity is referred to as a capacity for change "for better and for worse" (Belsky et al., 2007). Note that no environmental

context is ever purely positive or negative, or “neutral”. How a context is perceived is always subjective and relational.

Carhart-Harris and Nutt were careful to highlight that mood and mental health effects of psychedelics are highly sensitive to the context in which the treatment occurs (Johnson et al., 2008; Hartogsohn, 2016, 2017), developing an extra-pharmacological model of drug action (Carhart-Harris and Nutt, 2017). While drugs are generally considered based on their ligand-receptor interactions, an extra-pharmacological model posits that non-pharmacological factors of internal (*set*) and external (*setting*) nature can modulate the acute response to a psychedelic drug and the subsequent long-term outcomes (Carhart-Harris and Nutt, 2017). The emotional and mental context that an individual brings into a psychedelic experience is referred to as the *set,* while the physical, social, and cultural environmental context in which this experience is occurring is the *setting* (Hartogsohn, 2016). Set refers to both psychological traits, such as personality, but also biological traits, e.g., receptor polymorphisms. The terms of “set” and “setting” were first introduced by Timothy Leary (1963) who argued that psychedelic drugs act as nonspecific magnifiers of whatever already existed in one’s mind.

Despite the widespread adoption of the set and setting theory among psychedelic researchers, few have tested the relationship between psychedelics and context in a controlled manner. The limiting factors are the practical and ethical considerations for providing a sub-optimal or possibly adverse context for a psychedelic experience in humans, although this issue may be circumvented

by testing lower doses. Contemporary psychedelic-assisted therapy is administered in an environment designed to allow the recipient to feel prepared and supported. Extensive psychological preparation is provided by a psychotherapist during one or more repeat visits before the psychedelic treatment. During the treatment, guides trained specifically for supporting psychedelic therapies help the recipient throughout their experience, being available to engage in therapy if the recipient initiates it. The room décor is meant to reflect a familiar living-room-type environment, with low lighting and carefully curated music playlists. After the psychedelic experience, there are again one or more repeat visits with a psychotherapist who helps the recipient integrate the content and meaning of their acute psychedelic experiences.

Some of the earliest research on psychosocial determinants of psychedelic drug action was done in the 1960s by Robert Hyde using LSD. Hyde (1960) manipulated the non-pharmacological factors to shape the LSD response using dimensions such as: goal rigidity-flexibility, attitudes of acceptance-rejection of self, common-foreign culture, and familiarity-novelty of the environment. Hyde found that individuals who took the drug in isolation had more negative reactions than those who took the drug in a group setting. Notably, Hyde also found that if individuals were expected to undergo tests and perform some tasks while under psychedelics, they reported more negative effects than those individuals who could choose what they do while under LSD.

A contemporary investigation of the factors which contribute to predicting the intensity of the acute response to psilocybin in healthy humans confirmed

that, while the drug dose was the most significant predictor of drug response intensity, multiple non-pharmacological factors had contributing effects (Studerus et al., 2012). A more active and energetic state prior to intoxication predicted a more pleasant and mystical-type experience, as did a high personality trait of absorption and low prior occurrence of psychological problems. In contrast, a younger age and an experimental setting (e.g., a brain scanner) were associated with more anxious and unpleasant reactions to psilocybin. In fact, an experimental setting was the strongest predictor of anxiety, being twice as strong as the drug dose predictor. Emotional excitability was a positive predictor of both more intense synaesthesia and more frequent mystical-type experiences, but also of anxiety during intoxication (Studerus et al., 2012). Additionally, time of assessment was negatively correlated with cognitive measures, showing how fewer cognitive disturbances were being reported when subjects were tested later in the acute experience.

It has been shown that the duration of negative affect *but not its intensity* can predict negative long-term outcomes after psychedelic therapy (Carbonaro et al., 2016). It is important to note that having a challenging experience acutely does not predispose an individual to negative long-term outcomes. In fact, it could be the opposite. For example, higher neuroticism increased the likelihood of experiencing negative side effects following LSD, psilocybin, MDMA, and ayahuasca, but it also increased the likelihood of a positive mood change (Mason et al., 2020a).

Previous work on environmental factors of acute animal psychedelic responses is limited to housing conditions (Sakaue et al., 2002), prenatal stress (Holloway et al., 2013), and strong acute physical stressors (Chaouloff et al., 1994; Yamada et al., 1995b; Peričić, 2003). Studies using different stressors reported conflicting results. A combination of tail pinch, immobilization by taping, and repeated foot shocks rendered rats less sensitive to 1mg/kg DOI (Yamada et al., 1995b), but restraint stress enhanced rat sensitivity to the same DOI dose (Chaouloff et al., 1994). Other stressors such as the forced swim test or cold stress failed to affect DOI sensitivity in mice (Zamfir et al., 1992; Yamada et al., 1995b). Whether subtler differences in the quality and/or valence of the environment affect animals' sensitivity to psychedelics has not been widely explored. Published preclinical research employs a mix of environmental contexts, injecting animals in novel and home cages, enriched and bare environments, under and outside of task conditions. Because of the lack of controlled and direct comparisons of acute effects across many different types of environments, it is unclear if environmental influences could contribute to variability across preclinical findings of acute and post-acute psychedelic effects.

Experience-dependent plasticity effects are evocative of the impact of experience during early life and adolescence, developmental stages that are marked by elevated brain plasticity that can be regulated by 5-HT (Dayer, 2022). For example, the early-life critical period of the visual system development has been studied extensively with monocular deprivation experiments that showed how experiencing specific external stimuli are required for functional development (Hubel and Wiesel, 1970). An equivalent high-plasticity state can be

pharmacologically reinstated with chronic SSRI fluoxetine treatment (Vetencourt et al., 2008) or local 5-HT infusions (Vetencourt et al., 2011) to the visual cortex, demonstrating how 5-HT can control periods of developmental plasticity. Experience-dependent plasticity is also apparent in sensitive periods when functional development can occur in the absence of a specific stimuli, but environmental factors greatly shape the long-term functioning. For example, early-life stress can affect how various cortical circuits mature and this effect is mediated by the 5-HT system (Dayer, 2022).

Experience drives the wiring and rewiring of neural circuits and the behaviours they mediate, driving the individual's predisposition to effectively respond to the ever-evolving environment across its lifespan. Just as early-life stress can delay or truncate sensitive periods of functional development, the environmental factors defining the psychedelic experience could shape the extent and the duration of expression of enhanced plasticity after psychedelic treatment. Additionally, just as early-life stress can affect specific cortical circuits differently, environment could influence what neural circuitry psychedelics affect acutely, priming them for longer-term plasticity changes that follow. Therefore, high plasticity states induced by psychedelics share the characteristic sensitivity of developmental high plasticity periods, reopening a window where experiences can again reform long-term functioning of neural circuitry in a mature brain.

1.5 An integrative model of neuroplasticity

Neuroplasticity is the ability of the brain to change in both structure and function in response to experience. Neuroplasticity occurs on a variety of levels, ranging from molecular/cellular changes to large-scale structural changes in the brain. An integrative model of neuroplasticity has been suggested by Rebecca Price and Ronald Duman (2019) (from here on referred to as the *Price-Duman model*) to encompass the neurobiological, cognitive, and psychological adaptations that might support the treatment of depression and other disorders of negative affect. The fundamental underlying question is how could neuronal plasticity mechanisms profoundly alter the complex multifaceted human experience?

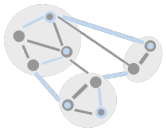
Why increased neuroplasticity explains therapeutic outcomes on mood is explained by considering some of the hallmark structural and functional differences in mental health patients compared to healthy individuals (Player et al., 2013). For example, on a neuronal level, stress and depression are associated with reduced neuronal plasticity in the PFC, hippocampus, and the amygdala (Duman and Aghajanian, 2012; McEwen et al., 2016). Structural abnormalities of neurons translate to structural abnormalities across brain regions. Patients with major depressive disorder have a volume decrease as high as 12% in the PFC, especially in anterior cingulate cortex (ACC) and the orbitofrontal cortex (OFC), with moderate reductions observed in the hippocampus, putamen, and caudate nucleus (Koolschijn et al., 2009). Given that brain structure constrains functional networks (Park and Friston, 2013), these

volumetric changes are possibly associated with abnormalities observed in functional neuroimaging of the same circuits. On a network level, depression has been associated with hypoconnectivity within the frontoparietal networks and between frontoparietal systems and parietal regions of the dorsal attention network (Kaiser et al., 2015). Additionally, hyperconnectivity within the default mode network (DMN, see section 1.6.c), and its connectivity with the frontoparietal systems. Neuronal, structural, and network alterations may contribute to deficits of depressed patients in cognitive and neuropsychological tasks. Depressed patients have impairments in psychomotor speed, learning, visual memory, and executive functions (Vives et al., 2015), including pronounced deficits in adaptive behaviour (Wagner et al., 2012). Clinical phenomenology of depression is broadly consistent with a decreased capacity of the brain to flexibly respond to a changing complex environment.

Increasing neuronal plasticity would, according to the Price-Duman model, simultaneously reverse deficits across all levels of analysis (Table 1.2). This model predicts that if a drug were to promote molecular neuroplasticity, there should be a correlated and simultaneous facilitation of higher, cognitive, and psychological levels of plasticity. For example, increased levels of neurotrophic factors and synaptogenesis might feed forward to improved functional integration across PFC and limbic circuits (e.g., hippocampus, amygdala, and striatum), which in turn might improve behavioural and cognitive flexibility that might ultimately lead to new more positive thoughts/perceptions and a diversified behavioural repertoire. In the context of therapy, enhanced neuroplasticity may lead to enhanced capacity for learning, to changes in thought patterns and

emotional responses, and, ultimately, to changes in behaviour. What intermediary mechanisms would allow neuronal and molecular changes to propagate up to cognition and behaviour remain to be empirically elucidated.

Table 1.2 Signatures of brain plasticity across levels of analysis. The remaining gaps are at the structural level of whole brain regions and cognition, where current findings are limited or only studied in individuals whose prior drug experience was extensive, and at cognitive level, where improvements in cognitive function are suggested but were not measured. sEPSC: spontaneous excitatory post-synaptic current. PFC: prefrontal cortex. DMN: default mode network. Asterisk signifies that the finding was only found with long-term use of psychedelics.

Level of analysis		Dysfunctional state	Psychedelic state
	*Neuron*	Loss of synapses Dendritic atrophy Neuronal atrophy sEPSC frequency ↓ (Duman and Aghajanian, 2012; McEwen et al., 2016)	Spino- and synaptogenesis Dendritogenesis Hippocampal neurogenesis sEPSC frequency ↑ (Catlow et al., 2013; Cameron et al., 2018; Ly et al., 2018; Morales-Garcia et al., 2020; Shao et al., 2021)
	*Region*	Grey matter loss (Koolschijn et al., 2009)	Cortical thickness ↑* (Bouso et al., 2015)
	*Network*	PFC-limbic connectivity ↓ Hyperactive DMN (Bennett, 2011; Kaiser et al., 2015)	PFC recurrent activity ↑ Hypoactive DMN (Roseman et al., 2014; Lord et al., 2019)
	*Cognition*	Inflexibility Negative bias (Wagner et al., 2012; Vives et al., 2015; Weisholtz et al., 2017)	Flexibility More positive thoughts (Kuypers et al., 2016; Davis et al., 2020; Murphy-Beiner and Soar, 2020)
	*Behaviour*	Repetitive maladaptive behaviour Low mood (van Praag, 1998; Hsu et al., 2015; Huys et al., 2015)	Personality changes openness & agreeableness ↑ Improved mood (Vollenweider and Kometer, 2010; MacLean et al., 2011)

The Price-Duman model considers cases where there are deficits in plasticity, but it also predicts a falsifiable hypothesis that if a compound increases molecular and neuronal plasticity, there should be *correlated and simultaneous* facilitation of plasticity at each of the higher levels of analysis. Available findings

on psychedelic-mediated neurobiological and psychological plasticity in humans and preclinical models, both on- and off-drug, are consistent with the Price-Duman model of neuroplasticity (Table 1.2). These will be discussed in detail in the next section where we review the evidence for signatures of psychedelic-enhanced plasticity at different levels of analysis, ranging from sub-cellular and cellular processes to cognition and behaviour, identifying the gaps in research.

1.6 Reviewing the evidence for plasticity effects of psychedelics

1.6.a Level 1: Neurons

Molecular plasticity entails changes in expressions of genes and proteins, including post-translational modifications (Gulyaeva, 2017). In the rodent cortex, psychedelics can promote gene expression related to synaptic plasticity within hours of treatment, including immediate early genes (IEGs) (Jefsen et al., 2019), such as *c-FOS* (Frankel and Cunningham, 2002) and *Arc* (Benekareddy et al., 2013), and BDNF (Vaidya et al., 1997; Gewirtz et al., 2002). Epigenetic modifications can stretch across the first week following a single treatment. A single injection of DOI leads to the reorganization of chromatin, most notably at enhancer regions of genes associated with synaptic assembly (de la Fuente Revenga et al., 2021).

Molecular changes can lead to structural changes in neurons, such as formation/elimination and/or modification of dendrites, spines, and synapses. Neuronal structural plasticity was first observed in rodent neuronal cultures where bath application of psychedelic drugs increased spine size and dendritic

branching (Ly et al., 2018, 2020). Application of DMT, psilocin, DOI, MDMA, and LSD, but not 5-HT, led to significant structural modifications. Transient stimulation can be sufficient to induce these changes. Only 15min of treatment with LSD resulted in robust increases in dendritic branching in cortical neuron culture, although a 6h period was optimal for increasing spine and synapse density (Ly et al., 2020). While details of the signalling pathways responsible for psychoplastogenic effects of psychedelics remain elusive, it appears that initial activation of TrkB, a high affinity receptor for BDNF, is required, followed by sustained activation of AMPA receptors and mammalian target of rapamycin (mTOR) (Ly et al., 2018, 2020).

In vivo, these results were confirmed across species. LSD and DOI increased dendritic branching of sensory neurons in *Drosophila* larvae and rat PFC pyramidal neurons (Ly et al., 2018). In chicken embryos, DOI dose-dependently increased synapse density by 20%, even in the presence of a 5-HT_{2A}R antagonist ketanserin (Niitsu et al., 1995). In pigs, one day after an injection of psilocybin, there was a significantly higher synaptic density in the hippocampus and PFC, as inferred by radiolabelling for synaptic vesicle protein 2A as molecular marker of synapses where SV2A density is thought to reflect presynaptic density (Raval et al., 2021). Note that SV2A density increase was still visible seven days post-intervention in the aforementioned study.

There has also been an attempt to track psychedelic effects on spine plasticity longitudinally, *in vivo* in mouse cortex. When the spines of the primary sensory cortex were tracked in mice injected with 10mg/kg DOI with transcranial

two-photon imaging before and 24h after injection, an increase in spine formation was observed, with no effect on spine elimination (Cameron et al., 2021). A longitudinal two-photon imaging study of spine dynamics with psilocybin also showed increased rate of spine formation within 24h, as well as increased spine density and spine size (Shao et al., 2021). These effects were observed in cortical pyramidal neurons of PFC, cingulate cortex, prelimbic and infralimbic cortex, and primary and secondary motor cortex. Increased spine density, but not spine size, was persistent a month later, although only in female mice. In contrast, the rates of spine formation returned to baseline levels by day 7 in both males and females.

However, spines that grew during the higher rates of spine formation can mature into functional synapses and are no less stable than spines formed under non-psychedelic conditions. Approximately half of newly formed spines remain stable on day 7, and approximately 30-40% of psilocybin-evoked spines were also found 34 days after treatment (Shao et al., 2021). The authors also noted the locations of lost spines and reported some dendritic branches losing most of their newly formed spines, while other branches retain most of their spines. They suggested this to be due to a putative difference in responsivity of different pyramidal neuron subpopulations, but it is also possible that both spines and dendrites undergo remodelling after the period of their increased formation. Newly formed dendritic branches have not been tracked over time yet, but they could also be undergoing further remodelling and pruning.

In some regions, like the hippocampus, neurogenesis can also occur (Gage, 2019). Reports on neurogenesis following psychedelics have been mixed.

In rats, LSD and DOI had no effect on adult neurogenesis (Jha et al., 2008), and, in mice, psilocybin slightly reduced it (Catlow et al., 2013). DMT activated adult hippocampal neurogenesis in the subgranular zone of the mouse dentate gyrus, an effect that was associated with better performance in a spatial memory task (Morales-Garcia et al., 2020). Furthermore, DMT had a direct effect on the differentiation of neural progenitors toward astrocytes and oligodendrocytes. Interestingly, DMT's effects were not linked to 5-HT receptors, but the sigma-1 receptor instead, for which DMT is an endogenous ligand. Considering other psychedelics have lower affinity for sigma-1 receptors, this could potentially explain the discrepancies between neurogenesis effects of different drugs. Nonetheless, DMT was administered 4-10 times in the aforementioned study, so single dose effects remain unclear. Classic antidepressants can also increase hippocampal neurogenesis, but they simultaneously increase elimination of neurons via apoptosis, making the net effect that of neuronal turnover (Sairanen et al., 2005). It is not yet known if psychedelics modulate hippocampal apoptotic cell death.

Structural modifications are accompanied by functional changes. The size and shape of dendritic spines relates to functional plasticity (Bourne and Harris, 2008). Thin spines are highly dynamic in response to neural activity, while stubby spines are the transitional structures that grow into the mature mushroom spines. This is an example of how, at the cellular level, neuroplasticity is activity-dependent, which translates to experience-dependent plasticity at the level of cognition and behaviour. In mice injected with 2mg/kg DOI, the density of both thin and stubby spines in the frontal cortex, but not mature mushroom spines, is

increased 24h after (de la Fuente Revenga et al., 2021). The number and strength of synapses is reflected by the frequency and amplitude of miniature and spontaneous excitatory postsynaptic currents (mEPSCs and sEPSCS), and psychedelics have been found to regulate both. Slice recordings of rat layer 5 pyramidal neurons following DMT treatment showed increased frequency and amplitude of sEPSCs. The frequency of mEPSCs in layer 5 mouse pyramidal neurons was increased 24h after psilocybin injection (Shao et al., 2021). 2mg/kg DOI enhances the magnitude of sEPSCs and long-term potentiation in layer 2/3 frontal cortex pyramidal neurons (de la Fuente Revenga et al., 2021).

Psychedelic effects on neuronal plasticity are dose and time dependent. It has been shown that higher doses of DOI induce greater changes in gene expression (Vaidya et al., 1997; Jefsen et al., 2019) and dendritic branching (Ly et al., 2018). While neuroplasticity may increase by a significant amount within hours, peak plasticity is suggested to occur in the following days. This is due to the results showing higher structural plasticity 72h after exposure than that seen at the 24h mark (Ly et al., 2018, 2020; Shao et al., 2021). Neuronal structural plasticity then likely diminishes by the end of the first week. Spine formation returns to baseline levels by the fifth day (Shao et al., 2021), but this does not mean that the newly formed spines and dendrites cannot outlast this period. Spine density was still higher when measured at day 34, and 30% of newly formed spines form functional synapses that persist for at least four weeks (Shao et al., 2021).

Other determining factors of psychedelic neuronal plasticity are less clear. Most notably, whether psychedelic activation of 5-HT_{2A}Rs is necessary for the induction of neuronal plasticity is still under debate. Some studies suggest that neural plasticity effects of psychedelics might require 5-HT_{2A}R activation (Ly et al., 2018; Cameron et al., 2021), but such findings were not replicated by others (Niitsu et al., 1995; de la Fuente Revenga et al., 2021; Hesselgrave et al., 2021; Shao et al., 2021). Therefore, the consensus has not been reached yet on whether the acute psychedelic effects are required for the therapeutic effect and whether non-psychedelic analogues can have comparable therapeutic effects.

Human data on psychedelic-induced neuronal plasticity is limited by available methods. Human studies mostly relied on peripheral BDNF levels as indicators of neuroplasticity. Results have been mixed. Some find increased BDNF levels 6h after LSD (Hutten et al., 2020) and 48h after ayahuasca (Almeida et al., 2019), while others report no changes in the first 12h after psilocybin nor LSD (Holze et al., 2022). There is some preliminary evidence of human synaptic plasticity since increased long-term potentiation was evoked by visual responses in healthy individuals acutely treated with psilocybin (Olson, 2018). Neuroimaging studies of altered neural connectivity (section 1.6.c) are interpreted as evidence of drug-induced neuroplastic changes, even though we cannot measure neuronal structure directly with invasive methods such as those used in preclinical models.

1.6.b Level 2: Brain regions

Regional structural plasticity can be measured as changes in regional volumes of grey and white matter. These can be assessed with structural brain

magnetic resonance imaging (MRI) (see section 2.4 for further details on how MRI is used to measure structural plasticity changes). The long-term impacts of single psychedelic use on the brain remain unexplored despite several suggestions of potent plasticity-inducing effects of psychedelics (Frankel and Cunningham, 2002; González-Maeso et al., 2007; Antoniadou et al., 2018; Ly et al., 2018). Previous work on cellular and molecular plasticity had to focus on specific regions of the brain due to the limitations of the methods available, but structural changes in grey matter volume could potentially be simultaneously found across several brain regions beyond the frontal and sensory cortices. The extent and timing of these changes may not be comparable across regions so elevated plasticity could vary by region and so affect the cross-regional control of behaviour.

The therapeutic need for induction of regional volume increase is necessitated by atrophies seen in neuropsychological disorders. For example, meta-analyses of MRI studies done on patients with major depression, including those taking antidepressants, suggest hippocampal atrophy (McKinnon et al., 2009) and cortical thinning (Koolschijn et al., 2009). A non-pharmacological treatment of depression with electroconvulsive therapy is known to normalize hippocampal volumes (Wilkinson et al., 2017), but long-term antidepressant treatment has so far only been shown to have modest protective effects against hippocampal atrophy (Frodl et al., 2008). There are no published studies describing the long-term effects of psychedelic treatment on hippocampal volume in depressed patients or healthy controls.

There has only been one study of cortical thickness changes with psychedelics by Bouso and colleagues (2015) who studied how *sustained* psychedelic use affects the brain in the long-term. Only chronic users of ayahuasca, who had over 50 exposures to ayahuasca in the previous two years but minimal exposure to other drugs, were included in the study. These participants were members of the Santo Daime church where ceremonial use of ayahuasca is typically this frequent. Structural MRI showed both cortical thinning and thickening across the cortex. Cortical thinning in ayahuasca users was reported in posterior cingulate cortex (PCC), in middle, inferior, and superior frontal gyrus, and in the precuneus. Cortical thickening was found in ACC and the precentral gyrus. These structural modifications correlated with personality differences between ayahuasca users and non-users. Increased PCC thinning was associated with greater scores on a personality trait of self-transcendence which refers to expansion of personal boundaries such as transpersonal identification and connectedness with the universe. Considering the study participants had on average over 100 prior exposures to ayahuasca, it is likely that a single dose would not be sufficient to induce such effects, although cortical volume differences were never measured in human or animal studies in the days and weeks after single dosing.

Regional functional plasticity are related to physiological changes such as altered metabolism and neurotransmission. There have been several efforts to look at regional neurometabolic changes. Some of the earliest work was done on mescaline where single photon emission computed tomography (SPECT) measures of cerebral blood flow in healthy subjects indicated *hyperfrontality*

whereby frontal cortex showed markers of increased blood flow while posterior cortical regions showed reduced blood flow under mescaline (Hermle et al., 1992). Hyperfrontality was also reported in healthy volunteers treated with psilocybin and imaged with a positron emission tomography (PET) scan testing for cerebral metabolic rates of glucose (Vollenweider et al., 1997; Gouzoulis-Mayfrank et al., 1999). Confusingly, a baseline left-greater-than-right asymmetry of glucose metabolic rates in the frontolateral cortex was reported as increased by psilocybin (Vollenweider et al., 1997), but others suggest a greater right hemisphere activation instead (Gouzoulis-Mayfrank et al., 1999).

Neurometabolic changes can be measured with MR spectroscopy that allows us to measure concentrations of glucose, but also of inhibitory neurotransmitter γ-Aminobutyric Acid (GABA), and other neurometabolites, such as creatinine (Cr), choline-containing compounds (Cho), inositol (Ins), glutamate (Glx), and total N-acetylaspartate plus N-acetylaspartylglutamate (NAA-NAAG) (Rae, 2014). 24h after ingesting ayahuasca, healthy volunteers had significant neurometabolite changes compared to 24h before ayahuasca only in PCC, and not in ACC or the cerebellum (Sampedro et al., 2017). In the post-ayahuasca assessment in PCC, there were significant decreases only in Cr and NAA-NAAG levels, and marginal decreases in Glx. The post-acute decrease in Glx could be the result of increased glutamatergic excitatory activity in the acute phase and is consistent with the decreases in Cr and NAA-NAAG that are both associated with metabolic activity, with NAAG being directly linked to glutamatergic pathways. Glx changes have also been reported following psilocybin treatment, but these were only measured acutely, 1-1.5h into the peak subjective drug effects (Mason

et al., 2020b). In the acute phase, Glx levels were higher with psilocybin in medial PFC, but lower in the hippocampus. There were also higher concentrations of NAA and GABA in PFC, but no other significant differences in the hippocampus. Acute effects of psilocybin on regional neurotransmitter levels were also replicated in rodents. Rat microdialysis experiments measured extracellular levels of neurotransmitters in frontal cortex and found increased levels of glutamate and GABA, as well as increased 5-HT and dopamine (Wojtas et al., 2022). However, the post-acute period remains greatly unexplored in both human and animal studies, so we cannot yet know if regional neurometabolism is affected by psychedelics in the long-term.

1.6.c Level 3: Networks

Brain function involves coordinated integration and segregation of information over networks linking spatially distributed specialized brain areas. Structural brain networks refer to the patterns of anatomical connections between brain areas that make up the nodes of a network, and structural plasticity refers to the physical changes in these connections, as discussed in the previous section. Functional brain networks on the other hand refer to the temporal correlation of neurophysiological activity occurring at the network's nodes (Lord et al., 2017). Functional communication between brain regions plays a key role in complex cognitive processes and functional dysconnectivity is found in psychiatric brain disorders (van den Heuvel and Pol, 2010).

Investigations of functional networks are usually derived from neuroimaging data with methods such as functional MRI (fMRI). fMRI detects low

frequency fluctuations in the blood oxygen level dependent (BOLD) signal. Temporal correlations of these fluctuations across different brain regions define *functional connectivity*. Functional connectivity can also be measured in no-task conditions using resting-state fMRI (rsfMRI) to look at how resting-state functional connectivity patterns change after drug manipulations.

The first rsfMRI investigations of acute psychedelic effects were performed in healthy subjects intravenously injected with LSD (Carhart-Harris et al., 2016a) and psilocybin (Carhart-Harris et al., 2012). The results implied decreased activity and functional connectivity in the brain's key connector hubs in the thalamus, PCC, and ACC. A way of visualising this idea is that normally the brain's functional networks act like a clique – most of the strongest connections are short-range and between members of the same community, i.e., network nodes that share functionality. In contrast, a more intercommunicative mode of function emerges in the less constrained psychedelic state, such that stronger and more long-range functional connections are becoming more prominent (Petri et al., 2014).

Selection of anatomically relevant regions from functional connectivity maps is mainly done by the experimenter and psychedelic research has largely focused on the default mode network (DMN) and executive control network (ECN). DMN is a collection of correlated areas in PCC, medial prefrontal, lateral parietal, and perihippocampal cortices (Buckner et al., 2008). DMN's association with the "default mode" of brain function came from observations that its structures are most correlated in the absence of any task, when the brain is idle,

and the DMN is then deactivated during task performance. While DMN is active during resting awake states and is implicated in internal mental activity, ECN is active during cognitive tasks where it is responsible for decision-making and problem-solving to facilitate goal-directed behaviour (Menon, 2011).

Because most functional connectivity findings have been the results of a seeded analysis limited to a handful of regions, the interpretations drawn remain subjective and dependent on the number of components chosen for the analysis. Critically, the results of functional connectivity analysis are highly dependent on scanning and analysis parameters, such that comparisons across studies are only valid for exactly comparable set-ups. Additionally, psychedelic drugs can affect neurovascular coupling (Spain et al., 2015), further complicating the interpretation of BOLD signal findings.

Aside from changing patterns of network connectivity, psychedelics have also been found to change the brain's spatiotemporal dynamics. Such findings have led to a theory of an entropic brain (Carhart-Harris et al., 2014; Carhart-Harris, 2018). *Brain entropy* refers to the index of both the richness of information processed by the brain, as well as how much uncertainty there is about how this system will behave in the future and how ordered is its functioning. Therefore, a brain state that has high entropy is very content-rich, but also unpredictable and potentially unstable as it exhibits "criticality", i.e., entropic states are near a critical transition point between order and disorder. Criticality confers sensitivity to perturbation, intrinsic or extrinsic, which may translate as increased environmental sensitivity. Under favourable conditions, this sensitivity could

translate to greater well-being, but, under adverse conditions, it could lead to greater mental vulnerability instead (Belsky et al., 2009; Branchi, 2011).

Using connectome harmonics, a frequency-based analysis of fMRI, signatures of criticality in brain dynamics have been found in psychedelic-induced states (Atasoy et al., 2018). Elevated entropy of brain function implies a greater variance of intra-network synchrony. LSD and psilocybin, compared to a placebo, reduce the control energy required for brain state transitions, an effect that correlates with more frequent state transitions and increased entropy of brain state dynamics (Singleton et al., 2022).

Increased flexibility of functional networks has been suggested as the mechanism underlying the psychedelic antidepressant effect as distinct from SSRIs (Daws et al., 2022), but this has been contested due to spurious statistical reasoning (Doss et al., 2022a). The debate surrounding these findings has highlighted the extensive practice of reanalysis of the same rsfMRI data using different methods and hypotheses generated after seeing previous results based on the same data. The most recent review of psychedelic resting-state neuroimaging (McCulloch et al., 2022) quotes that 52% of published rsfMRI analyses included in their review are derived from the two original rsfMRI data sets on LSD (Carhart-Harris et al., 2016a) and psilocybin (Carhart-Harris et al., 2012). These are the only two data sets available that used intravenous administration (oral administration is favoured in more recent studies) and only included participants with prior experience of psychedelic drug use. There is a

clear need for independent replication of these findings using other data sets, especially those from more generalizable populations.

Aside from the entropic brain model, other prominent models tested include: (i) the thalamic gating theory (Vollenweider and Geyer, 2001), suggesting that the acute hallucinogenic-like effects of psychedelics arise from the disruption of thalamic filtering of external and internal information to the cortex, (ii) the claustro-cortical model (Doss et al., 2022b), suggesting the key role of 5-HT_{2A}R activation in the claustrum for the network disruption under psychedelics, and (iii) the relaxed beliefs under psychedelics (REBUS) model (Carhart-Harris and Friston, 2019), referring to the ability of psychedelics to reduce top-down control to disrupt typical predictive coding. The REBUS model is in fact linked with the entropic brain hypothesis as reduced top-down control, and the resulting increase in bottom-up information flow, would be expressed as increased entropy. A promising aspect of the thalamic gating theory is that it may open doors to non-psychedelic treatment with psychedelic-like drugs. If the perceptual effects of psychedelics were found to be modulated only by the thalamic filtering, and if this process was found to be unrelated to the therapeutic effects of psychedelics, this would suggest that the mechanisms for the acute psychedelic state and the long-term therapeutic state could be separated. This would mean that non-psychedelic analogues could be developed to provide therapeutic benefits of psychedelics to populations currently excluded due to safety concerns over induced psychoses.

How do these models of psychedelic effects on functional networks link back to the clinical findings in patients? Many neuropsychiatric disorders are characterized by rigid cognitive and behavioural patterns and compulsive traits arising from overweighted priors (Weisholtz et al., 2017). For example, a drug addiction may begin with a prior belief that taking a particular drug is associated with a large rewarding feeling. As a person starts abusing the drug the negative aspects of drug dependence start becoming more apparent and the rewarding feeling gets harder to replicate as the drug deregulates the brain's reward system (Feltenstein and See, 2008). This new information is supposed to update the prior belief to better reflect the new state of the world. However, in an addicted state, the prior belief about the stimulus-outcome values is too rigid to be updated to reflect adjusted predictions about future outcomes (Lucantonio et al., 2012). This overlearning is also coupled with drug euphoria and fear of withdrawal to reinforce relapse behaviour (Robinson et al., 2013). Relaxing predictive coding under the REBUS model would work against pathologically rigid priors underpinning such perseverative states of mood and behaviour in mental disorders (Clark et al., 2018). The psychological consequence of this would be a reduced influence of maladaptive beliefs. Preliminary empirical evidence for this has been found in a small sample of healthy individuals treated with psilocybin who then reported decreased confidence in the negative beliefs they had about themselves (Zeifman et al., 2022).

1.6.d Levels 4 & 5: Cognition and behaviour

Measures of neural plasticity alone do not tell us how behaviour is changing. We need measures of behaviour to determine whether and how neural

plasticity supports the improvements in mood and function are associated with psychedelic-assisted psychotherapy. With the support of an improved neural structure and functionality discussed in the earlier sections, we can predict that the enriched brain would show enhanced cognitive capacities to better respond to changes in the environment.

The ability to adapt one's thinking and behaviour to changes in the external or internal environment is defined as cognitive and behavioural flexibility, respectively. Behavioural and cognitive flexibility require an inhibition of an old, no longer optimal strategy, and a search for and maintenance of new, more effective strategies (Scott, 1962). Compromised flexibility results in excessively rigid adherence to habitual responses and existing models of the world, and an inability to adapt to changes (Weisholtz et al., 2017). Hypothetically, treatments that enhance cognitive/behavioural flexibility could therefore alleviate a whole spectrum of disorders characterized by cognitive/behavioural rigidity.

A large set of evidence supports the association between 5-HT and its receptors with flexibility (Branchi, 2011). 5-HT neurons are activated when assumptions are violated, independent of their associations with rewards (Matias et al., 2017). Inactivating or depleting 5-HT in the PFC or OFC impairs cognitive flexibility in marmoset monkeys, mice, and rats (Clarke et al., 2007; Matias et al., 2017; Alsiö et al., 2021), possibly due to decreased basal activation of 5-HT_{2A}Rs (Boulougouris et al., 2008; Furr et al., 2012). When a 5-HT_{2A}R antagonist M100907 was injected into the rat OFC, it dose-dependently worsened

performance on an attentional set shifting reversal learning task[3], and it opposed the effect of chronic SSRI citalopram treatment that normally improves reversal learning in stressed rats (Furr et al., 2012). These results suggested that the role of 5-HT_{2A}R is to improve reversal learning and to contribute to the beneficial cognitive effects of chronic SSRI treatment. When M100907 was administered in rats performing an instrumental two-lever spatial reversal learning task, it also significantly impaired reversal learning by increasing perseverative behaviour (Boulougouris et al., 2008), but spatial learning impairments were not OFC-specific (Boulougouris and Robbins, 2010). Notably, other 5-HT_2 receptors can have opposing effects – a 5-HT_{2C}R antagonist SB242084 decreased perseveration in the two-lever spatial reversal learning task (Boulougouris et al., 2008), and these effects were mediated by OFC (Boulougouris and Robbins, 2010). The 5-HT_{1A}Rs are also implicated in cognitive flexibility – their direct role on cognitive flexibility may be limited to restoring reversal learning deficits in disease models (Depoortère et al., 2010), but they can also indirectly affect flexibility by regulating the serotonergic tone via their autoreceptors (Garcia-Garcia et al., 2014).

While the link between psychedelic pharmacological activation of the 5-HT system would suggest effects on cognitive flexibility, existing evidence is surprisingly limited. In humans, LSD increased trait openness for at least 2 weeks after treatment which has been interpreted as a “loosening” of cognition (Carhart-

[3] How reversal learning tasks are used to test cognitive flexibility will be discussed in detail in section 2.3.

Harris et al., 2016c). New data suggest that healthy subjects doing a probabilistic reversal learning task under LSD had higher rates of both reward and punishment learning, and decreased repetitive choices, reflecting heightened exploratory behaviour in the task (Kanen et al., 2021). Tests of cognitive flexibility have not been used extensively in the post-acute phase of psychedelic action. 24h after ayahuasca use, cognitive flexibility measured by both the cognitive flexibility scale and the Wisconsin Picture Card Sorting Task (WPCST) was improved 24h after ayahuasca relative to before treatment (Murphy-Beiner and Soar, 2020). Previous experience with ayahuasca was not found to be a significant factor for either CFS or WPCST although others have shown that regular ayahuasca users also have better performance on the WPCST and that these effects were maintained at the one-year follow up used in the study (Bouso et al., 2012). However, these results might differ across different types of psychedelics and across time since LSD in healthy subjects was linked with increased perseveration and higher error rate in the WPCST 24h after treatment (Wießner et al., 2022).

Behavioural and mood effects of psychedelics in humans have been studied more extensively than cognition. Mood benefits of psychedelic-assisted psychotherapy are known to persist for many months, even years, both in patients suffering from mental health problems (Griffiths et al., 2016; Ross et al., 2016; Johnson et al., 2017; Carhart-Harris et al., 2018a; Bogenschutz et al., 2022) and in healthy individuals (Studerus et al., 2011; Schmid and Liechti, 2018; Uthaug et al., 2018). Psilocybin's ability to decrease negative affect but also increase positive affect was found one week after treatment, with the effects on positive

affect persisting one month after suggesting enduring increased emotional plasticity (Barrett et al., 2020).

Preclinical models recapitulate the extended timeline of behavioural change. Notably, LSD's antidepressant-like effects in rats were found for as long as 5 weeks post-administration (Hibicke et al., 2020). DOI's antidepressant-like effects were apparent as soon as 24h after treatment and persistent for at least one week (de la Fuente Revenga et al., 2021). Nonetheless, there is a gap in our understanding of the after-effects of psychedelic drugs in the context of more complex cognitive tasks that would enable us to parcel out the specific aspects of cognitive flexibility being modulated and how they would relate to any improvements in mood.

1.6.e What makes psychedelics unique?

Psychedelics, like SSRIs, exert their effects via the 5-HT system, but they do so differently. SSRIs, as their name suggests, block the reuptake of 5-HT from the synaptic cleft by the presynaptic cell, which results in a prolonged increased level of 5-HT. Efficacy of SSRIs in treating depression implicated 5-HT, specifically a decrease in its levels, as a cause of depression. The belief that depression is caused by a chemical imbalance in the brain was used to explain the efficacy of antidepressants. Patients are required to take their SSRI pill every day, echoing that the chronic administration of the drug is needed to correct an imbalance, whether of chemical or some other nature, to manage the symptoms. However, direct evidence to suggest low 5-HT levels *cause* depression is lacking.

While SSRIs decrease negative mood, but they do so by leading to a more “flattened” mood state. Emotional blunting is a dose-dependent side-effect that is resolved by discontinuing the SSRI (Sansone and Sansone, 2010). In contrast, psychedelics increase acceptance of both positive and negative emotions. When amygdala’s activation was measured in subjects exposed to fearful or happy faces, subjects tested a week after psilocybin treatment showed significantly increased responses to both types of faces (Roseman et al., 2018a), while those subjects that were treated with an SSRI showed only a reduced activation by sad faces (Fu et al., 2004). Psilocybin’s ability to decrease negative affect but also increase positive affect was found one week after treatment, with the effects on positive affect persisting one month after suggesting enduring increased emotional plasticity (Barrett et al., 2020).

Different hypotheses on SSRIs’ antidepressant effects also rest on the 5-HT’s role in controlling neuroplasticity (Mattson et al., 2004). The differential susceptibility hypothesis conceptualizes the differences in susceptibility to stress not by categorizing individuals as vulnerable or resilient, but by considering the degree of plasticity as an indicator of how responsive individuals are to experiences, the direction of that responsivity being determined by their environment (Belsky et al., 2007, 2009). Branchi (2011) suggested that biological sensitivity to context is, at least in part, determined by 5-HT levels. He hypothesizes that SSRI’s ability to increase levels of 5-HT does not affect mood directly, but rather acts a catalyst for neuroplasticity. The consequent opportunity to change does not determine the direction of that change. If a supportive environment is available, capacity to recover will be increased, but in

unfavourable conditions, there will be a risk of further deterioration. Therefore, for SSRIs and for psychedelics, enhanced serotonergic activation is proposed not as the cause but as the permissive factor of therapeutic effects.

Drug-induced neuroplasticity is a well-established phenomenon (Castrén and Antila, 2017). Duman and colleagues were the first to show that chronic, but not acute, treatment with antidepressant drugs, such as SSRI sertraline and tricyclic mianserin, significantly increased BDNF mRNA levels the hippocampus (Nibuya et al., 1995). These effects were demonstrated in humans too. Post-mortem samples of patients on chronic antidepressants treatment at the time of death also showed increased BDNF mRNA levels compared to untreated patients (Chen et al., 2001). SSRI fluoxetine can also promote cortical remapping of ocular dominance columns and improve fear extinction learning (Castrén and Antila, 2017). However, the plasticity effects of antidepressants parallel their behavioural effects – chronic administration is required, and the onset of effects is slow.

Ketamine, a dissociative anaesthetic, was discovered to produce fast-acting and long-lasting antidepressant effect, being termed as a rapid-acting antidepressant (RAAD) (Lee et al., 2015). Ketamine is also a psychoplastogen, inducing growth of dendritic spines and new synapses in PFC within 24h of a single treatment (Li et al., 2010), and the behavioural effects follow the same timeline. But, while ketamine's effects on mood dissipate in a week, psychedelic-mediated mood improvements last for months. Comparisons of neuronal plasticity effects have also pointed to psychedelics being more potent

psychoplastogens than ketamine (Ly et al., 2018, 2020; Cameron et al., 2021). This reinforces the idea that while psychedelic effects on mood and plasticity are not unique in their occurrence or possible mechanisms, they are uniquely faster and longer lasting.

We were guided not by the promise of psychedelics to overturn the market of antidepressant drugs, but their ability to change behaviour quickly and enduringly, which is the goal of any mental health therapy. Studying their mechanism of action has the potential to elucidate what are the biological requirements for a fast and lasting behavioural change. Therefore, the value of psychedelics is not reserved for the clinic but is significant for advancing our basic understanding of psychological and neurobiological processes as well.

1.7 Research aims

Data reviewed in the previous section suggest that various signatures of enhanced neuroplasticity arise after psychedelic treatment. The earliest changes are those in gene expression, occurring within hours of treatment, followed by changes in neuron structure and synaptic organization and function that peak within 72h. Increased rate of dendritogenesis and spinogenesis tapers off within five days, although the neuroplastic changes that have occurred in this period persist for weeks after. However, it remains unclear if enhanced neuronal plasticity is simply something we can measure with psychedelics or if these changes have meaningful direct consequences on behavioural outcomes of mood and learning. We know that the changes in the morphology and activity of

the synaptic landscape can affect information transfer – changes in brain function have been uncovered in humans and they have been shown to occur within days, lasting across the following weeks. The critical gap in the multi-level plasticity chain is that we do not yet understand how functional and structural changes in neurons relate to large-scale structure of brain regions that make up neural networks, and how network dynamics would map onto the enduring changes in cognition and behaviour. Specific markers at different levels of analysis may also have different windows of plasticity than those seen with neuronal plasticity.

To understand how the enhanced molecular plasticity induced by psychedelics might ultimately translate to shifts in behaviour, we looked at plasticity markers at "middle" and "higher" levels of analysis – brain structure and cognitive function. Existing evidence of plasticity at these levels is limited to either the acute and immediate post-acute phase or to human populations with extensive experience of psychedelic drug use. There is a pressing need to elucidate whether a single dose can have long-term consequences on the brain and research in preclinical models where we have strict control over drug history and environmental context will be crucial in this endeavour (further discussion on our choice of animal model can be found in section 2.1). Therefore, we investigated how long-term psychedelic-modulated heightened cellular plasticity could manifest in a mouse model past the acute drug phase with a single dosing regimen.

Most of the previous preclinical studies in mice and rats, as well as human studies in healthy volunteers, focused on studying the acute effects of the

drug, and investigating receptor targets and signalling pathways. This is despite the evidence that subjects appear relatively insensitive to conventional task-based stimuli under psychedelics since the stimuli's ability to engage attention is diminished (Timmermann et al., 2018). Furthermore, one of the most unique aspects of psychedelic therapeutic effects is how long-lasting they are – subject's behaviour is not just changed quickly but enduringly. The elucidation of the mechanism underlying these long-term effects are urgently needed to optimize not just psychedelic-assisted therapies, but potentially other pharmacological mental interventions as well.

Notably, the beginning of the window of plasticity for both neurons and neural networks falls within the acute phase of psychedelic drug action, meaning that psychedelic experiences take place within a highly plastic brain. Acute psychedelic experiences therefore have the power to re-shape the neural circuitry that is undergoing plasticity, and the association between the windows of plasticity and states of higher environmental sensitivity has been highlighted from the start (Carhart-Harris and Nutt, 2017), but preclinical studies have greatly overlooked the importance of set and setting. This is why we also attempted to validate the extra-pharmacological model of psychedelic action in our animals.

We used a mouse model to test for three signatures of a comprehensive high plasticity state induced by a psychedelic substituted amphetamine DOI (further discussion on our choice of drug can be found in section 2.2): (1) acute enhancement of environmental sensitivity measured as environmentally dependent intensity of psychedelic responses, (2) post-acute enhancement of

cognitive flexibility tested with a multi-step reversal-learning paradigm, and (3) post-acute changes in whole-brain structure in the days following drug treatment quantified with magnetic resonance imaging. Our approach will be discussed in detail in the next chapter. The specific aims were as follows:

Aim 1: To examine context-dependent dose-responses to DOI in a mouse model (chapter 3). Enhanced plasticity is linked to heightened environmental sensitivity in humans so we hypothesized that acute behavioural responses to psychedelics would also be modulated by environmental factors in mice. Psychedelic-assisted psychotherapy guidance stresses the importance of environmental familiarity for humans, so we used the novelty of environment as our factor of interest. Our hypothesis was that the dose-response curve of the frequency of acute psychedelic-like responses (head twitches and ear scratches) would not be identical in a novel environment as in a familiar environment, without explicit predictions as to which environment would result in higher drug sensitivity.

Aim 2: To explore the cognitive flexibility effects of a single dose of DOI in the weeks after treatment (chapter 4). The previously reported neuronal plasticity effects of psychedelics could create a rich synaptic landscape that should favour the encoding of new information. Our hypothesis was that we would observe enhanced speed and/or accuracy of animal's learning in a cognitive flexibility task in the days and weeks following DOI treatment.

Aim 3: To test for the presence of regional brain structure changes in the days and weeks following a single DOI treatment (chapter 5). The strong cellular plasticity enhancements induced by psychedelics in the days following treatment (specifically, days 1-3 since treatment, dissipating past the first week) could be sufficiently extensive to result in regional brain volume changes in the same time frame. Our hypothesis was that DOI would be able to induce increased grey matter volume within the first three days of treatment, but that these changes would not be observable past the first week.

2 | Approach

While we introduced our research questions and the motivation behind them in the previous chapter, we want to elaborate on the choice of our experimental approach. In this chapter, we will discuss: (i) why we chose to study the psychedelic-induced higher plasticity state in the mouse model, (ii) why DOI was our psychedelic drug of choice, (iii) why and how we will study cognitive plasticity in the form of cognitive flexibility, and finally (iv) why and how we will study whole-brain structural plasticity with *ex vivo* MRI. The details of experimental procedures will be discussed in the following chapters, but this section is meant to guide the reader as to why those methods were used and what they allowed us to measure.

2.1 Animal model

The complex ethical approval process for psychedelic research in humans often restricts the inclusion of participants to those who have used psychedelics in the past, to limit the possibility of an adverse reaction for safety purposes. This implies that we cannot know for certain what a single dose is able to achieve if we use a human model. Another significant confound is the expectancy effect. Humans will always have preconceived notions of what a psychedelic experience and its effects *should* be, especially since psychedelic science has become more prominent in the media and the public. As a result, many have argued that psychedelic studies cannot have a placebo control and consistent blinding since it is very likely that both the subject and their therapist

can easily tell the difference between a psychedelic and non-psychedelic experience, thus effectively unblinding the study. Randomized controlled trials (RCTs) being conducted to investigate the therapeutic effectiveness of psychedelics might be confounded by de-blinding and expectancy. A systematic review of psychedelic RCTs argued that the reported treatment effect sizes are likely over-estimated due to the unblinding and response expectancy, neither of which is routinely measured within the studies (Muthukumaraswamy et al., 2021). Additionally, recruitment of participants for non-clinical human studies is done via online forums and word of mouth, which usually attracts the kind of participants who already have some opinions about the potential effects of psychedelics. This further increases the expectancy effects and makes random sampling from a diverse population difficult.

Several studies show behavioural effects of psychedelics reported in humans also occurring in rodents (Catlow et al., 2013; Young et al., 2015; Cameron et al., 2018; Mollinedo-Gajate et al., 2020). For example, putative antidepressant-like effects have been widely studied in rodents using a variety of tests and models, the choice of which influences the effects observed. One of the early studies of psilocybin in a genetic model of depression, the Flinders Sensitive Line rats, reported no rescue effects in the forced swim test (Jefsen et al., 2019). However, this genetic line has abnormally low central 5-HT_{2A} expression (Österlund et al., 1999; Du Jardin et al., 2017) and psychedelic effects are thought to be primarily mediated by 5-HT_{2A} agonism (Nichols, 2012), so it is likely that benefits of psychedelic 5-HT_{2A}R agonism could not be imparted on such animals. When studies were done using a different genetic model of depression-like

symptoms, the Wistar−Kyoto rats, a single dose of psilocybin and LSD were both able to induce robust antidepressant-like effects of reduced immobility in the forced swim tests (Hibicke et al., 2020). These effects persisted for at least five weeks after injection, reflecting the same characteristic of human psychedelic antidepressant action – a rapid and lasting reduction in symptoms from single treatment.

We have chosen the rodent model because it allows for observations of anatomical and cognitive changes to be coupled with precise control of environmental and personal history factors not possible in humans. Dosing and randomization are controlled by the experimenter, and an animal would not have any expectancy bias, although blinding the experimenter is still not easily feasible in observational studies. We have opted for the use of mice as there was a wealth of preclinical data available for both mice and rats, but mice offer a greater range of molecular and genetic tools which may be required for follow-up mechanistic studies.

Improvements in overall wellbeing and cognitive performance, as well as psychedelic-induced neurometabolic and functional connectivity changes, have all been reported in healthy individuals (Roseman et al., 2014; Bouso et al., 2015; Carhart-Harris et al., 2015; Soler et al., 2016; Sampedro et al., 2017; Murphy-Beiner and Soar, 2020), not just various clinical populations. Therefore, our approach was not specific to any disease model but is a proof of principle in a healthy wild-type organism that can then be applied to various disease models. We wanted to avoid having to narrow down our hypotheses to a specific model of stress or addiction which will inevitably have its own limitations and debates

regarding its translational value. The window of plasticity theory that guided our hypotheses is not specific to a depressive state, or any other disorder specifically. Structural and functional plasticity changes at the levels of neuron and network have been found in healthy organisms (as discussed in section 1.6), suggesting that enhancement of plasticity is not restricted to situations where there is a deficit to correct. We therefore decided to do our studies in healthy mice to show general effects of just enhancing plasticity in absence of any predetermined plasticity deficit. We discuss the potential generalizability of our findings to disease models in section 6.4, but our study cannot account for the large diversity of plasticity changes implicated in various animal models of neuropsychiatric disorders.

The mouse behavioural proxy of human psychedelic potential is the head-twitch response (HTR). This behaviour is characterized as a rapid side-to-side rotational movement of the head. It is part of the normal repertoire of spontaneous mouse behaviours similar to the pinna reflex, an acoustic startle response (Carlson and Willott, 1998), but psychedelic drugs greatly increase its frequency. This effect is not induced by other psychoactive drugs such as cocaine or amphetamine (Hanks and González-Maeso, 2013; Jaster et al., 2022a), and is therefore a reliable rodent model of psychedelic action.

HTR is easily detectable, and therefore prevents complete blinding of the experimenter, but independent measures by different observes display remarkable consistency with low within- and between-subject variability (Keller and Umbreit, 1956). Importantly, HTR potency of psychedelics in mice is highly correlated with the drugs' hallucinogenic potency in humans (Halberstadt et al., 2020). Additionally, pharmacological and genetic tools have demonstrated that

blocking or ablating 5-HT_{2A}Rs completely abolishes the HTR in mice (Canal and Morgan, 2012), showing 5-HT_{2A}Rs are direct mediators of mouse psychedelic action, as they are in humans (Vollenweider et al., 1998; Kometer et al., 2013). While HTR could have some validity as an animal model of psychedelic hallucinations or schizophrenic psychosis, considering how an imagined auditory tone could cause an acoustic startle reflex, HTR is most suitable as a model of 5-HT_{2A} receptor activity. Therefore, we consider HTR as a pharmacological outcome with a cross-species translational relevance, but not as a model of a psychedelic state of consciousness seen in humans.

Only male wildtype C57BL/6J (Charles River) mice (*n*=124) were used in our experiments as several studies reported strain-dependent sexually dimorphic effects of psychedelic drugs in rodents (Brookshire and Jones, 2009; Páleníček et al., 2010; Tylš et al., 2016; Miliano et al., 2019; Jaster et al., 2022b). In humans, females have significantly higher 5-HT_{1A} receptor and lower 5-HT transporter binding potentials throughout the cortical and subcortical brain regions (Jovanovic et al., 2008). Many studies have suggested that oestrogen and progesterone increase density, expression, and/or sensitivity of 5-$HT_{2A/C}$ and 5-HT_{1A} receptors (Haleem et al., 1990; Frankfurt et al., 1994; Sumner and Fink, 1995; Fink et al., 1999; Cyr et al., 2000; Birzniece et al., 2002; Zhou et al., 2002; Landry and Di Paolo, 2003; Le Saux and Di Paolo, 2005). Therefore, sex is likely to play a role in the sensitivity of the serotonergic system to psychedelic behavioural effects, as several animal studies have shown for LSD, DOI and psilocin (Blanchard et al., 1992; Meehan and Schechter, 1998; Brookshire and Jones, 2009; Páleníček et al., 2010; Tylš et al., 2016; Jaster et al., 2022b). For

example, DOI induced a stronger HTR in female than in male C57BL/6J mice (Jaster et al., 2022b). Pharmacokinetic properties, such as brain and plasma concentrations of DOI, also differed between the sexes (Jaster et al., 2022b).

We originally wanted to investigate the effect of sex and oestrus cycle on DOI in a separate study where we would be able to include sex as an independent experimental variable, but this was suspended due to licensing and time limitations (see a note on the impact of the COVID-19 pandemic in section 8). Therefore, all our experiments only used male mice for consistency, but we discuss our predictions on potential findings in females in section 6.4. However, we stress the need for extending preclinical psychedelic research to include the female model as enhanced vulnerability of this sex to a variety of mental health issues is well-documented (Rubinow and Schmidt, 2019).

2.2 Drug

Our drug of choice was DOI. DOI belongs to the phenylalkylamine class of compounds, meaning it consists of a phenyl ring attached to an alkyl chain that is attached to an amine. DOI's alkyl structure is ethyl, and it has a methyl group attached to the α carbon, making its core structure an α-methylphenethylamine, or an amphetamine. Hence, DOI is also identified as a substituted amphetamine.

The use of DOI is widespread in psychedelic studies in animals, although its clinical use is not determined, unlike for LSD or psilocybin. In humans, DOI has a long duration of effects, 16-30h with 1.5-3.0mg doses (Shulgin and Shulgin, 1995), making it one of the most long-lasting phenethylamine psychedelics. The

prolonged acute experience is what limits clinical studies with DOI, as they would be arduous to perform in a clinical setting. The quality of the acute experience has been reported as similar to LSD, with clear eyes-closed imagery of delineated patterns, pictures, and colours (Shulgin and Shulgin, 1995).

We chose DOI over psilocybin as the preparation of DOI is simpler due to its high solubility in saline, which is advantageous when minuscule amounts are used and for avoiding adjustments for neutral pH. The commercially available forms of psilocybin at the time of our study design could only be used with were particularly difficult to dissolve, compromising the accuracy of the dose the experimenters believe they inject, and tartaric acid needs to be used as the vehicle. DOI is chemically stable in solution and is one of the few psychedelics considered to be *relatively* selective. DOI is a potent agonist for most 5-HT_2 receptor subtypes, but it is reported to have up to 40-fold higher affinity for 5-HT_{2A} than for 5-HT_{2C} sites (Nelson et al., 1999), which is advantageous for any future experiments on specific receptor pharmacology. Although, we do note that the more diverse pharmacological profile of other psychedelic drugs might be the basis of their therapeutic effects (although there is no evidence to suggest superiority of any of the classic psychedelics for specific behavioural effects), but we discuss how generalizable our effects are to other psychedelic drugs in section 6.5.

ESR is a rapid scratching of the head or neck with either limb. Like HTR, it is normally seen in mice, especially during grooming episodes. ESR is produced by other psychedelics of the phenalkylamine group, such as 1-(2,5-dimethoxy-4-methylphenyl)-2-aminopropane (DOM). ESR is partly mediated by 5-HT_{2A} but

primarily by 5-HT_{2C} receptor activation, and its inhibition is modulated by 5-HT_{1B} receptors (Darmani et al., 1990c).

DOI has a chiral centre, meaning it can exist as two enantiomers: (+)-DOI and (-)-DOI. The (-)-DOI enantiomer is the more potent of the two, exhibiting higher behavioural potency in both mice (Darmani et al., 1990c) and humans (Shulgin and Shulgin, 1995). We use racemic DOI in all our experiments as ESR is stereoselective with the (-)-enantiomers (Darmani et al., 1990c), but we wanted to avoid the high potency of (-)-DOI to avoid a 5-HT syndrome due to higher activation of other 5-HT receptors at smaller doses.

Low (0.5 and 1mg/kg) and moderate (2mg/kg) doses of DOI were chosen based on previous findings with this psychedelic. Dose-dependent effects of DOI demonstrated in mice suggest increases in HTR over the doses ranging from 0.1mg/kg (sub-psychedelic, no HTR) up to 2-10mg/kg (maximum HTR) (Darmani et al., 1990a, 1990b; Schreiber et al., 1995; Yamada et al., 1995a; Miyata et al., 2004; Canal et al., 2010). A biphasic U-shaped dose-response curve was reported, with the increasing HTR reaching a peak and then a decrease in frequency with increasing doses. The ascending limb of the response curve is due to increasing activation of 5-HT_{2A}Rs, while the descending limb of the response curve is believed to be mediated by the HTR-supressing effect of 5-HT_{2C} receptor activation (Fantegrossi et al., 2010) – with increasing doses, DOI can activate its lower potency receptors more strongly. There are strain differences in the shape of the dose-response curves, such that some studies in C57BL/6J mice also report a linear increase in HTR that reaches a maximum at 1.6mg/kg and then plateaus at higher doses up to 12.8mg/kg (Canal et al., 2010).

For the case of ESR, previous reports suggest a linear increase in frequency up to doses of 2.5mg/kg (Darmani and Gerdes, 1995), but high-enough doses of DOI were not measured to capture a potential decline or plateau so a U-shaped curve is suggested due to inhibitory action of 5-HT_{1B} receptors (Darmani et al., 1990c), but it has not been defined yet. Such discrepancies between reports and gaps in the literature urged us to determine the dose-response curves in our lab setting ourselves, rather than selecting only a single dose of interest to test environmental influences.

2.3 Studying cognitive flexibility

Cognitive flexibility enables an individual to adapt to environmental changes. A synthesized research definition of cognitive flexibility is a switch in thinking in new situations, whether that be because of a switch in rules or because of a need to switch one's previous beliefs or thoughts that have become habitual but no longer optimal. As flexibility involves a disengagement from ongoing behaviour, it requires multiple components of decision-making. Learning to make decisions that lead to best possible outcomes is critical for success in a particular environment. Flexibility is comprised of both cognitive and behavioural domains that are closely intertwined to refer to the abilities to change one’s thinking and behaviour according to a specific context. Since laboratory tasks of cognitive flexibility require a behavioural output, they can be considered as tasks of both cognitive and behavioural flexibility, and so the two terms will be used interchangeably in this text.

Experimental tasks designed to test flexible decision-making usually rely on reversal learning, which can be employed in multiple species (Izquierdo et al., 2017), including humans, so it has a high translational value. Reversal learning involves repeated pairing of an action (e.g., the pressing of a lever) with an outcome (e.g., a food reward) according to a learned rule. Over time, subjects in the task become very proficient at associating the action with the desired outcome. Typically, once a learning criterion is reached for the initial association, the reversal phase is implemented where the reward contingencies are reversed. The trained response no longer leads to reward, so the task measures the subject's ability to disengage from previously learned behaviour by effortfully emitting a different response, i.e., the ability to exhibit flexibility of responses.

The rules determining the action-outcome association can be deterministic (fully predictive) or probabilistic, and the steps of actions required to reach the outcome can vary. Probabilistic multi-step decision making tasks better mimic real-world situations where multiple steps are required to achieve a probabilistic reward, and thus may have higher translational value. The rules used in human reward-guided flexible decision-making tasks are also most commonly probabilistic. Therefore, we used a multi-step decision-making task to monitor how DOI treatment affects the adaptation of cognitive strategies and behaviour in changing task conditions. To operationalize probabilistic flexible adaptation, we first needed a framework that theorizes how a subject makes decisions in general.

Reinforcement learning (RL) frameworks describe how an agent interprets its environment to learn values of actions by making choices and

experiencing rewards (Sutton and Barto, 1998). An agent can engage in two types of computations – model-free or model-based. In model-free learning, an agent learns value functions such that chosen actions are directly associated with an experienced reward value and previously rewarded actions are repeated. This is computationally simple but not very flexible, giving rise to habit-like and automatically evoked behaviours (Dickinson and Balleine, 1994; Daw et al., 2011). In model-based learning, an agent learns value functions, but it also makes a model of the world, considering likely outcomes of actions given some knowledge about the structure of the environment (Daw et al., 2011; Doll et al., 2015). An additional step called *planning* involves the agent using its model of the world to generate additional "imaginary" data, from which it can also learn. Planning serves to predict consequences of the agent's actions and to evaluate value functions by simulating behavioural trajectories. This confers flexibility, as future implications of new information can be evaluated using the learned model and not by trial and error. Model-based RL is therefore more robust to changes in the task structure than model-free RL and is believed to support cognitive flexibility processes (Tolman, 1948; Daw and Dayan, 2014; Doll et al., 2015). It is computationally expensive and slow to use these simulations, so a habitual system would be preferred in familiar environment with well-practiced actions.

In humans, sequential decision-making tasks have been developed to allow studies of model-based and model-free learning across time. One of the most established tasks is the two-step task developed by Daw and colleagues (2011) (Fig.2.1A). Each trial begins with a choice between two options (*step 1*) that probabilistically leads to one of two possible states where a subject again

needs to make a choice between two options (*step 2).* Each of the two possible step 1 choices is associated with a higher/common (70%) or lower/rare (30%) probability of transitioning to one of the two possible step 2 states. Each of the four possible step 2 choices is associated with a different reward probability. To incentivize continued adaptive learning, the reward probabilities of step 2 choices are changed throughout the task, independently, and according to Gaussian random walks with reflecting boundaries at 25% and 75% reward probabilities.

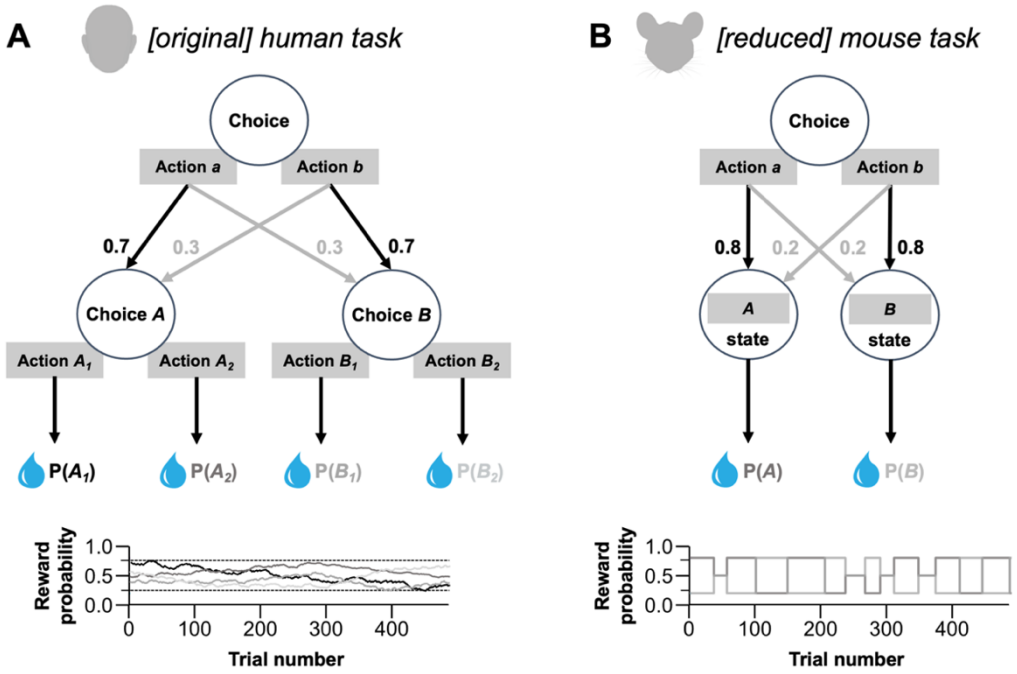


Fig.2.1 Human and mouse two-step task design. (A) In the human version, steps 1 and 2 require a choice between two options. The transitions between steps are either common (70% of trials) or rare (30%). Each step 2 action is associated with its own reward probability that changes according to Gaussian random walks between 25-75%, independent of other reward probabilities. **(B)** In the mouse version, only step 1 requires a choice. Step 2 has two possible states (A or B). The transitions between steps are either common (80%) or rare (20%). The reward probabilities of the two step 2 states, P(*A*) and P(*B*), are anti-correlated such that P(*B*)=1-P(*A*) where P(A) can be 80% or 20%.

This task allows for the differentiation between model-free and model-based behaviour based on step 1 choice behaviour which is a function of reward and transition history. A purely model-free subject is expected to repeat the same

step 1 choice if the previous trial was rewarded, regardless of whether the transition between steps was common or rare (Fig.2.2A). A model-free subject merely follows what previously happened, ignoring the transition structure underlying the task. A model-based subject is expected to include both their reward history and the task's transition structure, showing a reward X transition interaction identifiable as a decreased likelihood of repeating the same step 1 choice if it had led to a reward via a rare transition (Fig.2.2B). Real human behaviour measured in the two-step task is not purely model-free or purely model-based, it instead reflects contributions of each strategy (Fig.2.2C).

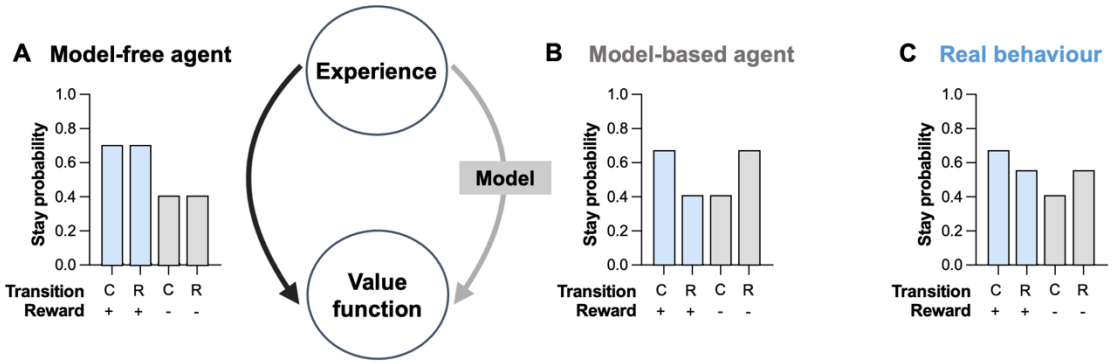


Fig.2.2 Model-free versus model-based behaviour in the two-step task. (A) A model-free agent associates experienced rewards directly to the value functions of choices such that all rewarded choices are reinforced, no matter the type of transition in the trial. **(B)** A model-based agent learns from experience but also from an internal model of the state of the world such that not all rewarded trials are reinforced, only those associated with common transitions. **(C)** Real behaviour of a human or animal is not a reflection of any one strategy alone, but a mix of both model-free and model-based learning.

Hypothetically, inducing more efficient model-based learning could be protective against forming persistent maladaptive habits and repetitive behaviours that dominate in neuropsychiatric disorders. The two-step task has been used to investigate potential differences in model-based versus model-free behaviour in psychiatric disorders (Sebold et al., 2014; Voon et al., 2015; Heller et al., 2018). A bias towards a model-free strategy was reported for a binge-eating

disorder, methamphetamine addiction, and OCD, where this bias was also associated with lower regional grey matter volume (Voon et al., 2015). In contrast, alcohol addiction was reported to impair model-based function, rather than increase the model-free strategy (Sebold et al., 2014). This effect was selective to trials with reward omission. Similarly, higher depression levels were associated with lower model-based function, but this effect emerged only under stress (Huys et al., 2015; Heller et al., 2018). Gillan et al. (2016) found that the deficits in model-based behaviour were most strongly associated with symptoms of OCD, eating disorders, and substance abuse – symptoms which they term "compulsive behaviour and intrusive thought" – but there was no association with symptom severity.

The two-step task has since been adapted for use in mice (Akam et al., 2015) (Fig.2.1B) where it has also been used as a test of cognitive flexibility (Korn et al., 2021). As in the original task, the subjects need to make a choice between two "step 1" actions that lead probabilistically to a "step 2" state in which reward could be obtained from one of the two reward ports. Each step 1 action commonly leads to one of step 2 states and rarely to the other. However, several modifications were required to simplify the task for mice. Step 2 has only one action available, instead of a choice between two actions. While the original task has stochastic transition and reward probabilities, the mouse task has a greater contrast between the common/rare transitions and reward probabilities. In the original, the timings of reward reversals involved random walks, but a block-based probability distribution is used for mice to promote task engagement.

When the same reversal problem is faced repeatedly, sophisticated automatization strategies may be developed which enable the animal to identify the relevant states of the world which have a fixed value. In the mouse two-step task, the animal does not need to relearn the reward structure each time a reversal happens, it only needs to learn that there are two states of the world (choose action X → more reward on port A or choose action Y → more reward on port B). Only one state can be true, and it can be inferred by observing where the rewards are obtained. Such agents have been previously termed as "latent-state" agents (Akam et al., 2015), as they use the location of an experienced reward as a cue for what latent state of the world is true, i.e., which step 2 state port, up or down, is "good" in the current task state. After a reversal occurs, the animal then only needs to infer the other state is now true and switch to that already learned fixed mapping strategy. This approach is essentially a stimulus-response habit with minimal cognitive demand of continued value learning.

Inference learning is not "wrong". In the case of the two-step task with repeating reward reversals, updating reward prediction errors after every reversal is the inefficient choice as previously encountered situations are continuously revisited. Using that prior experience makes inference-based behavioural flexibility a "smarter" choice as the subject just redeploys learned values from the previous encounters and updates the values associated with the step 2 up or down ports. However, to take advantage of this approach, the animal would need to accrue evidence for the regularity of the task structure which would only become apparent after experiencing many reversals in reward probabilities. This

strategy would then likely emerge after substantial experience with the task, which extensive training of animal subjects provides.

While detailed characterization of specific strategies animals use in this task is beyond the scope of our project, and our goal was not to make claims specific to model-free or model-based behaviour, there was one way we could modify the two-step task to break the predictability of the original task in order to test the more classical aspect of flexibility that looks at adaptation after the *first* reversal in choice-outcome mapping which has previously been shown to be more sensitive to drug effect due to its novelty (Boulougouris et al., 2008). Previous implementations of the mouse two-step task included repeated block-based reversals in both transition and reward probabilities (Akam et al., 2015; Korn et al., 2021). However, it proved harder to categorize animals' behavioural strategies in response to the serial transition reversal, so more recent versions switched to using a fixed transition probability structure (Blanco-Pozo et al., 2021). In our version of the task, we used a hybrid of these two approaches: we kept the block-based reward reversals, but the transition probabilities between the two steps were fixed during training, and we introduced a single reversal in the transition probabilities after drug treatment, making the previously common transition between step 1 choice and the available step 2 reward port switch to being rare and vice versa. We anticipated this novel transition reversal would disrupt the subjects from using any habit-like strategies as the long-run predictive relationship between rewards and step 1 actions was broken, requiring more reliance on the classical model-based strategy.

Learned reversals encourage automatized switching and planning for anticipated reward contingencies, and their underlying neural mechanism is different to situations when only one reversal is presented. By combining continued reward reversals with a single transition reversal in the two-step task, we were able to test both learned and novel cognitive flexibility.

2.4 Studying brain structure

Structural brain plasticity measures are limited to examining selected brain regions, either because of the technology (e.g., the limited field of views in multi-photon microscopy) or by the amount of labour required for whole-brain coverage (e.g., in immunohistochemistry). However, magnetic resonance imaging (MRI) is a tool that enables a rapid search of the whole brain to find regions undergoing structural plasticity changes. While the current "gold standard" for investigating neurobiological substrates in mouse models is histology, it has recently been complemented by *ex vivo* and *in vivo* MRI.

The MRI scanner applies an electromagnetic field to the tissue's hydrogen protons and measures the electromagnetic signals these atoms emit in response. The signals are localized by applying spatially varying magnetic gradients. The result is a three-dimensional signal pixel called the *voxel*. The intensity of a voxel's signal is its *contrast* which depends on how many hydrogen protons a voxel contains and on the local microenvironment of the tissue. Different contrasts, and thereby different tissue microenvironments, can be

detected by varying the timings of the magnetic field manipulations (pulse sequences).

Tissue contrasts depend on how the protons' magnetic properties, or its *spins,* change after electromagnetic pulses are applied. Two independent processes describe spin changes. T1 represent the time constant for a system of protons to return to equilibrium after electromagnetic application. T1 depends on water content, water binding, and concentration of macromolecules. The transverse T2 relaxation is a signal decay observed when spins are taken out of alignment with each other because of local tissue microenvironment variations. Gray matter has a longer T2 relaxation time than white matter so their contrasts would be different. Structural MRI uses "weighted imaging" – signal intensity is related to T1 and T2, but it is not a direct quantification of these properties. Such approach is more efficient and results in a greater signal to noise ratio (SNR). MRI is therefore an indirect measure of the cellular compartments our research questions are based on and is limited by the resolution of the technology. Therefore, a correct interpretation is confounded and requires caution when extrapolating to make neurobiological conclusions.

Studying neuroanatomy across voxels in an unbiased way, i.e., without the prior constraint of defined regions of interest, is the domain of voxel-based and deformation-based morphometry (VBM and DBM, respectively). In VBM, local amounts of tissue types (white matter, grey matter, or cerebrospinal fluid, CSF) are blurred with a Gaussian kernel and compared across subjects after linear or nonlinear alignment (Ashburner and Friston, 2000). In DBM, brains are nonlinearly deformed into a common space or a study template, a process called

registration. Because anatomical variability in inbred mouse strains is much lower than in humans, a study average is used over an atlas. The objective of registration is to find the deformation fields that match homologous points between images based on minimizing a cost function, that is the sum of all the deformations required. The deformation fields at each voxel can be analysed directly (Cao and Worsley, 1999) or measured by a scalar called the Jacobian determinant (JD) – these are then compared across brains (Chung et al., 2001). The JDs are a univariate measure of local volume changes so statistical significance of differences across brains can be assessed using a Student's *t*-test. Because the number of simultaneous *t*-tests across all voxels is in the range of thousands and millions, the risk of making false discoveries is unacceptable inflated such that no conclusions can be drawn before controlling for multiple testing with a false discovery rate (FDR) that controls for the expected proportion of falsely rejected hypotheses (Benjamini and Hochberg, 1995). In addition to a voxel-wise comparison, DBM can also be applied across multiple voxels in a region-wise manner to detect changes of regions of interest (ROI). The ROI volume change is equivalent to the average of the local voxel-wise volume changes taken across the entire ROI area (Chung et al., 2001). Reinforcing once again that MRI does not a provide a direct measure of anatomy, any VBM or DBM measurements will depend on the hardware and the sequences used.

Neuroanatomy within and across voxels is also studied by diffusion-weighted MRI (DWI) (O'Donnell and Westin, 2011). Diffusion MRI detects the local microenvironment via the restriction of random motion of water molecules that points to how the tissue is organized. The motion of diffusing water molecules

is modelled by an ellipsoidal shape termed *tensor.* Different shape metrics of the tensor, and therefore the variations in water diffusions, are then evaluated: fractional anisotropy (FA) is a measure of tensor's elongation, while diffusivity is a measure of tensor's radius along different axes. Estimates of greater specificity along multiple diffusion directions are enabled by multi-shell acquisitions using multiple strength and timings of magnetic gradients. A different type of sequence utilizes phase information that is typically discarded from sequences described previously that rely on the magnitude information. The method of quantitative susceptibility mapping (QSM) uses phase images to quantify mean magnetic susceptibility of the tissue in a voxel (Weiskopf et al., 2021). This is a more direct measure of tissue magnetism than relaxation times, and variations in the signal have been shown to depend on tissue iron, myelin, and cell membranes.

Various forms of brain plasticity have been studied with MRI in humans. Grey matter changes attributed to learning, memory, and training have been found in London taxi drivers (Maguire et al., 2000), juggling tasks (Draganski et al., 2004; Scholz et al., 2009), video games (Sagi et al., 2012), musical training (Hyde et al., 2009), and motor coordination tasks (Taubert et al., 2010). Many sophisticated imaging methods have also been implemented in mice, such as DWI (Xue et al., 2001; Kim et al., 2006) and fMRI (Beckmann et al., 2003; Nair and Duong, 2004; Guilfoyle and Hrabe, 2006). The successful application of these imaging sequences implies that clinical imaging can be translated and applied to the mouse. As in humans, learning in animals has also been found to cause changes in regional brain volumes (Lerch et al., 2011) and diffusion properties (Blumenfeld-Katzir et al., 2011), as quickly as in one day and lasting

for weeks (Scholz et al., 2015; as reviewed in Markham and Greenough, 2004). Lerch and colleagues (2011) have shown that training mice in the Morris water maze induced grey matter volume increases in specific brain regions rapidly and at a scale detectable by MRI (as low as 1.4% volume change).

In animal models, MRI assessments can be followed up by histology and immunohistochemistry to provide mechanistic explanations underlying MRI signal changes. Linking molecular mechanisms to MRI outcomes, besides neurogenesis and increased neuronal or glial size, grey matter volume changes have been found to correlate with synaptic markers (Golub et al., 2011; Lerch et al., 2011), dendritic spine counts (Keifer et al., 2015), and glutamate concentrations (Biedermann et al., 2012). These are all examples of plasticity changes found with psychedelics (section 1.6.a-b), so we can expect that they would be able to drive structural plasticity at the level of whole brain regions. More accurate estimates and direct measures of neural morphometry are still needed to establish a more accurate and robust mapping of volume measurements to tissue biophysical properties. Until then, our conclusions will always be confounded by unknown cellular mechanisms. For example, when age-dependent grey matter volume changes detected by VBM were correlated with cellular metrics from two-photon *in vivo* microscopy of mouse brains, physical alterations such as tissue expansion, volume of cell nuclei, and cell density explained only 35.6% of volume variance (Asan et al., 2021). Neuronal structural plasticity can therefore influence brain volume readouts beyond a solely volumetric mechanism. Others have shown that higher spine density explained 20% of VBM signal variance in the auditory cortex of mice trained in a fear

conditioning paradigm (Keifer et al., 2015). Certainly, stress-related loss of grey matter volume in mice has not been found to be related to neuronal nuclei volume, but instead to decreased synaptic spine density and cumulative dendritic length (Kassem et al., 2013). MRI outcomes further depend on ever-present artifacts and subtle differences between subjects, such as hydration status (Streitbürger et al., 2012) and time of day (Trefler et al., 2016).

Our approach involved an *ex vivo* imaging pipeline that included a DBM-based structural scan, DWI, and QSM. This combination allowed us to measure both grey and white matter plasticity. Compared to *in vivo* imaging*, ex vivo* imaging offered us enhanced sensitivity to subtler morphological alterations (Holmes et al., 2017), which were anticipated in our study of healthy individuals and single dose drug treatments. *Ex vivo* imaging enabled us to use longer scan times with limited motion and higher-concentration contrast, all factors boosting resolution, SNR and contrast-to-noise ratio (CNR) (Lerch et al., 2012). To extract the brain for *ex vivo* MRI studies, chemical fixation is needed to preserve the macromolecular structure and prevent tissue breakdown during long-term storage, analogous to brain tissue preparation for histology and immunohistochemistry. Transcardiac perfusion is preferred over immersion fixation as the vascular network delivers the fixative rapidly and evenly across the brain. MRI is especially useful when multiple regions could be affected across a wide area of the brain. While *in vivo* measures of cellular plasticity studies with psychedelics are limited to PFC and the somatosensory cortex (Ly et al., 2018; Cameron et al., 2021; Shao et al., 2021), there is no evidence yet for the localization of effects. Biased analysis of specific brain regions is therefore not

warranted, especially considering the only acute MRI studies done with psychedelics in rodents showed activation patterns across the whole brain (Malkova et al., 2014; Spain et al., 2015). A whole-brain coverage of our MRI analyses allowed us to identify any region that possibly changed its volume in a drug-dependent manner. That is the advantage of MRI over the other methodologies used to investigate cellular plasticity, such as immunohistochemistry, multi-photon microscopy, or electron microscopy, slice or *in vivo* electrophysiology – they are limited to examining specific brain regions. While a whole-brain analysis has reduced power, we maximized our discovery rate by using an exploratory discovery threshold to identify any possible regions affected by drug treatment, also reporting which regions survived the conservative discovery threshold.

Anatomical measures from fixed specimens are widely used in phenotyping studies (Chen et al., 2006; Spring et al., 2007; Lau et al., 2008; Lerch et al., 2008; Ellegood et al., 2010) and are validated against stereology (Lerch et al., 2008; Spring et al., 2010), where MRI had greater sensitivity at discriminating between groups than slice-based techniques. Therefore, there is sufficient verification from published research to show that our imaging pipeline was sensitive enough to detect drug-induced changes as similar methods have been used in earlier animal imaging studies with the potential for extension to clinical studies, including studies of drug effects (Chandran et al., 2012; Schobel et al., 2013; Wheeler et al., 2013; Wu et al., 2016) and 5-HT function (Preece et al., 2009; Spain et al., 2015).

3 | The behavioural level: Environmental sensitivity under DOI

In this chapter we report a behavioural signature of an acutely environmentally sensitive state induced by DOI. High-plasticity states are known to be associated with vulnerability to the internal and external environment in humans. Therefore, in this experiment, we tested whether the acute phase of DOI's action in mice would also exhibit environmental sensitivity, here measured as a putative difference between the behavioural responses to DOI in two environments defined by their contextual novelty or familiarity.

3.1 Introduction

As the window of plasticity hypothesis predicts, a state associated with increased sensitivity to the environment is induced by, or is a by-product of, a highly plastic psychedelic state (Carhart-Harris and Nutt, 2017). Therefore, we can consider an environmentally dependent intensity of acute drug response to be a behavioural proxy signature of a highly plastic psychedelic state.

We previously outlined what factors contribute to predicting the intensity of the acute response to psychedelics in humans (section 1.4.a). In addition to the drug dose, multiple non-pharmacological factors have contributing effects, such as personality, physical and emotional state, and the environmental setting (Studerus et al., 2012). Previous work on environmental factors of acute animal psychedelic responses mostly revolved around developmental stressors (Holloway et al., 2013) or strong physical stressors administered in the acute phase (Chaouloff et al., 1994; Yamada et al., 1995b; Peričić, 2003).

Instead of physical stressors, we chose to address familiarity as one of the main environmental factors emphasized in clinical settings, both historically (Hartogsohn, 2017) and in current-day psychedelic-assisted psychotherapy (Garcia-Romeu and Richards, 2018). Familiarity of the environment was one of Hyde's (1960) key extra-pharmacological dimensions, and, as we described earlier, a less familiar experimental setting was the strongest predictor of anxiety during intoxication in humans. Even recreational users reported a preference for a familiar context, consuming classic psychedelics more often at home and not in a party setting (Mason et al., 2020a).

In rats, effects of familiarity were reported for locomotor and investigatory responses after psychedelic injection, but not for acute behavioural responses such as the head-twitch response (HTR) and the ear-scratch response (ESR). In a novel arena, rat locomotion was suppressed by LSD (Geyer and Light, 1979; Adams and Geyer, 1982), but this effect was absent in a familiar arena (Adams and Geyer, 1985a, 1985b). This was interpreted as a potentiation of neophobia by the psychedelic, but these studies had no direct comparisons between familiar and novel environments, so it is unclear whether the lack of locomotor suppression in a familiar arena is due to a floor effect in already lower exploration due to habituation. In mice, the locomotor effects of psychedelics are very variable and likely strain-dependent (Darmani et al., 1996; Dhonnchadha et al., 2003; González-Maeso et al., 2007; Halberstadt et al., 2009). Most studies test the animals in a novel environment, like a novel recording box, following a drug injection that occurs in the novel box or the home cage, so some variability across

studies is likely explained by different environmental contexts, although this prediction has not been formally tested.

In this study, we investigated whether changing the familiarity of the external environment would modulate DOI's acute drug responses in mice – HTR and ESR. Specifically, we tested whether the shape of the dose-response relationships for HTR and ESR would be different across environments of different novelty. We also explored the more general effects of DOI on the degree and the manner of environmental exploration and whether these are modulated by the environmental novelty too. Following the window of plasticity model (section 1.4), if a particular drug dose was associated with a stronger induction of neuronal plasticity, it would also be associated with greater environmental sensitivity. DOI's effects on neuronal plasticity are dose-dependent, with higher concentrations of DOI resulting in greater branching effects in cultured neurons (Ly et al., 2018). Therefore, we hypothesized that moderate doses of DOI, which are more likely to induce a robust enhancement in neuronal plasticity, would be associated with a greater environmental sensitivity, i.e., greater differences in HTR and ESR across different environments.

3.2 Methods

3.2.a Animals

Care and testing of all animals were conducted under the Animal (Scientific Procedures) Act 1986, United Kingdom, and the Local Ethical Review Committee at the University of Oxford. Six-week-old wild-type JAX^{TM} C57BL/6J

(Charles River, Strain Code 632) male mice (*N*=68) were acclimatized for one week upon arrival, and ear punched for identification. The housing room was temperature- (21±2°C) and humidity-controlled (55±10%). All animals were observed daily for health and welfare.

Animals were under a 12h light/dark cycle with lights off at 7PM. Procedures were done between 8AM and 1PM. Food (Envigo Teklad 2916 standard diet) and water were provided *ad libitum* in the home cage, but no food or water was available during behavioural testing. All animals were housed in open-top cages (NKP Isotec, model M3, 48 X 15 X 13cm polyproplylene) with sawdust (Datesand Ltd eco-pure premium bedding) and enrichment (Datesand Ltd Sizzle Nest, a cardboard tunnel, and a cardboard house) in groups of four mice. All cage mates underwent identical procedures at the same time. No cage cleaning was done on injection days. Each animal received only one injection, making the study design between-subjects.

Four animals (2mg/kg DOI, familiar environment group) were excluded from analysis due to a camera failure during acute drug response recordings, making the final *N*=64 with n_{group}=8 for each of the four drug doses (0, 0.5, 1.0, and 2.0mg/kg) in each of the two treatment environments (familiar and novel).

3.2.b Video recordings of behaviour

The recording box was a 42 X 20 X 20cm clear Plexiglass box covered with a clear lid with air breathing holes. Revotech I706-POE cameras (approx. 20fps variable frame rate) were used for video recordings in a room with dim white light. For offline manual scoring of head twitches and ear scratches after

injection, a camera was mounted next to the cage for a side view. For offline automated scoring of locomotion and exploration, an overhead camera was mounted for a top-down view.

3.2.c Establishing contextual familiarity versus novelty

All animals were habituated to handling and daily weighing for a minimum of three days before the drug injection. All animals in one cage were randomly assigned as a group to one of the environmental contexts, *familiar* or *novel* (Fig.3.1). As all animals within a cage received the same type of drug injection in the same environmental context, the animal cages as a whole were randomly assigned to a particular environment and drug treatment group.

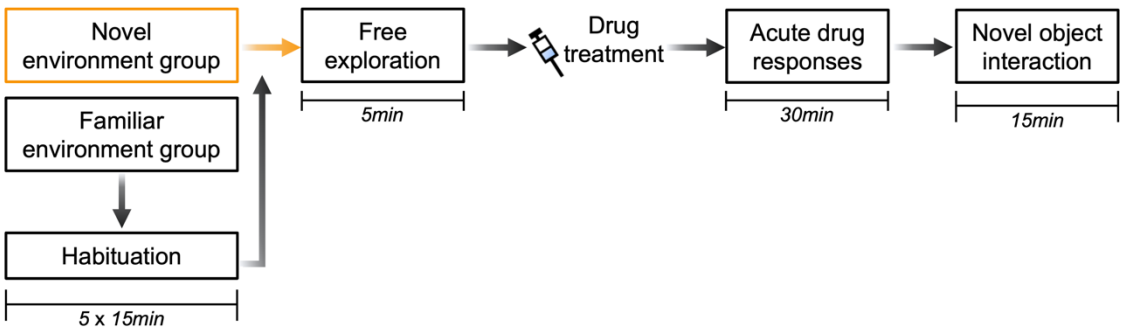


Fig.3.1 Experiment timeline for the study of the effect of novelty on the acute behavioural responses to DOI. A subset of animals was habituated to the recording box before drug treatment (*familiar environment group*), while *the novel environment group* was exposed to the recording box only on the day of treatment. Both groups had 5min of free exploration of the box before an injection of either vehicle saline or increasing doses of DOI (0.5, 1.0, or 2.0mg/kg). Animals were recorded for quantification of acute psychedelic and explorative responses in the first 30min after injection, and for a separate test of novel object interaction 30-45min after injection.

The familiar group was habituated to the recording box for five days of daily habituation sessions before injection to establish the *familiar context*. For the habituation sessions, the mice were transported to the testing room at least 30min before recording and were then allowed 15min of free exploration of the recording box containing clean wood shaving bedding and some nesting material

from their home cage. The habituation sessions were performed at the same time every day (between 8AM-12PM), the same time period that was used for the eventual drug treatment, and in the same recording box that was used for the drug treatment of that animal. Video recordings were taken for each habituation session for offline assessment of the degree of locomotion. In contrast, the novel group remained in their home cages and was not exposed to the recording box before the injection day to maintain a *novel context*. We note that there was a gap of 2-4 days between completing the habituation sessions and performing the drug treatment as we could not inject all animals on the same day, so there was a gap while some of the mice were undergoing drug treatment, but no additional habituation sessions were used on the other mice yet to injected to keep the amount of habituated consistent across animals.

On the testing day, prior to injection, the animals from both the familiar and novel group were allowed 5min of free exploration of the recording box to initiate a reaction to the environment before the drug was administrated. Mice were then taken out of the box and injected with the drug or the vehicle. Video recordings were taken for offline assessment of pre-drug locomotion.

3.2.d Drug treatment and behavioural observations

(±)-DOI hydrochloride (CAS Number 42203-78-1; Sigma-Aldrich, Product no. D101-10MG) was dissolved in 0.9% saline vehicle. Injections were administered with weight-adjusted volume (10mL/kg for 2.0mg/kg DOI; 5mL/kg for 0.5 and 1.0mg/kg DOI, and for saline). Serum levels tend to rise more slowly and peak at significantly lower concentrations after subcutaneous (SC) injection (Verma et al., 2010; Turner et al., 2011) so intraperitoneal (IP) administration was

preferred to complete the behavioural observations efficiently. When DOI is administered IP, the absorption is fast with maximal concentrations being reached within the first 30min (Jaster et al., 2022b).

HTR and ESR (Video 1) were quantified manually from the side recordings of the first 30min after injection with the Behavioral Observation Research Interactive Software (BORIS), freely available at https://www.boris.unito.it/ (Friard and Gamba, 2016). The experimenter was not blinded to dose nor treatment environment during injections, and while we aimed to ensure blinding for behavioural analysis, due to the recognizable frequency of HTR and ESR, the experimenter was effectively unblinded during analysis.

Two novel objects were placed in the recording box for the next 15min (30-45min after injection) to record the degree of novel object interaction. Both objects had a 5 X 5cm base and measured 3.4cm in their widest diameter and 8.6cm in height. Both were made of shiny metallic material and could be climbed on and jumped through as objects that can only be touched have shown a more rapid habituation (Heyser and Chemero, 2012) and we wanted to maintain exploration levels throughout the recording.

3.2.e Behavioural analysis using DeepLabCut

DeepLabCut v.2.1.6.4 toolbox (Mathis et al., 2018), freely available at https://github.com/DeepLabCut, was used for high-throughput video analysis of exploration as it is more reliable than common tracking software in environments with reflective walls and motion blur. 200 frames were extracted uniformly (20 frames/video) from five distinct recordings and manually labelled for body, object,

and recording box points (Fig.3.2A). The data were split randomly into a training set (95% of extracted frames) and a test set (5% of extracted frames). A ResNet was trained using the training set for 1,030,000 iterations. Evaluation of labelling accuracy was achieved by comparing the labels acquired from the ResNet on the test set. Once trained, this network was used to apply labels to all recorded videos, resulting in *x*- and *y*-coordinates corresponding to the position of each labelled body/object part within each frame, and a confidence score, which reports how probable the ResNet's prediction of a label's location is (Video 2).

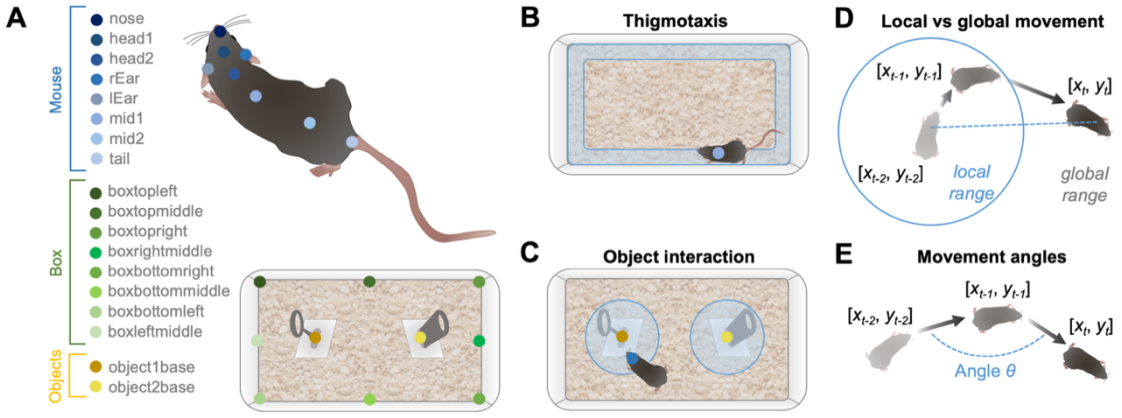


Fig.3.2 Animal movement analysis with DeepLabCut. (A) The parts of the animal and the recording box labelled for tracking. **(B)** An animal's tendency to stay near the box walls (thigmotaxis) was measured as the total time body point *mid1* was within 3cm away of the box walls. **(C)** Object interaction was counted as the times when the average of the animal's head coordinates (*nose, head1, head2, lEar, rEar*) was within the 3cm radius from any of the two objects' bases. **(D)** A movement sequence was defined by the coordinates of the body point *mid1* position at time *t* ($[x_t, y_t]$) and finding its prior position at *t-1* ($[x_{t-1}, y_{t-1}]$) and again at *t-2* ($[x_{t-2}, y_{t-2}]$). A sequence was termed "local" when $[x_t, y_t]$ was within a 9cm radius from $[x_{t-2}, y_{t-2}]$, or "global" if beyond the 9cm radius. **(E)** Turning angle (θ) for movement sequences was calculated as the angle between vectors drawn between $[x_t, y_t]$ and $[x_{t-1}, y_{t-1}]$, and between $[x_{t-1}, y_{t-1}]$ and $[x_{t-2}, y_{t-2}]$.

All further analyses were done with custom-written code in MATLAB version 9.12.0 (R2022a; The MathWorks Inc.). Time stamps for each frame were extracted from videos using the *videoframets* function v.0.1 (by David Bulkin) and the FFmpeg toolbox (freely available at http://ffmpeg.org/).

Distance travelled was calculated by finding the distance between the *x*- and *y*-coordinates of the front body midpoint (*mid1*, higher confidence scores overall than for the head coordinates) sampled every 1s (smaller resolution would be confounded by movement jitters).

Thigmotaxis (Fig.3.2B) was calculated by summing the times when the front body midpoint (*mid1*) was found within 3cm from the walls of the box. The range of 3cm was decided based on mouse body dimensions. 10-week-old C57BL/6J mice have an average body length of approximately 8.60cm (Chakraborty et al., 2017) and body width of approximately 2.5cm (Amende et al., 2005). Therefore, to measure thigmotaxis, requiring the animal's body to be adjacent to the walls of the box, 3cm allows for the presumed width of the mice used in our study. The assumption underlying the use of thigmotaxis as an index of anxiety is that rodents tend to avoid open spaces due to fear of aerial predators (Treit and Fundytus, 1988). Thigmotaxis does have some cross-species translational validity as humans exploring a virtual reality open field also preferred to stay near the walls, although the degree of thigmotaxis in virtual reality was not clearly correlated with anxious traits of participants (Gromer et al., 2021).

Object interaction time (Fig.3.2C) was calculated by summing the duration in which the averaged coordinates of all head points (*nose*, *head2*, *head1*) were found within a 3cm radius from the midpoint of either of the two objects' bases (*object1base*, *object2base*) and expressed as the percentage of time of the entire session. The 3cm radius was chosen to account only for the times when the animals head was directly adjacent to the object where we approximated the size of the mouse head as a third of the body length.

Additionally, we developed ways of quantifying the geometry of animals' movements to test their patterns of exploration – how the animal moves through space, considering the geometry of the paths it takes and coverage of the available territory. We isolated movement sequences by tracking the position of an animal (via the *mid1* point) at time *t* ([x_t, y_t]) back to its prior position at *t-1* ([x_{t-1}, y_{t-1}]) and *t-2* ([x_{t-2}, y_{t-2}]) based on a sampling frequency f_s. Multiple values for f_s were tested to check for ceiling and floor effects in the probability distributions to determine what sampling frequency fits the natural behaviour best, meaning that an animal had sufficient time to realistically complete the behaviour being measured. A 3s gap between positions was selected as that was the smallest time gap that resulted in an even probability distribution of events (Fig.3.3).

Whether the animal was travelling across space in long-range movements or staying in a restricted region was quantified by local vs global movement (Fig.3.2D). This was calculated as a ratio of the number of local and global movement sequences. Local sequences reflect the times an animal's final position in the sequence ([x_t, y_t]) was contained to a 9cm radius from its starting position ([x_{t-2}, y_{t-2}]), compared to global sequences when the animal has advanced beyond the local limit. The 9cm radius was chosen to consider the local range as within one body length of the animal.

To investigate the angular nature of an animal's path through space, movement angles (Fig.3.2E) were defined as the average angle θ between the two vectors connecting the movement sequences. For more straight-line movements through space, the average θ would be closer to 180° than if the animal was taking many turns on its paths.

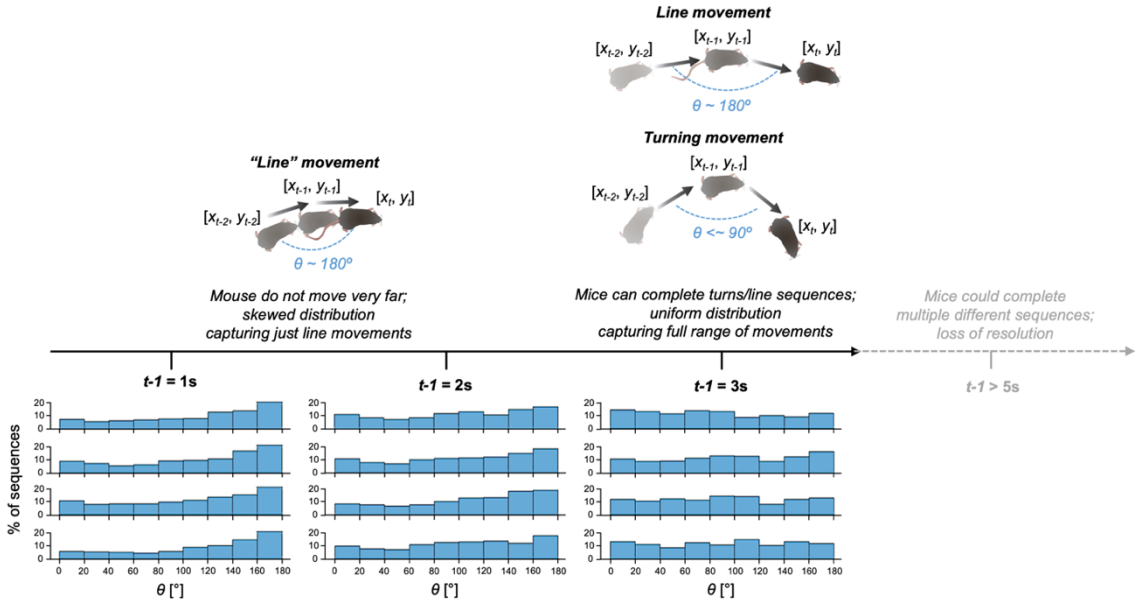


Fig.3.3 Probability distributions for the turning angles of movement sequences separated by increasing time-gaps. To determine what should be the time interval between frames that define a movement sequence, we looked at the probability distribution of observed angles with different sampling frequencies. Sampling the frames every 1s resulted in a strong ceiling effect with most values being close to 180° as there was not enough time for an animal to complete a turn, making most sequences appear as straight-line movements. With a time-gap of 2s, the animal could realistically complete a rapid turning sequence in that time frame, so we saw a much more varied spread of different types of movements, both straight line and turning, although there was still an apparent ceiling effect. Sampling frames every 3s, when an animal could realistically complete slower turning sequences, was the smallest sampling frequency that resulted in an even distribution of turning angles. Increasing the sampling frequency further risked a loss of resolution. Note that the direction of effects did not change when using the sampling frequencies between 2-4s. Separate graphs represent separate representative animals, including both saline- and DOI-treated mice.

An additional index of exploration, independent of the amount of locomotion, was roaming entropy (RE), a measure of how much an animal explored the full range of the recording box. RE has previously been calculated as Shannon entropy of the roaming distribution of an animal whose location was recorded by antennas in a RFID-based tracking system (Freund et al., 2013). Adapting this analysis to the data available from DeepLabCut, I first defined a 1cm X 1cm grid to which all *x-y* coordinates of an animal's position sampled every

1s were rounded to. Then we calculated a probability distribution *p* of the positions rounded to the grid. The roaming entropy of a mouse *i* was defined as:

$$RE = -\sum_{i=1}^{k}(p_i \times \log_{10} p_i) \div \log_{10} k$$

where *k* is the number of grid points in the box. RE values range from 0 to 1, where lower RE signals an animal had several spots of regular attendance, while higher RE signals that the animal had an evenly distributed coverage of the territory. An online simulation of RE by Freund and colleagues is freely available at http://brandmaier.de/roamingentropy/ (Freund et al., 2015).

3.2.f Statistics and reporting

HTR and ESR dose-response curves: Comparisons of the numbers of head twitches or ear scratches induced by different doses of DOI have previously been reported using a classic analysis of variance (ANOVA) (Darmani et al., 1990a, 1990c). However, such reports were only interested in whether a specific dose induces a response significantly higher than that of the vehicle-injected control animals. Therefore, the ANOVA factor of interest was the main effect of drug, and the relevant post-hoc comparisons were Dunnett's tests of difference between the vehicle group and each dose tested. In our study, the question of interest is not whether the drug was effective, but whether the effect of DOI depended on the treatment environment, i.e., the main effect of drug was not relevant here, but instead how the effect of drug differs across environments.

To examine the relationship between DOI and contextual novelty, we used a nonlinear regression analysis. We chose this over an ANOVA as an

ANOVA tests for a difference in means but does not consider any relationship between the data. It treats the different doses the same way it would treat different drugs. The fact that the different doses are sequential or numerical is ignored by ANOVA, e.g., that the 1mg/kg dose is higher than 0.5mg/kg dose, and that the distance between 2mg/kg dose data and the 1mg/kg data on the response curve is twice the distance between the 0.5mg/kg and 1mg/kg data. If we scrambled the order of the doses, we would get the same ANOVA result. An additional problem is that HTR and ESR are counts of discrete events which are not continuous and are left-censored at zero, while an ANOVA in general requires continuous data, or at least very large count numbers to avoid the censoring at zero. Therefore, we decided to use nonlinear regression instead to answer a focused question regarding the overall relationship between DOI and the treatment environment. Nonetheless, we also report the effects of the ANOVAs for transparency, complemented by Bayesian ANOVAs. All detailed statistical analysis is reported in the appendix (section 8) and any discrepancies are also discussed in the main text.

The presence of the drug effect was confirmed by the quadratic fit as an inverted U-shape model (Fig.3.4A; quadratic fit was the better fit compared to line regression for both HTR and ESR). If there was no effect of drug dose, the best fit would have been a horizontal line. For the effect of the treatment context, our null hypothesis was that one curve fits datasets from both the familiar and novel group. A second order polynomial equation

$$y = B_2 * x^2 + B_1 * x + B_0$$

was used, with B_2 constrained to be <0, as previously reported dose-response curves for psychedelic drugs describe an inverted U-shaped curve (Canal and Morgan, 2012). Considering our dependent variables were counts of events, a Poisson regression was used. The comparison of whether a global fit is adequate for all data was assessed by the likelihood ratio test at P<0.05. A P<0.05 in fit comparison signals that separate fits for each treatment environment were warranted, so this is used as a measure of a significant effect of treatment environment. We additionally used the Akaike Information Criterion corrected for small sample sizes (AICc) to report the relative probability of whether separate fits (alternative hypothesis, H_1) or the global fit (the null, H_0) model was more likely to have generated the data, to indicate the degree of evidence in our data for the effect of environment.

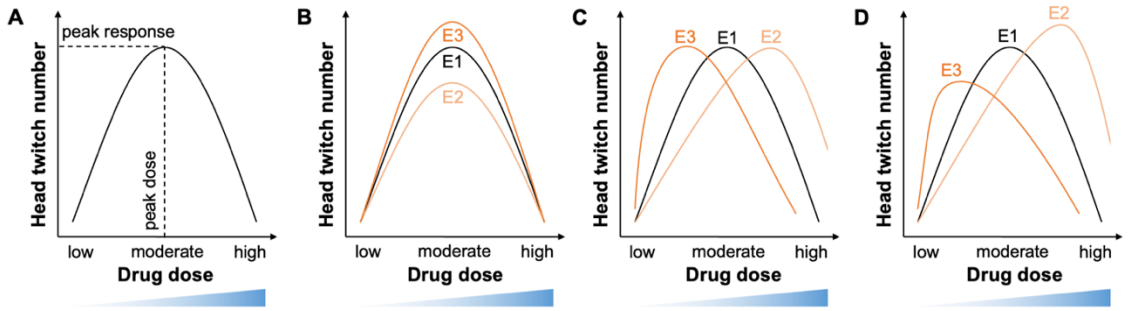


Fig.3.4 The inverted U-shape of psychedelic dose-response curve. (A) The ascending limb of the curve is the rising number of psychedelic responses with increasing drug dose, up until the peak response, which defines the turning point. The descending limb of the curve is the fall in psychedelic responses with further increases of drug dose. In different environments (E), the sensitivity to the psychedelic drug could change such that **(B)** peak psychedelic response decreases (E2) or increases (E3), **(C)** the dose at which peak psychedelic response occurs is higher (E2) or lower (E3), or **(D)** overall shape of the dose-response curve could change such that both the peak response and the dose at which occurs is different depending on the environmental context.

If separate fits were suggested, we followed up these results by Bonferroni corrected comparisons of best-fit regression weights for the linear (B_1)

and quadratic term (B_2). B_2 alone controls the curvature of the graph – the negative sign of B_2 reflects that a curve follows an *inverted* U-shape, and the greater absolute values ($|B_2|$) are associated with a more closed, sharply curved U-shape. B_2 and B_1 both control the turning point (the vertex) of the curve. The *x*-*y* coordinates of the vertex define at what dose of DOI is the highest HTR or ESR and what is the magnitude of that peak response (Fig.3.4A):

$$peak\ dose = -\frac{B_1}{2B_2}\ , \qquad peak\ response = -\frac{B_1^2}{4B_2} - B_0\ .$$

Therefore, for a negative B_2, the peak dose is positively correlated with B_1, and inversely correlated with $|B_2|$, and the peak response is positively correlated with squared B_1, and inversely correlated with $|B_2|$. The ways in which the coordinates of the turning point could affect the dose-response relationships is shown in Fig.3.4B-D.

Habituation: We used nonlinear regression analysis to test how locomotion changed over the five habituation sessions. We chose this approach over a repeated-measures ANOVA as the previously discussed limitation of using ANOVA for comparisons across drug doses also applies to comparisons made across several time points. If an ANOVA was used for the comparison of distance travelled across the five habituation sessions, the different time points would be treated the same as regardless of their order – this is not appropriate to answer the question of how the dependent variable changes continuously *over time*.

We calculated nonlinear line regression model fits using unweighted least squares regression, considering each replicate *y*-value as an individual point. Whether the animals exhibited lower locomotion as a result of habituation was

determined by checking if the best-fit slope was significantly different from zero (H_0 being that habituation did not affect the rates of exploration). An extra sum-of-squares *F* test is supplemented with the AICc ratio to indicate the degree of evidence for the effect. Distances travelled in the 5min before injection were compared across environments using an unpaired *t*-test supplemented by a Bayesian *t*-test (Rouder et al., 2009) with the Cauchy prior (scale of 0.707).

Exploration: To answer whether the dose-response relationships for the exploration measures differ between the novel and familiar treatment environments, we used nonlinear line regression model fits as there was no strong prior belief that the inverted U-shape curve would be expected like for HTR and ESR. A least squares regression fitting method was used with no weighting and considering each replicate as an individual point. The effect of drug dose was considered significant if the 95% confidence intervals (CIs) of the linear fit slopes were not overlapping with zero. The effect of environment was considered significant if separate fits were suggested by an extra sum-of-squares *F* test supplemented with the AICc ratio. In the case of separate fits, the post-hoc comparison of the best-fit slopes was reported.

Bayesian analysis: We used Bayesian analysis to assess the strength of evidence to which the data supports the effects reported. The implementation of Bayesian ANOVA was based on the *BayesFactor* package developed by Morey and Rouder (2015). The default uniform prior was used without enforcing the principle of marginality. To exclude random processes influencing the analyses and to ensure reproducibility of results, the seed was set to “123” (the choice of seed is arbitrary, as long as it is consistent and reported for replication purposes).

Analysis of effects is reported in the form of inclusion Bayes factors (BF_{incl}) which gives the odds ratio considering all models where the effect is included as H_1. All Bayes factors are reported as BF_{10} to show evidence for the two-sided H_1 relative to H_0. Evidence categories for Bayes factors are based on previously established guidelines (van Doorn et al., 2021). For the evidence in support of H_1, the range of 1-3 was considered “weak”, the 3-10 range was considered “moderate”, and any values greater than 10 were considered “strong”. Quantifying evidence in favour of H_0, the 0.33-1 range was considered “weak”, the 0.1-0.33 range was considered “moderate”, and values <0.1 were considered “strong”. The same evidence categories were used to interpret the AICc test. We remind the reader that these classifications are only used to facilitate communication. The advantage of the Bayes factor is that evidence can be assessed on a continuous scale.

The general approach: The experimenter was not blinded to group assignments during injections or during statistical analysis. All tests were two-sided with significance defined as $P<0.05$. Outliers were identified with the ROUT method (Motulsky and Brown, 2006) at FDR Q=1%. All 95% CIs are reported as “CI [lower limit, upper limit]”. CIs of all nonlinear regression fits were calculated as asymmetrical profile likelihood CIs. Normal distribution of the data was verified with a D'Agostino-Pearson (omnibus K2) normality test and the normality of residuals was assessed in Q-Q plots. For repeated-measures, if Mauchly’s test of sphericity was significant, Greenhouse-Geisser correction was applied. Data visualization and statistical analyses were done in Prism version 9.4.0 for Mac OS (GraphPad Software Inc.). Effect size calculation and Bayesian statistics were

done in JASP version 0.16.3 for MacOS Apple Silicon (JASP team). Details of all statistical analyses are reported in section 8.

3.3 Results

3.3.a Habituation established familiarity of the injection environment

To establish two different treatment environments, one group of animals was habituated to the recording box in five 15min-long daily sessions, while the second group of animals was not exposed to the recording box prior to the injection day. We first investigated whether our habituation protocol established familiarity with the recording boxes by looking for diminished locomotor exploration across habituation sessions.

Total distance covered across the full 15min sessions did not decrease significantly over time (Fig.3.5A, extra sum-of-squares $F_{1,158}$ =986.4, P=0.124, slope -0.84, CI [-1.91, 0.23]), although the AICc test (=1.18) suggested weak evidence. The post-hoc comparisons revealed a significantly lower locomotion only on the third habituation session compared to the first (Dunnett's P=0.005).

However, habituation sessions were 15min long and the initial recognition of environment likely occurs in the first few minutes (Leussis and Bolivar, 2006). We confirmed the presence of a within-session habituation by analysing the sessions in 5min time bins (Fig.3.5B) and detecting a significant moderate main effect of time ($F_{1.49,46.3}$=168.28, P<0.001, η_p^2=0.84, BF_{incl}>>100), and, importantly, a large interaction between habituation session and time (Time X Session $F_{5.65,175}$=9.28, P<0.001, η_p^2=0.23, BF_{inc}>>100). As predicted, in the first

5min, the initial explorative response to the environment decreased over the five habituation sessions (Fig.3.5B right, extra sum-of-squares $F_{1,158}$=14.95, P<0.001, AICc>>100), signalling that the animals were exploring it less in the later habituation sessions. The latter 10min of the habituation sessions did not exhibit a session-dependent change in locomotion (Fig.3.5B centre, extra sum-of-squares $F_{1,158}$=2.50, P=0.116, AICc=1.24; Fig.3.5B left, extra sum-of-squares $F_{1,158}$=1.95, P=0.164, AICc=0.94), likely due to the floor effect of the within-session habituation.

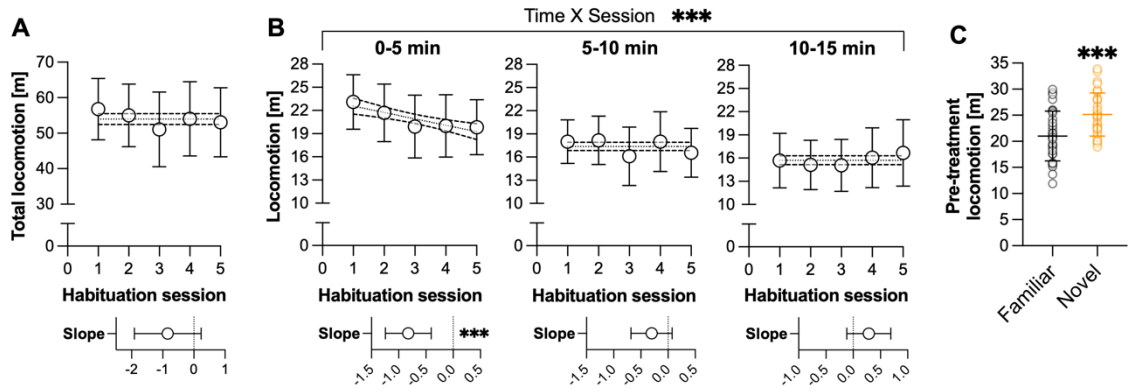


Fig.3.5 Habituation reduced the locomotor response to the recording box. (A) Total distance travelled in 15min recordings did not change across sessions (line fit slope test against zero P=0.124). **(B)** There is a significant degree of within-session habituation (Time X Session P<0.001). In the first 5min, the initial exploration response of animals significantly decreased across habituation sessions (P<0.001). In the latter parts of the sessions, within-session habituation had already led to a lowered locomotion which did not exhibit further decreases across different sessions (5-10min P=0.116; 10-15min P=0.164). **(C)** In the 5min free exploration time before the drug injections, habituated mice displayed a significantly lower (P<0.001) degree of locomotion compared to the mice being exposed to the recording box for the first time. Scatter plot represents individual subjects. Data shown as mean with SD error bars. Dotted line: mean model fit. Dashed lines: borders of the 95% confidence intervals for the model fit. Slopes shown as mean with 95% CI. n_{group}=32. ***P<0.001.

To confirm that the familiar group of mice was still able to recognize the familiarity of the recording box on the injection day, we looked at whether the animals' exploration levels were lower in the 5min of free exploration before injection compared to the non-habituated mice who were seeing the box for the

first time. Habituated mice travelled 4.1m (CI [1.9, 6.4]) less distance than the non-habituated mice (Fig.4C, unpaired *t*-test, t_{62}=3.706, *P*<0.001, Cohen's *d*=0.93, BF_{10}=60.54), confirming that the familiar and novel environment groups were responding to their surroundings differently prior to the injections.

3.3.b Acute psychedelic dose-response curves of DOI varied between the two treatment environments

To investigate whether the novelty of the treatment environment modulated acute psychedelic responses – head twitches and ear scratches – in the initial 30min after injection of increasing doses of DOI, we compared the dose-response curves in the familiar and novel environments.

Injections of DOI induced a dose-dependent increase in HTR and ESR, but these dose-response curves were modulated by environmental novelty at the time of injection. Fit comparisons for HTR suggested strong evidence (AICc=59.5) for separate fits for each treatment environment (Fig.3.6A, Poisson likelihood ratio =15.2, *P*=0.002). We judge this difference between dose-response fits to be subtle since neither the linear or quadratic terms were significantly different (*P*=0.516 and *P*=0.565, respectively).

We observed the same direction of environmental effects in ESR, but ESR effects were stronger. The evidence for separate curve fits across environments was extremely strong (Fig.3.6B, likelihood ratio =80.0, *P*<0.001, AICc>>100). While the linear terms were comparable across the two fits (*P*=0.646), the quadratic term was significantly less negative in the novel environment (*P*=0.002).

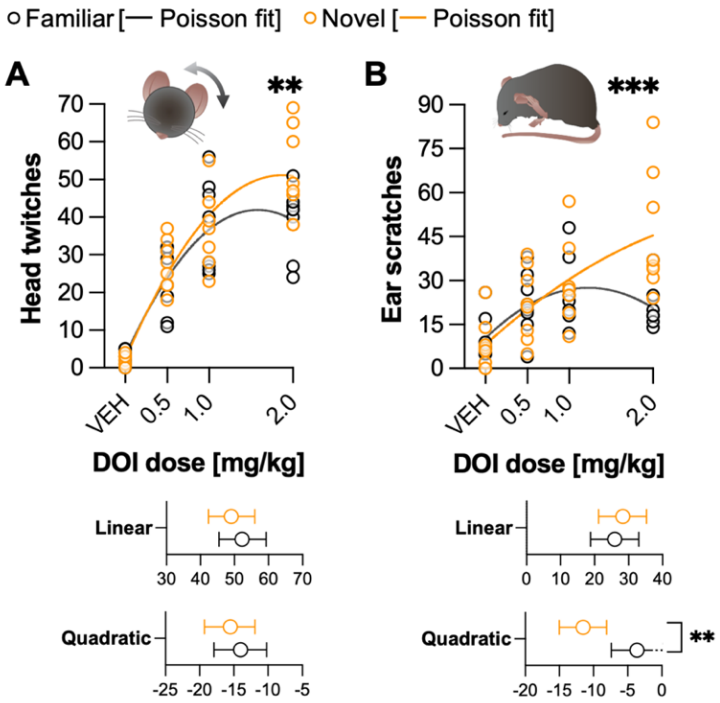


Fig.3.6 The degree of DOI's modulation of psychedelic responses was dependent on the treatment environment. (A) Dose-dependent increase in the number of head twitches followed the ascending limb of an inverted U-shaped curve. Poisson quadratic fit for the total head twitches suggested separate fits for each environment (P=0.002). Linear (P=0.516) and quadratic term (P=0.565) of the model were not significantly different. **(B)** Poisson quadratic fit for the total ear scratches suggested separate fits for each environment (P<0.001). The quadratic term (P=0.002), but not the linear term (P=0.646), in the novel environment was significantly higher than in the familiar, suggesting a later- and/or higher peaking model. Scatter plots represent individual subjects. Linear and quadratic terms shown as mean with 95% CI. n_{group}=8. N_{total}=64. **P<0.01. ***P<0.001.

A less negative quadratic term means that the curvature of the dose-response relationship was less sharp, more "open" or protracted. A less negative quadratic term also means that the absolute value of the quadratic term was lower in the novel than in the familiar environment, which would correlate with a right-shift in peak dose (where the turning point of the dose-response curve lies) and/or a greater peak ESR (Fig.3.4). The average peak dose (based on the regression model fit) was 1.2mg/kg in the familiar environment, while the mean predicted peak dose for ESR in the novel environment was 3.5mg/kg. This would indicate

that, past the 1.0mg/kg dose, the familiar curve goes into the descending limb, while the novel curve continues to rise, appearing to be still in the linear ascending limb phase. The peak ESR was also predicted to be higher (=54) in the novel environment, than in the familiar (=28 ear scratches).

For ESR, the classic ANOVA also suggested strong evidence for the interaction between drug dose and the type of environment ($F_{3,56}$=4.25, P=0.001, η_p^2=0.19, BF_{incl}=5.14). Post-hoc Bonferroni-corrected tests confirmed that the ESR of the familiar and novel environment group were significantly different past the 2.0mg/kg dose (P<0.001), in line with our prediction that the difference across environments would be more likely at higher doses of a psychedelic. For HTR, the effect of environmental context did not reach statistical significance (P=0.074), but exploratory Fisher's least square difference tests confirmed the same trend as in ESR data – the dose-response curves begin to diverge only at the higher 2mg/kg dose of DOI (P=0.006).

3.3.c Increasing doses of DOI reduced locomotion and exploration in both treatment environments

Exploration levels were continuously tracked during the first 30min after injection to monitor the effects of familiarity on any stimulatory or suppressive effects of DOI. All regression models, except for thigmotaxis, pointed to a single dose-response fit for both treatment environments (extra sum-of-squares P>0.05, for details see section 8), indicating that there was no overall effect of treatment environment on these exploration measures.

We looked at general locomotion by calculating the total distance travelled across the full 30min (Fig.3.7A). Locomotion decreased with increasing doses of DOI (negative slope -9.5, CI [-14.9, -4.1]). Dunnett's post-hoc comparisons showed a significantly lower locomotion only at the highest dose tested, 2.0mg/kg of DOI, compared to the vehicle control (P=0.001). To measure the animal's tendency to avoid open areas, the percentage of time the animals spent near the walls of the box is compared to the exploration time of the centre. Time spent near the walls was significantly different across treatment environments (Fig.3.7B, extra sum-of-squares $F_{2,59}$=3.63, P=0.033, AICc=2.67), such that the thigmotaxis in the novel group was significantly lower than that in the familiar group only at the 2.0mg/kg dose (Bonferroni P=0.013). The effect of DOI was not significant. While thigmotaxis appeared to increase with DOI in the familiar group (positive mean slope 0.21) and decrease in the novel group (negative mean slope -1.61), neither slope was significantly different from zero (familiar CI [-1.71, 2.13], novel CI [-3.95, 0.74]), so an induction of an anxiety-like thigmotaxis with DOI was not indicated.

We next examined how different doses of DOI influenced patterns of exploration. Mice treated with higher doses of DOI were more prone to (i) straight-line short-range movements, (ii) covering a smaller area, and (iii) avoiding novel objects, regardless of which environment they were injected in (Fig.3.7C-F).

The average turning angle (Fig.3.7C) increased with DOI (positive slope 4.6, CI [2.3, 6.9]). Post-hoc tests revealed that the drug effect was again linked only to the 2mg/kg dose (Dunnett's P<0.001). Despite taking less convoluted paths, DOI-treated mice were covering less territory, likely due to travelling

smaller distances overall. The range of movement was more local with DOI – the percentage of local sequences significantly increased with increasing doses of DOI (Fig.3.7D, positive slope 4.7, CI [1.6, 7.8]). Post-hoc tests revealed, once again, that the difference between the DOI-treated mice and the controls was only at the 2mg/kg dose (Dunnett's P=0.017).

A further way of characterising changes in animals' movements was roaming entropy (RE), a measure of probabilistic coverage of territory that is independent of the distance covered. RE decreased with increasing DOI doses (Fig.3.7E, slope -0.009, CI [-0.014, -0.004]). As with previous measures of exploration, the difference was apparent only at the 2mg/kg dose (Dunnett's P=0.011).

Finally, we examined if DOI affected how the animals responded to novel objects being introduced into their environment. To investigate whether DOI affected the animals' ability to interact with objects in their environment, we placed two novel objects in the recording boxes 30min after injection for a further 15min of recording to measure the time spent interacting with the novel objects. The percentage of time mice spent interacting with the novel objects showed a marginal decrease in presence of DOI (Fig.3.7F, slope -1.0, CI [-2.0, -0.1]). In an ANOVA, the drug effect ($F_{1,56}$=0.88, P=0.352, BF_{incl}=0.36) and the drug X environment interaction ($F_{3,56}$=2.50, P=0.069, BF_{incl}=1.22) were not found as statistically significant.

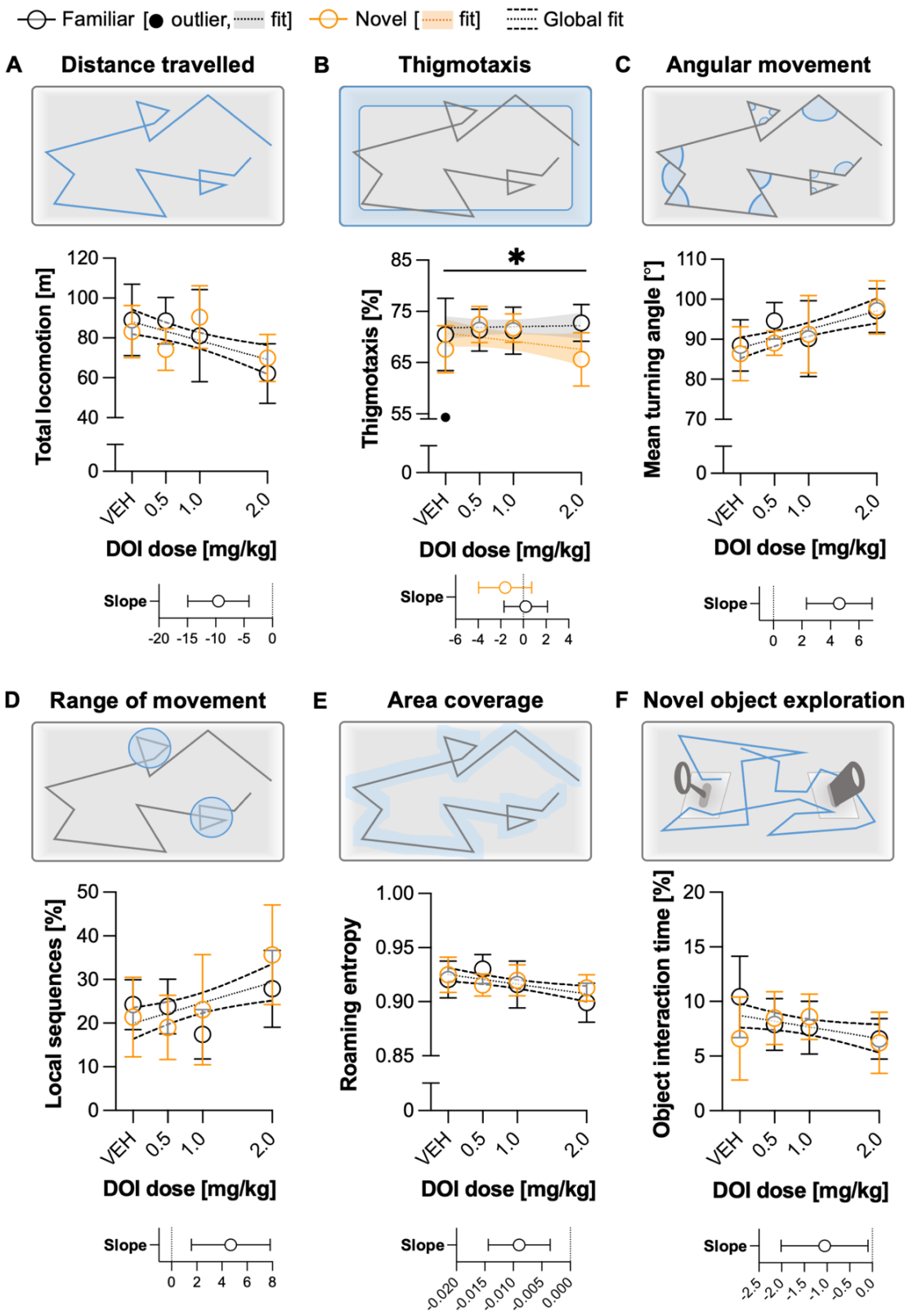


Fig.3.7 *legend on the next page*

Fig.3.7 The degree of DOI's modulation of locomotion and exploration was not dependent on the treatment environment. (A) Nonlinear regression least squares fits were not different across the treatment environments for the total distance travelled in 30min after injection (P=0.225), but the negative slope indicates that there was a reduction in locomotion with increasing doses of DOI. **(B)** Separate fits for thigmotaxis were warranted for each treatment environment separately (P=0.033), but while the line fits were moving in opposite directions depending on the environment (rising in the familiar, and falling in the novel), neither slope was significantly different from zero, signalling no marked change in thigmotaxis across drug doses. **(C)** The average turning angle of movement sequences was increasing with higher doses of DOI regardless of the treatment environment (P=0.438). **(D)** The proportion of local movement sequences was increasing with higher doses of DOI regardless of the treatment environment (P=0.108). **(E)** The roaming entropy exhibited a decrease over increasing doses of DOI but did not depend on the treatment environment (P=0.317). **(F)** The time spent interacting with novel objects marginally decreased over time, but was comparable across environments (P=0.265). Data shown as mean with SD error bars. Dotted line: mean model fit. Dashed lines or shaded areas: borders of the 95% confidence intervals for the model fit. Slopes shown as mean with 95% CI. n_{group}=8. N_{total}=64. *P<0.05.

3.4 Discussion

In this study, we examined the influence of environmental novelty on DOI-induced HTR and ESR, as well as locomotion and exploration changes. One group of animals was habituated to the test environment extensively prior to injecting them with the drug, whereas the environment was novel for the second group. We confirmed that animals habituated to the recording box recognized it as familiar before drug treatment (Fig.3.5C).

3.4.a The degree of novelty of the injection environment modulated DOI's dose-dependent effects on head-twitch and ear-scratch responses

Previous reports on DOI-induced HTR and ESR suggested inverted U-shaped dose-response curves (Fig.3.4) such that increasing doses of DOI increase the numbers of head twitches and ear scratches up to a point, after which the frequency of psychedelic responses declines (Arnt and Hyttel, 1989;

Darmani et al., 1990b; Schreiber et al., 1995; Canal et al., 2010; Fox et al., 2010; Canal and Morgan, 2012). The start of the descending limb of the inverted U-shape curve was reported to be at doses as high as 10mg/kg DOI or as low as 2.0mg/kg (Darmani et al., 1990b, 1990a; Schreiber et al., 1995; Yamada et al., 1995a; Miyata et al., 2004; Canal et al., 2010). The reasons for such variability were attributed to differences in species, strain, and age, but environmental factors are likely to also be involved.

We showed how novelty of the drug injection environment influenced the shapes of the dose-response curves (Fig.3.6). For ESR, the dose-response curve was more drawn-out in a more novel environment with a later and higher turning point. For HTR, the same direction of effects was observed, albeit to a lesser degree, as the difference in individual fit terms did not reach statistical significance. These effects cannot be interpreted to simply indicate greater or lower sensitivity to DOI in the more novel/familiar environment. A higher peak dose would suggest that a higher dose of DOI was required to induce a peak response, meaning that the animals were less sensitive to DOI, or, at least, to DOI's activation of 5-HT_{2A} or 5-HT_{2C} receptors whose activation is responsible for the increase in HTR and ESR, respectively (Darmani et al., 1990c; Canal and Morgan, 2012). However, a higher peak psychedelic response would suggest higher sensitivity to DOI, or, at least, to DOI's activation of 5-HT_{1B} or 5-HT_{2C} receptors whose activation is responsible for the decrease in ESR and HTR, respectively (Darmani et al., 1990c; Fantegrossi et al., 2010) and for which DOI exhibits lower affinity compared to the 5-HT_{2A} receptor (Table 1.1).

The difference in the effect sizes for HTR and ESR is likely due to the differential involvement of 5-HT_{2C} receptors in these responses – while 5-HT_{2C} activation inhibits head twitches, it potentiates ear scratches. If the effects of environment were mediated by increasing 5-HT_{2C} activation, we would observe an earlier and lower peak HTR, which we do not. If the effects of environment were mediated by decreasing 5-HT_{2C} activation, we would observe a later and higher peak HTR, but also a reduced ESR that is primarily potentiated by 5-HT_{2C} agonism – this is also not what our data showed. If the effects of environment were mediated by increasing 5-HT_{2A} activation, we would observe a later and a higher peak HTR and ESR, but with greater effect sizes in HTR, since ESR is only partially potentiated by 5-HT_{2A} agonism. Instead, we see the opposite pattern of effect sizes being greater for ESR, not HTR. We can, therefore, infer that the effects of environment were more likely partially mediated via 5-HT_{1B} receptors. Decreasing 5-HT_{1B} activation would reduce ESR inhibition, shifting the ESR response-curve turning point to be later and higher, but its effects on HTR would be minimal as 5-HT_{1B} agonism only partially modulates the frequency of head twitches. Nonetheless, DOI's affinity for other receptors which could modulate HTR and ESR cannot be discounted.

In humans, ingesting psilocybin in an experimental setting, like inside an MRI scanner, was associated with more anxious and unpleasant reactions to the psychedelic (Studerus et al., 2012). This is thought to be mainly because an experimental setting is less familiar and harder to relax in. An experimental setting in the novel environment group of mice used in our study was also less familiar – the recording box was not similar in dimensions or appearance to the home cage,

and it did not have any enrichment or social interaction available. These factors would be diminished by habituation in the familiar environment group. However, novelty in laboratory rodents can be more or less anxiogenic depending on the degree of novelty and the situation in which it is encountered which will affect the balance between curiosity-based approach and fear-based avoidance (Hughes, 2007). C57BL/6J mice are generally more likely to exhibit approach than avoidance in response to novelty (Oliverio et al., 1973; Kronenberger and Médioni, 1985; Peeler and Nowakowski, 1987; Griebeii et al., 1993), suggesting a smaller anxiogenic competing drives for approach versus avoidance. Novelty in our case could have just resulted in a more active and excitable state, i.e., an increase in arousal that was then associated with more intense peak psychedelic responses, as emotional excitability in humans was also a positive predictor of more intense effects of psilocybin on perception (Studerus et al., 2012).

3.4.b C57BL/6J mice did not display a neophobic reaction in presence of DOI

Our data suggest that the locomotor and exploration effects of DOI were not a function of novelty or any anxiogenic properties of the environment. Why environmental habituation affected the psychedelic-like behaviour but not locomotion and exploration could be explained by the different mechanisms which orchestrate these behaviours. DOI-induced hypoactivity has been found to be mediated by 5-HT_{2C} not 5-HT_{2A} receptors (Halberstadt et al., 2009). So, while both 5-HT_{2C} and 5-HT_{2A} are involved in both the psychedelic-like and activity effects of DOI, effects of 5-HT_{2C} receptor activity on locomotion do not seem to have been affected the environment. And, we have discussed in the previous section how the environmental differences in HTR and ESR are also unlikely to

have resulted from differential activity of either 5-HT_{2C} and 5-HT_{2A} receptors. In addition, while frontal cortical regions are believed to be the main orchestrator of psychedelic-like effects (section 1.3), while locomotion and initiation requires a brain-wide interaction between the brainstem, cerebellum, subcortical and cortical structures (Pernía-Andrade et al., 2021). Different behaviours are therefore orchestrated differently by the brain and would differ in the nature of environmental factors that are able to modify them with and without the presence of drugs.

The only measure of exploration that was different across environments was thigmotaxis (Fig.3.7B). Neither environment group showed a significant change in thigmotaxis across the different doses of DOI, but the novel group had significantly lower thigmotaxis compared to the familiar group at the 2mg/kg dose of DOI. While there is a statistically significant difference, there may not be a biologically relevant one – the differences compared to the vehicle-treated controls were not sufficient to suggest a neophobic or an anxiolytic effect in either environment, although a separate anxiety test (e.g., an elevated plus maze) would be needed to confirm this.

Our data do not suggest a strong neophobic response like the one observed in LSD-treated rats (Mittman and Geyer, 1991), which is not surprising considering the aforementioned observation of C57BL/6J mice being generally less likely to display defensive behaviours in response to novelty (Oliverio et al., 1973; Kronenberger and Médioni, 1985; Peeler and Nowakowski, 1987; Griebeii et al., 1993). Therefore, previous results that include increased avoidance of novel and central areas in rodents treated with psychedelics (Mittman and Geyer,

1991) may be a part of a species- and strain-specific behavioural response to the drug, rather than an anxiogenic effect of the drug itself. In fact, a recent report of 2mg/kg DOI's effects on anxiety in mice, using standard anxiety tests, such as the elevated mazes and the passive avoidance test, suggested an anxiolytic, rather than an anxiogenic, effect (Pędzich et al., 2022).

3.4.c Dose-dependent decrease in exploratory drive with DOI was not modulated by the novelty of the treatment environment

DOI, at doses ranging from 0.27mg/kg to 2.4mg/kg, induces a suppression of locomotor activity in rats that is limited to the first 30min after injection (Wing et al., 1990; Mittman and Geyer, 1991; Paulus and Geyer, 1993), an effect we observe in our mice injected with 2mg/kg DOI (Fig.3.7A). Locomotive suppression was also observed for other psychedelic derivatives of amphetamine, such as DOM, for other phenethylamines, such as mescaline, as well as for tryptamines, such as 5-methoxy-dimethyltryptamine (5-MeO-DMT) (Adams and Geyer, 1985a). The hypolocomotor effect of DOI was blocked by the administration of ritanserin, a 5-HT_2 antagonist, but not propranolol, a 5-HT_1 and β-adrenergic antagonist (Mittman and Geyer, 1991), suggesting that the ability of DOI to reduce locomotor exploration is mediated by 5-HT_2 family receptors.

We do note some discrepancies on DOI's locomotor effects in the literature. While we and others (Wing et al., 1990; Mittman and Geyer, 1991; Paulus and Geyer, 1993) report locomotion suppression at moderate doses of DOI, a previous study by Darmani et al. (1996) reported enhanced locomotor activity due to DOI, although these effects were present only up until 7 weeks of age, with no significant differences observed after. A separate study by

Halberstadt and colleagues (2009) described a delayed locomotion increase with 1.25mg/kg DOI in C57BL/6 mice, with the high 10mg/kg dose resulting in an immediate locomotion decrease. However, Halberstadt et al. injected their animals in the home cage and transferred them to the recording chamber for data collection 15min after, but hypolocomotor effects reported by us, and others (Mittman and Geyer, 1991), were limited to the first 30min after injection. The combined exposure to both novel and familiar environments during drug treatment and lack of data from the initial 15min post-drug complicate any direct comparison with our studies. A more recent report investigated the locomotor effects of 2mg/kg DOI in a circular corridor to which male C57s were thoroughly habituated (Pędzich et al., 2022). They found no significant locomotor changes, but the patterns of exploration available to the animals are much more constrained in the circular corridor than in an open field.

Locomotion alone is not a complete measure of exploration, as it does not assess the sequential and geometrical aspects of an animal's movement through space. To distinguish nonspecific motor activity and specific exploratory responses to the environment and environmental stimuli, we quantified additional aspects of animal movement, such as the angularity and range of movement sequences, probabilistic coverage of territory, and exploration of novel objects. We showed how DOI-treated mice had a dose-dependent (i) increased frequency of short-range, more straight-line paths, (Fig.3.7C-D) (ii) reduced area covered by their exploration (Fig.3.7E), and (iii) reduced novel object interaction times (Fig.3.7F). When others also attempted to quantify the microstructure of rodent behaviour following DOI, they found that rats treated with 0.27mg/kg DOI also

showed reduced locomotor activity with the animals more frequently taking long straight paths along the edges of a recording cage (Paulus and Geyer, 1993).

The reduced novel object interaction times with increasing doses of DOI could be a sign of a cognitive shift from external to internal processing with the animal's attention shifting from the environment and externally generated stimuli to its emotional and/or physical state and internally generated stimuli. However, an additional test may be required where we test the animals' ability to recognize the object they encountered during the acute psychedelic intoxication the next day, when the psychedelic effects have dissipated. If their object interaction times were indeed significantly lower, the mice would exhibit some deficits in recognizing the should-be-familiar object in the second session and would still spend a significant portion of time interacting with that object, and not a new object introduced only in the second testing session.

While not statistically significant, we note the apparent difference in object interaction across contexts in the vehicle data (Fig.3.7F). The control animals exposed to a familiar environment had slightly longer object interaction times, which was likely a result of habituation to the background context. Lowered object interaction in the novel environment was probably due to competition for attention with the environment – exploratory attention of these animals was split between the objects and the still relatively novel box, while animals in the familiar environment could direct a larger proportion of their attentional resources to the novel objects.

3.4.d Possible mechanisms

As we initially predicted, and as was reported previously by others (Wing et al., 1990; Nichols, 2016), behavioural responses to lower doses of DOI were not modulated by environmental novelty/habituation, so they were less sensitive to environmental influences. The peak of HTR and ESR dose-response curves were modulated by the environment, but the initial phase of the ascending limb of the curve, at doses around 0.5 and 1.0mg/kg appeared to be comparable for both treatment environments (Fig.3.6).

We originally hypothesized that the higher environmental sensitivity at higher doses of the drug could be due to higher psychedelic doses having an increased likelihood of inducing a sufficiently higher plasticity state that would be associated with higher environmental sensitivity. When given in a novel environment compared to the home cage, other psychoactive drugs, such as amphetamine (Badiani et al., 1998; Uslaner et al., 2001), cocaine (Uslaner et al., 2001; Ostrander et al., 2003), and morphine (Ferguson et al., 2004) induce significantly greater levels of *c-fos* expression in brain areas such as the caudate putamen, nucleus accumbens, and several cortical regions. These studies show that the neural circuitry engaged by such drugs could depend on the familiarity of the environmental context in which the drugs were administered. Inducing gene expression is one of the steps in most (though not all) synaptic plasticity processes, so environmental novelty could be affecting the ability of psychoactive drugs to initiate molecular and neuronal plasticity. In fact, cocaine-dependent increases in spinogenesis were also reported to be higher in a novel environment (Li et al., 2004). Hence, another likely scenario of how psychedelics exhibit

environmentally sensitive behaviours is that different environments would prime different neural circuitry for enhanced plasticity.

Being in a state of high plasticity here reflects the ability to affect brain structure and function easily, and higher psychedelic doses would be expected to activate a much wider set of serotonergic, and other, receptor systems, as there is more drug available to activate even the receptors for which DOI normally exhibits lower affinity and that lower doses of DOI would not activate to a significant degree. The pattern of acute receptor activation would then further be affected by the receptors regulating each other in turn (Darmani et al., 1990c, 1990b). The environment could therefore modulate the acute psychedelic experience by determining the pattern of acute brain activation, conferring the ability to have set- and setting-dependent priming of specific neural circuits for long-term effects of psychedelics, including neuroplasticity changes.

Thinking about how specific circuits can be primed by the environmental setting, the putative mechanisms may not be region-specific. The exact brain regions which modulate DOI-induced psychedelic responses are still unknown. While the frontal cortical pyramidal neurons are believed to be the main orchestrator of HTR (Canal and Morgan, 2012), lesioning of serotonergic projections in the hippocampus (Lombardi et al., 1987) and from the nucleus raphe obscurus (Wieland et al., 1990) suggest involvement of other brain systems too. Therefore, environmental sensitivity may not be dependent only on the frontal cortex.

Exposure to a novel environment can influence the secretions of the brain's neurotransmitter system, including dopamine (Handa et al., 1993; Berridge et al., 1999; Horvitz, 2000) and 5-HT. In rats, novel environmental conditions increased endogenous 5-HT levels across the brain, increased 5-HT turnover, and decreased the input resistance of dorsal raphe serotonergic neurons' plasma membranes (Laaris et al., 1999; Miura et al., 2002). Changes in the 5-HT signalling system that are due to novelty alone would affect how susceptible the brain is to 5-HT receptor activation by DOI and its downstream signalling.

In a novel environment, animals' endocrine secretions of acetylcholine and corticosterone can also be increased (Muir and Pfister, 1987; Handa et al., 1993; Laaris et al., 1999). Acetylcholine and 5-HT have opposing roles on the modulation of layer 6 pyramidal neurons, which are involved in the psychedelics' glutamate-dependent change in excitatory signalling in the prefrontal cortex (Sparks et al., 2018). While elevated corticosterone can have direct effects on 5-HT receptor sensitivity (Laaris et al., 1999), its secretion is linked with stress responsivity, making it likely that environmental challenge of novelty can also impact drug pharmacokinetics. Psychophysiological stress can modify the function of hepatic drug-metabolizing enzymes of the cytochrome P450s (CYP) family (Konstandi, 2013). Additionally, stress can alter binding of drugs to plasma and tissue proteins, via an increase of free fatty acids due to corticosterone-induced fat mobilisation, as well as blood flow rate and vascular function, which can in turn alter drug distribution and pharmacokinetics (Antonia et al., 2012). One way to check if these parameters were different across the familiar and novel

environment would be to study the concentration of DOI in systemic blood and brain samples taken from a separate cohort of mice sacrificed at different time-points after administration of 2mg/kg DOI (the dose at which the difference between dose-response curves was the greatest).

An interesting recent hypothesis on the psychosomatic mechanisms of action of psychedelics posits that psychedelic drugs may affect gut microbes that promote production of 5-HT that can cross the blood-brain barrier (BBB) to reach the brain in as little as 10min (Császár-Nagy et al., 2022). The authors suggest that increased plasma 5-HT can cross the BBB: (i) by temporarily increasing BBB permeability by modulating the function of microvascular endothelial cells, (ii) via BBB's serotonin transporters, and/or (iii) with the help of platelet-derived extracellular vesicles (Császár-Nagy et al., 2022). Therefore, gut-derived 5-HT production could act as a hormone-like regulatory signal influencing blood-brain barrier permeability and, via volume transmission, potentially even modulate excitatory and inhibitory neurotransmission in the central nervous system.

While we discussed how novelty can affect endogenous levels of 5-HT and dopamine, could there also be environmentally dependent differences in the pattern of 5-HT receptor activation? Some functional changes that should be considered are changes in agonist affinity and in modulatory actions on other neuronal systems, like the noradrenergic system or other 5-HT receptors. 5-HT receptor trafficking, including both internalization and addressing to the membrane, can occur within minutes of activation by 5-HT or a 5-HT agonist (Berry et al., 1996; Bhattacharyya et al., 2002). But functional changes in the 5-HT receptors could also be present without any change in their numbers. For

example, in rats, a 5-HT_2 agonist mianserin blocks discrimination of quipazine, a 5-HT reuptake inhibitor and a 5-HT_{2A} and 5-HT_3 receptor agonist, for over 48h (Smith et al., 1990). Changes in both receptor density and receptor sensitivity were candidate mechanisms of mianserin's prolonged activity. Available 5-HT_2 receptor sites, as measured by [3H]-ketanserin binding, while initially downregulated, recovered sooner than behaviour. However, the recovery of 5-HT_2 receptor sensitivity, measured as a degree of 5-HT-mediated phosphoinositide hydrolysis, overlapped more closely with recovery of the discrimination behaviour (Smith et al., 1990). Therefore, the effects of psychedelics may depend on the receptor sensitivity states which may in turn be modulated by a variety of internal and external (set and setting) factors. Additional changes in physiological parameters and arousal, in the sense of responsiveness and response effectiveness to a stimulus, are likely to contribute as they would involve changes in activity of all the neuromodulatory systems. Furthermore, note that our experimental design does not allow us to distinguish between effects due to novelty versus habituation.

4 | The cognitive level: Flexibility in the weeks after DOI

In this chapter we report a behavioural signature of post-acute enhancement of cognitive flexibility with DOI. A high-plasticity state should facilitate faster adaptation and better strategies at the cognitive level. Therefore, in these studies we tested whether DOI's induction of plasticity would, in the long-term, result in changes in adaptability, here measured as the speed of learning following changes in the rules of a decision-making task.

4.1 Introduction

Therapeutic benefits of psychedelics have been reported across a wide spectrum of mental disorders. A common denominator is that many of those disorders are characterized by rigid cognitive and behavioural patterns and compulsive traits. These include ruminations and negative cognition in anxiety and depression (Hsu et al., 2015), attentional switching difficulties in PTSD (Newman, 1998), and compulsive rituals in eating disorders (Tchanturia et al., 2011) or in addiction and obsessive-compulsive disorder (Figee et al., 2016). In all these cases, the persistence of a maladaptive response is combined with a restricted search for a novel response strategy, implying impairments of cognitive and behavioural flexibility. Greater cognitive flexibility has been associated with higher resilience to negative life events and stress (Genet and Siemer, 2011), and so it is not unlikely that increasing cognitive flexibility has a protective and/or remedying effect on maladaptive stress responses.

LSD and psilocybin have been implicated in improving cognitive flexibility in both rats and primates. Both LSD and psilocybin improved monkeys'

performance on the delayed visual discrimination task up to 96h after injection (Roberts and Bradley, 1967). In rats, LSD caused improved learning on brightness discrimination reversal, for as long as 90min after injection (King et al., 1974). Contrastingly, in mice, 5-HT_{2A} agonist 25CN-NBOH was not found to improve performance in a touchscreen-based reversal learning test (Odland et al., 2021), but performance was only assessed acutely and with serial reversals. Studies on psychedelic effects on cognition have so far been largely limited to simple memory or impulsivity tasks in the acute or immediate sub-acute drug phase only (Njung'e and Handley, 1991; Matsushima et al., 2009; Egashira et al., 2012; Rambousek et al., 2014).

The window of plasticity hypothesis posits that the key effect of psychedelics on brain 5-HT transmission is the engagement of plasticity processes that facilitate change when change is necessary (Carhart-Harris and Nutt, 2017), which is the goal of flexibility processes. The integrated model of plasticity further suggests that enhanced neuronal plasticity, characterized by increased growth of new dendrites and spines, should create a rich synaptic landscape that can facilitate learning and memory in the long-term. However, there have been no preclinical studies on whether learning and memory changes can be observed in the weeks after psychedelic drug action, when neuronal plasticity begins to normalize back to the baseline levels, but persistent behavioural effects are still observed.

Using a multi-step decision making task called the two-step task (see section 2.3) we monitored reversal learning changes in the first three weeks following a single DOI treatment. We hypothesized that DOI might lead to long-

term improved flexibility in this task by influencing the speed of relearning following a change in rules.

4.2 Methods

4.2.a Animals

Care and testing of all animals were conducted under the Animal (Scientific Procedures) Act 1986, United Kingdom, and the Local Ethical Review Committee at the University of Oxford. Five-week-old wild-type JAX^{TM} C57BL/6J (Charles River, Strain Code 632) male mice (N=56) acclimatized for one week upon arrival before ear punching for identification and starting experimental procedures. The housing and care were outlined in section 3.2.a. Animals were housed in groups of three or four with all cage mates undergoing behavioural tasks and drug injections at the same times. All mice were habituated to handling and daily weighing for a minimum of two days before experiments began. All procedures were done during the light phase.

One animal was excluded from analysis as it did not pass the learning criterion for the penultimate training stage (section 4.2.c, see training stage 4.6), making the final N=55 with n_{group}=13-15 across two separate experimental groups (section 4.2.c, see Group 1 vs. 2).

4.2.b Water restriction

At 6-weeks-old, animals were weighed for two consecutive days before starting water restriction. These bodyweights were averaged to give a pre-restriction baseline bodyweight for each animal that was age-corrected by 2% every week until 14-weeks-old, after which animal bodyweights plateau so a 1%

correction was used (https://www.jax.org/jax-mice-and-services/strain-data-sheet-pages/body-weight-chart-000664#). One day after starting water restriction, the animals were given 1h of unrestricted water access in their home cage, and behavioural training commenced the next day. During all training and testing sessions, the animals were weighed before and after the task, and their bodyweight calculated as a percentage of the pre-restriction age-corrected baseline. If the animal's bodyweight dropped below 85%, they had free water access in their home cage with food available until the bodyweight percentage was above 85%.

During the 90min-long daily two-step task testing sessions, the animals would on average get 0.88mL (CI [0.87, 0.90]) of water when fully trained. All animals had a food pellet available in the operant box during behavioural training and testing. This helped the animals maintain their bodyweight by reducing the likelihood of dehydration-related anorexia and hemodilution (Toth and Gardiner, 2000). Animals were given 1h of free water access in their home cage once a week. Under this protocol, pre-test bodyweight typically dropped to 89.8% (CI [89.5, 90.1]) of pre-restriction levels in the first week of training and was then maintained at 91.8% (CI [91.4, 92.3]) when fully trained. Post-test, after the animals received their daily water, bodyweight typically increased to 95.5% (CI [95.0, 95.9]).

4.2.c Two-step decision-making task

Setup: Custom-built 12 X 12cm operant boxes controlled using pyControl (freely available at https://github.com/pyControl) were used to run the two-step task (Akam et al., 2022). Five nose poke ports were located on one of the operant

box walls. A central port was flanked by two choice ports 4.0cm to the left and right, and by two second-step state ports 1.6cm above and below the central poke. The two second-step ports had a solenoid for delivering water rewards. A speaker located above the ports delivered auditory stimuli. An active port, i.e., the port that a mouse could interact with by nose pokes, was indicated by illuminating those ports. To ensure mice knew when they had made a nose poke on the active port, a click sound was presented whenever the mice poked the illuminated port. No click sound was presented if a mouse was poking inactive ports.

Task design: The original human two-step task (Daw et al., 2011) was adapted for use in mice (Akam et al., 2015; Korn et al., 2021) (Fig.2.1). We used the version of the mouse task with serial reward reversals only, described by Blanco-Pozo et al. (2021) (Fig.4.1A). Each trial started with the central port lighting up. By poking the central port, the mouse initiated either a free-choice trial, or a forced-choice trial.

In free-choice trials, both left- and right-side choice ports lit up in *step 1* and the mouse had to choose between the two. Poking one of the choice ports triggered a 200ms delay followed by a transition to the up or down port lighting up (*step 2*). A 1s-long auditory cue signalled the location of the step 2 transition (5 or 12kHz for up/down states, counterbalanced assignment across animals). Poking the illuminated step 2 port triggered another 200ms delay, after which a 500ms cue signalled if the water reward would be delivered at that port at cue offset. The same 5kHz or 12kHz tone that signalled the step 2 transition pulsed at 10Hz for rewarded trials, or a white noise cue would signal omissions. Once the

animal's nose was out of the step 2 port for at least 250ms, a variable 2-4s inter-trial interval would precede the next trial.

In forced-choice trials, only one (either right or left) randomly selected choice port lit up during *step 1* and the mouse had to poke that active side, it could not choose its step 1 action. Forced-choice trials comprised a maximum of 25% of trials of any given session and were used to ensure that the animals continued to try out both step 1 choice states. Poking the illuminated step 1 port triggered a 200ms delay followed by a transition to step 2, following the same rules of transitions and reward delivery as for the free-choice trials.

Task structure and types of reversals: The (i) transitions between step 1 and step 2, and (ii) the reward deliveries followed a probabilistic schedule (Fig.4.1B). Each step 1 choice port was associated with a *common transition* (occurring in 80% of trials) to one step 2 state port and a *rare transition* (occurring in 20% of trials) to the other step 2 state port. The two possible types of common transitions were: (1) left→up & right→down (Type A), and (2) left→down & right→up (Type B). The transition structure remained fixed within and across sessions, its type (A or B) counterbalanced across animals. Transition probabilities remained fixed throughout testing, apart from one single reversal implemented by the experimenter (*transition reversal*, i.e., mice performing Type A transitions were switched to Type B, and vice versa, see Fig.4.1B), either one day or one week after drug injections (Fig.4.2).

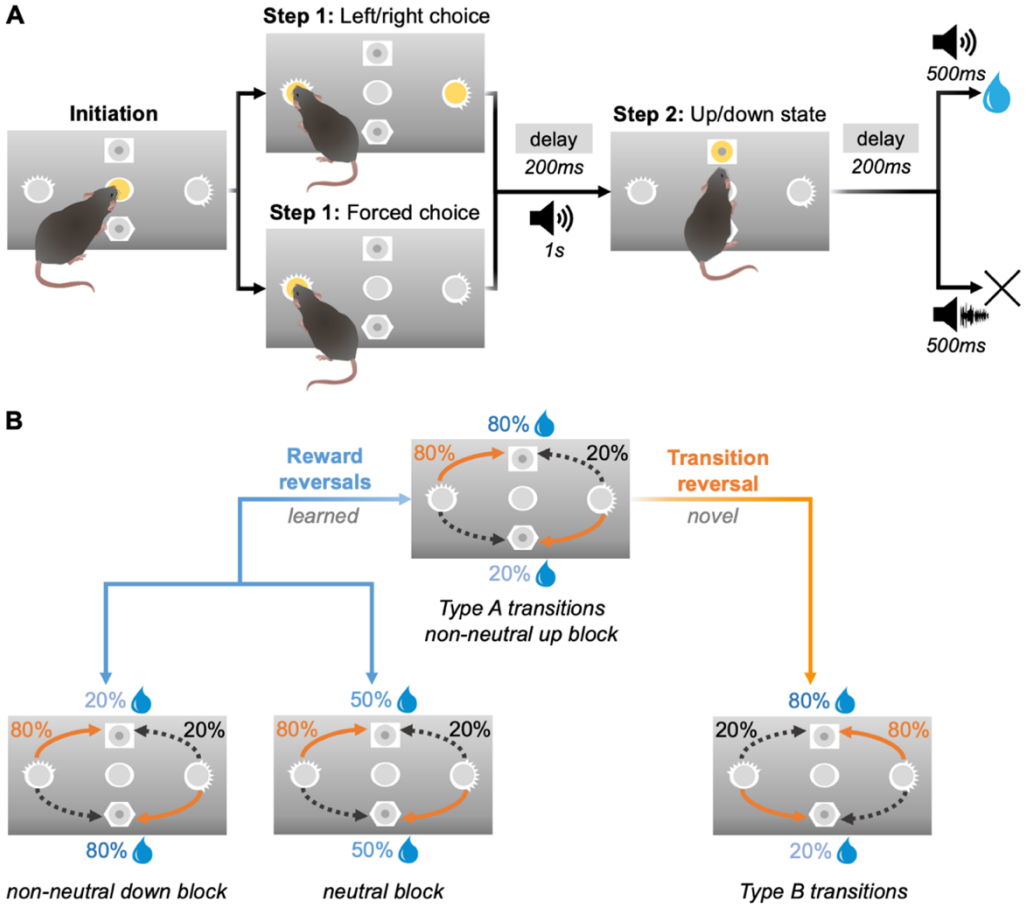


Fig.4.1 Two-step task design. (A) Trial events. Initiation: central port lit up for the mouse to poke. Step 1: either both side ports lit up for the animals to choose which one they poke (a free choice) or only one of the side ports lit up to force the animal to explore that choice (max. 25% of trials per session). Step 2: only one of the water delivery ports lit up for the animal to poke. A tone or white noise cue would signal water reward delivery or omission, respectively. **(B)** The probabilistic structure and the types of reversals. The three possible states of reward probabilities for the up/down ports were: 80/20 or 20/80 for non-neutral blocks, or 50/50 for a neutral block. Reward block reversals were triggered based on a behaviour criterion for non-neutral blocks or after a random interval between 20-30 trials for the neutral block. As animals were trained on reward reversals and learned to perform multiple reward reversals within each session, these were considered "learned" adaptations. The two possible states of left→up & right→down (Type A) transition probabilities were: 80/20 or 20/80 (where the common structure was Type B, left→down & right→up). Transition structure (counterbalanced across animals) remained fixed during training and initial testing so the single experimenter-directed reversal in the transition structure was considered a "novel" adaptation.

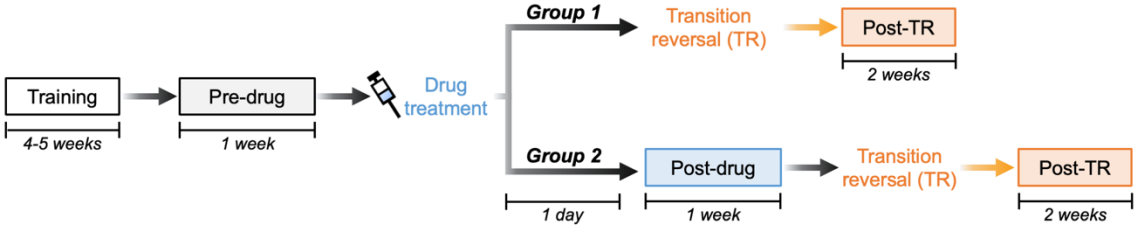


Fig.4.2 Experimental timeline. Group 1 animals were treated with either saline vehicle or 2mg/kg DOI when fully trained on the two-step task and given a single transition reversal (TR) the next day. **Group 2** animals were treated with either saline vehicle or 2mg/kg DOI when fully trained on the two-step task and given a single TR after one week.

Reward probabilities for the two second-step ports were anticorrelated and changed in blocks (*reward reversals*) (Fig.4.1B). Subjects started each daily session in the same reward block that the previous session finished on. Reward blocks could be non-neutral or neutral. In non-neutral blocks, one step 2 port (either the up in an *up block* or a down in a *down block*) had 80% reward probability and the other 20%. In neutral blocks, both the up and down step 2 state ports were being rewarded with 50% probability. Reward reversals from non-neutral blocks were based on animal's performance – after the exponential moving average of correct choices (time constant =8 free-choice trials) crossed a threshold of 75%, a reversal was triggered following a random delay of 5-15 trials. Reward reversals from neutral blocks did not depend on animal's performance and were triggered after a random interval between 20-30 trials from the start of the neutral block.

Training: Animals were put on water restriction 48h before the first training session as described in section 4.2.b. Training consisted of multiple stages with increasing complexity to build the sequence of multiple steps required by the task (Table 4.1). Training and testing would occur as one session per day,

for 6 days/week. The initial training sessions lasted 60min, and then 90min-long sessions were used for all following testing. Water reward size in the task started at 15µl and was decreased to 4µl across training to increase the number of trials and reward blocks that the animals were doing. Animals required 14-26 sessions to reach the final stage of training (the times taken for separate stages are indicated in Table 4.1).

Table 4.1 Two-step task training stages. Grey-shaded areas indicate when task conditions changed. U: up. D: down. L: left. R: right. C: centre.

Stage	Learning outcome	Available Pokes	Transition Probability *-Common-*	Transition Probability *-Rare-*	Reward Probability *-Common-*	Reward Probability *-Rare-*	Reward Probability *-Neutral-*	% Free Choice	Reward Volume [µL]	Learning criterion	Sessions to criterion (min – max)	Change from previous stage
1.1	U/D pokes deliver reward	UD	NA	NA	NA	NA	1	0%	15	>50 trials	1	
1.2		UD	NA	NA	NA	NA	1	0%	12	>70 trials	1 - 2	auditory cue (different frequency for up and down) before reward is delivered
2	L/R → U/D sequence	UDLR	0.8	0.2	1	1	1	0%	12/10	>50 trials	1 - 3	left & right ports, auditory cues with different frequency for transitions with 80/20% common/rare probabilities
3	C → L/R → U/D sequence	UDLRC	0.8	0.2	1	1	1	0%	12/10	>70 trials	1 - 3	initiation (centre) port
4.1	finding the 'correct' choice based on different reward probabilities that reverse across blocks	UDLRC	0.8	0.2	0.9	0.7	0.8	0%	12/10	>70 trials	1	reward probabilities, block switch after 20-30 trials, white noise signals no reward
4.2		UDLRC	0.8	0.2	0.9	0.5	0.7	25%	10	>70 trials	1	25% free choice trials, rare/neutral reward probabilities
4.3		UDLRC	0.8	0.2	0.9	0.3	0.6	25%	10	>70 trials	1	rare/neutral reward probabilities
4.4		UDLRC	0.8	0.2	0.9	0.1	0.5	25%	10	>70 trials	1	rare/neutral reward probabilities
4.5		UDLRC	0.8	0.2	0.9	0.1	0.5	50%	10	>70 trials	1	50% free choice trials, block switch in non-neutral blocks triggered by animal's behaviour
4.6		UDLRC	0.8	0.2	0.9	0.1	0.5	75%	10/8/6	>5 blocks for 3 consecutive sessions	4 - 16	75% free choice trials, 90min session length for slow learners
4.7		UDLRC	0.8	0.2	0.8	0.2	0.5	75%	6/4	>=8 blocks in >6 sessions	1 - 20	common/rare reward probabilities, 90min session length

At the first training stage, only the up and down step 2 state ports were visible to the animal (the other ports were taped over), and the animal needed to learn that these ports deliver water. At stage 1.1, step 2 state ports were illuminated in a pseudorandom order with a 2-4s inter-trial interval without any auditory cues. Poking the illuminated port resulted in water reward delivery with

100% probability. When the animals completed >50 trials in one session at stage 1.1, they transitioned to stage 1.2 on the next session during which the auditory cues for the step 2 state ports and the rewards were introduced. The delay in introducing auditory cues only at stage 1.2 was to ensure that the animals do not get startled by the sounds such that they fail to explore the nose poke ports and get the water. When the animals completed >70 trials in one session in stage 1.2, they transitioned to stage 2 on the next session.

At the training stage 2, the step 1 choice ports were revealed to build the sequence of poking left/right and then up/down. All trials were forced-choice trials, so only one step 1 choice port was illuminated on each trial, but the common/rare transition structure was used from the start. When the animals completed >50 trials in one session at stage 2, they transitioned to stage 3 on the next session.

At stage 3, the central port was revealed to complete the centre-left/right-up/down task sequence. Mice were switched to stage 4 when they completed >70 trials in one session.

At the fourth and final training stage, mice gradually learned how to find the “correct” choice based on different reward probabilities that change across blocks. Free-choice trials and omissions were introduced. Across seven substages, reward probabilities gradually changed (see Table 4.1) until reaching the final task parameters and progressively more free choice trials per daily session were added. Mice transitioned from 4.1 to 4.6 substage if they completed >70 trials in one session. Mice transitioned to the final stage 4.7 (the final task structure) when they were able to complete at least five blocks in a single session

for at least three consecutive sessions. At stage 4.7, session length was increased to 90min and the reward size reduced to 4µl to maximize the number of trials per session. Animals were considered fully trained once they were consistently completing eight or more reward blocks per session.

4.2.d Drug treatment and recording

Drug treatment was done only after there were at least six sessions of mice performing 6 or more reward reversals per session in the final training stage of the two-step task. (±)-DOI hydrochloride (CAS Number 42203-78-1; Sigma-Aldrich, Product no. D101-10MG) was dissolved in 0.9% saline vehicle. Injections were administered IP with weight-adjusted volume (10mL/kg for both 2.0mg/kg DOI and for saline). Each animal received only one injection. While all animals within a cage underwent injections at the same time, individual mice in the cage were randomly assigned to the DOI or vehicle group before any two-step task training (i.e., assignment to the treatment groups was not based on pre-drug task performance).

As reports on administration of DOI under water restriction were limited, several safety precautions were in place in case of a quicker and/or greater weight drop after injection as the animals did not have access to water until the next day. First, injections were performed the day after the animals had 1h of free water access in their home cage, so that the animals had higher pre-test weights. Second, the drug injections were always performed only after the daily two-step task testing was completed, such that the animals already had their daily water access. Third, all animals had to be at or above 90% pre-restriction age-corrected baseline weight before receiving the injections, otherwise they had to be topped

up with water after the two-step testing and before injections. Finally, for a subset of animals (n_{group}=13, N_{total}=26) we monitored the animals' weights hourly for at least 3h after injections. The average weight loss at the end of the 3h monitoring period compared to the post-test pre-drug weight, was 0.31g (CI [0.14, 0.48]) for vehicle-injected animals and 0.49g (CI [0.27, 0.71]) for DOI-injected animals (unpaired *t*-test, t_{24}=1.42, *P*=0.168). The average pre-test weight loss the day after injection compared to the pre-test weights on the day of injection was 0.45g (CI [0.26, 0.63]) for vehicle-injected animals and 0.40g (CI [0.15, 0.66]) for DOI-injected animals (unpaired *t*-test, t_{24}=0.32, *P*=0.753). We judged there were no short-term or long-term detrimental effects on body weight of administering DOI under our water restriction protocol, which also implied that there were likely no effects on the levels of motivation during subsequent task testing.

The injections were administered in a different room to where the two-step task testing took place. Each injected animal was placed in a 42 X 20 X 20cm clear Plexiglass box covered with a clear lid with air breathing holes and recorded for 30min by a Revotech I706-POE camera (variable frame rate of approximately 20fps) placed on the side of the cage for offline manual scoring of head twitches and ear scratches. The recording box was a novel environment to all animals. The half-life of HTR following 1mg/kg DOI was found to be 1.12h on average (de la Fuente revenga et al., 2019) and predicted to be somewhat longer for 2mg/kg DOI used in this study. Therefore, the mice remained in the recording box for further 30min after the behavioural recordings were completed to allow time for most of HTR and ESR effects to dissipate before returning the animals to their home cage.

The animals underwent the drug injections after completing the two-step task testing and were tested again in the two-step task the next day, when DOI was supposed to have cleared from the system. Most psychedelics are rapidly cleared from the body – the half-life of 1mg/kg DOI was found to be on average 1.90h in whole blood and 1.52h in the forebrain, with no concentration of DOI detected 24h after injection (de la Fuente Revenga et al., 2019). Even though the higher, 2mg/kg dose used in the study would be associated with a longer half-life, we still expect DOI to have cleared from the system by the next day. On the first testing day after drug injections, the transition probabilities were reversed for all animals and daily testing then proceeded as before, but the animals were faced with a novel challenge of adapting to a single transition reversal. For one subset of animals (*Group 1*, *n*=29) this reversal occurred immediately the next day after drug treatment, while the other set of mice (*Group 2*, *n*=26) had an additional week on the original task before facing the transition reversal (Fig.4.2).

4.2.e Analysis of overall task performance

We examined drug effects on (i) the number of trials performed across sessions, as a measure of task engagement and experience, and (ii) the number of correct choices across sessions (expressed as a ratio of correct choices over total choices made by that animal, excluding all forced-choice trials and choices made under a neutral reward block), as a measure of task accuracy, and (iii) the number of reward reversals (from a non-neutral block to either the other non-neutral block or to a neutral block) completed across sessions, as a measure of reward reversal performance.

4.2.f Analysis of choice behaviour and transition reversal adaptation

For initial assessment of the animals' learning of the task structure, we calculated stay probabilities – the probabilities of the animal repeating the same step 1 choice in a free-choice trial as a function of the transitions and outcomes of the previous trial (common/rare transition followed by a reward/omission).

Behavioural logistic regression model: To assess how the animals learned the underlying structure of the task, we performed multiple logistic regression of the probability of repeating a choice based on the trial events (transitions and outcomes) of the previous choice(s) using additional regressors that alleviate potential biases. The dependent variable in logistic regression analyses were the animal's choices (excluding all forced-choice trials) coded as stay/switch. Therefore, positive regression coefficients signal that the predictor promoted repeating the same choice. The predictors were coded as a function of trial events as:

Correct (repeat correct choice): +0.5 for choosing an option which commonly leads to the step 2 state with higher reward probability (*correct choice*), -0.5 for choosing an option which commonly leads to the step 2 state with lower reward probability, 0 for any choices made during a neutral block. This predictor tracks the cumulative effect of past choices and outcomes and prevents correlations across trials from causing spurious loading on the *Transition* X *Outcome* interaction predictor (Akam et al., 2015).

Choice (repeat choice, side bias): +0.5 for repeated choices, -0.5 for different choices.

Outcome (repeat rewarded choice): +0.5 for rewarded trials, -0.5 for unrewarded trials

Transition (repeat choices followed by a common transition): +0.5 for trials with a common transition, -0.5 for trials with a rare transition.

Transition X Outcome interaction (repeat choices followed by rewarded common and unrewarded rare transitions): +0.5 for rewarded trials with a common transition and unrewarded trials with a rare transition, -0.5 for unrewarded trials with a common transition and rewarded trials with a rare transition.

To assess how rewarded and unrewarded trials are evaluated by the animal separately, we also implemented a second type of model that, in addition to the *Correct*, *Choice*, and *Outcome* predictors as described above, also included the following:

Reward by transition (repeat rewarded choices with a common transition): +0.5 for rewarded trials with a common transition, -0.5 for rewarded trials with a rare transition, 0 for any unrewarded trials.

Omission by transition (repeat unrewarded choices with a common transition): +0.5 for unrewarded trials with a common transition, -0.5 for unrewarded trials with a rare transition, 0 for any rewarded trials.

All sessions to be included in the regression analysis for one animal were concatenated such that each trial counted equally for each animal. The logistic regression was implemented using the scikit-learn function *linear_model.LogisticRegression* with the newton-cg solver.

Lagged logistic regression: To test how trial events impacted multiple choices into the future, logistic regression analysis was adapted to include the history of trial events over the last 12 trials (lags of 1, 2, 3-4, 5-8, and 9-12 trials, where the range of lags refers to the sum of the individual trial predictors over the specified range). The *Correct* predictor was not included in the lagged regressions as here the effects of earlier trials are accounted for by the lagged predictors.

4.2.g Analysis of reward and transition reversal adaptation

Adaptation to the transition reversals across sessions was assessed with logistic regression model of trial-to-trial learning applied on a session-by-session basis, concatenating across three sessions to supply enough trials for the model to be fitted accurately.

Adaptation to reward reversals was assessed by calculating post-reversal choice probability trajectories (excluding forced-choice trials) starting 10 trials before reversal and ending at 20 trials after reversal, averaging across all reversals from non-neutral blocks (including transition to another non-neutral block, or to a neutral block) occurring across all six sessions (occurring either pre- or post-drug), such that each reversal contributed equally. Then, the data was averaged across individual subjects and compared across drug treatment groups.

Exclusions: Technical failures led to some sessions ending earlier than 90min. In these cases, the animals were taken out of the operant box and topped up with water if they had not received enough water in the task. The trial-by-trial

data from these sessions could still be used for logistic regression models and reward reversal adaptation trajectories, but incomplete sessions had to be excluded from the per-session counts of trials, reward reversals, and correct choices.

4.2.h Statistics and reporting

All behavioural analyses were performed in Python version 3.9.7 (Python Software Foundation) using both custom code and code adapted from Blanco-Pozo et. al. (2021) and Akam et. al. (2021).

Stay probability: A 2-way RM ANOVA was used to assess the effects of outcome, transition, and their interaction on repeating choices with the Bonferroni method of correction for multiple post-hoc comparisons.

Reward reversal choice probability trajectories: As in previous reports (Akam et al., 2021; Korn et al., 2021), reward reversal adaptation was analysed via double exponential model fits. The starting value was determined by the mean choice probability in the final 10 trials before the reversal. Permutation testing was used to assess the significance of differences in double exponential adaptation curves between sessions from DOI- and vehicle-injected animals. The double exponential fit was calculated in Python, minimizing the error using the scikit-learn *minimize* function with the L-BFGS-B algorithm method. The model was fitted to sessions from DOI- and vehicle-injected animals to give two sets of population level parameters

$$\theta_{DOI} = \{\mu_{DOI},\ \Sigma_{DOI}\} \text{ and } \theta_{VEH} = \{\mu_{VEH},\ \Sigma_{VEH}\}$$

where θ_{DOI} are the parameters (tau_{fast} and tau_{slow}) for trials from DOI-injected animals, and θ_{VEH} are the parameters (tau_{fast} and tau_{slow}) for trials from vehicle-injected animals. The difference between the population means for the DOI and vehicle conditions were calculated as

$$\Delta\mu_{true} = \mu_{DOI} - \mu_{VEH}$$

An ensemble of *N*=5000 permuted datasets was then created by shuffling the labels on sessions such that sessions were randomly assigned to the "DOI" and "vehicle" conditions. The double exponential was fit separately to sessions from DOI- and vehicle-injected animals for each permuted dataset and the difference between population level means of tau_{fast} and tau_{slow} in the DOI and vehicle conditions was calculated for each permuted dataset *i* as

$$\Delta\mu^{i}{}_{perm} = \mu^{i}{}_{DOI} - \mu^{i}{}_{VEH}$$

The distribution of $\Delta\mu_{perm}$ over the population of permuted datasets approximates the distribution under the null hypothesis that drug treatment does not affect the double exponential fit parameters (tau_{fast} and tau_{slow}). The *P* values for the observed distances $\Delta\mu_{true}$ are then given by

$$P = 2min\left(\frac{\mathbf{M}}{N}, 1 - \frac{\mathbf{M}}{N}\right)$$

where **M** is the number of permutations for which $\Delta\mu^{i}{}_{perm} > \Delta\mu_{true}$. Permutation testing was also used to assess significant differences in the probabilities of correct choices at the start or end of reward reversal blocks, with permuted datasets again generated by permuting sessions between the two drug treatment groups of subjects.

Logistic regressions: Significance of coefficients was assessed using a one-sample *t*-test (or Wilcoxon signed-rank test) comparing the distribution of the individual subjects' coefficients against zero. For lagged regression, Bonferroni multiple comparison correction was used applied to a family of one predictor for all lags. Significance of differences in coefficients across treatment groups was assessed using unpaired *t*-tests (or Mann-Whitney tests). Significance of differences between pre- and post-drug coefficients across treatment groups was assessed using 2-way RM ANOVA.

For assessing the significant differences in coefficients across sessions, our research question was concerned with how animals adapted *over time*, so keeping the sequential nature of our data points in our analysis was key. As discussed previously (section 3.2.f), an ANOVA ignores the order of data such that separate sessions are considered the same as separate treatments. Therefore, we again opted for nonlinear regression model fits using the least squares regression method with outlier detection as described before (section 3.2.f). Since there were no previous reports on how regression coefficients change over time with single transition reversals, we had no prior regarding what model to use, so the first step in these analyses was checking what the best model fit was (either linear, single exponential, or double exponential, like for reward reversal adaptation curves).

The main effect of time was implied by adaptation, and therefore not explicitly tested, although a non-zero slope (if the 95% CIs of the linear fit slopes were not overlapping with zero), or presence of a single or double exponential fit, signal a significant main effect of time (H_0: a straight line fit across all post-

reversal sessions). To test the effect of drug treatment, the models fitted to each treatment group separately were compared with an extra sum-of-squares *F* test, supplemented with reports of AICc probability differences, to test whether a shared global fit is sufficient (H_0) or separate fits were warranted for each treatment group separately (H_1). If separate fits were suggested, this was followed up by Bonferroni-corrected comparisons of the slopes or of the plateau and the time constants for the linear or exponential fits, respectively. For transparency, ANOVA results are also reported in section 8 and any discrepancies are discussed in the main text.

Note that the exponential time constants (*tau*) do not have a direct behavioural interpretation – they are simply the terms determining the shape of the exponential fit curve, i.e., how quickly the function decays (or grows, in the case of exponential association). The lower the time constant, the faster the exponential decay, and vice versa. In the case of a double exponential curve, there are two *tau* values, tau_{fast} and tau_{slow}, which also determine the shape of the fit curve, except the curve now has a fast and a slow component. The two-phase model is therefore the sum of the fast and slow components, each defined by their own rate constants, tau_{fast} and tau_{slow}, respectively. Both phases are happening at all time points – it is not that the fast phase finishes and then the slow phase begins. Likewise, it is not that tau_{fast} and tau_{slow} reflect how long the system is in the fast or slow phase – they are only mathematical terms of the model fit equation, like the linear and quadratic component of a second-order polynomial equation in section 3.2.f.

Session characteristics: The number of trials, reward reversals, and correct choices pre- and post-drug were compared using 2-way RM ANOVAs. For assessing the significant differences across sessions after transition reversal, nonlinear regression fits were used as for logistic regression predictors.

The experimenter was not blinded to group assignments during behavioural testing or during statistical analysis. All tests were two-sided with significance defined as $P<0.05$. All 95% confidence intervals are reported as "CI [lower limit, upper limit]". CIs of nonlinear regression fits were calculated as asymmetrical (profile-likelihood) CIs. As outlined previously (section 3.2.f), normality, sphericity, and homodescacity assumptions were verified and corrected. Outliers were identified with the ROUT method (Q=1%). ANOVAs and *t*-tests were supplemented by Bayesian statistics. Data visualization and statistical analyses were done in Prism version 9.4.0 for Mac OS (GraphPad Software Inc.). Effect size calculation and Bayesian analyses were done in JASP version 0.16.3 for MacOS Apple Silicon (JASP team). Detailed results of all statistical analyses are reported in section 8.

4.3 Results

We trained healthy wild-type C57BL/6 mice on a sequential two-step decision making task (Fig.4.1A) where they learned to make a choice between a left and right option to gain access to an up or down reward port. Rewards were delivered probabilistically and were anti-correlated between the up and down port, reversing over time based on subject's performance. This required the subjects to continuously search for the "correct", more highly rewarded, choice

(Fig.4.3A). The transitions between the two steps were probabilistic but initially fixed (no transition reversals). After drug treatment, our task included reversals in both reward and transition probabilities (Fig.4.1B). This allowed us to examine the post-acute influence of DOI over different aspects of cognitive flexibility, both learned (when the location of high probability reward changes) and novel (when the initial choice required to reach the high probability reward changes).

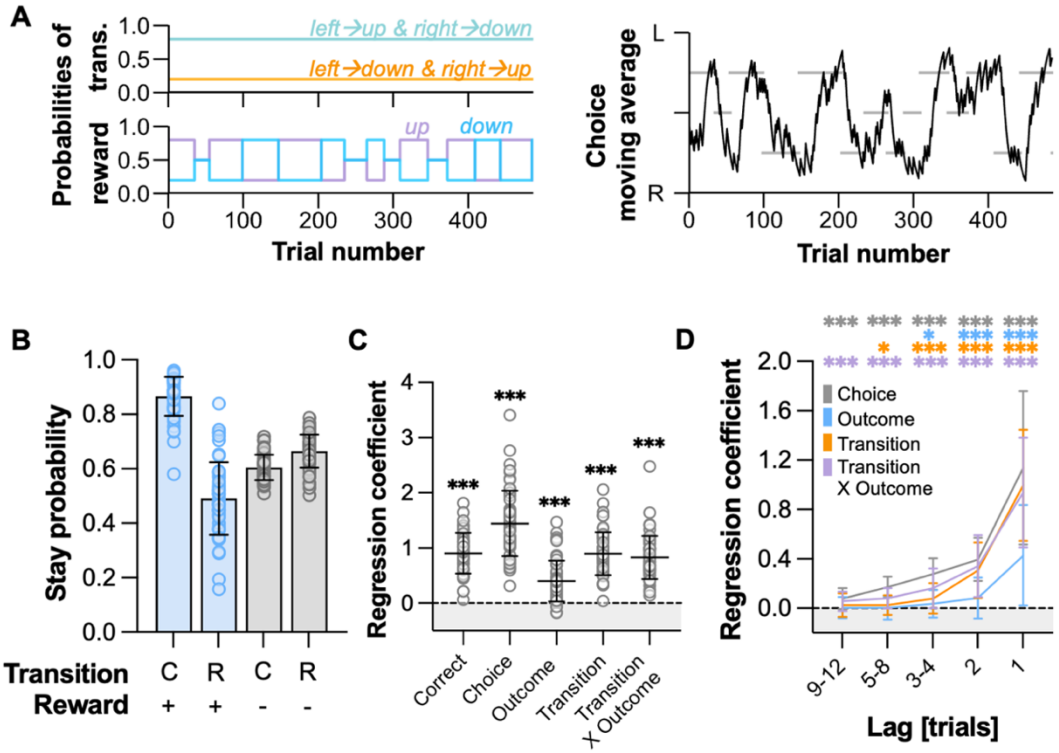


Fig.4.3 Pre-drug choice performance on the two-step task. (A) Example session. Left top: Probabilities of common and rare transitions remained fixed within a session. Left bottom: reward probabilities for the up and down ports were anticorrelated and changed in blocks multiple times across a single session. Right panel: exponential moving average of choices across 8 trials. Grey lines: reward blocks, the *y*-position represents the correct choice (left, right, or neutral). **(B)** Stay probabilities for the step 1 choice were a function of subsequent common (C) or rare (R) transitions ($P<0.001$) and rewarded (+), or not (-), trial outcome ($P<0.001$), and their interaction ($P<0.001$). **(C)** Logistic regression analysis quantifying how transitions, outcomes, and their interaction predict repeating the same step 1 choice on the next trial. *Correct* and *Choice* predictors capture any side bias and correct for cross-trial correlations. All predictors were significantly different from zero ($P<0.001$). **(D)** Lagged regression analysis shows how the repeated step 1 choices were influenced by trial history (one-sample *t*-tests against 0). Data shown as mean with SD error bars. Scatter plots represent individual subjects. $n=55$. *$P<0.05$. ***$P<0.001$.

4.3.a Baseline performance

Mice became proficient at the task in 27 (CI [26, 28]) training sessions on average. During the six baseline sessions before any drug treatment (*pre-drug*, Fig.4.2), animals were performing on average 405 (CI [389, 421]) trials and 6 (CI [6, 7]) reward reversals in a single 90min session.

To gain insight into the subjects' decision-making strategies and trial-by-trial learning, we looked at how the frequency of repeating a particular step 1 choice was a function of subsequent trial events for that choice – stay probability (Fig.4.3B). The mice were not only sensitive to the outcome, repeating rewarded choices (RM 2-way ANOVA *Outcome* $F_{1,54}$=23.9, P<0.001, η_p^2=0.84, BF_{incl}>100), and the transition type, finding common transitions reinforcing (*Transition* $F_{1,54}$=282.6, P<0.001, η_p^2=0.84, BF_{incl}>>100), but trial outcome interacted with the transition (*Transition X Outcome* $F_{1,54}$=343.0, P<0.001, η_p^2=0.86, BF_{incl}>>100). This implies that not all rewarded choices were simply reinforced – rewards preceded by common transitions promoted staying, but rewards preceded by rare transitions promoted switching to the other choice on the next trial. Further analyses using a logistic regression confirmed that the *Transition X Outcome* interaction predicted both the immediate repeated choices (Fig.4.3C, Wilcoxon signed-rank test for non-zero predictor loading P<0.001, BF_{10}>>100) and the recent history of choices (Fig.4.3D).

4.3.b Group 1: DOI did not affect task performance

In Group 1, animals underwent a transition reversal one day after drug treatment (Fig.4.2), and, over the next two weeks, we tracked how well and how quickly the animals adapted to a change in the task's transition structure.

Group 1 mice did not differ in their general task performance. The number of trials completed per session (Fig.4.4A) was comparable between vehicle- and DOI-treated mice both in sessions before drug injections (unpaired *t*-test t_{27}= -0.26, *P*=0.798, BF_{10}=0.36) and after drug administration when the transition reversal occurred (extra sum-of-squares $F_{2,108}$=0.18, *P*=0.840, AICc=0.14). Regression analysis suggested that task engagement did not change after the transition reversal in either group (slope 6.6, CI [-1.1, 14.4]), though, the 2-way RM ANOVA reported the main effect of time effect to be marginally significant ($F_{3,78}$=2.8, *P*=0.048, η_p^2=0.10) with weak evidence (BF_{incl}=1.04).

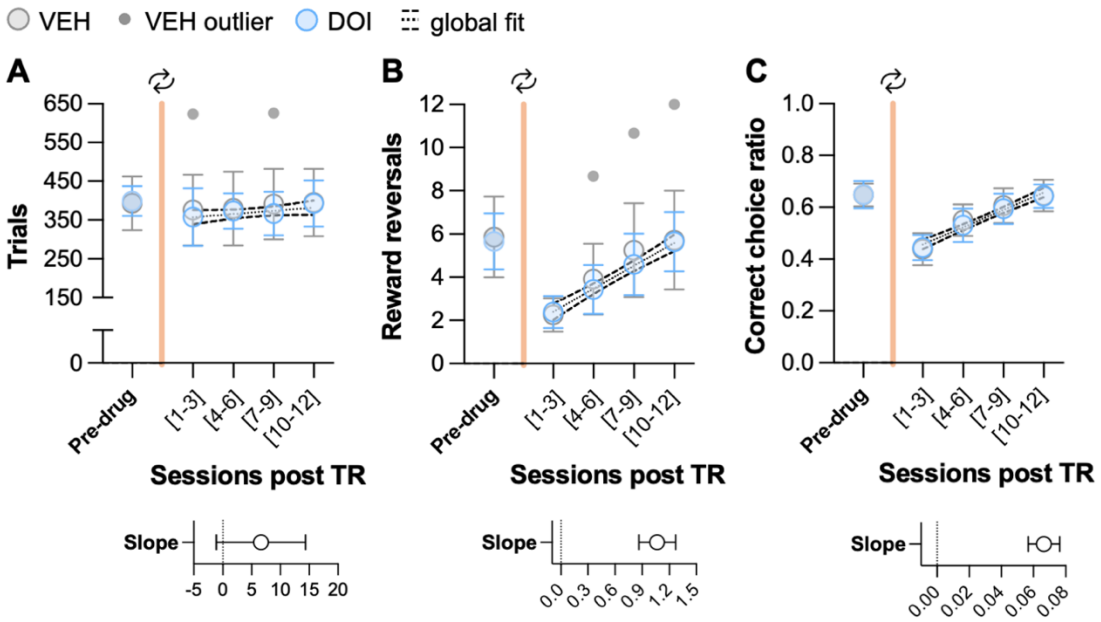


Fig.4.4 Group 1 overall task performance. Both vehicle (VEH) and DOI treatment groups were comparable after the transition reversal (TR) in **(A)** the number of trials per session (*P*=0.840), **(B)** the number of reward reversals per session (*P*=0.954), and **(C)** the correct choices per session (*P*=0.804). Data shown as mean with SD error bars. Dotted line: mean model fit. Dashed lines: borders of the 95% confidence intervals for the model fit. The orange vertical line denotes when TR has occurred.

As expected, performance accuracy initially dropped after the transition reversal. All mice initially completed fewer reward reversals per session (Fig.4.4B, slope 1.1, CI [0.9, 1.3]) and made fewer correct choices (Fig.4.4C,

slope 0.067, CI [0.057, 0.076]), recovering their pre-drug performance over time. There were no effects of drug treatment (extra sum-of-squares Fig.4.4B $F_{2,109}$=0.047, *P*=0.954, AICc=0.12; Fig.4.4C $F_{2,112}$=0.22, *P*=0.804, AICc=0.14).

4.3.c Group 1: DOI did not affect transition reversal adaptation

In the week preceding the drug injections, the treatment groups did not differ in terms of their trial-by-trial choice strategy (Fig.4.5A-C, pre-drug unpaired *t*-tests *Outcome* t_{27}= -1.03, *P*=0.313, *Transition* t_{27}=1.00, *P*=0.327, Mann-Whitney test *Transition X Outcome* W=120, *P*=0.533).

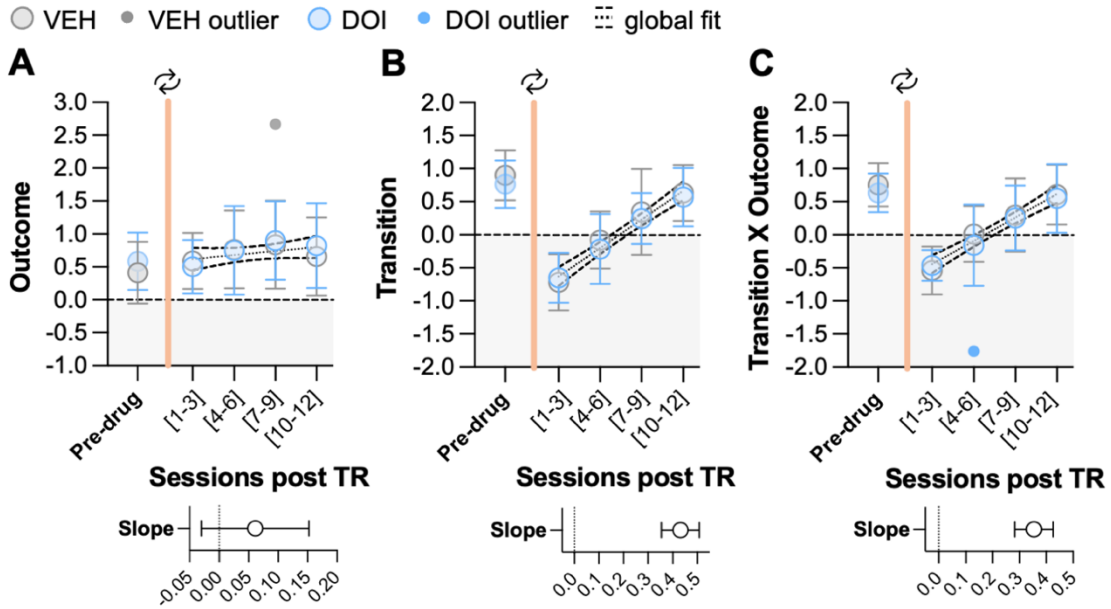


Fig.4.5 No differences in adaptability to the transition reversal (TR) in Group 1. Pre-drug trial-to-trial learning of animals selected for the DOI group was comparable to the animals selected for the control group (saline vehicle, VEH). Post-TR, **(A)** *Outcome* loadings did not change across groups (*P*=0.474) or across time. The *Transition* **(B)** and *Transition X Outcome* **(C)** loadings switched in sign after TR as initially the animals were still following the prior task structure and then they learned how to reverse their strategy over time. The speed of this adaptation was not different with DOI (*Transition P*=0.726, *Transition X Outcome P*=0.837). Data shown as mean with SD error bars. Dotted line: mean model fit. Dashed lines: borders of the 95% confidence intervals for the model fit. The orange vertical line denotes when TR has occurred.

The transition reversal did not affect how trial outcome influenced subsequent choice (Fig.4.5A, slope 0.06, CI [-0.03, 0.15]) in either drug or vehicle treatment group (extra sum-of-squares $F_{2,111}$=0.75, P=0.474, AICc=0.23). A 2-way RM ANOVA suggested a significant main effect of time ($F_{3,78}$=4.1, P=0.009, η_p^2=0.14, BF_{incl}=4.18), but post-hoc comparisons were significant only for the difference between post-reversal sessions [1-3] and [7-9] (P=0.006), signalling that the animals transiently relied more on simple reinforcing effects of rewards in sessions [7-9].

Animals' choice strategies initially continued to reflect the previous transition structure, reflected by the negative sign of the *Transition* and the *Transition X Outcome* predictor (Fig.4.5B-C). As animals learned the new transition structure, the predictor loadings returned to the pre-reversal positive values (slope *Transition* 0.43, CI [0.36, 0.51] & *Transition X Outcome* 0.35, CI [0.28, 0.43]). Importantly, the rate at which this learning occurred was comparable across treatment groups for both predictors (extra sum-of-squares *Transition* $F_{2,112}$=0.32, P=0.726, AICc=0.16 & *Transition X Outcome* $F_{2,111}$=0.17, P=0.837, AICc=0.14).

4.3.d Group 1: DOI did not affect reward reversal adaptation

The speed of adaptation to reward reversals was comparable across all animals before drug treatment (Fig.4.6, permutation test Tau_{fast} P=0.093, and Tau_{slow} P=0.088). We could not compare the performance after transition reversal as animals were completing too few reward blocks per session initially and varied on when they restarted doing more blocks, so the data were too variable for accurate model fitting.

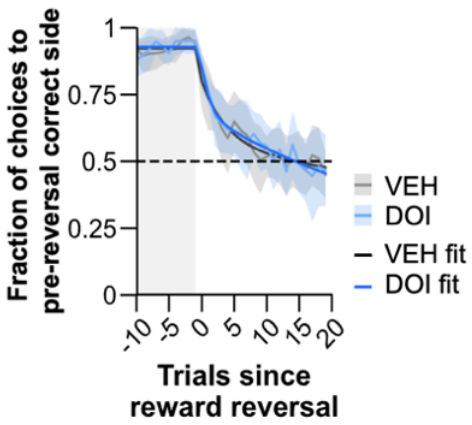


Fig.4.6 The pre-drug performance of Group 1 on reward reversals. Double exponential fit Tau_{fast} P=0.093 and Tau_{slow} P=0.088. Data shown as the average trajectory: pale grey line for saline vehicle (VEH), pale blue line for DOI, with shaded areas representing cross-subject SD. Double exponential fits: black or dark blue for VEH and DOI group respectively. n_{VEH}=15. n_{DOI}=14.

4.3.e Group 2: DOI did not affect task performance

In Group 2, animals continued testing on the unchanged task during the first six sessions after drug injections and they only underwent a transition reversal one week after drug treatment (Fig.4.2). As in Group 1, task engagement and overall performance were not modulated by DOI.

The number of trials per session increased marginally (by 16, CI [3, 30], trials) post-drug, regardless of the type of treatment (Fig.4.7A, 2-way RM ANOVA Time $F_{1,24}$=6.4, P=0.018, η_p^2=0.21, BF_{incl}=3.03, Drug $F_{1,24}$=0.8, P=0.391, BF_{incl}=0.69, Time X Drug $F_{1,24}$=0.6, P=0.456, BF_{incl}=0.44), but after the transition-reversal there were no changes across time (slope -6.4, CI [-15.8, 2.9]) and no differences across groups (extra sum-of-squares $F_{2,100}$=0.24, P=0.786, AICc=0.14).

The average number of reward reversals completed per session also increased marginally post-drug for both treatment groups (Fig.4.7B, mean

difference 0.70, CI [0.19, 1.20], 2-way RM ANOVA Time $F_{1,24}$=8.1, P=0.009, η_p^2=0.25, BF_{incl}=5.67, Drug $F_{1,24}$=1.6, P=0.064, BF_{incl}=0.80, Time X Drug $F_{1,24}$=0.003, P=0.959, BF_{incl}=0.36), and the rate of performance recovery following the transition reversal was comparable across treatment groups (extra sum-of-squares $F_{2,100}$=0.032, P=0.968, AICc=0.12).

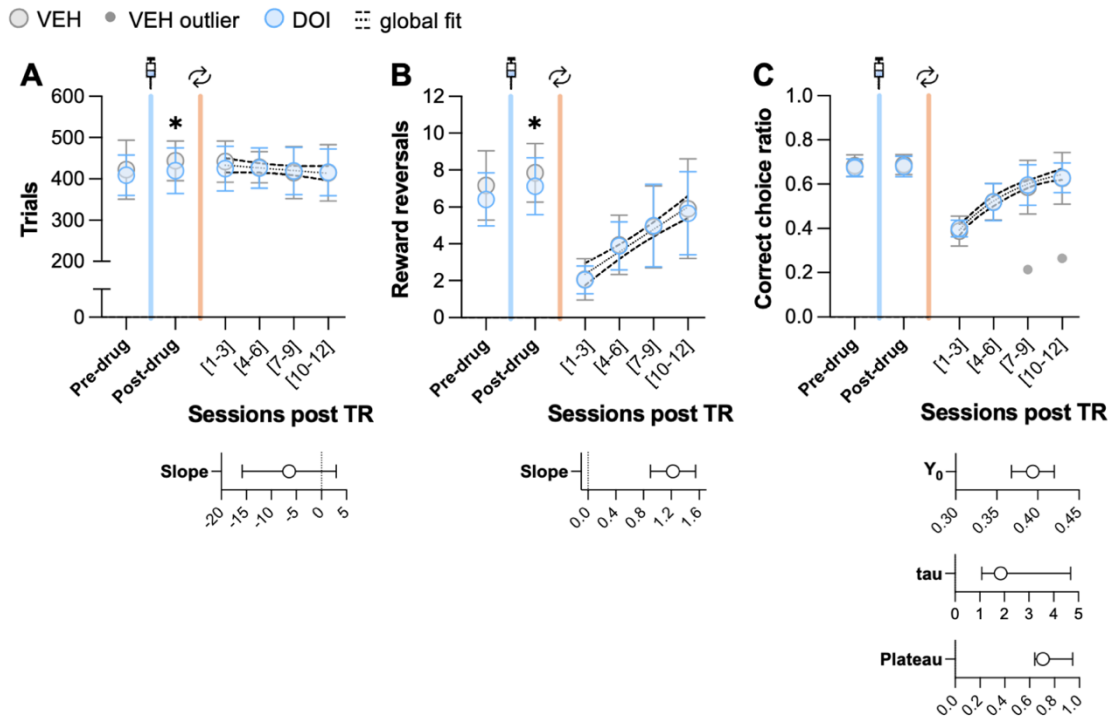


Fig.4.7 Group 2 overall task performance. (A) The number of trials completed per session increased in the first week post-drug (Time P=0.018) but remained comparable across treatment groups (Drug P=0.391), including after transition reversal (TR, P=0.840). **(B)** Similarly, the number of reward reversals completed per session increased in the first week (Time P=0.009) regardless of treatment (Drug P=0.064), without any drug-related differences post-TR (P=0.954). **(C)** The number of correct choices per session remained comparable across treatment groups both after the injections (P=0.521) and after TR (P=0.599). Data shown as mean with SD error bars. Dotted line: mean model fit. Dashed lines: borders of the 95% confidence intervals for the model fit. The blue vertical line denotes when drug injections have occurred. The orange vertical line denotes when TR has occurred. *P<0.05. **P<0.01.

The percentage of correct choices the mice were making across sessions did not change post-drug, before the transition reversal, (Fig.4.7C, 2-way RM ANOVA Time $F_{1,24}$=0.42, P=0.521, BF_{incl}=0.33, Drug $F_{1,24}$=0.34, P=0.566,

BF_{incl}=0.50, Time X Drug $F_{1,24}$=0.002, P=0.967, BF_{incl}=0.36) and the time course of adaptation to the transition reversal was not affected by drug treatment (extra sum-of-squares $F_{3,96}$=0.63, P=0.599, AICc=0.09).

4.3.f Group 2: DOI-treated animals showed quicker transition reversal adaptation

In the week preceding the drug injections and in the six sessions after drug injections, prior to the transition reversal, the two treatment groups did not differ by their learning from outcomes (Fig.4.8A, 2-way RM ANOVA, Time $F_{1,24}$=2.1, P=0.161, BF_{incl}=0.62; Drug $F_{1,24}$=2.5, P=0.127, BF_{incl}=0.97; Time X Drug $F_{1,24}$=3.3, P=0.082, BF_{incl}=1.12), transitions (Fig.4.8B, Time $F_{1,24}$=3.8, P=0.063, BF_{incl}=1.23; Drug $F_{1,24}$=0.2, P=0.624, BF_{incl}=0.53; Time X Drug $F_{1,24}$=0.4, P=0.520, BF_{incl}=0.41), or their interaction (Fig.4.8C, Time $F_{1,24}$=1.4, P=0.246, BF_{incl}=0.49; Drug $F_{1,24}$=1.3, P=0.261, BF_{incl}=0.66; Time X Drug $F_{1,24}$=0.4, P=0.528, BF_{incl}=0.41).

After the transition reversal one week after drug injections, the animals did not become more reliant on the simple reinforcing effects of rewards as the *Outcome* regression coefficient did not change significantly over time (Fig.4.8A, slope -0.02, CI [-0.11, 0.07]) and was comparable across treatment groups (extra sum-of-squares $F_{2,100}$=1.28, P=0.283, AICc=0.42). The simple reinforcing effects of transitions again changed over time to reverse to tracking the now-common, previously rare transitions (Fig.4.8B, tau 1.27, CI [0.76, 2.52]), but again was not modulated by the drug (extra sum-of-squares $F_{3,98}$=1.06, P=0.372, AICc=0.18).

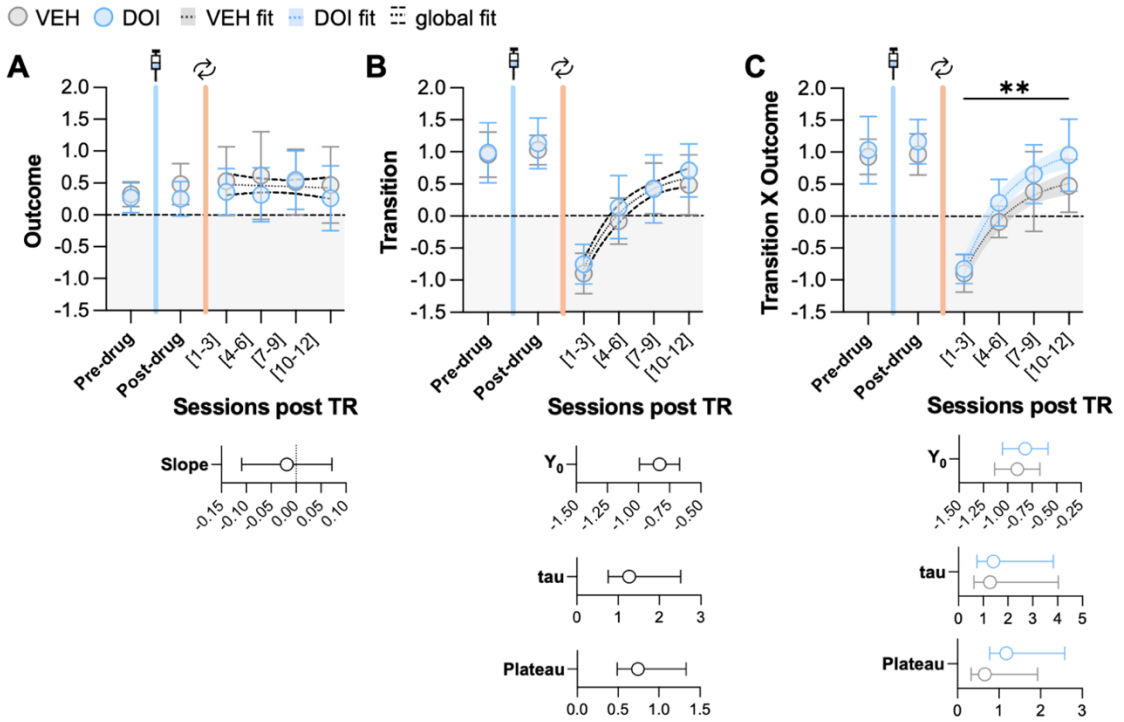


Fig.4.8 Group 2 DOI-treated animals had faster transition reversal (TR) adaptation. **(A)** The loading on the *Outcome* predictor was not different post-drug (Time P=0.161 & Drug P=0.127), or post-TR (P=0.161). The *Transition* **(B)** and *Transition X Outcome* **(C)** loadings did not change post-drug (*Transition* Time P=0.063 & Drug P=0.624, and *Transition X Outcome* Time P=0.246 & Drug P=0.261) but they switched in sign post-TR reflecting the animals initially keeping with the prior task structure and then learning over time how to reverse. The speed of this adaptation was not different with DOI for the reinforcing effects of common transitions (P=0.372), but DOI-treated animals were quicker in their *Transition X Outcome* loading reversal (P=0.004). Data shown as mean with SD error bars. Dotted line: mean model fit for DOI (blue), VEH (grey), or global fit (black). Dashed lines or shaded areas: borders of the 95% confidence intervals for the model fit. The blue vertical line denotes when the drug injections have occurred. The orange vertical line denotes when TR has occurred. **P<0.01.

However, DOI treatment altered how the mice's choices were influenced by the outcome they received *and* the transition that preceded it. DOI affected the recovery of the *Transition X Outcome* predictor to pre-drug levels, as indicated by separate curves being warranted for control and DOI data (Fig.4.8C, extra sum-of-squares $F_{3,98}$=4.76, P=0.004, AICc=40.10). The 2-way RM ANOVA suggested a main effect of drug ($F_{1,24}$=5.0, P=0.035, η_p^2=0.17, BF_{incl}=2.11), though not a significant interaction with session ($F_{2.09,50.23}$=1.79, P=0.177, BF_{incl}=0.54). The ANOVA main drug effect would imply that the DOI group's

regression coefficient was higher *overall*, across all sessions. But, the post-hoc comparisons in the regression analysis do not suggest a significant difference in the initial perseverance (Y_0 [1-3] P=0.919) or the post-adaptation predictor values (predicted plateau P=0.226), implying that the DOI-treated animals were as affected by the transition reversal as the vehicle-treated animals (i.e., there was no "protective" effect of DOI) and the vehicle-treated animals were still able to recover a strategy comparable to DOI-treated animals (i.e., the controls understood the task structure at the end of the adaptation period). Exploratory uncorrected Fisher's LSD post-hoc comparisons across vehicle- and DOI-treated mice showed that the two treatment groups were significantly different at post-reversal sessions [4-6] (P=0.023) and [10-12] (P=0.022). It is the way in which the DOI-treated animals were recovering their strategy that was different, as it was the shape of the adaptation curve after the comparable start points that was significantly different.

4.3.g Group 2: A change in strategy in DOI-treated mice

DOI-treated animals appear to have been able to relearn the task structure more quickly but what could have helped them to do that? An improvement in cognitive flexibility can be mediated not just by learning rates, but also cognitive strategies. We next asked whether the strategy that mice were employing to adapt to the transition reversal was different if the animals received an injection of DOI or the vehicle.

Previous research in mice performing the two-step task consistently showed that the influence of outcomes is asymmetrical – mice appear to be sensitive only to rewards and not update their preferences following omissions

(Blanco-Pozo et al., 2021). We asked whether the added challenge of a novel transition reversal affected a mouse's drive to learn from omissions. To do this, we adapted our original logistic regression model (Fig.4.3C) to model how transitions interact with rewards and omissions separately (*Reward by transition* & *Omission by transition*, respectively, section 4.2.f), rather than jointly as they were modelled in the original regression.

Prior to drug injections, the *Reward by transition predictor* was strongly positive (Fig.4.9A, one sample *t*-test against zero, vehicle t_{12}=12.74, P<0.001, Cohen's d=3.53, BF_{10}>>100, DOI t_{12}=7.70, P<0.001, Cohen's d=2.14, BF_{10}>>100) as rewards preceded by common transitions are strongly reinforced. This effect was comparable in both treatment groups (unpaired *t*-test t_{24}= -0.45, P=0.659, BF_{10}=0.39), confirming the choice strategies were identical in all animals prior to drug treatment. In contrast, the pre-drug *Omission by transition* predictor was not significantly different from zero (Fig.4.9A, one sample *t*-test against zero, vehicle t_{12}=0.30, P=0.768, BF_{10}=0.29, DOI t_{12}= -0.52, P=0.610, BF_{10}=0.31) and was comparable across all mice (unpaired *t*-test t_{24}=0.58, P=0.567, BF_{10}=0.41). A predictor whose regression coefficient is on average not significantly different from zero is not a significant factor for predicting repeated choices. For the *Omission by transition* predictor, this means that, on average, mice did not include the effect of experiencing omissions in their choice strategy, as we originally predicted based on previous reports of learning asymmetries in mice (Cieślak et al., 2018; Blanco-Pozo et al., 2021).

During the post-drug period, before the transition reversal, the treatment groups remained comparable for the *Reward by transition* predictor (Fig.4.9B, 2-

way RM ANOVA Time $F_{1,24}$=3.4, P=0.079, BF_{incl}=1.04; Drug $F_{1,24}$=0.8, P=0.387, BF_{incl}=0.61; Time X Drug $F_{1,24}$=0.6, P=0.444, BF_{incl}=0.44) suggesting that DOI did not affect how positive feedback was evaluated with regards to the transition type. The same was true for the *Omission by transition* predictor (Fig.4.9C, 2-way RM ANOVA Time $F_{1,24}$=0.13, P=0.725, BF_{incl}=0.29; Drug $F_{1,24}$=0.76, P=0.392, BF_{incl}=0.47; Time X Drug $F_{1,24}$=0.01, P=0.907, BF_{incl}=0.36).

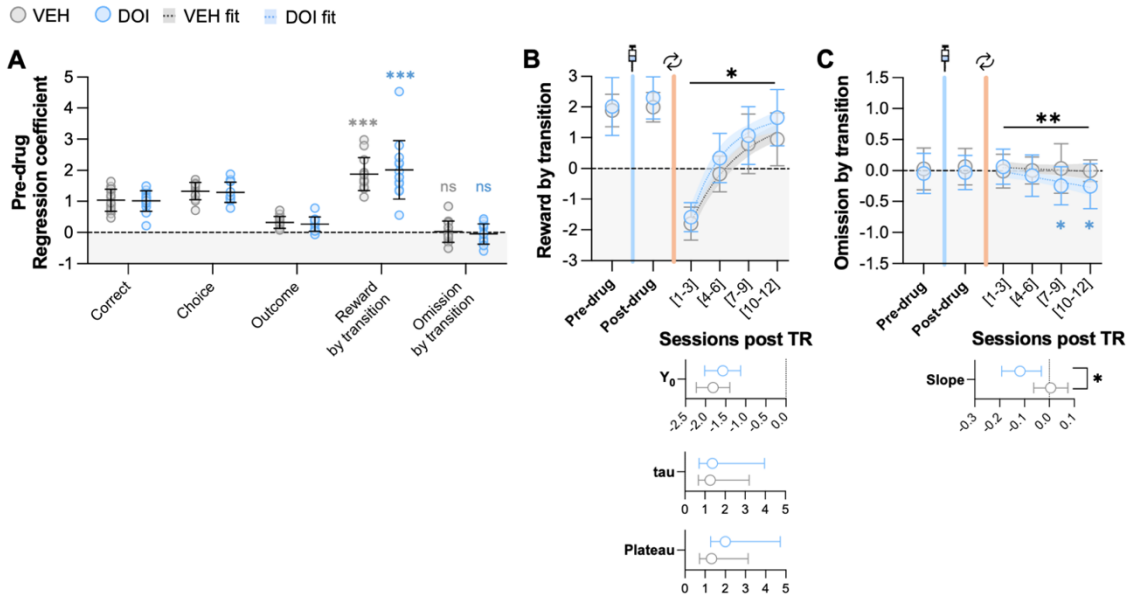


Fig.4.9 Group 2 DOI-treated animals started learning from omissions after the transition reversal. (A) Pre-drug, the reinforcing value of rewards was modulated by the type of transition (*Reward by transition* predictor for VEH and DOI P<0.001), but omissions were not contributing to trial-to-trial learning in general (*Omission by transition* predictor for saline vehicle VEH P=0.768 and DOI P=0.610). Scatter plot represents individual subject data. **(B)** After the transition reversal (TR), *Reward by transition* predictor adaptation pattern was marginally quicker for DOI animals than the controls (P=0.043). **(C)** While the *Omission by transition* predictor was not contributing to the choice strategy pre- nor post-drug, nor after the TR for VEH mice, for the DOI-treated mice the regression coefficient became significantly more negative as animals adapted to the TR (slope -0.112, CI [-0.192, -0.032], line fits difference P=0.007), signalling that they have started incorporating omission in their strategy (regression coefficient significantly non-zero only for DOI-treated animals by session [7-9] post-TR P=0.015, and [10-12] P=0.029). Data shown as mean with SD error bars. Dotted line: mean model fit for DOI (blue) or VEH (grey). Shaded areas: borders of the 95% confidence intervals for the model fit. The blue vertical line denotes when the drug injections have occurred. The orange vertical line denotes when TR has occurred. *P<0.05. **P<0.01. ***P<0.001. Grey *: one-sample t-tests on VEH data. Blue *: one-sample t-tests on DOI data.

After the transition reversal, as expected, *Reward by transition* predictor reversed its sign as animals adapted to the transition reversal (Fig.4.9B). The speed of this adaptation was again different for DOI-treated animals (extra sum-of-squares $F_{3,98}$=2.82, P=0.043) but this effect was weaker compared to the original *Transition X Outcome* predictor (AICc=2.53) and did not reach significance in the 2-way ANOVA (Drug $F_{1,24}$=3.2, P=0.085, BF_{incl}=1.78, Time X Drug $F_{1.96,47.10}$=1.0, P=0.372, BF_{incl}=0.26).

Strikingly however, following the transition reversal, the vehicle-treated animals did not change their learning from omissions (Fig.4.9C, slope =0.006, CI [-0.063, 0.074]), but the DOI-treated mice began incorporating learning from omissions. They significantly decreased their loading on the *Omission by transition* predictor (Fig.4.9C, slope -0.112, CI [-0.192, -0.032], fit comparison vehicle vs. DOI extra sum-of-squares $F_{2,100}$=5.22, P=0.007, AICc=19.62; slope difference P=0.027) such that there was a significantly negative influence of omissions in the DOI group by the second week post-reversal (one-sample t-tests against zero P>0.400, BF_{10}=0.38 for sessions [1-6], but for sessions [7-9] t_{12}= -2.82, P=0.015, Cohen's d= -0.78, BF_{10}=4.08, and [10-12] t_{12}= -2.48, P=0.029, Cohen's d= -0.69, BF_{10}=2.46). In contrast, the vehicle group continued not to exhibit any influence of omissions on their subsequent choices (one-sample t-tests against zero P>0.700, BF_{10}<0.29 for all sessions [1-12]). The significant negative loading implies that omissions following a common transition increased the value of the state that would be more commonly reached from the action that was not chosen on that trial *or* decreased the value of the chosen commonly reached state. A 2-way RM ANOVA on these data confirmed the difference

across treatment groups (drug $F_{1,24}$=5.5, P=0.027, η_p^2=0.19, BF_{incl}=0.98). As with the *Transition X Outcome* predictor, our data suggests the difference in the *Omission by transition predictor* is something that developed *over time*, as animals were having to adapt to the transition reversal. Exploratory uncorrected Fisher's LSD post-hoc comparisons across vehicle- and DOI-treated mice showed that the two treatment groups were significantly different only [10-12] sessions after the transition reversal (P=0.037).

To investigate whether this change in sensitivity to reward omissions was specific to the transition reversal that happened one week after drug treatment, we ran the same analysis on the Group 1 mice that underwent the transition reversal one day after injections. Pre-drug, *Omission by transition* predictor loading was not significantly different from zero for the DOI group (Fig.4.10, one sample *t*-test against zero t_{13}=1.85, P=0.087, BF_{10}=1.04). For the control animals, the predictor loading was marginally positive (t_{14}=2.18, P=0.048, BF_{10}=1.60), i.e., these mice were exhibiting a wrong strategy of repeating unrewarded trials preceded by a common transition. Post-drug, which here coincided with the transition reversal, the treatment groups were not significantly different from each other (extra sum-of-squares $F_{2,112}$ =0.02, P=0.979, AICc=0.12). Moreover, the DOI-treated animals did not start including learning from omissions as the predictor loadings did not change over time (slope 0.07, CI [-0.02, 0.16]). For the control animals, the slope was marginally positive (0.07, CI [0.02, 0.13]), but this again reflects the wrong strategy. Therefore, Group 1 animals did not incorporate learning from omissions as we saw Group 2 DOI-treated animals did.

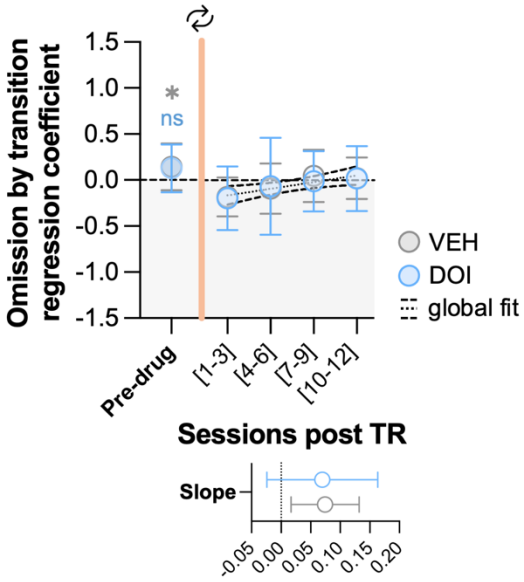


Fig.4.10 Group 1 animals did not include trial-to-trial learning from omissions. The loading on the *Omission by transition* predictor was not significantly different from zero before the drug for the would-be DOI-treated (*P*=0.087) animals. The vehicle (VEH) control had a marginally positive loading (*P*=0.048, but BF_{10} =1.60) that is a wrong strategy. After the transition reversal (TR), the DOI-treated animals did not change their loading. The VEH group had a marginally positive increase in their loading, reflecting a wrong strategy. Data shown as mean with SD error bars. Dotted line: mean model fit. Dashed lines: borders of the 95% confidence intervals for the model fit. The orange vertical line denotes when TR has occurred. n_{VEH}=15, n_{DOI}=14. *P<0.05. **P<0.01. Blue "ns": one-sample *t*-test on DOI data. Grey *: one-sample *t*-test on VEH data.

To confirm how reliable the general lack of learning from omissions in this task is, we re-analysed a separate C57-background mouse cohort (n_{group}=18), from Blanco-Pozo et al. (2021), trained on the same task structure with only reward reversals and without any drug treatment. When we fitted the logistic regression model, using the same number of sessions as the pre-drug period in our experiments, the loading on the *Omission by transition* predictor was not significantly different from zero (Fig.4.11A, one-sample *t*-test against zero t_{17}=1.77, *P*=0.095, BF_{10}=0.88). We also confirmed that the predictor loading does not change significantly from zero when analysing grouped consecutive sessions across two weeks, mimicking the adaptation period we investigated following the transition reversal (Fig.4.11B, extra sum-of-squares test of slope against zero

P>0.093). We therefore conclude that the significant negative *Omission by transition* predictor loading observed in Group 2 was a unique occurrence in mice solving the two-step task after a novel rule reversal following DOI treatment.

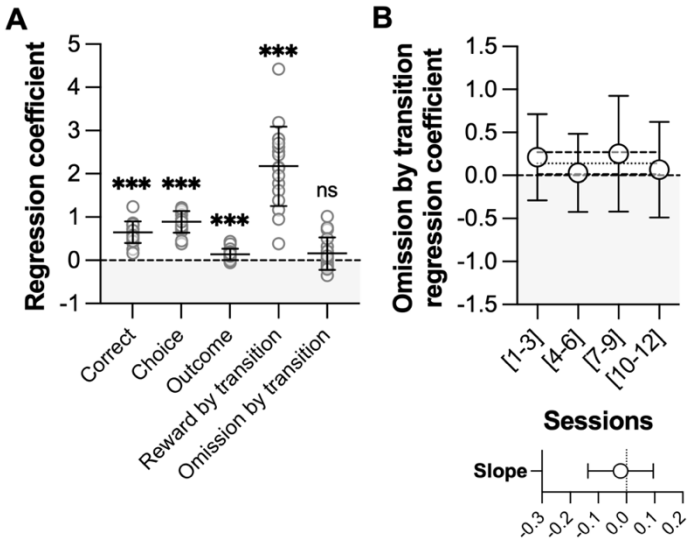


Fig.4.11 In general, C57-background mice do not include trial-to-trial learning from omissions. Investigating a same-strain mouse cohort (n_{group}=18) which was tested on the original two-step task structure but without any transition reversal, the loading on the *Omission by transition* predictor was not significantly different from zero when **(A)** fitting the logistic regression model to the same number of sessions as the pre-drug period in our experiments (*P*=0.095) or when **(B)** fitting the model on groups of three sessions followed over time for two weeks as the post-reversal period in our experiments (line fit slope = -0.02, CI [-0.14, 0.10], *P*=0.724). Dotted line: mean model fit. Dashed lines: borders of the 95% confidence intervals for the model fit. Scatter plots represent individual subjects. ***P<0.001.

4.3.h Group 2: DOI-treated animals showed quicker reward reversal adaptation

We asked if the improvement in cognitive flexibility was restricted to updating choice strategies after the novel reversal in transition probabilities, or whether there was evidence for improvement in performance during the serial reward reversals too. To do this, we examined adaptation to reward reversals occurring in the first week after drug injections, prior to the transition reversal.

Before the injections, all animals were comparable in terms of the speed of their adaptation to a reward reversal (Fig.4.12A, double exponential fit permutation test Tau_{fast} P=0.659, Tau_{slow} P=0.821). In the first week post-drug, despite the mice being highly proficient at reward reversals, there was a small but statistically reliable speeding of reversal performance of DOI-treated animals compared to the controls (Fig.4.12B, permutation test Tau_{fast} P=0.073, Tau_{slow} P=0.036). The lower time constant indicates a faster fall in the fraction of choices made to the wrong step 1 port, i.e., a more rapid serial reward reversal learning in DOI-treated mice before the transition reversal.

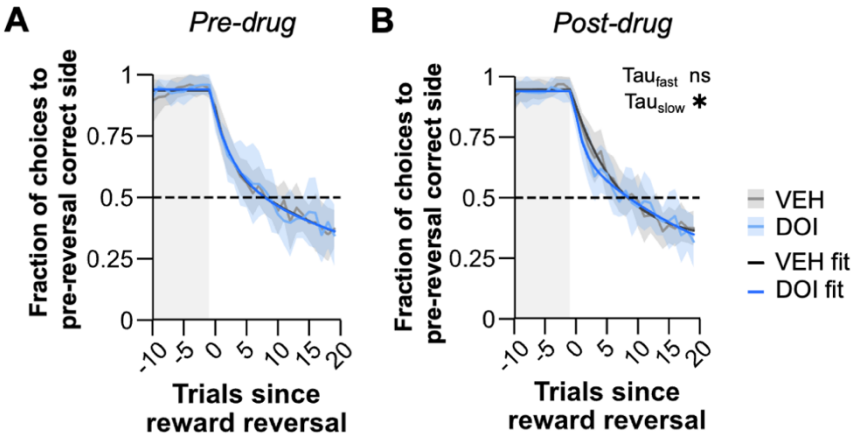


Fig.4.12 Group 2 reward reversal adaptation is faster post-DOI. (A) Pre-drug reward reversal performance was not significantly different across the treatment groups (Tau_{fast} P=0.659, Tau_{slow} P=0.821). **(B)** In the first week after drug injections, before the transition reversal, DOI treated animals were quicker at reversing their choice strategy following reward reversals (Tau_{fast} P=0.073, Tau_{slow} P=0.036). Data shown as the average trajectory: pale grey line for saline vehicle (VEH), pale blue line for DOI, with shaded areas representing cross-subject SD. Double exponential fits: black or dark blue for VEH and DOI group respectively. n_{group}=13. *P<0.05.

We checked whether the significant difference across treatment groups were due to significant differences across time within-subjects. Meaning, were the VEH-DOI differences post-drug due to the DOI group being not only quicker than the VEH group, but also quicker than themselves before the drug. We

compared the pre- and post-drug reward reversal adaptation curves for each treatment group separately and found that vehicle-treated group was slower in the post-drug compared to the pre-drug sessions (Fig.4.13A, within-subject permutation test, Tau_{fast} P=0.052, Tau_{slow} P=0.012). This effect was not discovered in the 2-way RM ANOVA (Time X Drug $F_{8.0,\ 192.8}$=1.7, P=0.094, BF_{incl}=0.89). In contrast, DOI group's performance was no different post-drug compared to before treatment (Fig.4.13B, within-subject permutation test Tau_{fast} P=0.081, Tau_{slow} P=0.159). This would suggest the DOI group's apparent improvement compared to the VEH-injected mice after injections was not due to the DOI's enhancement of reward reversal adaptation, but due to a possible drop in performance in the control group. This suggest DOI's effects on learned reward reversals were distinct from those on the novel transition reversal.

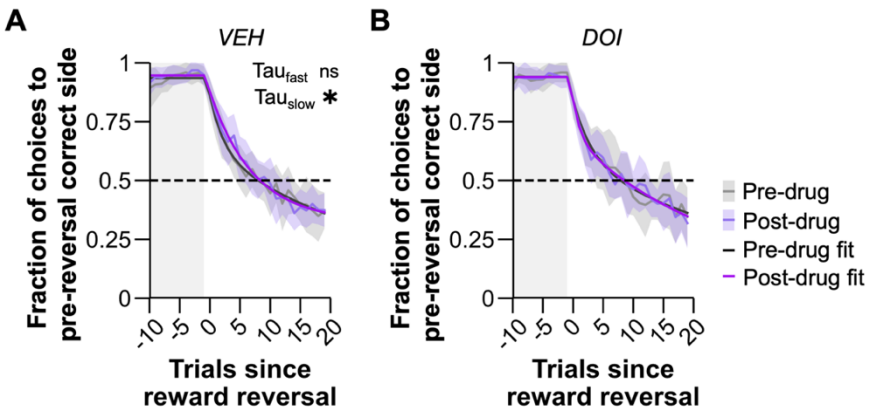


Fig.4.13 Comparing reward reversal adaptation across time. (A) In the VEH group, the animals had marginally worsened performance after injections (Tau_{fast} P=0.052, Tau_{slow} P=0.012). **(B)** There were no changes in performance after drug treatment in DOI-treated animals (Tau_{fast} P=0.081, Tau_{slow} P=0.159). Data shown as the average trajectory: pale grey line for pre-drug, pale purple line for post-drug, with shaded areas representing cross-subject SD. Double exponential fits: black or dark purple for pre- and post-drug period respectively. *P<0.05.

4.3.d The differences in adaptability between Group 1 and Group 2 were not due to differences in the intensity of acute drug effects

The divergent effects of DOI in the groups experiencing the transition reversal at different times after drug treatment could be due to a difference in the strength of DOI's acute effects. To assess this, we examined the frequency of head twitches and ear scratches occurring in the first 30min after injection. Both measures were comparable across Groups 1 and 2 (Fig.4.14, unpaired *t*-tests, head twitch: t_{25}=1.84, *P*=0.078, BF_{10}=1.21; ear scratch: t_{25}=1.59, *P*=0.124, BF_{10}=0.90).

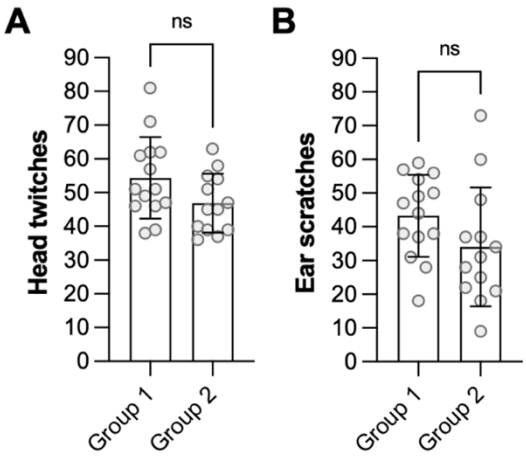


Fig.4.14 The intensity of the acute psychedelic effects of DOI were comparable across experimental groups. (A) The frequency of the psychedelic-like head-twitch responses in the first 30min after injection did not differ across experimental groups (*P*=0.078). **(B)** The frequency of the psychedelic-like ear-scratch responses in the first 30min after injection did not differ across experimental groups (*P*=0.124). Data shown as mean with SD error bars.

4.4 Discussion

In this study, we investigated putative enhancements in cognitive plasticity in the weeks following psychedelic treatment. We asked whether DOI

could increase cognitive flexibility by studying adaptations to both serial and novel reversal learning. Using an adapted version of the two-step decision-making task, we were able to monitor performance on learned serial reversals in reward probabilities, as well as how quickly mice were able to change their choice strategies following a single novel reversal in transition probabilities happening either one day or one week after a 2mg/kg DOI injection (Fig.4.2).

It is likely that mice understand that the transition probabilities linking the two steps of the task are fixed after extended training and experience with the task. This would mean that they would not update their estimates of transition probabilities based on trial-by-trial experience, suggesting their estimates of transition probabilities were averaged across several or many prior trials. This helps explain why adaptation to the transition reversal occurred on such a slower timescale compared to the reward reversal adaptation that occurred across only dozens of trials.

4.4.a A quicker adaptation, but only after a time

DOI differentially regulated specific aspects of cognitive flexibility. It did so by shaping trial-by-trial learning. DOI influenced reward-driven alternations in behavioural policies without shaping the motivational components of reward-guided behaviour. The alterations were specific to trial-by-trial reinforcement learning, where DOI shaped how quickly the animals detected a first-time change in the transition structure, but not if this change occurred only one day after drug treatment. The presence of significant improvements in cognitive flexibility in Group 2 but not in Group 1 was not due to any differences in the intensity of acute drug effects (Fig.4.14). When DOI conferred higher adaptability in the long-term

phase, it did so not only because the mice were better able to inhibit responding to the old model (the faster adaptation in the *Transition X Outcome* predictor, Fig.4.5C), but also because the mice were able to develop a new strategy of including novel types of learning (the significant *Omission by transition* predictor, Fig.4.9C).

4.4.b A richer strategy

Mice that displayed faster adaptation to the transition reversal after DOI also displayed a unique inclusion of learning from omissions in their choice strategy. This added sensitivity to frustrative reward omissions is the likely underlying mechanism of increased flexibility following a novel transition reversal.

While mice in the two-step task have high reward learning rates, they do not include learning from omissions (Fig.4.9A). This learning asymmetry has previously been shown using model-comparison of two-step task performance, as well as stay probability and logistic regression analyses (Blanco-Pozo et al., 2021). The same asymmetry in learning rates from positive and negative feedback was observed in mice solving a simpler single-step probabilistic reinforcement learning task (Cieślak et al., 2018). This effect is not unique to mice. Humans solving the two-step task and other reward-guided probabilistic tasks also show higher learning rates for positive feedback (Frank et al., 2004; Sebold et al., 2014b; Grogan et al., 2017; Wyckmans et al., 2019) and reduced loss aversion has been implicated in addictive disorders such as gambling and alcohol dependence (Genauck et al., 2017). One of the proposed explanations is that after learning that one choice has a higher average probability of reward,

single negative feedback is viewed as just noise and so ignored (Grogan et al., 2017).

While an experimenter designing the task imagines omissions to be informative in a probabilistically reward-guided task, this does not necessarily mean that the mouse solving the task will think in the same way. It has been suggested that frustrative omission of reward can act as an acquired drive, with “frustration” in this case referring to the emotional response to the withholding of a previously given reward (Amsel, 1958). For mice, it appears that omissions are not frustrative enough to generate a drive to change their reinforcement learning to include shifting away from unrewarded choices. This reduced sensitivity to omissions is not necessarily a “sub-optimal” strategy in the original task as the mice are still able to solve the task to a high level after training. In our task, 90min-long sessions with inter-trial intervals of only a few seconds long meant that the mice had enough training with serial reward reversals to anticipate that only following the rewarded choices leads to consumption of enough water across sessions. However, omissions become more informative after transition reversals, where they would not only signal the location of the more highly rewarded port, but also that the previously used transition structure was no longer relevant. Not learning the new structure quickly comes at a greater cost of losing many rewards in a session and no longer getting enough water as the mouse was used to before the transition reversal, so the frustrative value of omissions would be expected to increase.

It may be surprising that mice do not include learning from omissions to begin with, as not accounting for omissions is like adapting your learning on

exams based only on the correct answers and ignoring all the wrong answers. But, if a more complex decision-making strategy has only limited advantages, animal subjects have been shown to be more likely to switch to simpler strategies that require less cognitive effort, even if that means they obtain rewards at chance levels (Akam et al., 2015). For the mice in the two-step task, the cost of errors in reward reversals is not high, so animals do not care about omissions as they still solve the task to a very high success rate using learning only from rewarded trials. After transition reversal, the cost of errors is arguably much higher as overall success is decreased such that animals were getting fewer rewards across the session – they did not solve the task well enough to get as many rewards as they used to. The higher cost and motivational demand could be driving the change in strategy to include not only the experience of rewards but also of omissions.

Animals solving the original two-step task structure, with fixed transition probabilities, appear strongly model-based because of their high loading on the *Transition X Outcome* predictor, but this loading is in large part due to inference-based learning instead, supporting rapid adaptation to reward reversals but not transition reversals (Blanco-Pozo et al., 2021). However, we show that mice were able to adapt to a suddenly changing transition structure, and that this adaptation may not have required a change in strategy. VEH-treated animals in both Group 1 and Group 2 were still able to relearn the correct structure by using the same choice strategy as before, at least based on the logistic regression models used in our analyses, but we cannot say how much a model- versus inference-based strategy accounted for that. DOI-treated animals in Group 2 did change their choice strategy to incorporate learning from omissions, but we cannot exclude

the possibility that additional variables became relevant too as we did not explicitly test different reinforcement learning models with factors such as different learning and forgetting rates.

Our goal was not a detailed characterization of specific strategies since the session-by-session post-reversal data in our two-step task study does not provide enough data to fit reinforcement learning models with many terms. Therefore, we cannot make claims that psychedelic treatment enhances model-based (or any other) strategy specifically. There can be no guarantee that, when faced with a decision-making task, a mouse adopts the same task representation and strategy that the experimenter had conceived. Not all aspects of the task and the subject's engagement with it can be directly observed, but they would nonetheless influence observable events. A latent-state and model-based strategy would be distinguishable only by reinforcement learning model fitting and simulations, as they would both result in a significant *Transition X Outcome* interaction with a gradually decreasing predictive weight at increasing lags. Our logistic regression analysis results could be reflecting an added influence of a latent-state strategy, but its relative contribution could not be ascertained.

4.4.c Remaining questions

If novel adaptability differences were correlated and simultaneous with reported increases in neuronal plasticity that are at their strongest in the first few days after drug treatment, then we would expect to have seen a stronger effect when testing novel adaptability in the initial days following drug treatment when presumably the DOI's effects on dendrite- and spinogenesis would be at their highest. But this was not the case – we saw no adaptability differences when a

transition reversal was tested one day after DOI injection. This pointed to a critical time component which we will argue is due to the consolidation of neuronal plasticity changes taking place in that timeframe (see chapter 5).

However, in the week before transition reversal in Group 2, the mice were still gaining additional experience on the task which did result in marginal non-drug related increases in the number of trials and reversals performed. We cannot exclude the possibility that this additional training also conferred some benefits via experience-dependent drug-induced plasticity mechanisms, rather than solely due to the consolidation of neuronal plasticity.

A drug by training effect would need to be tested in a new group of animals that still have one week between drug injection and the transition reversal, but during this week the mice would not undergo any further two-step task testing until the transition probabilities have changed. If the additional week of experience on an unchanged task, but with the experience of DOI, is what is necessary for improved adaptation to novel reversals, then we would not see a difference between DOI and VEH animals in the time curves of *Transition X Outcome* and *Omission by transition* predictors in this new experiment. If instead, the prolonged time frame of drug effects on its own is sufficient, without any further training and experience-dependent modulation, the effects would still be present even if the mice were kept from performing the task.

In order to make conclusions specifically to plasticity, we would have to employ methods that would block or decrease induction of neuronal plasticity, such as selectively ablating newly formed synapses in the days following DOI

treatment (Moda-Sava et al., 2019) or employing transgenic animals with deficient BDNF signalling, such as *BDNF* Val66Met polymorphism mice (Chen et al., 2008), to prevent induction of neuronal plasticity in the first place (at least of those processes requiring BDNF). Considering plasticity mechanisms employed by psychedelic drugs are varied, selective removal of specific plasticity events might not be sufficient, and removal of multiple forms of neuronal plasticity might quickly prove a losing battle due to the limitations of the methods available and the compounding effects on general brain function.

5 | The structural level: Regional brain volumes after DOI

In this chapter we report a whole-brain structural signature of post-acute changes in grey matter volume with DOI. High-plasticity state at the structural level should facilitate regional brain volume changes or white matter structure differences. Therefore, in these studies we tested whether DOI's induction of plasticity would, in the long-term, result in changes in brain volume and structure, here measured as volumetric differences with whole-brain magnetic resonance imaging.

5.1 Introduction

While we know how the acute psychedelic experience can affect the function of brain regions across the whole human brain (dos Santos et al., 2016a), and comparable results have also been found in rodents (Malkova et al., 2014; Spain et al., 2015; Grandjean et al., 2021), evidence for long-term structural changes is extremely limited. A human study that compared MRI-derived measures of cortical thickeness from individuals with no psychedelic experience to those from individuals who had long-term use of ayahuasca found cortical thickness changes in the posterior and anterior cingulate, and frontal gyri (Bouso et al., 2015), but we cannot know if a single dose could have similar effects. There has been no attempt so far to study long-term whole-brain structural plasticity resulting from a single psychedelic treatment in neither humans nor animals.

In vivo evidence of off-drug enhancement in neuronal plasticity within one day of psychedelic treatment has been found in several prefrontal cortical and sensory areas of mice. Following 1mg/kg of psilocybin, changes in spine

formation and density, as well as frequency of post-synaptic excitatory currents, were found in neurons in anterior cingulate (ACC), prelimbic (PrL) and infralimbic (IL) cortices and primary and secondary motor cortex (M1/2) (Shao et al., 2021). After 10mg/kg DOI, higher spine formation was observed across the primary somatosensory cortex (S1) (Cameron et al., 2021). Repeated administration of 2mg/kg DMT across three weeks led to increased neurogenesis in the dentate gyrus of mouse hippocampus, and this was associated with better performance in memory tests (Morales-Garcia et al., 2020). It remains unknown if acute single-dose activation and potentiation of neuronal plasticity is sufficiently high and/or extensive to lead to structural changes at the level of whole brain regions.

If neuronal plasticity changes are reflected at the level of the whole brain, regional volume changes should accompany increases in neuronal plasticity. To investigate whether such anatomical plasticity changes can be induced by a single dose of DOI, we performed *ex vivo* MRI (section 2.4), either one day after treatment (*Experiment 1* in the sub-acute phase) or three weeks after treatment (*Experiment 2* in the long-term phase) (Fig.5.1). We chose time points in the sub-acute and long-term phase because, based on the available literature (Ly et al., 2018; Cameron et al., 2021; Shao et al., 2021), neuronal plasticity is at its highest in the first few days after drug exposure (when we did not observe any cognitive changes that early, sections 4.3.b-d) but it begins to dissipate by the end of the first week post-drug. While we found cognitive differences due to DOI after the first week has passed (sections 4.3.e-h), we could only image the brains of these animals when they completed the behavioural testing required to show this cognitive effect, which could only be done three weeks after drug treatment at the

earliest. This allowed us to compare putative whole-brain structural plasticity with periods of known plasticity at lower (neuronal) and higher (cognitive) levels.

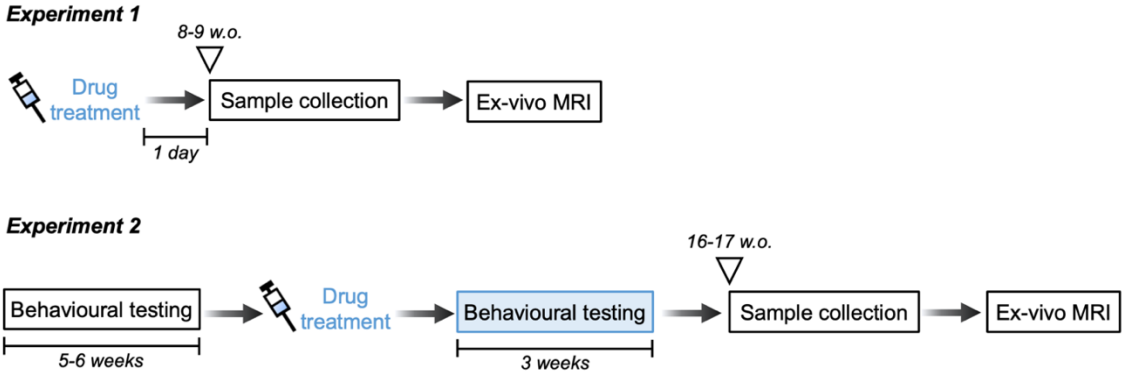


Fig.5.1 Experiment timelines. In **Experiment 1**, the brains for magnetic resonance imaging (MRI) were collected one day after drug injections with either saline vehicle or 2mg/kg DOI. In **Experiment 2**, the brain samples were collected from animals injected with either saline vehicle or 2mg/kg DOI three weeks before. These animals also underwent extensive behavioural training and testing both before and after drug treatment.

Lab mice maintained in the same environment have similar brain anatomy and there is low natural variability of regional brain volumes (Badea et al., 2007), but MRI signals can be altered by changes in neuronal structure at the level of dendrites and synapses (Golub et al., 2011; Lerch et al., 2011; Keifer et al., 2015). Our study is the first MRI study of long-term drug-induced structural plasticity applied to rodents treated with a psychedelic drug.

5.2 Methods

These experiments were a collaborative effort with Dr. Alberto Lazari and the lab of Prof. Jason Lerch. The contributions to outlined work are given in Table 5.1.

Table 5.1 Contribution to work outlined in chapter 5. MRI acquisition was delegated due to restricted access to the animal facility during the COVID-19 lockdowns. All the steps were supervised by Prof. Jason Lerch.

Experiment design	M.Š.
Sample collection	M.Š. *Training and supervisions by:* Lily Qui Claire Bratley
MRI acquisition	Claire Bratley Mohamed Tachrount Urs Schuffelgen Antoine Cherix Clemence Ligneul
Quality control	Alberto Lazari
Analysis	Alberto Lazari M.Š.
Visualizations	M.Š.

5.2.a Animals

Care and testing of all animals were conducted under the Animal (Scientific Procedures) Act 1986, United Kingdom, and the Local Ethical Review Committee at the University of Oxford. Wild-type JAX^{TM} C57BL/6J (Charles River, Strain Code 632) male mice (N=42) were used in all experiments. Housing and care were as outlined previously (sections 3.2.a and 4.2.a).

For Experiment 1, we performed the studies on sub-acute structural effects on the brains collected from a subset of animals (N=16, n_{group}=8) undergoing procedures outlined in chapter 3. The brains were collected one day (24-36h) after drug treatment with either saline or 2mg/kg DOI. These animals were between 8- and 9-weeks-old at the time of tissue collection. Several practical issues limited the number of animals used in the sub-acute study. Four out of eight animals used in the 2mg/kg DOI group were the subjects for which

there were no behavioural data available due to a technical failure. These animals were excluded from our analyses in section 3.3 but are nonetheless included here in the analysis of structural plasticity. However, we could not assess any correlations with behavioural outcomes. The animals were injected in either familiar or novel environmental context, but this study was not powered enough to test for any putative effect of the treatment environment. However, the treatment groups were fully balanced in terms of exposure to novelty and habituation – 4 out of 8 animals in each treatment group were treated in a novel environment, with the other 4 treated in a familiar environment.

In Experiment 2, we studied the long-term structural effects of DOI based on a subset of animals (N=26, n_{group}=13) undergoing procedures outlined in chapter 4. All animals underwent 9-10 weeks of two-step task testing (Group 2, as described in Fig.4.2, since these were the animals exhibiting significant cognitive differences due to DOI). The brains could be collected only after behavioural testing was completed, three weeks after drug treatment with either saline or 2mg/kg DOI. These animals were kept under water restriction for behavioural testing, so the brain samples were collected one day after the completion of behavioural testing and taking the mice off water restriction. These animals were between 16- and 17-weeks-old at the time of tissue collection. While all the samples were successfully scanned, ongoing registration issues with six samples prevented us from including them in the analysis reported here. The final sample sizes are N=20, n_{VEH}=10, n_{DOI}=10.

There was not enough prior information available to allow for predictions of specific effect sizes, so our power analysis check was focused on sensitivity

for detecting an at least 3% change in volume. Based on published power analyses, we judge that we were expected to be able to have 80% power for recovering volume differences around 10% using eight mice at the explorative significance levels of 20%, but at the stringent 5% significance threshold our power was likely under 80% (Lerch et al., 2012).

5.2.b Transcardiac perfusion and sample storage

Mice were anaesthetized via IP injection of 10mL/kg body weight of 150mg/kg ketamine and 10mg/kg xylazine in saline. The time between ketamine injection and death through perfusion was a maximum of 10-15min, so we believe that there was not enough time for ketamine's own neuronal plasticity-promoting effects to impact our findings. The first perfusion flush was 30mL of phosphate-buffered saline (PBS), 1µL/mL of heparin, and 2mM of Gadovist contrast administered at a rate of 1mL/min. A second flush was 30mL of 4% paraformaldehyde aqueous solution (PFA) and 2mM of Gadovist in PBS administered at a rate of 1mL/min. The low perfusion rate minimizes fixation artefacts (Cahill et al., 2012). Gadovist is a gadolinium-based contrast agent that reduces T1 relaxation time for improved SNR (Johnson et al., 2002). After perfusion, the mouse was decapitated and extracranial tissue removed, leaving the brain inside the skull. The presence of the skull preserves brain structure by limiting post-fixation structural changes, exposure to the surrounding medium, and tissue deformation due to handling.

5.2.c Sample storage and preparation

Perfusion fixation was followed by immersion in fixative to ensure the distribution of the fixative and contrast agent through the tissue and the formation

of protein cross-links (Thavarajah et al., 2012). The skull structure was soaked in a solution of 4% PFA and 2mM Gadovist overnight at 4°C, then transferred to a solution of 2mM Gadovist in PBS and 0.02% sodium azide. Leaving the brain and skull in the contrast-containing solution enables diffusive distribution of the contrast agent. Sodium azide additive improves cellular preservation and enhances deeper fixative penetration (Minassian and Huang, 1979). The samples were stored at 4°C until MRI acquisition, for a minimum of one month.

Pre-scanning sample preparation involved first placing the samples in a vacuum pump for 30-60min to remove any intracranial air-bubbles formed during storage. Any residual PBS was removed, and the sample was transferred to a holder filled with Fluorinert, a proton-free solution which minimizes MRI susceptibility artefacts. Samples were then kept at room temperature for 24h before scanning and during the acquisition. Following sample positioning in the scanner, a short multi-gradient echo (MGE) sequence was acquired to check for any remaining air-bubble artefacts. MGE sequence parameters were: 20 echoes, TE=3ms, 3ms inter-echo spacing, 200μm isotropic voxel resolution, and 120 X 40 X 55 matrix size.

5.2.d Image acquisition

MRI data were acquired with a 7T field strength Bruker BioSpec® 70/20 USR multipurpose high field MR scanner for preclinical research with a receive-only CryoProbe (Bruker BioSpin) coil. Three types of acquisitions were obtained in a one-sample overnight (~14 hour) imaging session: (1) a T2-weighted structural scan, (2) a multi-shell diffusion-weighted imaging (DWI) session, and 3) a gradient multi-echo quantitative susceptibility mapping (QSM). Acquisition

parameters are detailed in Table 5.2. As we have not discovered any drug-related changes in our DWI and QSM scans (linear model for the main drug effect was not statistically significant), only DBM results of grey-matter changes are discussed in this report (see discussion on white matter plasticity in section 5.4.d).

Table 5.2 Acquisition parameters for the *ex vivo* MRI. The protocol consisted of a single overnight scan with three modalities, a T2-weighted structural scan, diffusion-weighted imaging (DWI), and quantitative susceptibility mapping (QSM). TE: echo time. TR: repetition time. BW: bandwidth. TSE RARE: turbo spin echo rapid acquisition with relaxation enhancement. EPI: echo-planar imaging. δ: diffusion gradient duration, Δ: diffusion gradient separation. MGE: multi-gradient echo. FA: flip angle.

Modality	Voxel / matrix	Parameters	*TE*	*TR*	*BW*	Time
T2	60µm isotropic 400 X 160 X 200	TSE RARE 12ms echo spacing 6 echoes	12ms	350ms	60kHz	33min
DWI	100µm isotropic 240 X 96 X 120	segmented EPI 12 segments δ/Δ 6.7/13.5ms b = 0 s/mm^2 (4+1 phase-encoding reversed volumes) b = 2,500 s/mm^2 (volumes: 30) b = 10,000 s/mm^2 (volumes: 30) whole-shell and staggered directions	30ms	500ms	250kHz	13h
QSM	100µm isotropic 240 X 96 X 120	3D MGE FA = 15° 3ms echo spacing 20 echoes 2 repetitions	3ms	68ms	250kHz	26min

Quality control and pre-processing procedures were used to detect and correct artifacts (e.g., Gibb's ringing in T2 images) and to exclude those that could not be corrected, providing consistency for reliable deformation estimates. For some samples, persistent air-bubble artifacts required re-scanning.

5.2.e Analysis and statistics

Image analysis and visualization was performed using the RMINC library (https://mouse-imaging-centre.github.io/RMINC/) to R (R Foundation for Statistical Computing, https://www.R-project.org/) (Lerch, 2014). The experimenter was not blinded to group assignments during sample collection or during statistical analysis. The registration pipeline included alignment of all study samples onto the same coordinate space such that corresponding anatomical features are superimposed. We used the Mouse Build Model (MBM) pipeline from Pydpiper (Friedel et al., 2014) for non-linear deformation, required to align an individual sample image to the registered study average image (Fig.5.2), and to extract Jacobian determinants (JD) computed after smoothing the deformation fields. JDs are the measure of local volume change at a voxel level.

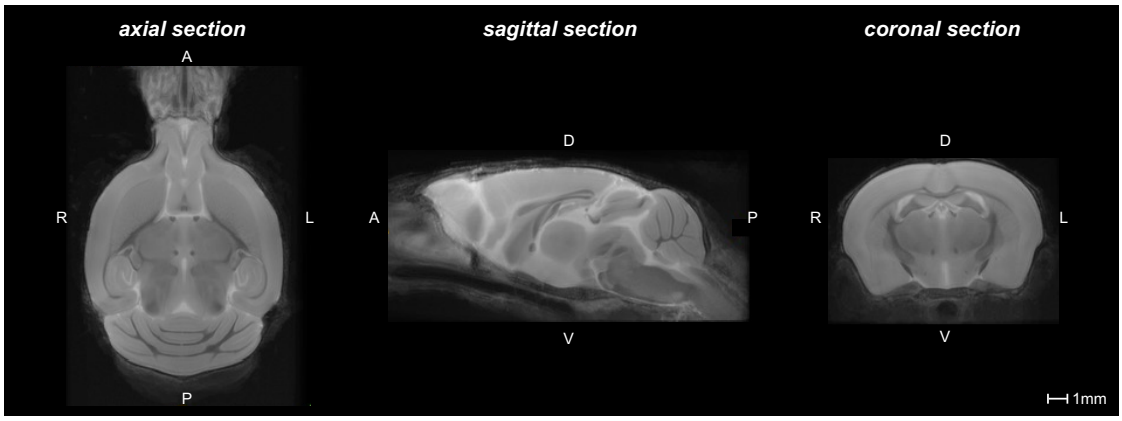


Fig.5.2 The registered T2-weighted study template. The study template is the average of all study samples that all individual subjects' samples are spatially registered to for the purpose of calculating the Jacobian deformation fields. This study template is based on samples taken one day after a DOI injection. A: anterior. P: posterior. D: dorsal. V: ventral. R: right. L: left.

In the voxel-wise analysis, an ANOVA for the main effect of the drug was computed at every voxel. To assess the relative differences across the groups, a *t*-test was computed at every voxel comparing the VEH and DOI brains. Multiple

comparisons were controlled for using FDR with the Benjamini and Hochberg (1995) method at either the explorative 20% level (i.e., 20% of significantly different voxels at this FDR level would be, on average, false positives), or conservative 5% level (a 5% rate of false positives, on average).

The hierarchical tree using ontogeny from the Allen Brain Institute (http://mouse.brain-map.org/static/atlas) was used for region of interest (ROI)-wise analysis where JDs were computed to measure local volume changes at the level of each structure, for each hemisphere separately. ROI segmentations were all done based on the DSURQE atlas (Qiu et al., 2018) through the MAGET algorithm (Chakravarty et al., 2013). To assess differences across groups, an ANOVA for the main effect of the drug was then computed at each structure with a *t*-test at every ROI comparing the VEH and DOI brains. FDR multiple comparison correction was done using the Benjamin and Yekutieli (2001) method because this method remains viable in the presence of dependence underlying a hierarchical tree. Only the ROIs where significance was retained after controlling for multiple comparisons with 20% FDR were visualized on the resulting maps on the DSURQE atlas (Qiu et al., 2018).

5.3 Results

5.3.a Structural differences one day after drug treatment

To determine if we can localise anatomical sites where DOI induces structural changes in the brain's grey matter, we used *ex vivo* MRI to image samples collected one day after treatment with a single 2mg/kg dose of DOI. The *F*-statistics representing the significance of the linear model for segmented

whole-brain ROIs were $F_{1,14}$= 12.19 at q<0.20 and $F_{1,14}$= 23.30 at q<0.05. The marginal t-statistic threshold at 20% FDR was t_{14}=3.49. The resulting map (Fig.5.3) showed that DOI-treated animals exhibited significant volume increases in grey matter, compared to the vehicle-treated controls, in sensory and posterior association cortex, particularly in the left hemisphere. Specifically, these were: left primary visual cortex (V1), left temporal association area (TeA), shoulder region of the left primary somatosensory cortex (S1Sh), trunk region of the left S1 (S1Tr), left retrosplenial area (RSA), left lateral parietal association cortex (LPtA), left ventral secondary auditory cortex (AuV), and left lateral secondary visual cortex (V2L). The enlargements ranged from 6.2% in RSA to 15-16.7% in shoulder and trunk areas of S1 (Fig.5.4, Table 5.3). At the conservative 5% FDR (t_{14}=4.83), left V1 and left TeA retained their significance, making these the most statistically robust drug-related differences.

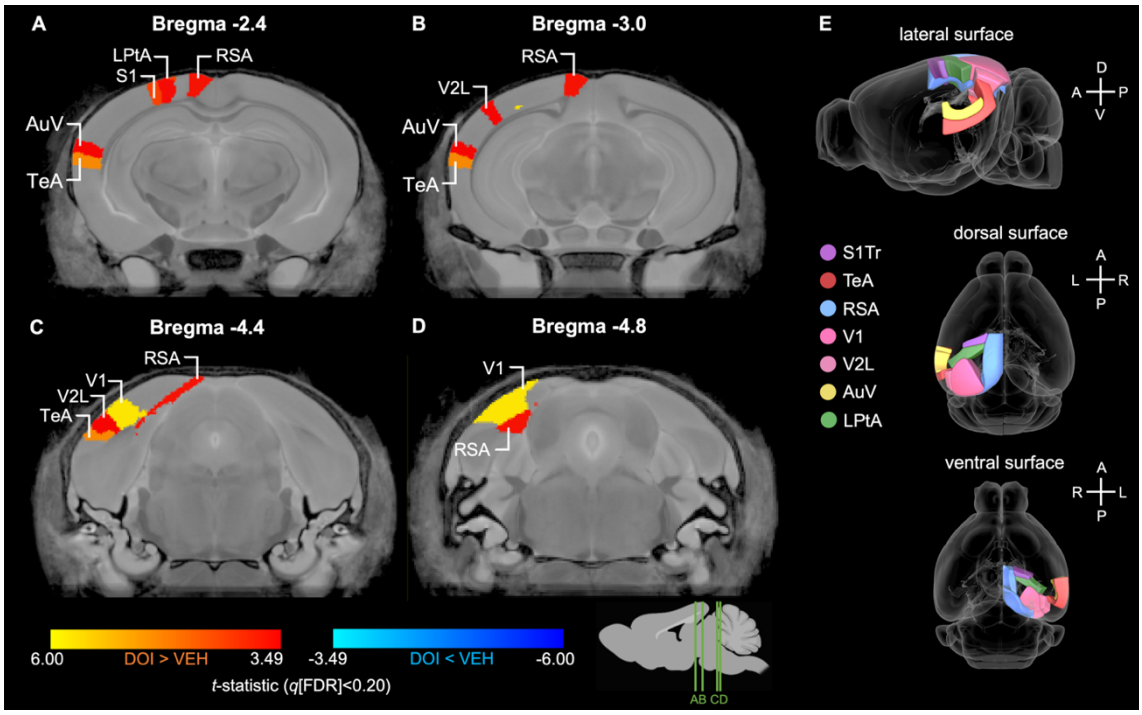


Fig.5.3 *legend on the next page*

Fig. 5.3 In one day, DOI increased the volume of several sensory and association areas. The False Discovery Rate (FDR) correction with q<0.20 resulted in the marginal t-statistic threshold=3.49. **(A-D)** Volume increases were found in: primary visual area (V1, t=5.75) and temporal association area (TeA, t=4.83) survived the strict q<0.05 (threshold t-statistic=4.83). Other significant differences were in primary somatosensory area (S1), specifically the shoulder (Sh) and the trunk (Tr) regions, retrosplenial agranular area (RSA), lateral parietal association area (LPtA), ventral secondary auditory area (AuV), lateral secondary visual cortex (V2L). n_{group}=8. The distances from bregma are based on the Scalable Brain Atlas (Bakker et al., 2015). **(E)** 3D brain anatomy images with significant regions highlighted. A: anterior. P: posterior. D: dorsal. V: ventral. L: left. R: right. Images created using the Scalable Brain Atlas 3D brain composer.

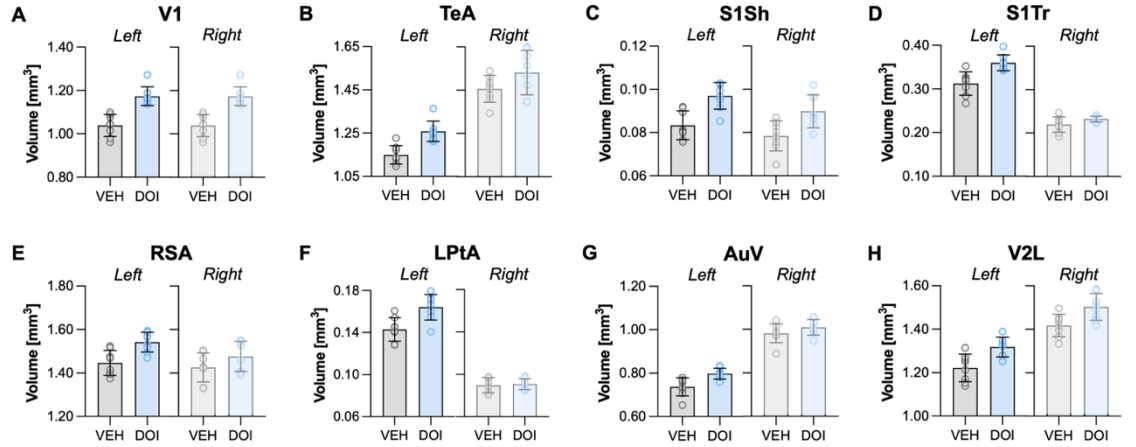


Fig.5.4 A post-hoc visualization of all regions which exhibited a significant volume change one day after DOI treatment. Significant differences were found only in the left hemisphere, but values of the corresponding right structures are given for reference. **(A)** Primary visual cortex (V1). **(B)** Temporal association area (TeA). **(C)** Shoulder region of the primary somatosensory cortex (S1Sh). **(D)** Trunk region of the primary somatosensory cortex (S1Tr). **(E)** Retrosplenial area (RSA). **(F)** Lateral parietal association area (LPtA). **(G)** Ventral secondary auditory cortex (AuV). **(H)** Lateral secondary visual cortex (V2L). Data shown as mean with SD error bars. Each data point represents volumetric data from one mouse (n_{group}=8). Regions shown were selected post-hoc based on a whole-brain analysis, and data is therefore shown for visualisation purposes only, rather than for statistical inference.

There were two unexpected aspects of the results. First, all significant changes only appeared for ROIs in the left hemisphere. To investigate hemispheric differences further, we examined the changes in homologous right hemisphere ROIs (Fig.5.4, Table 5.3). However, the only area where the mean difference was close to the marginal t-statistic threshold at 20% FDR was the shoulder region of S1 (t_{14}= 3.13). Second, it was noticeable that no PFC regions (Fig.5.5) reached significance, even though previous studies have suggested that

PFC and S1 are the main sites of psychedelic effects on neuronal plasticity based on the levels of 5-HT_{2A}R density (Ly et al., 2018, 2020; Shao et al., 2021). To investigate both characteristics further, we turned to voxel-wise analysis (Fig.5.6).

Table 5.3 Regional volume differences one day after DOI treatment. False discovery rate (FDR) threshold was set to q<0.20. The first column is the left or right region of interest (ROI) term, in decreasing order of significance: primary visual area (V1), temporal association area (TeA), primary somatosensory areas (S1) of the shoulder (Sh) and the trunk (Tr), retrosplenial area (RSA), lateral parietal association area (LPtA), ventral secondary auditory area (AuV), and lateral secondary visual area (V2L). The following columns are: drug effect t-statistics (degrees of freedom given in brackets), corresponding FDR-corrected q-values, the mean volumes for the DOI and control (VEH) group with 95% confidence intervals (CIs) shown as [lower limit, upper limit], and the approximate volume change compared to VEH (if q<0.20).

			VEH		*DOI*		
ROI	***t*(14)**	***q* value**	**Mean [mm³]**	**95% CI**	**Mean [mm³]**	**95% CI**	***% change***
Left V1	5.75	0.016	1.04	[1.00, 1.08]	1.17	[1.14, 1.21]	+12.5
Left TeA	4.83	0.043	1.15	[1.11, 1.19]	1.26	[1.22, 1.30]	+9.6
Left S1Sh	4.25	0.079	0.083	[0.078, 0.089]	0.097	[0.092, 0.102]	+16.7
Left S1Tr	4.15	0.079	0.313	[0.290, 0.335]	0.360	[0.345, 0.374]	+15.0
Left RSA	3.68	0.145	1.45	[1.40, 1.49]	1.54	[1.50, 1.58]	+6.2
Left LPtA	3.61	0.145	0.143	[0.134, 0.152]	0.164	[0.154, 0.174]	+14.7
Left AuV	3.53	0.145	0.737	[0.700, 0.772]	0.798	[0.777, 0.819]	+8.3
Left V2L	3.49	0.145	1.22	[1.17, 1.27]	1.32	[1.28, 1.36]	+8.2
Right S1Sh	3.13	0.240	0.078	[0.073, 0.084]	0.090	[0.083, 0.096]	ns
Right V2L	2.99	0.240	1.42	[1.37, 1.46]	1.50	[1.45, 1.56]	ns
Right V1	2.61	0.414	1.17	[1.12, 1.21]	1.26	[1.19, 1.33]	ns
Right S1Tr	1.88	0.808	0.220	[0.205, 0.235]	0.233	[0.227, 0.238]	ns
Right TeA	1.79	0.808	1.46	[1.41, 1.51]	1.53	[1.45, 1.62]	ns
Right RSA	1.48	0.808	1.43	[1.37, 1.48]	1.48	[1.42, 1.53]	ns
Right AuV	1.38	0.808	0.981	[0.945, 1.018]	1.009	[0.979, 1.040]	ns
Right LPtA	0.34	0.894	0.090	[0.084, 0.096]	0.091	[0.086, 0.095]	ns

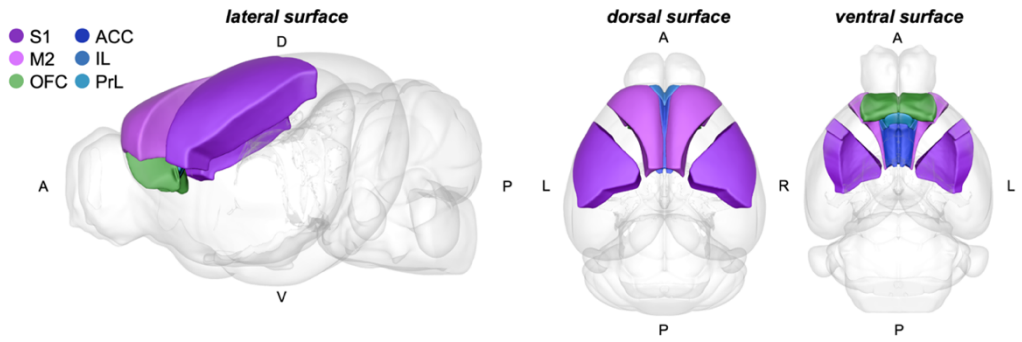


Fig.5.5 *legend on the next page*

Fig.5.5 Previous studies (Ly et al., 2018; Cameron et al., 2021; Shao et al., 2021) **reported psychedelic-induced cellular plasticity changes in the prefrontal cortex (PFC) and primary somatosensory cortex (S1) of rodents.** Subdivisions of mouse PFC shown here are secondary motor areas (M2), orbitofrontal cortex (OFC), anterior cingulate area (ACC), infralimbic cortex (IL), and prelimbic cortex (PrL). Images created using the Scalable Brain Atlas 3D brain composer. A: anterior. P: posterior. D: dorsal. V: ventral. L: left. R: right.

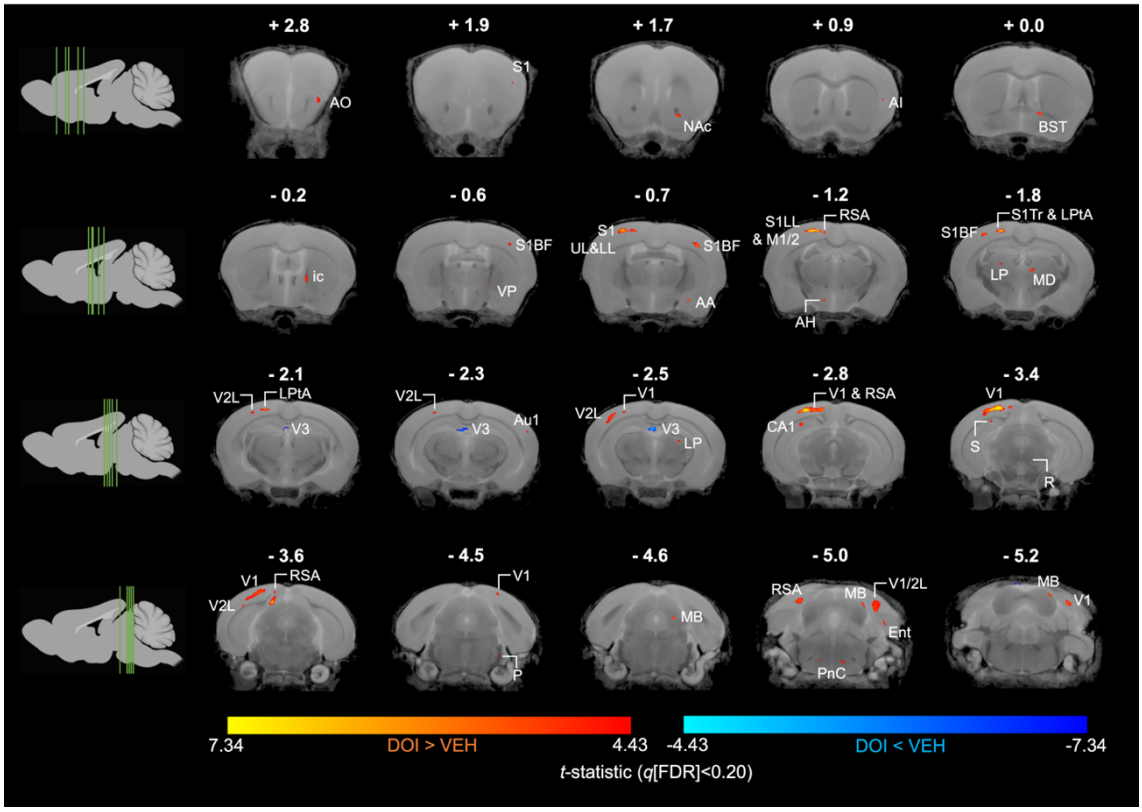


Fig.5.6 DOI-induced voxel-wise differences one day after treatment. The False Discovery Rate (FDR) correction was applied to whole-brain voxel-wise linear model analysis with an exploratory $q<0.20$ resulting in the marginal t-statistic threshold =4.43. All significant changes were volume increases ($t>0$), except for the third ventricle (V3). The maximum range of the colour legend represent the threshold t-statistic =7.34 at the strict $q<0.05$ to visualize which voxels pass the strict criterion. The distances from bregma are based on the Scalable Brain Atlas (Bakker et al., 2015). AA: anterior amygdaloid area. AH: anterior hypothalamic nuclei. AI: agranular insular area. AO: anterior olfactory nucleus. Au1: primary auditory cortex. BST: bed nucleus of stria terminalis. CA1: field CA1 of hippocampus. Ent: entorhinal cortex. ic: internal capsule. LP: lateral posterior thalamic nuclei. LPtA: lateral parietal association area. M1: primary motor area. M2: secondary motor area. MB: midbrain. MD: mediodorsal thalamic nuclei. NAc: nucleus accumbens. PnC: caudal pontine reticular nucleus. R: red nucleus. RSA: retrosplenial area. S: subiculum. S1: primary somatosensory cortex; BF barrel field, UL upper limbs, LL lower limbs, Tr trunk. V1: primary visual cortex. V2L: lateral secondary visual cortex. VP: ventral pallidum. $n_{group}=8$.

The main effect of drug treatment was significant at $q<0.20$ ($F_{1,14}= 19.61$) and at $q<0.05$ ($F_{1,14}= 53.84$). The marginal t-statistic threshold at 20% FDR was $t_{14}=4.43$. The resulting maps showed again a consistent pattern of volume increases in the DOI group; the only decreased voxels were in parts of the third ventricle. The voxels which crossed the 5% FDR threshold ($t_{14}=7.34$) were localized to the left V1 and posterior areas of left RSA.

Regarding our first question about left hemisphere asymmetry, this was not the case in voxel-wise comparisons – most of the significantly different left ROIs also had significantly different voxels in the right hemisphere. Namely V1, S1, and V2L had bilateral differences in local volumes. In contrast, RSA and LPtA had significantly different voxels only in the left hemisphere.

Regarding our second question about volume changes in PFC, we observed significantly increased voxels in small parts of the secondary motor cortex (M2), but none in the cingulate, prelimbic, and orbitofrontal areas. A summary of all brain regions where significant voxel-wise differences were found, including notes on any hemispheric asymmetry, is given in Table 5.4.

5.3.b Structural differences three weeks after drug treatment

To determine if DOI's ability to induce volumetric changes in the brain's grey matter persists in the weeks after treatment, we imaged brain samples collected three weeks after treatment with 2mg/kg DOI. These animals also underwent the two-step task testing where they showed higher cognitive adaptability post-DOI (chapter 4). For the segmented whole-brain ROIs, the linear model for the main drug effect was not statistically significant at $q>0.20$. Local

differences in voxel-wise analysis were also not significant at $q<0.20$. For comparison, we visualized the regional brain volumes for ROIs that showed significant differences in Experiment 1. As can be observed, in all cases the DOI and vehicle regional volumes were very similar (Fig.5.7). We could not directly compare Experiment 1 and experiment 2 due to a marked difference in age of the animals at the time of brain collection (9 vs. 17 weeks old) which would affect the deformations required for the study template.

Table 5.4 Regions showing significant voxel-wise differences in brains taken one day after DOI treatment. The regions are shown as those who had significantly different voxels at FDR=20% only in the left or right hemisphere, or if significant voxels were spread across both hemispheres. Regions shaded in blue were also significantly different in our analyses based on regions of interest.

Region	*Left*	*Right*
Primary somatosensory cortex	Y	Y
Primary visual cortex	Y	Y
Lateral secondary visual cortex	Y	Y
Lateral posterior thalamic nuclei	Y	Y
Caudal pontine reticular nucleus	Y	Y
Retrosplenial agranular area	Y	N
Lateral parietal association area	Y	N
Primary/secondary motor cortex	Y	N
CA1 of hippocampus	Y	N
Subiculum	Y	N
Anterior olfactory nucleus	N	Y
Nucleus accumbens	N	Y
Agranular insular area	N	Y
Anterior amygdaloid area	N	Y
Primary auditory cortex	N	Y
Bed nucleus of stria terminalis	N	Y
Entorhinal cortex	N	Y
Mediodorsal thalamic nuclei	N	Y
Midbrain reticular nucleus	N	Y
Pallidum	N	Y

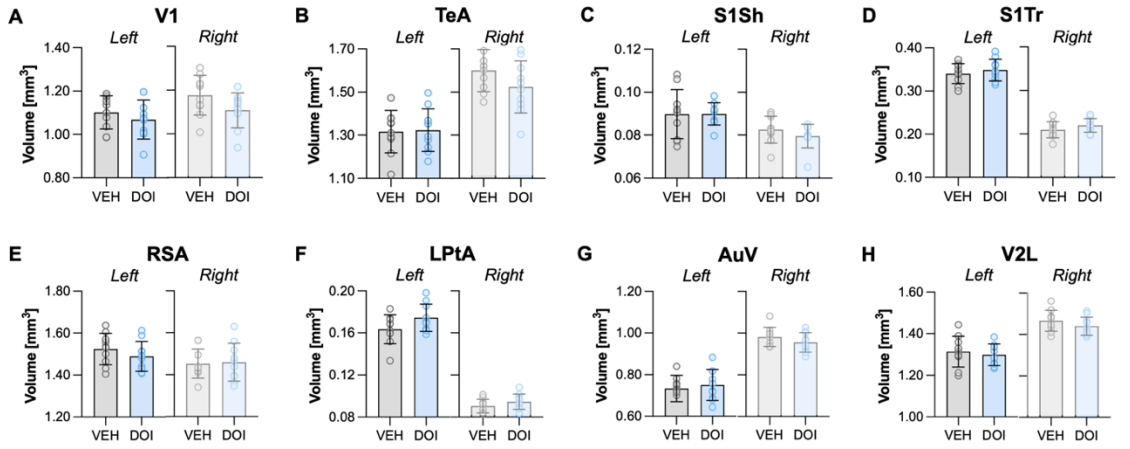


Fig.5.7 All regions which exhibited a significant volume change one day after DOI treatment had comparable volumes in brains taken three weeks after treatment. Note that the animals whose brains were taken at the three week point also underwent extensive behavioural testing in a decision-making task both before and after drug treatment. **(A)** Primary visual cortex (VISp). **(B)** Temporal association area (TEa). **(C)** Shoulder region of the primary somatosensory cortex (SSp-sh). **(D)** Trunk region of the primary somatosensory cortex (SSp-tr). **(E)** Retrosplenial area (RSP). **(F)** Lateral parietal association area (PTLI). **(G)** Ventral secondary auditory cortex (AUDv). **(H)** Lateral secondary visual cortex (VISl). Data shown as mean with SD error bars. Each data point represents volumetric data from one mouse (n_{group}=8). Regions shown were selected post-hoc based on a whole-brain analysis, and data are therefore shown for visualisation purposes only, rather than for statistical inference.

5.4 Discussion

In this study, we investigated putative increases in regional brain volumes in the weeks following psychedelic treatment. We asked whether DOI's effects on neuronal plasticity, previously shown as increased dendritic branching and spinogenesis that occurs in the days after treatment (Ly et al., 2018; Cameron et al., 2021), would be strong and/or extensive enough to result in regional brain volume increases in the same period. Using multimodal *ex vivo* imaging, we measured grey matter plasticity using T2-weighted MRI. We showed how mice injected with 2mg/kg DOI had significant increases in regional brain volumes of

midbrain sensory and association cortices, as well as the retrosplenial cortex, only when brains were sampled at the start of the sub-acute phase, one day after drug injection (Fig.5.3). Alternatively, when we imaged brain samples taken three weeks after drug injection, in the long-term phase of DOI action, following behavioural training, regional volume differences were not statistically different compared to the controls (Fig.5.7).

5.4.a Grey matter plasticity

The significant volume differences we observed were not in the frontal cortex (Fig.5.5), but in the primary sensory and association cortices found in the more posterior parts of the cortex. While preclinical studies of neuronal plasticity have focused on the PFC, due to its high density of 5-HT_{2A}R expression, the frontal cortex is not the only site of action for psychedelic effects on brain function and structure, and 5-HT_{2A}R expression is high in other parts of the brain too, including, but not limited to: auditory cortex, entorhinal cortex, hippocampus, primary motor cortex, primary and secondary somatosensory cortex, striatum, claustrum, and pontine nuclei (Pompeiano et al., 1994; Hamada et al., 1998; Andrade and Weber, 2010). Additionally, DOI and other psychedelic are not selective 5-HT_{2A}R agonists, so regional expression of 5-HT_{2A}Rs is not the only requirement for pharmacological action. It is likely that cognitive and behavioural effects of psychedelic-induced plasticity are driven not only by the changes in the PFC, but by the rebalancing of how distinct regions, including but not limited to the frontal cortex, control each other.

As initially predicted, based on known neuronal structural plasticity effects (Ly et al., 2018; Cameron et al., 2021), the volume differences we

observed were all volume increases. We judge the partial decrease in the volume of the third ventricle not to be indicative of any major effect of DOI on CSF levels or ventricle structure, since ventricular volume is highly susceptible to fixation and storage artifacts in *ex vivo* samples. Fixation alters tissue volume and shape, and these changes are non-uniform in their extent and time-course (de Guzman et al., 2016). While grey matter tissue shrinks, ventricles and other CSF spaces expand. There is very little substance inside the ventricles to maintain their shape, so the ventricles are emptying or filling according to pressures from the surrounding grey matter tissue. We note that the voxel-wise maps (Fig.5.6) do not show significance across TeA and AuV as they do for other significantly different ROIs. These kind of discrepancies between voxel-wise and ROI analyses are not unexpected because of how the data is pooled and corrected for. Lack of significant voxels in TeA and AuV could just be an effect of ROI analyses being less stringent, in the sense that there are fewer multiple comparisons to correct for (instead of correcting for each voxel, corrections are made for each ROI). ROI analysis may have pooled together a lot of voxels that had subtle effects individually, such that they were not significant in the voxel-wise comparisons, but once the deformations are averaged across the entire ROI, they become significantly different in the ROI analysis.

Although showing that psychedelics can change brain volume rapidly in a matter of one day is novel, some of the regions in which these changes occur have already been shown to be affected by psychedelics acutely in earlier functional studies (Malkova et al., 2014; Spain et al., 2015). Both of these studies were performed during the acute phase of psychedelic drug action, either using

(i) functional MRI in the first 45min after injection of psilocybin (Spain et al., 2015) or (ii) manganese-enhanced MRI 1h after injection of DOI (Malkova et al., 2014). While the findings of these studies on acute psychedelic-induced changes were obtained over a very short time interval when changes in plasticity were unlikely to occur, they point to the areas of the brain whose activity was modified by the psychedelic drug. This acute activation/inhibition could be what selects specific circuits for the induction of structural and functional plasticity in the next phase. To see if there was any overlap between the areas whose activity was modulated by psychedelics acutely and those that exhibited structural changes, we compared our findings to these earlier studies and noticed that the somatosensory and motor cortex, areas that also exhibit neuronal plasticity changes due to DOI and psilocybin (Cameron et al., 2021; Shao et al., 2021), were implicated across both functional studies and our structural (Fig.5.8).

The ROIs exhibiting significant volume differences would be potentially consistent with the possibility of visual and auditory psychedelic changes. We measured the mouse psychedelic-like behaviours, head twitches and ear scratches (section 3.3.b), but we cannot know the sensory origin of these responses and compare them to psychedelic states as we know them in humans. Most of the sensory regions affected by DOI are highly conserved across species. Primary and secondary representations of auditory, visual, motor, and somatosensory areas, and association areas are common to all mammalian cortices (Krubitzer, 1995). Our results may therefore reflect the acute MRI activations observed in humans too (dos Santos et al., 2016a). Sensory psychedelic effects in humans can be described as either perception of absent

external stimuli (e.g., visual imagery of geometric shapes, such as spirals, lattices, tunnels, and cobwebs), or as misinterpretation of external stimuli in space and/or time. Psychedelic visual imagery is thought to be generated by the brain, as, in most cases, images are seen by both eyes and maintain their relative positions in the visual field with movement. Mathematical models of V1 based on anatomical evidence suggest that the geometry of psychedelic visual imagery is a direct consequence of the architecture and the retino-cortical map of V1 (Ermentrout and Cowan, 1979; Bressloff et al., 2002).

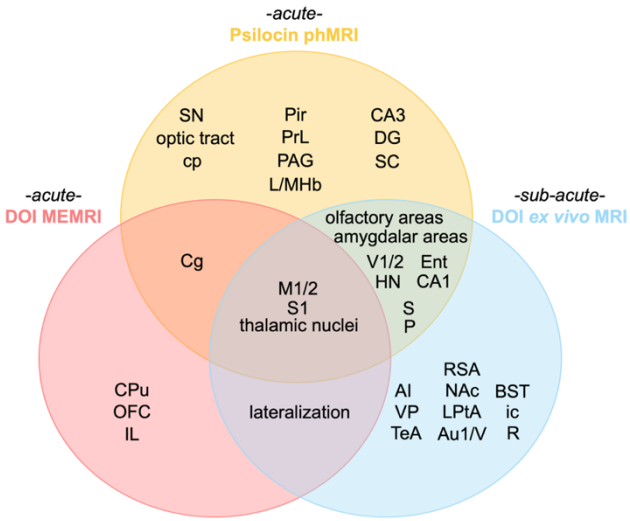


Fig.5.8 The overlap between brain areas that have shown psychedelic-dependent changes across two previous acute imaging studies and our results in the sub-acute phase. The overlapping results across all three studies are in primary and secondary motor cortices (M1/2), somatosensory cortex (S1), and various thalamic nuclei. There are overlaps with the acute psilocybin study (Spain et al., 2015) in olfactory and amygdalar areas, visual cortex (V1/2), hypothalamic nuclei (HN), subiculum (S), pontine nuclei (P), entorhinal cortex (Ent), and CA1 of hippocampus. The areas specific to the pharmacological MRI (phMRI) following psilocybin are substantia nigra (SN), optic tract, cerebral peduncle (cp), piriform cortex (Pir), prelimbic cortex (PrL), periaqueductal grey (PAG), lateral and medial habenula (L/MHb), dentate gyrus (DG), CA3 of the hippocampus, and superior colliculus (SC). The overlap between only the two acute studies is in cingulate cortex (Cg). The signal changes distinct to only the acute manganese-enhanced MRI (MEMRI) with DOI (Malkova et al., 2014) are in caudate putamen (CPu), orbital areas (OFC), and infralimbic area (IL). Lateralized effects are reported in both studies with DOI. Changes that are specific to our sub-acute study are in agranular insular cortex (AI), ventral pallidum (VP), temporal association area (TeA), the nucleus accumbens (NAc), lateral parietal association cortex (LPtA), primary and secondary ventral auditory cortex (Au1/V), bed nucleus of stria terminalis (BST), internal capsule (ic), red nucleus (R), and retrosplenial area (RSA).

In awake mice, 10mg/kg DOI administered SC was shown to acutely affect sensory processing in V1 neurons where DOI reduced the amplitude of visual responses and increased surround suppression (Michaiel et al., 2019). Similar findings were found in humans where psilocybin (Kometer et al., 2013) and LSD (Carhart-Harris et al., 2016a) induced an overall reduction in oscillatory synchronization in V1 too. While the temporal dynamics of visual responses were also affected in mice treated with DOI, the tuning properties and retinotopic organization of V1 remained intact (Michaiel et al., 2019). 10mg/kg SC dose is comparable to a 2.5mg/kg IP dose of DOI, so we can suppose that V1 responses were able to be affected acutely by the 2mg/kg DOI dose used in our study.

In addition to structural changes in sensory and association ROIs, we observed a significant volume increase in RSA. RSA has been mainly associated with spatial cognition in humans (Maguire, 2001) and in rodents (Czajkowski et al., 2013; Milczarek et al., 2018), but it is also implicated in processing of non-spatial information, specifically of subjective value representation, such as human representations of stable and consistent actions (Auger and Maguire, 2018). In mice who are trained to expert-levels in a value-based decision-making task, RSA representations of value-related signals were more stable than those in primary sensory and association cortices (Hattori et al., 2019). Acute inactivation of RSA inhibited a behavioural strategy based on reward history in that decision-making task, so the authors concluded that RSA supports adaptive behaviours via its involvement in stable encoding of value-related signals but flexible encoding of reward history (Hattori et al., 2019). RSA's role in reward-based decision-making is further warranted by its connectivity patterns – in rats, RSA is bidirectionally

connected to anterior cingulate cortex and central–medial OFC, and it projects to the dorsomedial striatum, a region involved in goal-directed decision-making (Monko and Heilbronner, 2021). Therefore, more recently, RSA is suggested to have a fundamental role in model-based decision-making (de Barros et al., 2021) based on experiments in mice showing RSA is necessary for both spatial and non-spatial latent/inference learning, which refers to the ability of a learning agent to create internal models of the world based on hidden, i.e., not explicitly reinforced, associations (see section 2.3 for explanation of inference learning).

Acute and post-acute activation of RSA, and possibly other decision-making circuits, would help explain psychedelic effects on performance in decision-making tasks such as the two-step task we used to measure cognitive flexibility. While RSA volume was not significantly different in the animals tested on the two-step task, because structural plasticity possibly normalized by the three-week time point at which the brains were sampled, transient structural remodelling in the post-acute period could be providing the foundation for improved model-based and inference learning. In chapter 6 we will compare the timelines of neuronal, regional, and cognitive plasticity in closer detail. A significantly greater RSA volume was not required for cognitive performance enhancements of DOI, so the role of transient structural remodelling is possibly to rewire and reprogram, but not to maintain more complex dendritic arborization and spine dynamics in the long-term.

Lastly, we wanted to comment on the significant voxel-wise volume increases in PnC. We discussed earlier (section 2.1) how the HTR mouse model of acute psychedelic effects is similar to the pinna reflex, a type of an acoustic

startle response (ASR). ASR is a behavioural reflex evoked by abrupt, intense sounds, a universal phenomenon in animals and in humans (Landis and Hunt, 1939). A key brain region involved in ASR is the PnC whose responses clearly parallel the latency, response threshold, and response sensitivity of ASR (Carlson and Willott, 1998). Our results suggest that PnC is a site of psychedelic-induced plasticity, raising the possibility that PnC is also acutely activated by psychedelics, furthering the similarities between HTR and the ASR.

We cannot be sure that the significant regional volume changes we observed were due to the DOI's action within those regions or elsewhere. We administered DOI systemically, so we cannot determine if local pharmacological action in V1 or RSA or any other ROI would be sufficient to drive the structural changes, or whether other regions and the pharmacological activation of the brain as a whole would be contributing to the observed effects. Nonetheless, none of the significant volume changes we observed one day after DOI injections were present in brains taken three weeks after DOI treatment, signalling that regional structural plasticity diminished and/or returned to the pre-drug levels in the long-term phase of the drug. The potential reasons for such effects will be discussed in section 6.1.c.

5.4.b Asymmetry of regional volume changes

Our findings of left-right asymmetry in volumetric differences replicate a previous report that demonstrated regional volume asymmetry in the thalamus, sensorimotor, and visual cortex in 12-week-old male C57BL/6 mice (Spring et al., 2010). This report showed smaller right compared to the left hemisphere volumes for each of these structures, after correcting for the observation that the left

hemisphere was significantly larger by 2.8% than the right. A greater regional volume may be more susceptible to drug-related changes, due to a floor-effect of smaller volumes and a likely smaller population of cells that can undergo structural plasticity changes. We did not explicitly analyse for hemispheric volume differences so we cannot make statistical inferences from our post-hoc ROI maps in Fig.5.4, we can only note trends. A smaller right hemisphere volume was suggested only for the trunk region of S1, and LPtA, among the ROIs whose left component was significantly different due to the drug.

The two brain hemispheres differ in their structure, function, and neurochemistry in humans and in other mammals, including mice (Toga and Thompson, 2003). Cerebrocortical asymmetry in rodents is known to be dictated by age, but also by sex and the environment (Diamond et al., 1983; Zilles et al., 1996). It is not unlikely that drug-induced regional changes could also affect the degree and/or the direction of hemispheric asymmetries, especially at an age that is characterized by lateralization (Spring et al., 2010). The brains we imaged in Experiment 1 were taken from 9-week-old mice and age-dependent lateralization in frontal and prefrontal areas, with lower right hemisphere volumes, has been shown in C57BL/6 background mice as old as 13 weeks (Asan et al., 2021).

Lateralization of drug activation would not be due to drug metabolism because we used IP injections that lead DOI to be metabolized by the body and the brain systemically, despite the injection site being predominantly into the left lower quadrant of the abdomen. This is especially the case considering the rate of absorption with IP injections – IP-administered substances were detected in systemic circulation as quickly as 10s after injection, although precise timings

would be substance-dependent (al Shoyaib et al., 2020). It is also unlikely that there would be lateralized brain activation due to asymmetries in receptor binding and signalling. 5-HT receptor subtypes are expressed across both hemispheres and human positron emission tomography (PET) scan measures of 5-HT_{2A}Rs in healthy individuals have not shown significant hemispheric asymmetry in receptor density or binding (Cho et al., 1999). Densities of other neurotransmitter receptors, such as NMDA and AMPA, have also not shown significant directional asymmetry, at least when measured in rat sensorimotor cortex (Zilles et al., 1996). There has been a hypothesis that 5-HT preferentially activates the right hemisphere (Fitzgerald, 2012), but direct evidence supporting this has been mixed. It could be that regional lateralization in activity of other neurotransmitter systems such as dopamine and acetylcholine could affect the overall pattern of activation induced by psychedelics. Nonetheless, our voxel-wise analysis showed regional differences that were not only left-specific, but also right-specific and bilateral too.

5.4.c Possible mechanisms underlying the volume changes

In general, cellular processes that could underlie volume increases are: (i) increased number of neurons and/or their size, (ii) increased number of astrocytes and/or their size, (iii) increased neurogenesis and/or survival of new neurons (although this process may possibly only occur in the hippocampus), (iv) neuronal processes remodelling. Immunohistochemical staining for specific markers can reveal differences in these processes, namely: (i) staining for NeuN for number and size of neurons, (ii) GFAP marker for astrocytes (although, not all astrocytes express GFAP, or do so only weakly (Xu, 2018)), (iii) DCX marker of

young neurons, and (iv) GAP-43 marker of synapses (GAP-43 is expressed throughout the neuron but is higher in axon terminals and growth cones). While GAP-43 mainly targets presynaptic changes (Benowitz and Routtenberg, 1997; Namgung and Routtenberg, 2000; Holahan et al., 2007), post-synaptic changes are believed to occur in parallel and are as important for structural plasticity (Bourne and Harris, 2008). In a study on training-induced changes in healthy wild-type C57 mice, GAP-43 staining has been found to positively correlate with structure volume, while there were no correlations with the other three IHC measures, so neuronal processes remodelling was believed to be one of the main explanatory factors for MRI-detectable volume changes (Lerch et al., 2011). However, correlations cannot fully account for all cellular plasticity components and different correlations could be found for drug-induced changes, or in non-healthy animals.

The speed of volume changes, occurring within 24-36h of drug treatment, restrict the potential underlying processes to fast events such as dendritogenesis and spinogenesis, the events previously shown to be induced by DOI in this timeframe, both *in vitro* and *in vivo* (Ly et al., 2018; Cameron et al., 2021). Cortical and hippocampal volume increases occurring as quickly as after two days of exposure to enrichment were linked with increased expression of genes associated with axonogenesis, dendritic spine development, synapse structural plasticity, and neurogenesis, suggesting these processes can underlie the fast volume changes detected with MRI (Vousden et al., 2018).

Grey matter volume composition estimates for the human neocortex outline that volume is dominated by dendrites (30%) and axon collaterals (29%),

followed by neuronal cell bodies (7.8%) and synapses (6%) (Bennett, 2011). Rodent estimates made using the same approach were comparable: dendrites (26%), axon collaterals (29%), neuronal cell bodies (11%), and synapses (5.7%) (Kassem et al., 2013). We tried to use these estimates to calculate what volume changes would be expected based on the estimates of dendritogenesis and spinogenesis in previous reports of structural neuronal plasticity following DOI (Ly et al., 2018; Cameron et al., 2021). If there was a 100% gain (i.e., a doubling) in the number of dendrites or spines, the grey matter volume should increase by 26% and 5.7%, respectively. Cell culture measurements of dendritic branching estimated a 60-75% increase in the number of branches within hours of DOI treatment (Ly et al., 2018). We have assumed the *in vivo* and *in vitro* rates of dendritogenesis were comparable, and so included a 60% increase in the number of dendrites in our calculations. Measurements of synapse changes in S1 of mice treated with DOI estimated a 39% increase in spine formation in mouse primary sensory cortex 24h post-drug (Cameron et al., 2021). The increase in spine formation does not necessarily directly translate to an equivalent increase in new synapses. Based on studies with psilocybin, about half of the newly formed spines remain stable throughout the first week, suggesting they have become functional synapses (Shao et al., 2021), so we used 19.5% increase in synapse number in our calculations.

Therefore, a 60% and a 19.5% increase in the number of dendrites and synapses, respectively, would result in an overall grey matter volume change of 16.7%. The approximated volume increases observed in our ROI analysis (Table 5.3) all fall below the 16.7% estimate, meaning that the observed increases in

ROI volumes one day after DOI could likely be mostly due to the gain of new dendrites and their synapses.

5.4.d White matter plasticity

While we attempted to measure changes in white-matter plasticity with our imaging pipeline, we did not find any significant findings with DWI at either the 24h or three-weeks mark (all $q>0.20$, data not shown). These analyses were purely exploratory as no currently available data shows psychedelics are able to induce white matter changes, although there is some evidence to suggest psychedelics could be activating the cells responsible for myelin plasticity.

Experience-dependent changes in myelination are an additional form of plasticity that could mediate long-lasting changes in neural circuit function, affecting learning and memory (Sampaio-Baptista and Johansen-Berg, 2017; Xin and Chan, 2020). Work in rodents has shown how external factors and sensory experience can not only affect the rate and pattern of myelination, but also the proliferation and differentiation of oligodendrocytes. Myelin plasticity has even been shown to be required for motor (McKenzie et al., 2014), spatial (Steadman et al., 2020), and fear learning (Pan et al., 2020). This is not surprising considering oligodendrocytes regulate neurotransmitter release and metabolism and are able to release glutamine and BDNF, and therefore affect not just axonal conductance, but also synaptic efficacy and excitability. This line of evidence was what urged us to consider myelin plasticity with psychedelics, considering the findings on neuronal excitability and BNDF increase following psychedelic treatment.

However, myelin plasticity may not be an acute effect considering evidence suggesting it takes between one to two weeks for new myelin to form in the PFC, at least in the context of fear learning (Pan et al., 2020), although we did not see any differences in DWI in brains taken three weeks post-drug. Nonetheless, existing oligodendrocytes can influence remodelling of existing myelin and ion channel clustering, and thus cell excitability and conductance, at much shorter timescales, so neuronal-level white matter plasticity changes could still be relevant, even if they do not propagate to structural changes at the resolution of whole white matter structures.

The possibility that psychedelics can affect white matter cells is suggested by the fact that the myelin basic protein, which maintains the correct structure of myelin and is also present in synaptosomal membranes, has a 5-HT binding site (Carnegie, 1971). LSD is known to compete for that site both *in vitro* and *in vivo* (Sansone and Sansone, 2010). A possible site of interaction is at the nodes of Ranvier where the myelin basic protein was suggested to be localized (Dickinson et al., 1970). Others have speculated that psychedelic drugs could be affecting the myelin sheath in the vicinity of the nodes of Ranvier rather than specifically at synapses, as interfering with the conduction properties of neurons would lead to temporal dispersion of neural impulse volleys and consequently to functional disturbance (Carnegie et al., 1972). This could potentially help explain the changes in intrinsic excitability of neurons observed after psychedelic treatment (Ly et al., 2018).

Myelin is derived from and maintained by oligodendrocytes and glial cells that change their pulsation in response to 5-HT in culture (Bornstein and Murray,

1958). Although changes measured in DWI are typically interpreted as changes in myelination, other cell types (such as astrocytes or oligodendrocytes) and structures (e.g., axons and blood vessels) would affect fractional anisotropy. One report has found increased *cFos* expression in oligodendrocytes of the rat PFC following LSD (Reissig et al., 2008), and so psychedelic-induced changes in oligodendrocyte activity cannot be discounted. Furthermore, certain hallucinogens, such as phencyclidine (PCP), can target sigma-1 receptors which stimulate differentiation of oligodendrocyte progenitor cells (Hayashi and Su, 2004). Together, these findings indicate that more attention should be paid to the influence of psychedelics on oligodendrocytes, especially considering oligodendrocytes restrict dendritic branching and spine turnover in the cortex (Zemmar et al., 2018), events which may come into play during the consolidation of the initial burst of psychedelic-induced neuroplasticity.

5.4.f Limitations of the imaging methods

Increased storage time of *ex vivo* samples before scanning allows post-fixation tissue changes to stabilize and has also been found to increase contrast-to-noise ratio (CNR) across the brain (de Guzman et al., 2016). The best-practice rule of scanning fixed samples that minimizes volume differences due to post-fixation tissue changes is to image all samples after the first month of storage and before the sixth month (de Guzman et al., 2016). We were not able to follow this rule in Experiment 2 due to equipment availability and ongoing issues with air bubbles. It may be possible that extended storage of the samples confounded our measures of volume differences, leading us to miss positive findings,

especially considering fixation can induce variations as high as 3% per month (de Guzman et al., 2016).

5.4.f Future directions

Neuroanatomical signatures of psychedelic drug effects are a highly translational avenue of research. Considering that MRI acquisition and analysis can be made comparable across species, studying the short- and long-term effects of psychedelics in rodents can help our understanding of the underlying cellular mechanisms of brain structure changes observed with MRI in humans, especially if the pattern of these changes across the brain are shown to be consistent across species. Mouse MRI, because of its whole-brain coverage, enables us to identify areas undergoing plasticity adaptations that may be of further interest for closer examination using immunohistochemistry, two-photon, or electron microscopy. Genetic mouse models of altered cellular processing and brain plasticity might prove critical for establishing causality and the sequence of events that underlie psychedelics' effects on brain structure.

We propose tracking the induction and duration of putative structural changes induced by either a single or double dose of DOI using *in vivo* MRI, to serially assess the same animal and observe morphological and functional changes over time (Lau et al., 2008; Zhang et al., 2010). Additionally, manipulating the number of injections would elucidate if a single exposure can be sufficient to induce lasting plasticity changes in the brain or if multiple exposures would facilitate stronger and/or more lasting results.

6 | Discussion

6.1 Summary of main results

6.1.a Environmental dependency

We showed that mice could distinguish between environments before the drug injection and that behavioural responses to DOI differed between the two drug injection environments. These changes were subtler for HTR than for ESR, and greater differences were found with higher doses of DOI.

The context of drug administration can modulate gene transcription, neural circuit activity, and neurotransmitter systems engaged by a drug, and influence the drug's ability to produce persistent neuroplastic adaptations that may mediate drug addiction. The pharmacology of psychedelics could therefore be working synergistically with the environment to create an acute experience conducive to specific outcomes. This confers a pluripotent quality to psychedelic experiences. Borrowing the term from stem cell biology, pluripotency refers to the fact that stem cells have no fixed developmental potential, they can differentiate into different cell types. In the case of psychedelics, pluripotency could refer to their ability to produce multiple distinct responses in an organism in terms of the specific cell signalling pathways downstream of their G-protein-coupled receptors and/or the nature and the content of the acute state of non-ordinary consciousness. A pluripotent psychedelic experience can therefore take on a different quality depending on the internal and external factors present during treatment.

Psychedelic drugs highlight the interaction between pharmacology and non-pharmacological factors, although a similar view is increasingly adopted for SSRIs too (Branchi, 2011). The extra-pharmacological model of drug action posits abstract factors that are not easily quantifiable as central to the result of psychedelic therapy. The awareness of psychosocial factors brings scientific rigour to areas which used to be considered external to science, enriching our understanding of goals of medicine.

6.1.b Cognitive flexibility

During the acute psychedelic experience, cognitive function has been shown as either intact (Pędzich et al., 2022) or compromised by impairments of working memory, attention, and cognitive control (Goldberger, 1966; Bouso et al., 2013; Bershad et al., 2019). Post-drug longer-term changes in cognition have not been sufficiently explored, despite the suggestions that the richer synaptic landscape resulting from neuronal plasticity changes should lead to improvements in learning (Carhart-Harris and Nutt, 2017). We showed how DOI could improve adaptation to novel reversals, but not if that novel reversal occurred at the start of the sub-acute phase, one day after treatment.

It is possible that cognitive benefits begin to develop during the sub-acute phase but require time to grow to confer benefits for novel and/or more challenging adaptations. In our experiments we implemented the novel transition reversal either one day or one week after treatment, but we cannot argue that adaptability to reversals occurring a few days after drug injections would not also be improved. Some benefit of DOI was noted in the first week after drug treatment for the learned serial reversals. This appeared more as a protective effect as DOI-

treated animals did not improve upon their pre-drug performance, but they did not exhibit a performance drop seen in vehicle-treated animals after drug injections. In our case, we tested healthy animals who were trained on reward reversals for weeks before and had been performing them to a high standard before drug treatment. DOI's effects may not be strong enough to increase their performance further, i.e., there is a ceiling effect and so only a small window for improvement.

There is likely to be an optimal level of cognitive flexibility for a given context such that excessive flexibility becomes unconducive to accurate reality testing and conventional cognition and behaviour. While increasing the dose of psychedelics might increase their effect on flexibility, it may also bring a risk of overshooting this optimal flexibility threshold through extreme 5-HT_{2A}R signalling. Furthermore, increasing the dose of psychedelics also implies stronger activation of a wider set of 5-HT receptors, some of which could have opposite effects on flexibility (Boulougouris et al., 2008). There would also be an optimal level of neuronal plasticity – plasticity-promoting effects of DOI are linked to increased extracellular glutamate concentrations, and excessive glutamate at high doses of DOI would have a toxic that could lead to neuronal atrophy instead (Olson, 2018).

Our observation of significant sensitivity to reward omissions was unique to DOI-treated mice more adaptable to the transition reversal. Omissions are not included in the choice strategies of any other mice we tested on the two-step task, and, to the best of our knowledge, others have also noted mice's sensitivity only to rewards in the two-step (Blanco-Pozo et al., 2021) and other decision-making tasks (Cieślak et al., 2018). Mouse reward learning systems may have adapted more to foraging environments, where reward omission is not as important as

reward amount and timing. In choosing between foraging patches, the mouse knows reward is always available somewhere, so its learning system only needs to be sensitive to the probability of reward at each patch in order to choose between staying where it is or going to explore a different patch. In the two-step task with only reward reversals, tracking reward probabilities alone allows the mice to maximize rewards to achieve great success. Following a reward reversal, it only takes a dozen trials for the mice to pick the correct side better than chance levels. However, following a transition reversal, continuing to track only reward probabilities made the vehicle-treated animals slower at adapting compared to the DOI-treated animals who also tracked probabilities of omissions. Notably, our data showing DOI-treated mice have a higher rate of learning from both rewards and omissions echoes the recent human data suggesting LSD increased both reward and punishment learning rates in healthy subjects doing a probabilistic reversal task, with the important difference of the human subjects performing the task in the acute phase (Kanen et al., 2021).

It has been suggested that subjects solving the two-step task with fixed transition probabilities would not be able to solve a new task with serial reversals in transition probabilities (Akam et al., 2021). For DOI-treated animals, the added learning from omissions does not confer a performance boost for the first reversal, where both DOI- and vehicle-treated animals require almost two weeks to adapt, because there were no overall differences in how many correct choices the animals were making. But it might be that the richer strategy would ensure better success on the next transition reversal, and on the one after that – DOI-treated animals might be better equipped to adapt to transition reversals not only

faster but also better the next time they face a similar challenge. We did not employ serial transition reversals in our experiments, but future experiments might benefit from either performing additional transition reversals occurring across sessions post-drug, or serial within-session transition reversals, as they have been used in earlier work (Akam et al., 2015; Korn et al., 2021).

6.1.c Regional volumetric differences

Parallel drug-induced changes at both structural and cognitive levels are suggested by the overlap in the brain regions implicated in psychedelic responses (e.g., PFC, hippocampus, and amygdala) and their involvement in modulating learning, memory, and cognitive task performance (Dalley et al., 2004; Zühlsdorff et al., 2022). Behavioural task training alone is known to induce regional brain differences (Lerch et al., 2011), so we originally expected the volume changes in the long-term study to be more pronounced than in the sub-acute one, due to the extensive behavioural training involved. Cognitive flexibility and two-step task performance is dependent on PFC, OFC, the insula, basal ganglia, anterior and posterior parietal cortex (Leber et al., 2008; Terracciano et al., 2008), so drug-dependent changes in these regions were of particular interest, especially since rule learning is known to enhance synaptic plasticity in OFC (Johnson et al., 2016).

However, our results showed no drug-dependent long-term changes in either the sensory regions which were affected one day after treatment, nor in the regions implicated in two-step task-related processes. The fact that structural plasticity in sensory regions does not persist for weeks is not too surprising considering previous reports that only a third of newly formed spines would

remain three weeks after psychedelic injections (Shao et al., 2021). Therefore, although the overall number of spines and dendrites may still be higher than it would be without DOI, the differences may be too subtle to be picked up with a whole-brain analysis.

Another possibility is that it is not only the presence of more “material” (the total number of dendrites and spines) that facilitates long-term changes observed with psychedelic, but rather the reshaping of the patterns of distribution and connectivity of dendrites and spines, i.e., the way in which the initial growth of new links was consolidated across time. This pattern of connectivity, affecting network structure and communication, would then feed into cognitive changes, such as the adaptability differences we observed in our decision-making task. Therefore, in the timeline used in our studies, we do not see structural and cognitive changes that coincide in time, but they seem to depend on the same underlying molecular mechanisms of neuronal plasticity.

The premise that persistent changes in behaviour are supported by persistent changes in neural circuitry is far from new but demonstrating it has never been trivial. There is always a debate as to whether specific brain areas can be proven necessary and sufficient for specific behaviours, especially complex ones, such as executive function, or those that are considered “states” rather than behaviours, as would be the case for euthymic mood. Furthermore, given the different ways in which neuroplastic change can manifest and be measured, correlating those changes to appropriate elements of behaviour can become another debate.

6.2 Integrative model – a reappraisal

As described previously (section 1.5), the integrative model of plasticity predicts that if a drug were to promote molecular neuroplasticity, there should be a correlated and simultaneous facilitation of higher, cognitive, and psychological, levels of plasticity. Our project did not assess the "correlated" aspect of plasticity changes as we did not measure cellular plasticity effects ourselves, and our studies of different plasticity levels were done across separate cohorts of animals. However, we can make some claims about the "simultaneous" aspect of plasticity changes since our studies of cognitive and structural plasticity spanned both the sub-acute and the long-term phase.

Converging evidence (see section 1.6.a) suggests that the rates of neuronal plasticity changes are at their highest in the first few days after psychedelic drug treatment (during the sub-acute phase) and dissipate around the one-week point (i.e., the start of the long-term phase). We found evidence of regional brain volume changes only when we looked at the brains taken out during the sub-acute phase, suggesting that the whole-brain plasticity effects, like the cellular plasticity effects, are strongest at the start of the sub-acute phase and do not persist into the long-term phase – the two appear to be simultaneous, at least within the restricted time points used in this study.

In contrast, we found evidence of cognitive plasticity changes only when we looked at the animals tested with the novel transition reversal in the long-term phase, not seeing any novel adaptability differences in animals tested in the sub-acute phase. While we saw enhanced adaptability to learned reversals in the sub-acute phase, or at least a protective effect of DOI to possible deficits in learned

adaptability, we believe the improvements in novel transition reversal learning required more time. The restricted time points tested in this study would suggest that the novel adaptability improvements and the neuronal plasticity enhancements might be correlated but are asynchronous. Our proposed timelines of psychedelic-induced plasticity changes across levels of analysis are summarized in Fig.6.1.

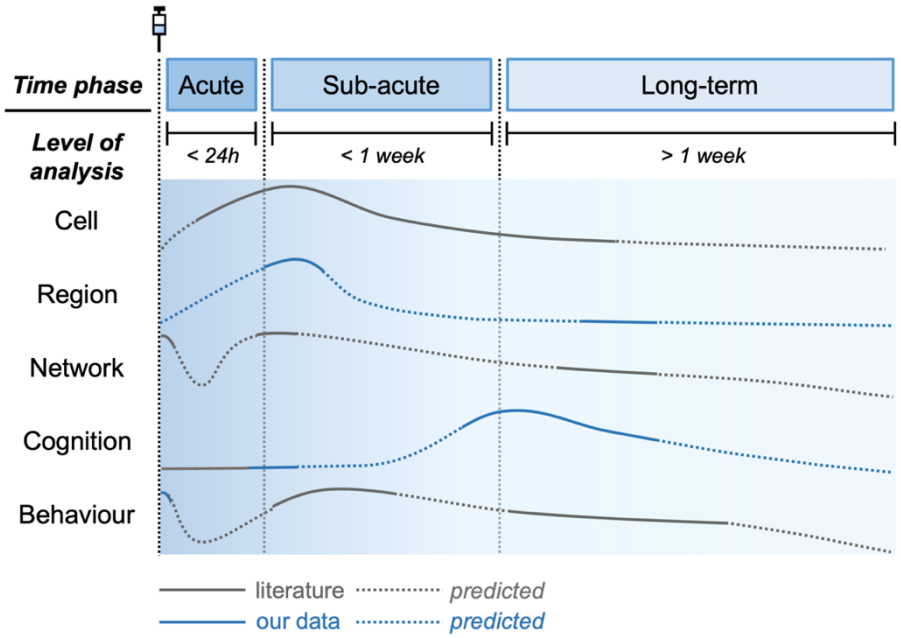


Fig.6.1 Signatures of a comprehensive high-plasticity state after psychedelic drug treatment. Phases of drug action are: acute (the first 24h after drug administration), sub-acute (starting at 24h after drug administration and lasting over the first week since the treatment), and long-term (over one week after drug administration). Levels of analysis of neuroplasticity range from single neurons to neural networks, to cognition and behaviour. **Cell** plasticity can occur within hours of treatment, is strongest in the first few days after treatment, and largely dissipates by the end of the first week, but an increase in spine density can remain detectable up to one month after initial treatment. **Region** structural plasticity was observable in the day following psychedelic drug administration, but not three weeks after treatment. Regional structural plasticity likely dissipates faster than neuronal structural plasticity, as the lower levels of formation of new dendrites and spines are not high and/or extensive enough to affect regional brain volumes. **Network** function is profoundly affected under psychedelics. Network-level plasticity differences are visible for weeks, although the directionality of effects is usually the opposite of those seen acutely. **Cognition** is either intact or compromised acutely. Enhanced cognitive flexibility is likely initiated in the first week after treatment and is the strongest in the first weeks of the long-term phase, i.e., after neuronal and regional structural plasticity effects have been consolidated. **Behaviour** changes profoundly in the acute phase, where environmental sensitivity is the highest. Mood and personality changes can start as early as few days after treatment and last for weeks (in rodents) or months (in humans).

We raise the possibility that the completion and consolidation of cellular plasticity changes could be not just a predecessor but a requirement for long-term improvement in new learning. This would go against the Price-Duman model's claim of *simultaneous* facilitation of higher levels of plasticity together with molecular plasticity enhancement (Price and Duman, 2019). Instead, our results suggest molecular plasticity might be a pre-requisite, paving the way for higher level changes that might follow, depending on the intensity and duration of changes at the neuronal level.

By "consolidation" we mean the process of synaptic pruning and strengthening that will determine which spines will persist long-term and which connections will be maintained and used by the brain long-term. An excess of dendritic spines can lead to behavioural and functional connectivity impairments if not kept in check by pruning (Zhan et al., 2014). Therefore, it is likely that the "usefulness" of psychedelic-induced dendritogenesis and spinogenesis is only revealed when new functional synapses are formed and consolidated. It is estimated that only about 30% of newly formed spines in the days following psychedelic treatment become functional synapses (Shao et al., 2021) – how this pruning process is regulated and whether it can be directed for a specific purpose is an intriguing area of future research. The previously discussed internal and external environmental factors may play a critical role in determining which foundations are laid down, i.e., which connections are maintained, and which ones are pruned away.

The initial explosion of neuronal plasticity may help build new roads in the brain, but not all of them will remain. Depending on ongoing experience, only

some of the roads will get chosen for consolidation into the synaptic landscape. As the work on plasticity mechanisms of neurorehabilitation (Warraich and Kleim, 2010) has shown, certain forms of plasticity appear to precede or depend on others. Therefore, discovering the nature of psychedelic higher-level plasticity and its behavioural relevance might not be so much a function of *how* one looks, but *when*.

The main limitation of our studies is the lack of causal inference. Although the foundation of our hypotheses was based on previous reports of psychedelic-induced neuronal plasticity, we did not measure nor manipulate structural and functional changes in neurons in the animals which we used to study whole-brain structure and cognitive plasticity. While change in structural neuroplasticity at a neuronal and regional level may occur simultaneously, and while cognitive plasticity appears to follow neuronal plasticity, whether neuronal changes mediated these effects remains an open question. Future studies are required to manipulate neuronal plasticity and observe how higher-level plasticity is affected in turn.

6.3 Experience-dependent plasticity

Neuroplasticity is a dynamic and complex cascade of molecular, cellular, structural, physiological, and network-level events across time, and, at each level, experience can direct this cascade. It is likely why clinical practice uses psychedelics in combination with psychotherapy – the plasticity-promoting effects of psychedelics could better the chances of significant restructuring of thought and behaviour achieved by psychotherapy. While plasticity enhancements itself

may have cognitive and behavioural effects without psychotherapy, the greater benefits might be found with the synergistic effects of drug and therapy combined.

Clinical experience has shown that treatment of depression is more effective using a combination of antidepressants and psychotherapy rather than using either treatment alone (Belmaker and Agam, 2008). Such drug-experience interaction has also been shown in preclinical models. In mice, chronic fluoxetine treatment in combination with extinction training was more effective in reducing a conditioned fear response than chronic fluoxetine or extinction on their own (Karpova et al., 2011; but see Burghardt et al., 2013). The combined effect was attributed to the fluoxetine-dependent increase in functional and structural plasticity that allows for more efficient fear erasure, but this process is further helped by training-guided remodelling of the memory circuitry.

Thus, the pharmacological plasticity-promoting effects of psychedelics may also be boosted when combined with training-guided reorganization of networks rendered more plastic by the drug. However, hippocampal and infralimbic infusions of BDNF can induce extinction without any behavioural training (Peters et al., 2010), signalling that purely pharmacological plasticity-promoting interventions can regulate behavioural extinction. This highlights the need for our control two-step task experiment where we eliminate additional training after drug treatment and observe whether we can still see improvements in cognitive adaptation.

Psychedelics are not the only drugs capable of inducing neuroplasticity. Drug-induced neuroplasticity has previously been suggested as the main

mechanism underlying antidepressant effects of SSRIs (Castrén and Antila, 2017). However, not all plasticity is therapeutic. Neuroplasticity allows subsequent stimuli to reshape neural circuits and not necessarily for the organism's benefit. For example, cocaine also induces formation of new dendritic spines in the NAc (Ferrario et al., 2005) and PFC (Muñoz-Cuevas et al., 2013) and, like for psychedelics, these adaptations can occur from a single dose and in a single day. But cocaine's induction of plasticity has been implicated in its abuse potential rather than any therapeutic effect (Li et al., 2004; Ferrario et al., 2005; Marie et al., 2012; Muñoz-Cuevas et al., 2013).

The difference between the effects of cocaine- versus psychedelic-induced plasticity has been demonstrated for the reopening of a critical period for social reward learning in mice. A critical period is a developmental stage characterized by elevated plasticity when specific environmental stimuli are required for proper nervous system development and organization. When the critical period ends, adaptability of the developed system/circuit is limited. The critical period for social reward learning, which in mice peaks around postnatal day 40 and closes by adulthood, is established by developmental regulation of oxytocin-dependent decreases in the frequency of EPSCs, i.e., a long-term depression, in the NAc (Nardou et al., 2019). A single dose of MDMA reinstated social reward learning and oxytocin-dependent long-term depression in NAc within 6h of injection and lasting up to four weeks, while cocaine had no effects on social reward learning nor on NAc EPSCs (Nardou et al., 2019). Reinstatement of this oxytocin-dependent critical period for social preference has now also been shown with LSD, psilocybin, ketamine, and ibogaine (Sawyer,

2022). Therefore, it is not enough to simply induce hyperplasticity – the therapeutic effect will be determined not just by where plasticity is initiated, but how it guides the rewiring of the more plastic synaptic landscape.

6.4 The generalizability of our findings and their translational significance

In section 2.1 we discussed the evidence suggesting differences in the acute psychedelic-like experience between males and females (Blanchard et al., 1992; Meehan and Schechter, 1998; Brookshire and Jones, 2009; Páleníček et al., 2010; Tylš et al., 2016; Jaster et al., 2022b) and how sex might play a role in the sensitivity of the serotonergic system to psychedelic behavioural effects. For DOI specifically, while both sexes showed a significant activity response to DOI, male and female mice had significant differences in the degree of their locomotor and vertical activity after doses smaller than 2mg/kg DOI (Brookshire and Jones, 2009). In terms of HTR, DOI induced more head twitches in female than in male C57BL/6J mice at the 2mg/kg dose, even though the concentrations of DOI were higher in brain samples of the male mice (Jaster et al., 2022b). It is unclear if such differences in the behavioural and pharmacokinetic properties of DOI would impact the effects seen past the acute phase, specifically the effects on plasticity.

A previous report on neuronal plasticity and behavioural effects with DOI included both male and female mice, but without investigating the interaction between drug and sex (Cameron et al., 2021). Shao and colleagues report their findings on spine structure and behaviour in a learned helplessness paradigm after psilocybin for both male and female mice separately, but the main effect of sex and the drug by sex interaction were not statistically significant for either spine density or spine head width changes in the medial frontal cortex (Shao et

al., 2021). However, region-specific changes in spine density and spine protrusion length in the cingulate/premotor area of the medial frontal cortex were significantly higher in the female than in male mice treated with psilocybin (Shao et al., 2021). Therefore, the ability of DOI to induce neuronal plasticity and therapeutic-like behavioural effects is not restricted to males but occurs in females too. While the presence of effect is currently not contested in the literature, a putative difference in effect size has not been sufficiently explored to suggest males or females as more responsive to the long-term effects of psychedelics. An added caveat is that the direct causative link between the strength of acute psychedelic-like experience and the magnitude of post-acute plasticity and behavioural changes is still under debate. We therefore believe that, while the acute behavioural effects of psychedelics in females and males could be different, this does not necessarily imply that their post-acute behavioural effects would be incomparable. As suggested earlier, we predict that we would observe the effects we saw in males also in female mice, but relative effect sizes may differ.

While our study was performed in a healthy organism, we predict that our findings of structural and cognitive plasticity likely translate to disease models where there has been, e.g., a loss in grey matter (such as in depression) or a drop in reversal learning rates (such as with stress). Our finding of improved cognitive flexibility exhibited a time-dependent pattern where maintenance of a stable performance was present within the first week of treatment, but a performance boost in novel reversals required more time. However, in animals where the performance is not optimal, DOI's effects might prove to be beneficial

earlier. For example, in animals that exhibit deficits in reward reversal performance, perhaps due to stress or some pharmacological treatment, the effect of DOI in the first week might be strong enough to rescue the performance deficit. This prediction is supported by recent data on mouse cognitive flexibility in a four-choice odour discrimination and reversal task following unpredictable mild stress. After stress exposure, mice were significantly slower at learning the new odour-reward contingencies, but an injection of 10mg/kg of plasticity-inducing non-psychedelic analogue of ibogaine, tabernathalog (TBG) immediately after the stress period normalized cognitive flexibility one day later (Lu et al., 2021). These findings demonstrate TBG's fast effects in combating behavioural impairments, but TBG did *not* increase cognitive flexibility past the levels seen in the non-TBG-treated controls one day after the injection. Therefore, while the effects of psychedelic-induced cognitive plasticity may be rapid in cases where there is an impairment, imparting added performance benefits appears to follow a slower timeline. Furthermore, various reports of the ability of psychedelic drug to rescue depressive-like and addictive-like behavioural impairments (Cameron et al., 2021, 2023; Lu et al., 2021; Shao et al., 2021) reinforces our prediction that various psychedelic drugs, including DOI, can have similar behavioural benefits across different disease models, but our study cannot account for the large diversity of plasticity changes implicated in various animal models of neuropsychiatric disorders. This remains a key area of future investigation.

Treatment development often involves continuous back-and-forth translation between basic and preclinical research and the clinical studies and practices, termed *bench to bedside*. The most recent wave of psychedelic research had more of a bedside to bench direction, with clinical findings inspiring preclinical mechanistic studies and optimized drug design to improve patient outcomes and treatment availability. For example, broad efficacy of psychedelic-assisted psychotherapy urged studies into non-psychedelic analogues that would enable patient populations currently being excluded due to risk factors (e.g., personal or family history of psychosis) to also benefit from plasticity-promoting effects.

Elevated plasticity of the post-psychedelic state is evocative of elevated plasticity in the adolescent brain, also characterized by synaptic overproduction and pruning. Many affective psychopathologies, such as anxiety, depression, substance abuse, and eating disorders, emerge during adolescence. In this case, elevated plasticity is seen as a vulnerability, but the work on plasticity-promoting effects of psychedelics advocates high-plasticity states as double-edged swords (Branchi, 2011) – on the other side of vulnerability lies a powerful opportunity for intervention to mitigate previously persistent maladaptive behavioural patterns. Perhaps insights from pharmacologically induced highly plastic states could be used to explore how the benefits of developmental high plasticity periods can be reaped to reduce vulnerabilities to mental health problems.

Tailoring experiments to better operationalize and isolate behaviours resulting from psychedelic-assisted psychotherapy and focusing neurobiological studies on clinically relevant phenotypes may promote hypothesis-driven

treatment optimization, replacing the lengthier explorative studies carried out in the first phase of the latest psychedelic renaissance. This process does require acknowledgement of the limitations in translating between preclinical research and clinical practice. While the overlap between some brain and cognitive features is apparent from rodents to humans, key differences exist in how the surrounding world is experienced and used to guide behaviour in humans, in addition to the complex socioeconomic and cultural factors that shape human set and setting.

6.5 The importance of psychedelic experience

While the acute psychedelic experience is believed to be mostly mediated by the 5-HT_{2A}Rs (section 1.3), not all 5-HT_{2A}R agonists exhibit strong psychedelic-like effects. For example, lisuride and ergotamine have not been found to induce a head-twitch response (González-Maeso et al., 2007). The difference in behavioural effects is believed to be due to “biased agonism” of G-protein coupled 5-HT_{2A}Rs. Lisuride targets the same population of 5-HT_{2A}Rs like LSD does, but it induced distinct effects on intracellular signalling, electrophysiology, and behaviour (González-Maeso et al., 2007). However, the branding of lisuride as a non-psychedelic 5-HT_{2A}R agonist is controversial. There is some generalization of the subjective effects of lisuride and LSD in lab animals as lisuride substituted for LSD in rats trained to differentiate between LSD and saline (Appel et al., 1999). In humans, high doses of lisuride were able to induce hallucination-like responses in humans (Lees and Bannister, 1981; Critchley et al., 1986), although these effects have only been observed with the use of lisuride as a treatment for Parkinson’s disease.

Finding a non-psychedelic analogue with plasticity and therapeutic effects comparable to those of classic psychedelic is becoming a fervent goal of the psychedelics field. Some of the initial work was done by Cameron and colleagues (Cameron et al., 2021) who chemical modified ibogaine into a non-psychedelic tabernanthalog (TBG). TBGs was able to induce rapid structural neuroplasticity effects like those of classic psychedelics, and to transiently reduce immobility time in a forced swim test following unpredictable mild stress, as well as reducing alcohol- and heroin-seeking behaviour in the first 24h. Importantly, TBG still activates 5-HT_{2A}Rs and its behavioural effects were dependent on 5-HT_{2A} activation since they were blocked by blocked by the 5-HT_{2A} antagonist ketanserin (Cameron et al., 2021). However, the label of a "non-psychedelic" could be contested since the only behavioural data supporting that conclusion came from observations of the head twitch response. The trouble is that ibogaine itself did not induce a strong head twitch response in the authors' data, especially at higher doses, so the behavioural effects produced by TBG were comparable to those of high dose ibogaine.

Recently, much wider screens of possible non-psychedelic molecules have been published. PyschLight, a genetically engineered fluorescent sensor whose structure is based on the 5-HT_{2A}R, can detect (i) endogenous 5-HT release in behaving animals, and (ii) conformations induced by psychedelic ligands *in vivo* and in *in vitro* medium-throughput assays (Dong et al., 2021). Using psychLight, the authors were able to identify a novel non-psychedelic highly selective 5-HT_2 agonist AAZ-A-154 which does not produce head twitches but increases dendritic branching, decreases immobility in the forced swim test,

and ameliorates anhedonia. Others have used 5-HT_{2A}R-selective docking of a virtual library of molecules with an LSD-based scaffold to identify putative non-psychedelics (Kaplan et al., 2022). Structure-based optimization of resulting molecules led to two new 5-HT_{2A}R agonists – (*R*)-69 and (*R*)-70. The numbers of head twitches induced by either agonist were significantly lower than those induced by LSD and were comparable to the vehicle control. In a tail suspension test of antidepressant activity, both agonists were able to significantly reduce immobility times in a genetic model of enhanced learned helplessness, a vesicular monoamine transporter 2 heterozygous (VMAT2 HET) mice, to a degree comparable to the SSRI fluoxetine.

When thinking about whether non-psychedelic analogues of psychedelics could have comparable behavioural effects as we have observed with DOI, there are two main factors to consider: 1) pattern of 5-HT receptor activity and its necessity for a behavioural effect, and 2) the duration of behavioural effect. The aforementioned non-psychedelics TBG, AAZ-A-154, (*R*)-69, and (*R*)-70 all exhibited 5-HT_{2A}R activity, albeit smaller compared to the psychedelic drugs. 5-HT_{2A}R activity was necessary for both the plasticity-promoting and the behavioural effects of TBG and AAZ-A-154 (Cameron et al., 2021; Dong et al., 2021), while (*R*)-69, and (*R*)-70 were not tested in combination with 5-HT_{2A}R antagonists. The same was found to be true for psychedelics such as LSD, DOI, DMT, psilocybin (Ly et al., 2018; Cameron et al., 2023), so while the acute behavioural experience is different across psychedelics and non-psychedelic analogues, their plasticity-promoting and therapeutic behavioural effects can be comparable and possibly due to a common underlying mechanism.

It could therefore be likely that the cognitive and structural effects we found with DOI, could also be expected for TBG and AAZ-A-154.

A similar pattern would be expected when comparing across different psychedelics. The plasticity-promoting effects of DOI were comparable to LSD, DMT, and psilocin/psilocybin in terms of the increase in dendritic arborization and spine formation, although note that LSD marginally outperformed all the other psychedelic compounds tested (Ly et al., 2018; Shao et al., 2021). The synaptic plasticity of DMT and psilocybin were also comparable (Ly et al., 2018; Shao et al., 2021), but effects of LSD and DOI have not yet been reported for sEPSC amplitude and frequency. Behavioural therapeutic-like effects have been found across different psychedelics in animals (Ly et al., 2018; Nardou et al., 2019; Odland et al., 2019; Shao et al., 2021; Cameron et al., 2023) and in humans (Goldberger, 1966; dos Santos et al., 2016b; Lebedev et al., 2016; Carhart-Harris et al., 2017; Johnson et al., 2017; Murphy-Beiner and Soar, 2020; Goodwin et al., 2022). Therefore, since these psychedelics share the plasticity-promoting effects that are a likely common mechanism of behavioural effects, we expect to find analogous cognitive and structural effects with LSD, psilocin/psilocybin, and DMT, as we found with DOI, with the added factor of the dosages across different drugs being pharmacologically comparable.

We also highlighted the second factor of effect durability. The behavioural effects of TBG were only investigated 24h after treatment (Cameron et al., 2021), while the behavioural effects of AAZ-A-154, (*R*)-69, and (*R*)-70 do appear to last for at least one week after treatment (Dong et al., 2021; Kaplan et al., 2022). It remains an open question whether non-psychedelic analogues have long-term

effects on behaviour, as their psychedelic counterparts do, and as we have shown for DOI in our cognitive tests. Additionally, while the presence of similar behavioural effects would be expected among different psychedelics, and across non-psychedelic analogues, their relative efficacy could differ in the scenario that it is the distinct pharmacological profiles that are the basis of some behavioural effects. For example, if an effect is not purely 5-HT_{2A}R-dependent but is also dependent on 5-HT_{2C}R or 5-HT_1R activity than those drugs that have a more mixed 5-HT receptor activity profile could be more effective than those exhibiting higher selectivity for 5-HT_{2A}Rs, such as DOI.

7 | Conclusions

One of the proposed mechanisms of how psychedelics induce a fast and lasting remission across very different symptomologies of mental disorders is that the psychedelics affect the 5-HT system to open a window of enhanced plasticity where significant learning and changes in the brain can occur. This is associated with enhanced environmental sensitivity allowing significant therapeutic work to be done. The two in combination putatively lead to the enduring mood and learning changes. While there is a growing body of evidence showing extensive enhancements in neuronal plasticity due to psychedelics, we did not know if and how these changes are consolidated or used by the brain in any meaningful manner. We predicted that high neuronal plasticity should facilitate enhancements at the higher levels of plasticity as well, such as regional brain structure and cognitive function.

We used a mouse model in order to have complete control of environment and drug history, which is not possible in humans. We used a triangulation of methods to find evidence of long-term higher-level plasticity changes caused by a phenethylamine psychedelic DOI. We combined pharmacology, behavioural testing, and brain imaging to answer if DOI can: 1) induce environmentally sensitive acute psychedelic-like responses, 2) improve cognitive flexibility post-acutely, and 3) increase the volume of whole brain regions post-acutely.

We reported that environmental novelty could modulate sensitivity to DOI's acute psychedelic-like effects. We also found that a single dose of a

psychedelic drug was capable of inducing volume increases in several areas of the brain's sensory and association cortices just 24h after injection. However, these effects did not persist at three weeks after injection. Additionally, in the first week post-DOI, we found a small but reliable difference in learned reward reversal adaptability, but a faster strategy adaptation to a novel transition reversal was detectable only after the first post-drug week, pointing to delayed improvement in cognitive flexibility with DOI.

In summary, we show that a single moderate dose of a psychedelic drug is capable of inducing changes in brain structure and cognition that are associated with enhanced plasticity. This indicates that the effects of psychedelics on neuronal plasticity can propagate up in the ladder of brain plasticity in a time-dependant manner.

8 | A note on the impact of the COVID-19 pandemic on the experiments reported in this thesis

I started my DPhil studies in October 2019. The COVID-19 pandemic and the national lockdowns required during it had several consequences on the work that could be done in the period of March 2020 to March 2022 when the majority of legal restrictions were lifted. The most significant impact was on the time and equipment available to perform experiments as they were originally proposed. The details are outlined below.

- At the time of the first national lockdown in March 2020, I was performing the experiments required for chapter 3. The experiments on one cohort of required animals had been completed earlier in January, but I was performing the drug treatment and behavioural testing on the second cohort when the Biomedical Sciences Building (BSB) had to be closed. We managed to negotiate that I am allowed to complete my last days of work in order to inject all the mice I had been testing, but then immediately sacrifice them after. This meant that I could not perform perfusions for brain collection as for my first cohort of animals as that required additional days of animal housing, me coming into the building, as well as one other person that was required to assist the perfusions. As a result, *Experiment 1* reported in chapter 5, which was the imaging study planned with the missing brain samples, was less powered that originally designed. Instead of n_{group}=16, our sample size was n_{group}=8.

  Additionally, in the first cohort of animals, there was a technical failure with the cameras for four of the animals that were meant to be included in the imaging study. While I gathered the behavioural data of the additional four mice that were used as a replacement in the second cohort, we could not collect their brains. This

is why in our imaging sample, four out of 8 mice in the 2mg/kg DOI group did not have behavioural data available and we therefore could not correlate our findings of the grey matter volume changes to the acute psychedelic-like effects of DOI.

- My original project proposal included experiments on females that would 1) determine if the acute psychedelic-like effects of DOI were comparable across male and female mice, accounting for low versus high oestrogen phase in the oestrus cycle, 2) test cognitive flexibility in female mice too, replicating our effects reported in chapter 4. The first experiment was initially delayed as I was trying to determine what kind of oestrus cycle screening I was allowed to do under our existing project licence. Then, because of the lockdowns and the restricted access to BSB, I prioritized the cognitive tests that formed chapter 4 of my thesis first.

  Once there was time available to revisit the case of the females, discussions among the project team led to a decision to table these studies. A simple visual screen, labelled as husbandry and not a regulated a procedure, would allow us to group females only into a low versus high oestrogen phase in the oestrus cycle, but not to a specific cycle stage, which could only be done with cytology. Taking a sample for cytology was not under our licence. Furthermore, my supervisor team advised me that, in order to appropriately test sex differences in psychedelic drug action, we would need additional experiments on ovariectomized females and additional procedures for which we are not approved for in our project licence. Obtaining amendments would have taken too long for me to finish my studies within my grant timeline. As all our experiments up to that point were completed on male mice, a decision was made to keep using males one for consistency.
- Once access to BSB was granted again, there was a lot of demand on equipment from other lab members needing to finish their projects too. This meant that the

availability of operant boxes and scanner time were limited. Availability of operant boxes, coupled to the fact that data collection for my two-step task experiments takes 2.5 months to complete for one cohort of animals, meant that we could not perform many variations of those experiments (such as, different time gaps between injection and novel reversal, different psychedelic drugs, or replicating positive findings).

The MRI scanner was continuously booked up for overnight *ex vivo* scans for 3-5 different people at a time. Coupled with re-scanning required due to scanner failure, air-bubbles, and other artifacts, it took a full year for all 26 samples to be scanned for our *Experiment 2* in chapter 5. I therefore did not plan for additional imaging experiments as I only had a few months left on my grant and could not guarantee we would have the data by then.

- Access to the scanner was another issue as initial regulations allowed only one person at a time in the scanner room, so I could not have a trainer with me to show how sample preparation and scanning is done. Scanning had to be delegated to the radiographer and other experienced members of the lab.

9 | Statistics appendix

Fig	Statistical method	Result	Post-hoc tests
3.5 A	Nonlinear line regression	*Null hypothesis: slope = 0* Extra sum-of-squares *F* test $F(1, 158) = 2.40$, $P = 0.124$ Slope = -0.84, CI [-1.91, 0.23] AICc test $P(H_1/H_0) = 1.18$	
	RM ANOVA	Session $F(4,124) = 2.96$, $P = 0.022$, $\eta^2 = 0.09$	Dunnett's Session 1 vs.: Session 2 $P = 0.698$ Session 3 $P = 0.005$ Session 4 $P = 0.335$ Session 5 $P = 0.113$
	Bayesian RM ANOVA	BF_{incl}[Session] =1.55	
3.5 B	Nonlinear line regression	*Null hypothesis: slope = 0* **0-5min** Extra sum-of-squares *F* test $F(1, 158) = 14.95$, $P < 0.001$ Slope = -0.82, CI [-1.24, -0.40] AICc test $P(H_1/H_0) >> 100$ **5-10min** Extra sum-of-squares *F* test $F(1, 158) = 2.50$, $P = 0.116$ Slope = -0.30, CI [-0.68, 0.08] AICc test $P(H_1/H_0) = 1.24$ **10-15min** Extra sum-of-squares *F* test $F(1, 158) = 1.95$, $P = 0.164$ Slope = 0.29, CI [-0.12, 0.69] AICc test $P(H_1/H_0) = 0.94$	

	RM 2way ANOVA	**Greenhouse-Geisser corrected* Time $F(1.49, 46.3) = 168.28$, $P<0.001$, $\eta_p^2 = 0.84$ Session $F(3.40, 105) = 2.96$, $P=0.030$, $\eta_p^2 = 0.09$ Time X Session $F(5.65, 175) = 9.28$, $P<0.001$, $\eta_p^2 = 0.23$	Dunnett's Session 1 vs.: **0-5min** Session 2 $P=0.137$ Session 3 $P<0.001$ Session 4 $P<0.001$ Session 5 $P<0.001$ **5-10min** Session 2 $P=0.995$ Session 3 $P=0.015$ Session 4 $P>0.999$ Session 5 $P=0.097$ **10-15min** Session 2 $P=0.844$ Session 3 $P=0.752$ Session 4 $P=0.978$ Session 5 $P=0.505$
	Bayesian RM 2way ANOVA	BF_{incl}[Time] >>100 BF_{incl}[Session] =2.11 BF_{incl}[Time X Session] >>100	
3.5 C	Unpaired *t*-test	$t(62) = 3.706$, $P<0.001$, Cohen's $d = 0.93$	
	Bayesian unpaired *t*-test	$BF_{10} = 60.54$	
3.6 A	Nonlinear quadratic Poisson regression	Quadratic fit over line: $P<0.001$ Likelihood ratio test Likelihood ratio =15.2, $P=0.002$ Linear [Familiar] = 49.1, CI [42.4, 56.0] Linear [Novel] =52.3, CI [45.5, 59.3] Quadratic [Familiar] = -15.5, CI [-19.3, -11.9] Quadratic [Novel] = -14.0, CI [-17.9, -10.2] Familiar vertex: Peak dose 1.9 [1.3, 2.9] Peak HTR 42 [25, 70]	Linear $P=0.516$ Quadratic $P=0.565$

		Novel vertex: Peak dose 1.6 [1.1, 2.4] Peak HTR 51 [30, 90] AICc test $P(H_1/H_0)$ =59.5	
	2way ANOVA	Environment $F(1, 56)$ =3.32, P=0.074 Dose $F(3, 56)$ =74.2, P=0.001, η_p^2 =0.80 Environment X Dose $F(3, 56)$ =1.89, P=0.142	Dunnett's VEH vs: 0.5mg/kg DOI P<0.001 1.0mg/kg DOI P<0.001 2.0mg/kg DOI P<0.001 Exploratory Fisher's LSD tests Familiar vs. Novel VEH P=0.818 0.5mg/kg DOI P=0.405 1.0mg/kg DOI P=0.863 2.0mg/kg DOI P=0.006
	Bayesian 2way ANOVA	BF_{incl}[Environment] =0.96 BF_{incl}[Dose] >>100 BF_{incl}[Environment X Dose] =0.70	
3.6 B	Nonlinear quadratic Poisson regression	Quadratic fit over line: P<0.001 Likelihood ratio test Likelihood ratio =80.0, P<0.001 Linear [Familiar] =28.3, CI [21.2, 35.3] Linear [Novel] =25.9, CI [18.9, 33.0] Quadratic [Familiar] = -11.5, CI [-15.0, -8.09] Quadratic [Novel] = -3.66, CI [-7.4, ???] Familiar vertex: Peak dose 1.2 [0.7, 2.2] Peak ESR 28 [17, 51] Novel vertex: Peak dose 3.5 [1.3, ???] Peak ESR 54 [18, ???] *NB: "???" indicates that a complete CI could not be calculated. In this case, the lower limit of CI is stable, so we can be 95% certain that the "true" parameters value is greater than the lower limit, but we have no real certainty about where the upper limit is (under the constraint that it is <0)*	Linear P=0.646 Quadratic P=0.002

		AICc test $P(H_1/H_0)$ >>100	
	2way ANOVA	Environment $F(1, 56)$ =4.01, P=0.050 Dose $F(3, 56)$ =11.25, P<0.001, η_p^2 =0.38 Environment X Dose $F(3, 56)$ =4.25, P=0.001, η_p^2 =0.19	Dunnett's VEH vs: 0.5mg/kg DOI Familiar P=0.058 Novel P=0.003 1.0mg/kg DOI Familiar P=0.009 Novel P<0.001 2.0mg/kg DOI Familiar P=0.068 Novel P<0.001 Bonferroni Familiar vs. Novel VEH P=0.992 0.5mg/kg DOI P>0.999 1.0mg/kg DOI P>0.999 2.0mg/kg DOI P=0.007
	Bayesian 2way ANOVA	BF_{incl}[Environment] =1.24 BF_{incl}[Dose] >>100 BF_{incl}[Environment X Dose] =5.14	
3.7 A	Nonlinear line regression	Extra sum-of-squares F test $F(2, 60)$ =1.53, P=0.225 Slope [Familiar] = -14.2, CI [-22.5, -5.8] Slope [Novel] = -4.9, CI [-11.9, 2.2] Slope [Global] = -9.5, CI [-14.9, -4.1] AICc test $P(H_1/H_0)$ =0.48	
	2way ANOVA	Environment $F(1, 56)$ =0.04, P=0.843 Dose $F(3, 56)$ =6.03, P=0.001, η_p^2 =0.24 Environment X Dose $F(3, 56)$ =2.18, P=0.101	Dunnett's VEH vs: 0.5mg/kg DOI P=0.730 1.0mg/kg DOI P>0.999 2.0mg/kg DOI P=0.001
	Bayesian 2way ANOVA	BF_{incl}[Environment] =0.25 BF_{incl}[Dose] =28.47 BF_{incl}[Environment X Dose] =0.96	
3.7 B	Nonlinear line regression	Extra sum-of-squares F test **excluding one outlier* $F(2, 59)$ =3.63, P=0.033	Slope different from 0: Familiar

		Slope [Familiar] = 0.21, CI [-1.71, 2.13] Slope [Novel] = -1.61, CI [-3.95, 0.74] AICc test $P(H_1/H_0)$ =2.67	*P*=0.824 Novel *P*=0.172
	2way ANOVA	**excluding one outlier* Environment *F*(1, 55) =6.77, *P*=0.012, η_p^2 =0.11 Dose *F*(3, 55) =1.48, *P*=0.229 Environment X Dose *F*(3, 55) =4.13, *P*=0.010, η_p^2 =0.18	Dunnett's VEH vs: **Familiar** 0.5mg/kg DOI *P*=0.823 1.0mg/kg DOI *P*=0.798 2.0mg/kg DOI *P*>0.999 **Novel** 0.5mg/kg DOI *P*=0.051 1.0mg/kg DOI *P*=0.113 2.0mg/kg DOI *P*=0.643 Bonferroni Familiar vs. Novel: VEH *P*=0.895 0.5mg/kg DOI *P*>0.999 1.0mg/kg DOI *P*>0.999 2.0mg/kg DOI *P*=0.013
	Bayesian 2way ANOVA	**excluding one outliers* BF_{incl}[Environment] =3.65 BF_{incl}[Dose] =0.36 BF_{incl}[Environment X Dose] =4.75	
3.7 C	Nonlinear line regression	Extra sum-of-squares *F* test *F*(2, 60) =0.84, *P*=0.438 Slope [Familiar] =5.7, CI [2.4, 9.0] Slope [Novel] =3.5, CI [0.11, 6.9] Slope [Global] =4.6, CI [2.3, 6.9] AICc test $P(H_1/H_0)$ =0.24	
	2way ANOVA	Environment *F*(1, 56) =0.72, *P*=0.400 Dose *F*(3, 56) =6.02, *P*=0.001, η_p^2 =0.24 Environment X Dose *F*(3, 56) =0.83, *P*=0.485	Dunnett's VEH vs: 0.5mg/kg *P*=0.182

			1.0mg/kg *P*=0.403 2.0mg/kg *P*<0.001
	Bayesian 2way ANOVA	BF_{incl}[Environment] =0.34 BF_{incl}[Dose] =33.94 BF_{incl}[Environment X Dose] =0.30	
3.7 D	Nonlinear line regression	Extra sum-of-squares *F* test *F*(2, 60) =2.31, *P*=0.108 Slope [Familiar] =7.8, CI [2.8, 12.9] Slope [Novel] =1.6, CI [-2.1, 5.2] Slope [Global] =4.7, CI [1.6, 7.8] AICc test $P(H_1/H_0)$ =1.06	
	2way ANOVA	Environment *F*(1, 56) =0.46, *P*=0.501 Dose *F*(3, 56) =5.78, *P*=0.002, η_p^2 =0.24 Environment X Dose *F*(3, 56) =2.01, *P*=0.122	Dunnett's VEH vs: 0.5mg/kg *P*=0.946 1.0mg/kg *P*=0.756 2.0mg/kg *P*=0.017
	Bayesian 2way ANOVA	BF_{incl}[Environment] =0.30 BF_{incl}[Dose] =22.31 BF_{incl}[Environment X Dose] =0.82	
3.7 E	Nonlinear line regression	Extra sum-of-squares *F* test *F*(2, 60) =1.17, *P*=0.317 Slope [Familiar]=-0.013, CI[-0.022, -0.004] Slope [Novel] = -0.005, CI [-0.012, 0.002] Slope [Global]= -0.009, CI [-0.014, -0.004] AICc test $P(H_1/H_0)$ =0.34	
	2way ANOVA	Environment *F*(1, 56) =0.20, *P*=0.655 Dose *F*(3, 56) =4.09, *P*=0.011, η_p^2 =0.18 Environment X Dose *F*(3, 56) =2.24, *P*=0.094	Dunnett's VEH vs: 0.5mg/kg *P*>0.999 1.0mg/kg *P*=0.720 2.0mg/kg *P*=0.011
	Bayesian 2way ANOVA	BF_{incl}[Environment] =0.27 BF_{incl}[Dose] =4.53 BF_{incl}[Environment X Dose] =0.99	

3.7 F	Nonlinear line regression	Extra sum-of-squares *F* test $F(2, 60) = 1.36$, $P = 0.265$ Slope [Familiar] = -1.7, CI [-3.0, -0.4] Slope [Novel] = -0.4, CI [-1.8, 1.0] Slope [Global] = -1.0, CI [-2.0, -0.1] AICc test $P(H_1/H_0) = 0.41$	
	2way ANOVA	Environment $F(1, 56) = 0.88$, $P = 0.352$ Dose $F(3, 56) = 1.89$, $P = 0.141$ Environment X Dose $F(3, 56) = 2.50$, $P = 0.069$	
	Bayesian 2way ANOVA	BF_{incl}[Environment] =0.36 BF_{incl}[Dose] =0.53 BF_{incl}[Environment X Dose] =1.22	
4.3 B	RM 2way ANOVA	Transition $F(1, 54) = 282.6$, $P < 0.001$, $\eta_p^2 = 0.84$ Outcome $F(1, 54) = 23.9$, $P < 0.001$, $\eta_p^2 = 0.31$ Transition X Outcome $F(1, 54) = 343.0$, $P < 0.001$, $\eta_p^2 = 0.86$	Bonferroni: C+ vs. R+ $P < 0.001$ C+ vs. C- $P < 0.001$ C+ vs. R- $P < 0.001$ C- vs. R- $P < 0.001$ C- vs. R+ $P < 0.001$ R+ vs. R- $P < 0.001$
	Bayesian RM 1way ANOVA	BF_{incl}[Transition] >>100 BF_{incl}[Outcome] >100 BF_{incl}[Transition X Outcome] >>100	
4.3 C	One-sample *t*-tests or Wilcoxon signed-rank tests	*Theoretical mean =0* **Correct** $t(54) = 18.4$, $P < 0.001$, Cohen's $d = 2.48$ **Choice** $V = 1540$, $P < 0.001$, Rank-Biserial Corr. =1.00 **Outcome** $V = 1489$, $P < 0.001$, Rank-Biserial Corr. =0.93 **Transition** $t(54) = 17.1$, $P < 0.001$, Cohen's $d = 2.31$ **Transition X Outcome** $V = 1540$, $P < 0.001$, Rank-Biserial Corr. =1.00	
	Bayesian one-sample *t*-tests or	**Correct** Student BF_{10} >>100 **Choice** Wilcoxon signed-rank BF_{10} >>100 **Outcome** Wilcoxon signed-rank BF_{10} >>100	

	Wilcoxon signed-rank tests	**Transition** Student BF_{10} >>100 **Transition X Outcome** Wilcoxon signed-rank BF_{10} >>100	
4.3 D	One-sample *t*-tests or Wilcoxon signed-rank tests	*Theoretical mean =0* **Choice** **[9-12]** *V* =1372, *P*<0.001, Rank-Biserial Corr.=0.78 **[5-8]** *V* =1539, *P*<0.001, Rank-Biserial Corr. =1.00 **[3-4]** *t*(54) =16.2, *P*<0.001, Cohen's *d* =2.18 **[2]** *t*(54) =16.9, *P*<0.001, Cohen's *d* =2.27 **[1]** *V* =1540, *P*<0.001, Rank-Biserial Corr. =1.00 **Outcome** **[9-12]** *t*(54) =0.4, *P*=0.702 **[5-8]** *t*(54) =0.3, *P*=0.757 **[3-4]** *t*(54) =2.3, *P*=0.023, Cohen's *d* =0.32 **[2]** *t*(54) =3.7, *P*<0.001, Cohen's *d* =0.50 **[1]** *V* =1474, *P*<0.001, Rank-Biserial Corr. =0.91 **Transition** **[9-12]** *t*(54) =2.0, *P*=0.053 **[5-8]** *t*(54) =2.3, *P*=0.027, Cohen's *d* =0.31 **[3-4]** *t*(54) =4.8, *P*<0.001, Cohen's *d* =0.65 **[2]** *t*(54) =10.2, *P*<0.001, Cohen's *d* =1.38 **[1]** *t V* =1540, *P*<0.001, Rank-Biserial Corr. =1.00 **Transition X Outcome** **[9-12]** *t*(54) =5.4, *P*<0.001, Cohen's *d* =0.72 **[5-8]** *t*(54) =7.3, *P*<0.001, Cohen's *d* =0.98 **[3-4]** *t*(54) =7.5, *P*<0.001, Cohen's *d* =1.01 **[2]** *t*(54) =10.1, *P*<0.001, Cohen's *d* =1.36 **[1]** *t V* =1540, *P*<0.001, Rank-Biserial Corr. =1.00	
	Bayesian one-sample *t*-tests or Wilcoxon signed-rank tests	**Choice** **[9-12]** Wilcoxon signed-rank BF_{10} >100 **[5-8]** Wilcoxon signed-rank BF_{10} >>100 **[3-4]** Student BF_{10} >>100 **[2]** Student BF_{10} >>100 **[1]** Wilcoxon signed-rank BF_{10} >>100 **Outcome** **[9-12]** Student BF_{10} =0.16 **[5-8]** Student BF_{10} =0.15 **[3-4]** Student BF_{10} =1.78 **[2]** Student BF_{10} =50.68 **[1]** Wilcoxon signed-rank BF_{10} >>100 **Transition** **[9-12]** Student BF_{10} =0.90	

		[5-8] Student BF_{10} =1.56 **[3-4]** Student BF_{10} >>100 **[2]** Student BF_{10} >>100 **[1]** Wilcoxon signed-rank BF_{10} >>100 **Transition X Outcome** **[9-12]** Student BF_{10} >>100 **[5-8]** Student BF_{10} >>100 **[3-4]** Student BF_{10} >>100 **[2]** Student BF_{10} >>100 **[1]** Wilcoxon signed-rank BF_{10} >>100	
4.4 A	Unpaired *t*-test	$t(27) = -0.26$, $P=0.798$	
	Bayesian unpaired *t*-test	BF_{10} =0.36	
	Nonlinear line regression	**excluding four outliers* Extra sum-of-squares *F* test $F(2, 108)$ =0.18, $P=0.840$ Slope [VEH] =5.4, CI [-5.7, 16.5] Slope [DOI] =7.8, CI [-3.5, 19.2] Slope [Global] =6.6, CI [-1.1, 14.4] AICc test $P(H_1/H_0)$ =0.14	
	2way RM ANOVA	**excluding four outliers* Time $F(3, 78)$ =2.8, $P=0.048$, η_p^2 =0.10 Drug $F(1, 26)$ =0.08, $P=0.774$ Time X Drug $F(3, 78)$ =0.8, $P=0.515$	Bonferroni: [1-3] vs. [4-6] $P=1.000$ [1-3] vs. [7-9] $P=1.000$ [1-3] vs. [10-12] $P=0.037$ [4-6] vs. [7-9] $P=1.000$ [4-6] vs. [10-12] $P=0.362$ [7-9] vs. [10-12] $P=0.870$
	Bayesian 2way RM ANOVA	BF_{incl}[Time] =1.04 BF_{incl}[Drug] =0.46 BF_{incl}[Time X Drug] =0.19	
4.4 B	Mann-Whitney test	W =88.5, $P=0.484$	
	Bayesian Mann-Whitney	BF_{10} =0.39	

	Nonlinear line regression	**excluding three outliers* Extra sum-of-squares *F* test *F*(2, 109) =0.047, *P*=0.954 Slope [VEH] =1.0, CI [0.7, 1.3] Slope [DOI] =1.1, CI [0.8, 1.4] Slope [Global] =1.1, CI [0.9, 1.3] AICc test $P(H_1/H_0)$ =0.12	
	2way RM ANOVA	**excluding four outliers* **Greenhouse-Geisser corrected* Time *F*(2.2, 57.3) =71.9, *P*<0.001, η_p^2 =0.73 Drug *F*(1, 26) =0.02, *P*=0.900 Time X Drug *F*(2.2, 57.3) =0.83, *P*=0.451	Bonferroni: [1-3] vs. [4-6] *P*<0.001 [1-3] vs. [7-9] *P*<0.001 [1-3] vs. [10-12] *P*<0.001 [4-6] vs. [7-9] *P*<0.001 [4-6] vs. [10-12] *P*<0.001 [7-9] vs. [10-12] *P*=0.016
	Bayesian 2way RM ANOVA	BF_{incl}[Time] >>100 BF_{incl}[Drug] =0.38 BF_{incl}[Time X Drug] =0.21	
4.4 C	Unpaired *t*-test	*t*(27) =0.096, *P*=0.924	
	Bayesian unpaired *t*-test	BF_{10} =0.35	
	Nonlinear line regression	Extra sum-of-squares *F* test *F*(2, 112) =0.22, *P*=0.804 Slope [VEH] =0.068, CI [0.053, 0.082] Slope [DOI] =0.066, CI [0.052, 0.079] Slope [Global] =0.067, CI [0.057, 0.076] AICc test $P(H_1/H_0)$ =0.14	
	2way RM ANOVA	**Greenhouse-Geisser corrected* Time *F*(2.0, 54.4) =86.9, *P*<0.001, η_p^2 =0.76 Drug *F*(1, 27) =0.2, *P*=0.637 Time X Drug *F*(2.0, 54.4) =0.4, *P*=0.361	Bonferroni: [1-3] vs. [4-6] *P*<0.001 [1-3] vs. [7-9] *P*<0.001 [1-3] vs. [10-12] *P*<0.001 [4-6] vs. [7-9] *P*=0.010 [4-6] vs. [10-12] *P*<0.001

			[7-9] vs. [10-12] *P*=0.010
	Bayesian 2way RM ANOVA	BF_{incl}[Time] >>100 BF_{incl}[Drug] =0.33 BF_{incl}[Time X Drug] =0.13	
4.5 A	Unpaired *t*-test	*t*(27) = -1.03, *P*=0.313	
	Bayesian unpaired *t*-test	Student BF_{10} =0.52	
	Nonlinear line regression	**excluding one outlier* Extra sum-of-squares *F* test *F*(2, 111) =0.75, *P*=0.474 Slope [VEH] =0.01, CI [-0.11, 0.14] Slope [DOI] =0.11, CI [-0.03, 0.25] Slope [Global] =0.06, CI [-0.03, 0.15] AICc test $P(H_1/H_0)$ =0.23	
	2way RM ANOVA	**excluding one outlier* Time *F*(3, 78) =4.1, *P*=0.009, η_p^2 =0.14 Drug *F*(1, 26) =0.47, *P*=0.499 Time X Drug *F*(3, 78) =1.3, *P*=0.271	Bonferroni: [1-3] vs. [4-6] *P*=0.108 [1-3] vs. [7-9] *P*=0.006 [1-3] vs. [10-12] *P*=0.241 [4-6] vs. [7-9] *P*=1.000 [4-6] vs. [10-12] *P*=1.000 [7-9] vs. [10-12] *P*=1.000
	Bayesian 2way RM ANOVA	**excluding one outlier* BF_{incl}[Time] =4.18 BF_{incl}[Drug] =0.53 BF_{incl}[Time X Drug] =0.33	
4.5 B	Unpaired *t*-test	*t*(27) =1.00, *P*=0.327	
	Bayesian unpaired *t*-test	Student BF_{10} =0.51	

	Nonlinear line regression	Extra sum-of-squares *F* test $F(2, 112) = 0.32$, $P = 0.726$ Slope [VEH] =0.45, CI [0.33, 0.56] Slope [DOI] =0.41, CI [0.31, 0.52] Slope [Global] =0.43, CI [0.36, 0.51] AICc test $P(H_1/H_0) = 0.16$	
	2way RM ANOVA	**Greenhouse-Geisser corrected* Time $F(2.26, 60.98) = 52.9$, $P<0.001$, $\eta_p^2 = 0.66$ Drug $F(1, 27) = 0.27$, $P = 0.606$ Time X Drug $F(2.26, 60.98) = 0.32$, $P = 0.751$	Bonferroni: [1-3] vs. [4-6] $P<0.001$ [1-3] vs. [7-9] $P<0.001$ [1-3] vs. [10-12] $P<0.001$ [4-6] vs. [7-9] $P<0.001$ [4-6] vs. [10-12] $P<0.001$ [7-9] vs. [10-12] $P = 0.036$
	Bayesian 2way RM ANOVA	BF_{incl}[Time] >>100 BF_{incl}[Drug] =0.32 BF_{incl}[Time X Drug] =0.13	
4.5 C	Mann-Whitney test	W =120, $P = 0.533$	
	Mann-Whitney test	Mann-Whitney $BF_{10} = 0.46$	
	Nonlinear line regression	**excluding one outlier* Extra sum-of-squares *F* test $F(2, 111) = 0.17$, $P = 0.837$ Slope [VEH] =0.37, CI [0.27, 0.48] Slope [DOI] =0.33, CI [0.23, 0.43] Slope [Global] =0.35, CI [0.28, 0.43] AICc test $P(H_1/H_0) = 0.14$	
	2way RM ANOVA	**excluding one outlier* **Greenhouse-Geisser corrected* Time $F(2.02, 52.62) = 45.9$, $P<0.001$, $\eta_p^2 = 0.64$ Drug $F(1, 26) = 0.00038$, $P = 0.985$ Time X Drug $F(2.02, 52.62) = 0.19$, $P = 0.832$	Tukey: [1-3] vs. [4-6] $P<0.001$ [1-3] vs. [7-9] $P<0.001$ [1-3] vs. [10-12] $P<0.001$ [4-6] vs. [7-9] $P = 0.016$

			[4-6] vs. [10-12] P<0.001 [7-9] vs. [10-12] P=0.015
	Bayesian 2way RM ANOVA	*excluding one outlier BF_{incl}[Time] >>100 BF_{incl}[Drug] =0.33 BF_{incl}[Time X Drug] =0.12	
4.6	Permuta-tion test for double exp fit time constants	Tau_{fast} P=0.093 Tau_{slow} P=0.088	
	2way RM ANOVA	*Greenhouse-Geisser corrected Post-reversal trials only Time F(8.7, 235.0) =29.6, P<0.001, η_p^2 =0.52 Drug F(1, 27) =0.12, P=0.736 Time X Drug F(8.7, 235.0) =1.2, P=0.290	
	Bayesian RM 2way ANOVA	BF_{incl}[Time] >>100 BF_{incl}[Drug] =0.25 BF_{incl}[Time X Drug] =0.07	
4.7 A	2way RM ANOVA	Time F(1, 24) =6.4, P=0.018, η_p^2 =0.21 Drug F(1, 24) =0.8, P=0.391 Time X Drug F(1, 24) =0.6, P=0.456	
	Bayesian 2way RM ANOVA	BF_{incl}[Time] =3.03 BF_{incl}[Drug] =0.69 BF_{incl}[Time X Drug] =0.44	
	Nonlinear line regression	Extra sum-of-squares F test F(2, 100) =0.24, P=0.786 Slope [VEH] = -9.4, CI [-23.1, 4.4] Slope [DOI] = -3.5, CI [-16.8, 9.8] Slope [Global] = -6.4, CI [-15.8, 2.9] AICc test $P(H_1/H_0)$ =0.14	
	2way RM ANOVA	*Greenhouse-Geisser corrected Time F(1.9, 45.7) =1.8, P=0.177 Drug F(1, 24) =0.03, P=0.858 Time X Drug F(1.9, 45.7) =0.5, P=0.597	
	Bayesian 2way RM ANOVA	BF_{incl}[Time] =0.39 BF_{incl}[Drug] =0.47 BF_{incl}[Time X Drug] =0.16	
4.7 B	2way RM ANOVA	Time F(1, 24) =8.1, P=0.009, η_p^2 =0.25 Drug F(1, 24) =1.6, P=0.064 Time X Drug F(1, 24) =0.003, P=0.959	

	Bayesian 2way RM ANOVA	BF_{incl}[Time] =5.67 BF_{incl}[Drug] =0.80 BF_{incl}[Time X Drug] =0.36	
	Nonlinear line regression	Extra sum-of-squares *F* test *F*(2, 100) =0.032, *P*=0.968 Slope [VEH] =1.3, CI [0.8, 1.8] Slope [DOI] =1.2, CI [0.8, 1.6] Slope [Global] =1.2, CI [0.9, 1.5] AICc test $P(H_1/H_0)$ =0.12	
	2way RM ANOVA	**Greenhouse-Geisser corrected* Time *F*(1.9, 44.6) =49.0, *P*<0.001, η_p^2 =0.67 Drug *F*(1, 24) =0.01, *P*=0.915 Time X Drug *F*(1.9, 44.6) =1.9, *P*=0.142	Bonferroni: [1-3] vs. [4-6] *P*<0.001 [1-3] vs. [7-9] *P*<0.001 [1-3] vs. [10-12] *P*<0.001 [4-6] vs. [7-9] *P*=0.012 [4-6] vs. [10-12] *P*<0.001 [7-9] vs. [10-12] *P*=0.079
	Bayesian 2way RM ANOVA	BF_{incl}[Time] >>100 BF_{incl}[Drug] =0.44 BF_{incl}[Time X Drug] =0.11	
4.7 C	2way RM ANOVA	Time *F*(1, 24) =0.42, *P*=0.521 Drug *F*(1, 24) =0.34, *P*=0.566 Time X Drug *F*(1, 24) =0.002, *P*=0.967	
	Bayesian 2way RM ANOVA	BF_{incl}[Time] =0.33 BF_{incl}[Drug] =0.50 BF_{incl}[Time X Drug] =0.36	
	Nonlinear one-phase associ-ation regression	**excluding two outliers* Extra sum-of-squares *F* test *F*(3, 96) =0.63, *P*=0.599 Tau [VEH] =1.94, CI [1.00, 8.47] Plateau [VEH] =0.74, CI [0.65, 1.33] Tau [DOI] =1.77, CI [0.76, 36.33] Plateau [DOI] =0.68, CI [0.60, 3.33] Tau [Global] =1.85, CI [1.08, 4.68] Plateau [Global] =0.71, CI [0.64, 0.95] AICc test $P(H_1/H_0)$ =0.09	

	2way RM ANOVA	**excluding two outliers* Time $F(3, 69) = 130.7$, $P<0.001$, $\eta_p^2 = 0.85$ Drug $F(1, 23) = 0.59$, $P=0.450$ Time X Drug $F(3, 69) = 0.48$, $P=0.700$	Bonferroni: [1-3] vs. [4-6] $P<0.001$ [1-3] vs. [7-9] $P<0.001$ [1-3] vs. [10-12] $P<0.001$ [4-6] vs. [7-9] $P<0.001$ [4-6] vs. [10-12] $P<0.001$ [7-9] vs. [10-12] $P=0.054$
	Bayesian 2way RM ANOVA	BF_{incl}[Time] >>100 BF_{incl}[Drug] =0.48 BF_{incl}[Time X Drug] =0.16	
4.8 A	2way RM ANOVA	Time $F(1, 24) = 2.1$, $P=0.161$ Drug $F(1, 24) = 2.5$, $P=0.127$ Time X Drug $F(1, 24) = 3.3$, $P=0.082$	
	Bayesian 2way RM ANOVA	BF_{incl}[Time] =0.62 BF_{incl}[Drug] =0.97 BF_{incl}[Time X Drug] =1.12	
	Nonlinear line regression	Extra sum-of-squares *F* test $F(2, 100) = 1.28$, $P=0.283$ Slope [VEH] = -0.029, CI [-0.173, 0.116] Slope [DOI] = -0.008, CI [-0.120, 0.103] Slope [Global] = -0.02, CI [-0.11, 0.07] AICc test $P(H_1/H_0) = 0.42$	
	2way RM ANOVA	Time $F(3, 72) = 1.5$, $P=0.230$ Drug $F(1, 24) = 0.8$, $P=0.378$ Time X Drug $F(3, 72) = 1.5$, $P=0.223$	
	Bayesian 2way RM ANOVA	BF_{incl}[Time] =0.26 BF_{incl}[Drug] =0.61 BF_{incl}[Time X Drug] =0.41	
4.8 B	2way RM ANOVA	Time $F(1, 24) = 3.8$, $P=0.063$ Drug $F(1, 24) = 0.2$, $P=0.624$ Time X Drug $F(1, 24) = 0.4$, $P=0.520$	
	Bayesian 2way RM ANOVA	BF_{incl}[Time] =1.23 BF_{incl}[Drug] =0.53 BF_{incl}[Time X Drug] =0.41	

	Nonlinear one-phase associ-ation regression	Extra sum-of-squares *F* test $F(3, 98) = 1.06$, $P = 0.372$ Tau [VEH] =1.24, CI [0.65, 3.14] Tau [DOI] =1.31, CI [0.56, 6.10] Tau [Global] =1.27, CI [0.76, 2.52] AICc test $P(H_1/H_0) = 0.18$	
	2way RM ANOVA	**Greenhouse-Geisser corrected* Time $F(2.02, 48.47) = 93.8$, $P<0.001$, $\eta_p^2 = 0.80$ Drug $F(1, 24) = 1.5$, $P = 0.232$ Time X Drug $F(2.02, 48.47) = 0.6$, $P = 0.522$	Bonferroni: [1-3] vs. [4-6] $P<0.001$ [1-3] vs. [7-9] $P<0.001$ [1-3] vs. [10-12] $P<0.001$ [4-6] vs. [7-9] $P<0.001$ [4-6] vs. [10-12] $P<0.001$ [7-9] vs. [10-12] $P = 0.408$
	Bayesian 2way RM ANOVA	BF_{incl}[Time] >>100 BF_{incl}[Drug] =0.59 BF_{incl}[Time X Drug] =0.19	
4.8 C	2way RM ANOVA	Time $F(1, 24) = 1.4$, $P = 0.246$ Drug $F(1, 24) = 1.3$, $P = 0.261$ Time X Drug $F(1, 24) = 0.4$, $P = 0.528$	
	Bayesian 2way RM ANOVA	BF_{incl}[Time] =0.49 BF_{incl}[Drug] =0.66 BF_{incl}[Time X Drug] =0.41	
	Nonlinear one-phase associ-ation regression	Extra sum-of-squares *F* test $F(3, 98) = 4.76$, $P = 0.004$ Tau [VEH] =1.28, CI [0.62, 4.03] Tau [DOI] =1.41, CI [0.75, 3.82] AICc test $P(H_1/H_0) = 40.10$	Y_0 [1-3] $P = 0.621$ Tau $P = 0.849$ Plateau [10-12] $P = 0.226$
	2way RM ANOVA	**Greenhouse-Geisser corrected* Time $F(2.09, 50.23) = 127.4$, $P<0.001$, $\eta_p^2 = 0.84$ Drug $F(1, 24) = 5.0$, $P = 0.035$, $\eta_p^2 = 0.17$ Time X Drug $F(2.09, 50.23) = 1.79$, $P = 0.177$	Exploratory Fisher's DOI vs. VEH: [1-3] $P = 0.500$ [4-6] $P = 0.023$ [7-9] $P = 0.217$ [10-12] $P = 0.022$
	Bayesian 2way RM ANOVA	BF_{incl}[Time] >>100 BF_{incl}[Drug] =2.11 BF_{incl}[Time X Drug] =0.54	

4.9 A	One sample *t*-tests	*Theoretical mean = 0* **VEH** **Correct** *t*(12) =10.43, *P*<0.001, Cohen's *d* =2.89 **Choice** *t*(12) =17.14, *P*<0.001, Cohen's *d* =4.75 **Outcome** *t*(12) =5.99, *P*<0.001, Cohen's *d* =1.66 **Reward by transition** *t*(12) =12.74, *P*<0.001, Cohen's *d* =3.53 **Omission by transition** *t*(12) =0.30, *P*=0.768 **DOI** **Correct** *t*(12) =11.15, *P*<0.001, Cohen's *d* =3.09 **Choice** *t*(12) =14.21, *P*<0.001, Cohen's *d* =3.94 **Outcome** *t*(12) =4.18, *P*=0.001, Cohen's *d* =1.16 **Reward by transition** *t*(12) =7.70, *P*<0.001, Cohen's *d* =2.14 **Omission by transition** *t*(12) = -0.52, *P*=0.610	
	Bayesian one sample *t*-tests	**VEH** **Correct** BF_{10} >>100 **Choice** BF_{10} >>100 **Outcome** BF_{10} >100 **Reward by transition** BF_{10} >>100 **Omission by transition** BF_{10} =0.29 **DOI** **Correct** BF_{10} >>100 **Choice** BF_{10} >>100 **Outcome** BF_{10} =32.25 **Reward by transition** BF_{10} >>100 **Omission by transition** BF_{10} =0.31	
4.9 B	2way RM ANOVA	Time *F*(1, 24) =3.4, *P*=0.079 Drug *F*(1, 24) =0.8, *P*=0.387 Time X Drug *F*(1, 24) =0.6, *P*=0.444	
	Bayesian 2way RM ANOVA	BF_{incl}[Time] =1.04 BF_{incl}[Drug] =0.61 BF_{incl}[Time X Drug] =0.44	
	Nonlinear one-phase associ-ation regression	Extra sum-of-squares *F* test *F*(3, 98) =2.82, *P*=0.043 Tau [VEH] =1.26, CI [0.66, 3.20] Plateau [VEH] =1.32, CI [0.72, 3.13] Tau [DOI] =1.37, CI [0.70, 3.96] Plateau [DOI] =2.01, CI [1.28, 4.73]	Y_0 [1-3] *P*=0.429 Tau *P*=0.867 Plateau [10-12] *P*=0.329

		AICc test $P(H_1/H_0)$ =2.53	
	2way RM ANOVA	**Greenhouse-Geisser corrected* Time $F(1.96, 47.10)$ =140.4, $P<0.001$, η_p^2 =0.85 Drug $F(1, 24)$ =3.2, P=0.085 Time X Drug $F(1.96, 47.10)$ =1.0, P=0.372	Exploratory Fisher's DOI vs. VEH: [1-3] P=0.290 [4-6] P=0.072 [7-9] P=0.482 [10-12] P=0.056
	Bayesian 2way RM ANOVA	BF_{incl}[Time] >>100 BF_{incl}[Drug] =1.78 BF_{incl}[Time X Drug] =0.26	
4.9 C	2way RM ANOVA	Time $F(1, 24)$ =0.13, P=0.725 Drug $F(1, 24)$ =0.76, P=0.392 Time X Drug $F(1, 24)$ =0.01, P=0.907	
	Bayesian 2way RM ANOVA	BF_{incl}[Time] =0.29 BF_{incl}[Drug] =0.47 BF_{incl}[Time X Drug] =0.36	
	Nonlinear line regression	Extra sum-of-squares F test $F(2, 100)$ =5.22, P=0.007 Slope [VEH] =0.006, CI [-0.063, 0.074] Slope [DOI] = -0.112, CI [-0.192, -0.032] AICc test $P(H_1/H_0)$ =19.62	Slope P=0.027
	2way RM ANOVA	Time $F(3, 72)$ =1.4, P=0.262 Drug $F(1, 24)$ =5.5, P=0.027, η_p^2 =0.19 Time X Drug $F(3, 72)$ =1.9, P=0.142	Exploratory Fisher's DOI vs. VEH: [1-3] P=0.506 [4-6] P=0.447 [7-9] P=0.059 [10-12] P=0.037
	Bayesian 2way RM ANOVA	BF_{incl}[Time] =0.28 BF_{incl}[Drug] =0.98 BF_{incl}[Time X Drug] =0.75	
	One-sample *t*-tests	**VEH** **Pre-drug** $t(12)$ =0.30, P=0.768 **Post-drug** $t(12)$ =0.78, P=0.452 **[1-3]** $t(12)$ = -0.07, P=0.943 **[4-6]** $t(12)$ =0.10, P=0.922 **[7-9]** $t(12)$ =0.34, P=0.739 **[10-12]** $t(12)$ =0.06, P=0.954 **DOI** **Pre-drug** $t(12)$ = -0.52, P=0.610	

		Post-drug $t(12) = -0.39$, $P=0.707$ **[1-3]** $t(12) =0.87$, $P=0.403$ **[4-6]** $t(12) = -0.87$, $P=0.406$ **[7-9]** $t(12) = -2.82$, $P=0.015$, Cohen's $d = -0.78$ **[10-12]** $t(12) = -2.48$, $P=0.029$, Cohen's $d = -0.69$	
	Bayesian one-sample *t*-tests	**VEH** **Pre-drug** $BF_{10} =0.29$ **Post-drug** $BF_{10} =0.36$ **[1-3]** $BF_{10} =0.28$ **[4-6]** $BF_{10} =0.28$ **[7-9]** $BF_{10} =0.29$ **[10-12]** $BF_{10} =0.28$ **DOI** **Pre-drug** $BF_{10} =0.31$ **Post-drug** $BF_{10} =0.30$ **[1-3]** $BF_{10} =0.38$ **[4-6]** $BF_{10} =0.38$ **[7-9]** $BF_{10} =4.08$ **[10-12]** $BF_{10} =2.46$	
4.10	Unpaired *t*-test	$t(27) =0.15$, $P=0.880$	
	Bayesian unpaired *t*-test	$BF_{10} =0.35$	
	One-sample *t*-tests	**VEH** $t(14) =2.18$, $P=0.048$ **DOI** $t(13) =1.85$, $P=0.087$	
	Bayesian one-sample *t*-tests	**VEH** $BF_{10} =1.60$ **DOI** $BF_{10} =1.04$	
	Nonlinear line regression	Extra sum-of-squares *F* test $F(2, 112) =0.02$, $P=0.979$ Slope [VEH] =0.07, CI [0.02, 0.13] Slope [DOI] =0.07, CI [-0.02, 0.16] Slope [Global] =0.07, CI [0.02, 0.13] AICc test $P(H_1/H_0) =0.12$	
	2way RM ANOVA	Time $F(3, 81) =3.3$, $P=0.025$, $\eta_p^2 =0.11$ Drug $F(1, 27) =0.02$, $P=0.887$ Time X Drug $F(3, 81) =0.1$, $P=0.954$	Bonferroni: [1-3] vs. [4-6] $P=0.923$ [1-3] vs. [7-9] $P=0.055$ [1-3] vs. [10-12] $P=0.049$ [4-6] vs. [7-9] $P=1.000$

			[4-6] vs. [10-12] *P*=1.000 [7-9] vs. [10-12] *P*=1.000
	Bayesian 2way RM ANOVA	BF_{incl}[Time] =2.38 BF_{incl}[Drug] =0.29 BF_{incl}[Time X Drug] =0.10	
4. 11A	One-sample *t*-tests	*Theoretical mean =0* **Correct** *t*(17) =10.99, *P*<0.001, Cohen's *d* =2.59 **Choice** *t*(17) =14.94, *P*<0.001, Cohen's *d* =3.52 **Outcome** *t*(17) =4.52, *P*<0.001, Cohen's *d* =1.07 **Reward by transition** *t*(17) =10.03, *P*<0.001, Cohen's *d* =2.36 **Omission by transition** *t*(17) =1.77, *P*=0.095	
	Bayesian one-sample *t*-tests	**Correct** BF_{10} >>100 **Choice** BF_{10} >>100 **Outcome** BF_{10} =105.73 **Reward by transition** BF_{10} >>100 **Omission by transition** BF_{10} =0.88	
4. 11B	Nonlinear line regression	*Null hypothesis: slope = 0* Extra sum-of-squares *F* test *F*(1, 70) =0.13, *P*=0.724 Slope = -0.02, CI [-0.14, 0.10] AICc test *P*(H_1/H_0) =0.36	
	1way RM ANOVA	Time *F*(3, 51) =1.4, *P*=0.257	
	Bayesian 1way RM ANOVA	BF_{incl}[Time] =0.31	
	One-sample *t*-tests	**[1-3]** *t*(17) =1.78, *P*=0.093 **[4-6]** *t*(17) =0.28, *P*=0.782 **[7-9]** *t*(17) =1.60, *P*=0.128 **[10-12]** *t*(17) =0.52, *P*=0.613	
	Bayesian one-sample *t*-tests	**[1-3]** BF_{10} =0.90 **[4-6]** BF_{10} =0.25 **[7-9]** BF_{10} =0.71 **[10-12]** BF_{10} =0.27	

4. 12A	Permu-tation test	Tau_{fast} P=0.659 Tau_{slow} P=0.821	
	2way RM ANOVA	**Greenhouse-Geisser corrected* *Post-reversal trials only* Time F(7.4, 177.3) =60.0, P<0.001, η_p^2 =0.71 Drug F(1, 24) =0.008, P=0.931 Time X Drug F(7.4, 177.3) =0.9, P=0.532	
	Bayesian RM 2way ANOVA	BF_{incl}[Time] >>100 BF_{incl}[Drug] =0.25 BF_{incl}[Time X Drug] =0.02	
4. 12B	Permu-tation test	Tau_{fast} P=0.073 Tau_{slow} P=0.036	
	2way RM ANOVA	*Post-reversal trials only* Time F(19, 456) =86.4, P<0.001, η_p^2 =0.78 Drug F(1, 24) =0.6, P=0.453 Time X Drug F(19, 456) =2.1, P=0.006, η_p^2 =0.08	
	Bayesian RM 2way ANOVA	BF_{incl}[Time] >>100 BF_{incl}[Drug] =0.34 BF_{incl}[Time X Drug] =4.20	
4. 13C	Permu-tation test	Tau_{fast} P=0.052 Tau_{slow} P=0.012	
	2way RM ANOVA	**Greenhouse-Geisser corrected* *Post-reversal trials only* Time F(8.0, 192.8) =87.3, P<0.001, η_p^2 =0.78 Drug F(1, 24) =0.5, P=0.509 Time X Drug F(8.0, 192.8) =1.7, P=0.094	
	Bayesian RM 2way ANOVA	BF_{incl}[Time] >>100 BF_{incl}[Drug] =0.27 BF_{incl}[Time X Drug] =0.89	
4. 13D	Permu-tation test	Tau_{fast} P=0.081 Tau_{slow} P=0.159	
	2way RM ANOVA	**Greenhouse-Geisser corrected* *Post-reversal trials only* Time F(7.5, 179.0) =58.9, P<0.001, η_p^2 =0.71 Drug F(1, 24) =0.01, P=0.916 Time X Drug F(7.5, 179.0) =1.2, P=0.331	
	Bayesian RM 2way ANOVA	BF_{incl}[Time] >>100 BF_{incl}[Drug] =0.28 BF_{incl}[Time X Drug] =0.07	
4. 14A	Unpaired *t*-test	t(25) =1.84, P=0.078	

	Bayesian unpaired *t*-test	BF_{10} =1.21	
4. 14B	Unpaired *t*-test	*t*(25) =1.59, *P*=0.124	
	Bayesian unpaired *t*-test	BF_{10} =0.90	

10 | References

Adams LM, Geyer MA (1982) LSD-induced alterations of locomotor patterns and exploration in rats. Psychopharmacology (Berl) 77:179–185.

Adams LM, Geyer MA (1985a) Effects of DOM and DMT in a proposed animal model of hallucinogenic activity. Prog Neuropsychopharmacol Biol Psychiatry 9:121–132.

Adams LM, Geyer MA (1985b) A proposed animal model for hallucinogens based on LSD's effects on patterns of exploration in rats. Behavioral neuroscience 99:881.

Aghajanian GK, Marek GJ (1999) Serotonin, via 5-HT2A receptors, increases EPSCs in layer V pyramidal cells of prefrontal cortex by an asynchronous mode of glutamate release. Brain Res 825:161–171.

Akam T, Costa R, Dayan P (2015) Simple plans or sophisticated habits? State, transition and learning interactions in the two-step task. PLoS Comput Biol 11:e1004648.

Akam T, Lustig A, Rowland JM, Kapanaiah SKT, Esteve-Agraz J, Panniello M, Márquez C, Kohl MM, Kätzel D, Costa RM, Walton ME (2022) Open-source, Python-based, hardware and software for controlling behavioural neuroscience experiments. Elife 11.

Akam T, Rodrigues-Vaz I, Marcelo I, Zhang X, Pereira M, Oliveira RF, Dayan P, Costa RM (2021) The Anterior Cingulate Cortex Predicts Future States to Mediate Model-Based Action Selection. Neuron 109:149-163.e7.

al Shoyaib A, Archie SR, Karamyan VT (2020) Intraperitoneal Route of Drug Administration: Should it Be Used in Experimental Animal Studies? Pharm Res 37:1–17.

Almeida RN de, Galvão AC de M, da Silva FS, Silva EA dos S, Palhano-Fontes F, Maia-de-Oliveira JP, de Araújo L-SB, Lobão-Soares B, Galvão-Coelho NL (2019) Modulation of serum brain-derived neurotrophic factor by a single dose of ayahuasca: observation from a randomized controlled trial. Front Psychol 10:1234.

Alsiö J, Lehmann O, McKenzie C, Theobald DE, Searle L, Xia J, Dalley JW, Robbins TW (2021) Serotonergic innervations of the orbitofrontal and medial-prefrontal cortices are differentially involved in visual discrimination and reversal learning in rats. Cerebral Cortex 31:1090–1105.

Amende I, Kale A, McCue S, Glazier S, Morgan JP, Hampton TG (2005) Gait dynamics in mouse models of Parkinson's disease and Huntington's disease. J Neuroeng Rehabil 2:1–13.

Amsel A (1958) The role of frustrative nonreward in noncontinuous reward situations. Psychol Bull 55:102.

Andrade R, Weber E (2010) Htr2a Gene and 5-HT2A Receptor Expression in the Cerebral Cortex Studied Using Genetically Modified Mice. Front Neurosci 4.

Antonia K, Anastasia A, Tesseromatis C (2012) Stress can affect drug pharmacokinetics via serum/tissues protein binding and blood flow rate alterations. Eur J Drug Metab Pharmacokinet 37:1–7.

Antoniadou I, Kouskou M, Arsiwala T, Singh N, Vasudevan SR, Fowler T, Cadirci E, Churchill GC, Sharp T (2018) Ebselen has lithium-like effects on central 5-HT2A receptor function. Br J Pharmacol 175:2599–2610.

Appel JB, West WB, Rolandi WG, Alici T, Pechersky K (1999) Increasing the selectivity of drug discrimination procedures. Pharmacol Biochem Behav 64:353–358.

Arnt J, Hyttel J (1989) Facilitation of 8-OHDPAT-induced forepaw treading of rats by the 5-HT2 agonist DOI. Eur J Pharmacol 161:45–51.

Asan L, Falfán-Melgoza C, Beretta CA, Sack M, Zheng L, Weber-Fahr W, Kuner T, Knabbe J (2021) Cellular correlates of gray matter volume changes in magnetic resonance morphometry identified by two-photon microscopy. Sci Rep 11:1–20.

Ashburner J, Friston KJ (2000) Voxel-based morphometry—the methods. Neuroimage 11:805–821.

Atasoy S, Vohryzek J, Deco G, Carhart-Harris RL, Kringelbach ML (2018) Common neural signatures of psychedelics: frequency-specific energy changes and repertoire expansion revealed using connectome-harmonic decomposition. In: Progress in Brain Research, pp 97–120. Elsevier.

Auger SD, Maguire EA (2018) Retrosplenial cortex indexes stability beyond the spatial domain. Journal of Neuroscience 38:1472–1481.

Badea A, Ali-Sharief AA, Johnson GA (2007) Morphometric analysis of the C57BL/6J mouse brain. Neuroimage 37:683–693.

Badiani A, Oates MM, Day HEW, Watson SJ, Akil H, Robinson TE (1998) Amphetamine-induced behavior, dopamine release, and c-fos mRNA expression: modulation by environmental novelty. Journal of Neuroscience 18:10579–10593.

Bakker R, Tiesinga P, Kötter R (2015) The Scalable Brain Atlas: Instant Web-Based Access to Public Brain Atlases and Related Content. Neuroinformatics 13:353–366.

Barrett FS, Doss MK, Sepeda ND, Pekar JJ, Griffiths RR (2020) Emotions and brain function are altered up to one month after a single high dose of psilocybin. Sci Rep 10:1–14.

Beckmann N, Schuler A, Mueggler T, Meyer EP, Wiederhold K-H, Staufenbiel M, Krucker T (2003) Age-dependent cerebrovascular abnormalities and blood flow disturbances in APP23 mice modeling Alzheimer's disease. Journal of Neuroscience 23:8453–8459.

Béïque J-C, Imad M, Mladenovic L, Gingrich JA, Andrade R (2007) Mechanism of the 5-hydroxytryptamine 2A receptor-mediated facilitation of synaptic activity in prefrontal cortex. Proceedings of the National Academy of Sciences 104:9870–9875.

Belmaker RH, Agam G (2008) Major depressive disorder. New England Journal of Medicine 358:55–68.

Belsky J, Bakermans-Kranenburg MJ, van IJzendoorn MH (2007) For better and for worse: Differential susceptibility to environmental influences. Curr Dir Psychol Sci 16:300–304.

Belsky J, Jonassaint C, Pluess M, Stanton M, Brummett B, Williams R (2009) Vulnerability genes or plasticity genes? Mol Psychiatry 14:746–754.

Benekareddy M, Nair AR, Dias BG, Suri D, Autry AE, Monteggia LM, Vaidya VA (2013) Induction of the plasticity-associated immediate early gene Arc by stress and

hallucinogens: role of brain-derived neurotrophic factor. International Journal of Neuropsychopharmacology 16:405–415.

Benjamini Y, Hochberg Y (1995) Controlling the False Discovery Rate: A Practical and Powerful Approach to Multiple Testing. Journal of the Royal Statistical Society: Series B (Methodological) 57:289–300.

Benjamini Y, Yekutieli D (2001) The control of the false discovery rate in multiple testing under dependency. Annals of statistics 29:1165–1188.

Bennett MR (2011) The prefrontal–limbic network in depression: A core pathology of synapse regression. Prog Neurobiol 93:457–467.

Benowitz LI, Routtenberg A (1997) GAP-43: an intrinsic determinant of neuronal development and plasticity. Trends Neurosci 20:84–91.

Berridge CW, Mitton E, Clark W, Roth RH (1999) Engagement in a non-escape (displacement) behavior elicits a selective and lateralized suppression of frontal cortical dopaminergic utilization in stress. Synapse 32:187–197.

Berry SA, Shah MC, Khan N, Roth BL (1996) Rapid agonist-induced internalization of the 5-hydroxytryptamine2A receptor occurs via the endosome pathway in vitro. Mol Pharmacol 50:306–313.

Bershad AK, Schepers ST, Bremmer MP, Lee R, de Wit H (2019) Acute subjective and behavioral effects of microdoses of lysergic acid diethylamide in healthy human volunteers. Biol Psychiatry 86:792–800.

Bhattacharyya S, Puri S, Miledi R, Panicker MM (2002) Internalization and recycling of 5-HT2A receptors activated by serotonin and protein kinase C-mediated mechanisms. Proceedings of the National Academy of Sciences 99:14470–14475.

Biedermann S, Fuss J, Zheng L, Sartorius A, Falfán-Melgoza C, Demirakca T, Gass P, Ende G, Weber-Fahr W (2012) In vivo voxel based morphometry: detection of increased hippocampal volume and decreased glutamate levels in exercising mice. Neuroimage 61:1206–1212.

Birzniece V, Johansson I-M, Wang M-D, Bäckström T, Olsson T (2002) Ovarian hormone effects on 5-hydroxytryptamine2A and 5-hydroxytryptamine2C receptor mRNA expression in the ventral hippocampus and frontal cortex of female rats. Neurosci Lett 319:157–161.

Blanchard DC, Shepherd JK, Rodgers RJ, Blanchard RJ (1992) Evidence for differential effects of 8-OH-DPAT on male and female rats in the anxiety/defense test battery. Psychopharmacology (Berl) 106:531–539.

Blanco-Pozo M, Akam T, Walton M (2021) Dopamine reports reward prediction errors, but does not update policy, during inference-guided choice. bioRxiv.

Blumenfeld-Katzir T, Pasternak O, Dagan M, Assaf Y (2011) Diffusion MRI of structural brain plasticity induced by a learning and memory task. PLoS One 6:e20678.

Bogenschutz MP, Forcehimes AA, Pommy JA, Wilcox CE, Barbosa PCR, Strassman RJ (2015) Psilocybin-assisted treatment for alcohol dependence: a proof-of-concept study. Journal of psychopharmacology 29:289–299.

Bogenschutz MP, Ross S, Bhatt S, Baron T, Forcehimes AA, Laska E, Mennenga SE, O'Donnell K, Owens LT, Podrebarac S (2022) Percentage of Heavy Drinking Days Following Psilocybin-Assisted Psychotherapy vs Placebo in the Treatment of Adult Patients With Alcohol Use Disorder: A Randomized Clinical Trial. JAMA Psychiatry 79:953–962.

Bornstein MB, Murray MR (1958) Serial observations on patterns of growth, myelin formation, maintenance and degeneration in cultures of new-born rat and kitten cerebellum. J Cell Biol 4:499–504.

Boulougouris V, Glennon JC, Robbins TW (2008) Dissociable effects of selective 5-HT 2A and 5-HT 2C receptor antagonists on serial spatial reversal learning in rats. Neuropsychopharmacology 33:2007.

Boulougouris V, Robbins TW (2010) Enhancement of Spatial Reversal Learning by 5-HT2C Receptor Antagonism Is Neuroanatomically Specific. Journal of Neuroscience 30:930–938.

Bourne JN, Harris KM (2008) Balancing structure and function at hippocampal dendritic spines. Annu Rev Neurosci 31:47.

Bouso JC, Fábregas JM, Antonijoan RM, Rodríguez-Fornells A, Riba J (2013) Acute effects of ayahuasca on neuropsychological performance: differences in executive function between experienced and occasional users. Psychopharmacology (Berl) 230:415–424.

Bouso JC, González D, Fondevila S, Cutchet M, Fernández X, Barbosa PCR, Alcázar-Córcoles MÁ, Araújo WS, Barbanoj MJ, Fábregas JM (2012) Personality, psychopathology, life attitudes and neuropsychological performance among ritual users of ayahuasca: a longitudinal study. PLoS One 7:e42421.

Bouso JC, Palhano-Fontes F, Rodríguez-Fornells A, Ribeiro S, Sanches R, Crippa JAS, Hallak JEC, de Araujo DB, Riba J (2015) Long-term use of psychedelic drugs is associated with differences in brain structure and personality in humans. European Neuropsychopharmacology 25:483–492.

Branchi I (2011) The double edged sword of neural plasticity: increasing serotonin levels leads to both greater vulnerability to depression and improved capacity to recover. Psychoneuroendocrinology 36:339–351.

Bressloff PC, Cowan JD, Golubitsky M, Thomas PJ, Wiener MC (2002) What geometric visual hallucinations tell us about the visual cortex. Neural Comput 14:473–491.

Brookshire BR, Jones SR (2009) Direct and indirect 5-HT receptor agonists produce gender-specific effects on locomotor and vertical activities in C57 BL/6J mice. Pharmacol Biochem Behav 94:194–203.

Brouwer A, Carhart-Harris RL (2021) Pivotal mental states. Journal of Psychopharmacology 35:319–352.

Buckner RL, Andrews-Hanna JR, Schacter DL (2008) The Brain's Default Network. Ann N Y Acad Sci 1124:1–38.

Burghardt NS, Sigurdsson T, Gorman JM, McEwen BS, LeDoux JE (2013) Chronic antidepressant treatment impairs the acquisition of fear extinction. Biol Psychiatry 73:1078–1086.

Cahill LS, Laliberté CL, Ellegood J, Spring S, Gleave JA, van Eede MC, Lerch JP, Henkelman RM (2012) Preparation of fixed mouse brains for MRI. Neuroimage 60:933–939.

Cameron LP, Benson CJ, Dunlap LE, Olson DE (2018) Effects of N, N-dimethyltryptamine on rat behaviors relevant to anxiety and depression. ACS Chem Neurosci 9:1582–1590.

Cameron LP, Patel SD, Vargas M v, Barragan E v, Saeger HN, Warren HT, Chow WL, Gray JA, Olson DE (2023) 5-HT2ARs Mediate Therapeutic Behavioral Effects of Psychedelic Tryptamines. ACS Chem Neurosci.

Cameron LP, Tombari RJ, Lu J, Pell AJ, Hurley ZQ, Ehinger Y, Vargas M v, McCarroll MN, Taylor JC, Myers-Turnbull D (2021) A non-hallucinogenic psychedelic analogue with therapeutic potential. Nature 589:474–479.

Canal CE, da Silva UBO, Gresch PJ, Watt EE, Sanders-Bush E, Airey DC (2010) The serotonin 2C receptor potently modulates the head-twitch response in mice induced by a phenethylamine hallucinogen. Psychopharmacology (Berl) 209:163–174.

Canal CE, Morgan D (2012) Head-twitch response in rodents induced by the hallucinogen 2,5-dimethoxy-4-iodoamphetamine: a comprehensive history, a re-evaluation of mechanisms, and its utility as a model. Drug Test Anal 4:556–576.

Cao J, Worsley KJ (1999) The detection of local shape changes via the geometry of Hotelling's T2 fields. The Annals of Statistics 27:925–942.

Carbonaro TM, Bradstreet MP, Barrett FS, MacLean KA, Jesse R, Johnson MW, Griffiths RR (2016) Survey study of challenging experiences after ingesting psilocybin mushrooms: Acute and enduring positive and negative consequences. Journal of Psychopharmacology 30:1268–1278.

Carbonaro TM, Eshleman AJ, Forster MJ, Cheng K, Rice KC, Gatch MB (2015) The role of 5-HT 2A, 5-HT 2C and mGlu2 receptors in the behavioral effects of tryptamine hallucinogens N, N-dimethyltryptamine and N, N-diisopropyltryptamine in rats and mice. Psychopharmacology (Berl) 232:275–284.

Carhart-Harris R, Giribaldi B, Watts R, Baker-Jones M, Murphy-Beiner A, Murphy R, Martell J, Blemings A, Erritzoe D, Nutt DJ (2021) Trial of psilocybin versus escitalopram for depression. New England Journal of Medicine 384:1402–1411.

Carhart-Harris RL et al. (2016a) Neural correlates of the LSD experience revealed by multimodal neuroimaging. Proceedings of the National Academy of Sciences 113:4853–4858.

Carhart-Harris RL (2018) The entropic brain - revisited. Neuropharmacology 142:167–178.

Carhart-Harris RL, Bolstridge M, Day CMJ, Rucker J, Watts R, Erritzoe DE, Kaelen M, Giribaldi B, Bloomfield M, Pilling S (2018a) Psilocybin with psychological support for treatment-resistant depression: six-month follow-up. Psychopharmacology (Berl) 235:399–408.

Carhart-Harris RL, Bolstridge M, Rucker J, Day CMJ, Erritzoe D, Kaelen M, Bloomfield M, Rickard JA, Forbes B, Feilding A (2016b) Psilocybin with psychological support for treatment-resistant depression: an open-label feasibility study. Lancet Psychiatry 3:619–627.

Carhart-Harris RL, Erritzoe D, Williams T, Stone JM, Reed LJ, Colasanti A, Tyacke RJ, Leech R, Malizia AL, Murphy K, Hobden P, Evans J, Feilding A, Wise RG, Nutt DJ (2012) Neural correlates of the psychedelic state as determined by fMRI studies with psilocybin. Proceedings of the National Academy of Sciences 109:2138 LP – 2143.

Carhart-Harris RL, Friston KJ (2019) REBUS and the Anarchic Brain: Toward a Unified Model of the Brain Action of Psychedelics. Pharmacol Rev 71:316–344.

Carhart-Harris RL, Goodwin GM (2017) The therapeutic potential of psychedelic drugs: past, present, and future. Neuropsychopharmacology 42:2105–2113.

Carhart-Harris RL, Kaelen M, Bolstridge M, Williams TM, Williams LT, Underwood R, Feilding A, Nutt DJ (2016c) The paradoxical psychological effects of lysergic acid diethylamide (LSD). Psychol Med 46:1379–1390.

Carhart-Harris RL, Kaelen M, Whalley MG, Bolstridge M, Feilding A, Nutt DJ (2015) LSD enhances suggestibility in healthy volunteers. Psychopharmacology (Berl) 232:785–794.

Carhart-Harris RL, Leech R, Hellyer PJ, Shanahan M, Feilding A, Tagliazucchi E, Chialvo DR, Nutt D (2014) The entropic brain: a theory of conscious states informed by neuroimaging research with psychedelic drugs. Front Hum Neurosci 8:20.

Carhart-Harris RL, Nutt DJ (2017) Serotonin and brain function: a tale of two receptors. Journal of Psychopharmacology 31:1091–1120.

Carhart-Harris RL, Roseman L, Bolstridge M, Demetriou L, Pannekoek JN, Wall MB, Tanner M, Kaelen M, McGonigle J, Murphy K (2017) Psilocybin for treatment-resistant depression: fMRI-measured brain mechanisms. Sci Rep 7:1–11.

Carhart-Harris RL, Roseman L, Haijen E, Erritzoe D, Watts R, Branchi I, Kaelen M (2018b) Psychedelics and the essential importance of context. Journal of Psychopharmacology 32:725–731.

Carlson S, Willott JF (1998) Caudal pontine reticular formation of C57BL/6J mice: responses to startle stimuli, inhibition by tones, and plasticity. J Neurophysiol 79:2603–2614.

Carnegie PR (1971) Properties, Structure and Possible Neuroreceptor Role of the Encephalitogenic Protein of Human Brain. Nature 1971 229:5279 229:25–28.

Carnegie PR, Smythies JR, Caspary EA, Field EJ (1972) Interaction of Hallucinogenic Drugs with Encephalitogenic Protein of Myelin. Nature 1972 240:5383 240:561–563.

Castrén E, Antila H (2017) Neuronal plasticity and neurotrophic factors in drug responses. Mol Psychiatry 22:1085–1095.

Catlow BJ, Song S, Paredes DA, Kirstein CL, Sanchez-Ramos J (2013) Effects of psilocybin on hippocampal neurogenesis and extinction of trace fear conditioning. Exp Brain Res 228:481–491.

Chakraborty R, na Park H, Tan CC, Weiss P, Prunt MC, Pardue MT (2017) Association of body length with ocular parameters in mice. Optom Vis Sci 94:387.

Chakravarty MM, Steadman P, van Eede MC, Calcott RD, Gu V, Shaw P, Raznahan A, Collins DL, Lerch JP (2013) Performing label-fusion-based segmentation using multiple automatically generated templates. Hum Brain Mapp 34:2635–2654.

Chandran P, Upadhyay J, Markosyan S, Lisowski A, Buck W, Chin C-L, Fox G, Luo F, Day M (2012) Magnetic resonance imaging and histological evidence for the blockade of cuprizone-induced demyelination in C57BL/6 mice. Neuroscience 202:446–453.

Chaouloff F, Baudrie V, Coupry I (1994) Effects of chlorisondamine and restraint on cortical [3H]ketanserin binding, 5-HT2A receptor-mediated head shakes, and behaviours in models of anxiety. Neuropharmacology 33:449–456.

Chen B, Dowlatshahi D, MacQueen GM, Wang J-F, Young LT (2001) Increased hippocampal BDNF immunoreactivity in subjects treated with antidepressant medication. Biol Psychiatry 50:260–265.

Chen XJ, Kovacevic N, Lobaugh NJ, Sled JG, Henkelman RM, Henderson JT (2006) Neuroanatomical differences between mouse strains as shown by high-resolution 3D MRI. Neuroimage 29:99–105.

Chen ZY, Bath K, McEwen B, Hempstead B, Lee F (2008) Impact of Genetic Variant BDNF (Val66Met) on Brain Structure and Function. Growth Factors and Psychiatric Disorders 289:180–192.

Cho R, Kapur S, Du L, Hrdina P (1999) Relationship between central and peripheral serotonin 5-HT2A receptors: a positron emission tomography study in healthy individuals. Neurosci Lett 261:139–142.

Chung MK, Worsley KJ, Paus T, Cherif C, Collins DL, Giedd JN, Rapoport JL, Evans AC (2001) A unified statistical approach to deformation-based morphometry. Neuroimage 14:595–606.

Cieślak PE, Ahn W-Y, Bogacz R, Parkitna JR (2018) Selective effects of the loss of NMDA or mGluR5 receptors in the reward system on adaptive decision-making. eNeuro 5.

Clark JE, Watson S, Friston KJ (2018) What is mood? A computational perspective. Psychol Med 48:2277–2284.

Clarke HF, Walker SC, Dalley JW, Robbins TW, Roberts AC (2007) Cognitive inflexibility after prefrontal serotonin depletion is behaviorally and neurochemically specific. Cerebral cortex 17:18–27.

Critchley P, Perez FG, Quinn N, Coleman R, Parkes D, Marsden CD (1986) Psychosis and the lisuride pump. The Lancet 328:349.

Császár-Nagy N, Bob P, Bókkon I (2022) A Multidisciplinary Hypothesis about Serotonergic Psychedelics. Is it Possible that a Portion of Brain Serotonin Comes From the Gut? J Integr Neurosci 21:148.

Cyr M, Landry M, Di Paolo T (2000) Modulation by estrogen-receptor directed drugs of 5-hydroxytryptamine-2A receptors in rat brain. Neuropsychopharmacology 23:69–78.

Czajkowski R, Sugar J, Zhang S-J, Couey JJ, Ye J, Witter MP (2013) Superficially projecting principal neurons in layer V of medial entorhinal cortex in the rat receive excitatory retrosplenial input. Journal of Neuroscience 33:15779–15792.

Dalley JW, Cardinal RN, Robbins TW (2004) Prefrontal executive and cognitive functions in rodents: neural and neurochemical substrates. Neurosci Biobehav Rev 28:771–784.

Darmani NA, Gerdes CF (1995) Temporal differential adaptation of head-twitch and ear-scratch responses following administration of challenge doses of DOI. Pharmacol Biochem Behav 50:545–550 Available at: http://www.sciencedirect.com/science/article/pii/0091305794003408.

Darmani NA, Martin BR, Glennon RA (1990a) Withdrawal from chronic treatment with (+/−)-DOI causes super-sensitivity to 5-HT2 receptor-induced head-twitch behaviour in mice. Eur J Pharmacol 186:115–118.

Darmani NA, Martin BR, Pandey U, Glennon RA (1990b) Do functional relationships exist between 5-HT1A and 5-HT2 receptors? Pharmacol Biochem Behav 36:901–906.

Darmani NA, Martin BR, Pandey U, Glennon RA (1990c) Pharmacological characterization of ear-scratch response in mice as a behavioral model for selective 5-HT2-receptor agonists and evidence for 5-HT1B- and 5-HT2-receptor interactions. Pharmacol Biochem Behav 37:95–99.

Darmani NA, Mock OB, Towns LC, Gerdes CF (1994) The head-twitch response in the least shrew (Cryptotis parva) is a 5-HT2− and not a 5-HT1C-mediated phenomenon. Pharmacol Biochem Behav 48:383–396.

Darmani NA, Shaddy J, Gerdes CF (1996) Differential ontogenesis of three DOI-Induced behaviors in mice. Physiol Behav 60:1495–1500.

Davis AK, Barrett FS, Griffiths RR (2020) Psychological flexibility mediates the relations between acute psychedelic effects and subjective decreases in depression and anxiety. J Contextual Behav Sci 15:39–45.

Daw ND, Dayan P (2014) The algorithmic anatomy of model-based evaluation. Philosophical Transactions of the Royal Society B: Biological Sciences 369.

Daw ND, Gershman SJ, Seymour B, Dayan P, Dolan RJ (2011) Model-based influences on humans' choices and striatal prediction errors. Neuron 69:1204–1215.

Daws RE, Timmermann C, Giribaldi B, Sexton JD, Wall MB, Erritzoe D, Roseman L, Nutt D, Carhart-Harris R (2022) Increased global integration in the brain after psilocybin therapy for depression. Nature Medicine 2022 28:4 28:844–851.

Dayer A (2022) Serotonin-related pathways and developmental plasticity: relevance for psychiatric disorders. Dialogues Clin Neurosci.

de Barros ACB, Baruchin LJ, Panayi MC, Nyberg N, Samborska V, Mealing MT, Akam T, Kwag J, Bannerman DM, Kohl MM (2021) Retrosplenial cortex is necessary for spatial and non-spatial latent learning in mice. bioRxiv.

de Guzman AE, Wong MD, Gleave JA, Nieman BJ (2016) Variations in post-perfusion immersion fixation and storage alter MRI measurements of mouse brain morphometry. Neuroimage 142:687–695.

de la Fuente Revenga M, Shin JM, Vohra HZ, Hideshima KS, Schneck M, Poklis JL, González-Maeso J (2019) Fully automated head-twitch detection system for the study of 5-HT2A receptor pharmacology in vivo. Sci Rep 9:14247.

de la Fuente Revenga M, Zhu B, Guevara CA, Naler LB, Saunders JM, Zhou Z, Toneatti R, Sierra S, Wolstenholme JT, Beardsley PM (2021) Prolonged epigenomic and synaptic plasticity alterations following single exposure to a psychedelic in mice. Cell Rep 37:109836.

de la Torre R, Farré M, Roset PN, Pizarro N, Abanades S, Segura M, Segura J, Camí J (2004) Human pharmacology of MDMA: pharmacokinetics, metabolism, and disposition. Ther Drug Monit 26:137–144.

Deacon BJ (2013) The biomedical model of mental disorder: A critical analysis of its validity, utility, and effects on psychotherapy research. Clin Psychol Rev 33:846–861.

Depoortère R, Auclair AL, Bardin L, Colpaert FC, Vacher B, Newman-Tancredi A (2010) F15599, a preferential post-synaptic 5-HT1A receptor agonist: activity in models of cognition in comparison with reference 5-HT1A receptor agonists. European Neuropsychopharmacology 20:641–654.

Dhonnchadha BÁN, Bourin M, Hascoët M (2003) Anxiolytic-like effects of 5-HT2 ligands on three mouse models of anxiety. Behavioural Brain Research 140:203–214.

Diamond MC, Johnson RE, Young D, Singh SS (1983) Age-related morphologic differences in the rat cerebral cortex and hippocampus: Male-female; right-left. Exp Neurol 81:1–13.

Dickinson A, Balleine B (1994) Motivational control of goal-directed action. Anim Learn Behav 22:1–18.

Dickinson JP, Jones KM, Aparicio SR, Lumsden CE (1970) Localization of encephalitogenic basic protein in the intraperiod line of lamellar myelin. Nature 227:1133–1134.

Doll BB, Duncan KD, Simon DA, Shohamy D, Daw ND (2015) Model-based choices involve prospective neural activity. Nat Neurosci 18:767.

Dong C, Ly C, Dunlap LE, Vargas M v, Sun J, Hwang I-W, Azinfar A, Oh WC, Wetsel WC, Olson DE (2021) Psychedelic-inspired drug discovery using an engineered biosensor. Cell 184:2779–2792.

dos Santos RG, Bouso JC, Alcázar-Córcoles MÁ, Hallak JEC (2018) Efficacy, tolerability, and safety of serotonergic psychedelics for the management of mood, anxiety, and substance-use disorders: a systematic review of systematic reviews. Expert Rev Clin Pharmacol 11:889–902.

dos Santos RG, Osorio FL, Crippa JAS, Hallak JEC (2016a) Classical hallucinogens and neuroimaging: A systematic review of human studies: Hallucinogens and neuroimaging. Neurosci Biobehav Rev 71:715–728.

dos Santos RG, Osório FL, Crippa JAS, Riba J, Zuardi AW, Hallak JEC (2016b) Antidepressive, anxiolytic, and antiaddictive effects of ayahuasca, psilocybin and lysergic acid diethylamide (LSD): a systematic review of clinical trials published in the last 25 years. Ther Adv Psychopharmacol 6:193–213.

Doss MK, Barrett FS, Corlett PR (2022a) Skepticism about Recent Evidence That Psilocybin “Liberates” Depressed Minds. ACS Chem Neurosci.

Doss MK, Madden MB, Gaddis A, Nebel MB, Griffiths RR, Mathur BN, Barrett FS (2022b) Models of psychedelic drug action: modulation of cortical-subcortical circuits. Brain 145:441–456.

Draganski B, Gaser C, Busch V, Schuierer G, Bogdahn U, May A (2004) Changes in grey matter induced by training. Nature 427:311–312.

Du Jardin KG, Müller HK, Sanchez C, Wegener G, Elfving B (2017) Gene expression related to serotonergic and glutamatergic neurotransmission is altered in the flinders sensitive line rat model of depression: effect of ketamine. Synapse 71:37–45.

Duman RS, Aghajanian GK (2012) Synaptic dysfunction in depression: potential therapeutic targets. Science (1979) 338:68–72.

Dursun SM, Handley SL (1996) Similarities in the pharmacology of spontaneous and DOI-induced head-shakes suggest 5HT2A receptors are active under physiological conditions. Psychopharmacology (Berl) 128:198–205.

Egashira N, Okuno R, Shirakawa A, Nagao M, Mishima K, Iwasaki K, Oishi R, Fujiwara M (2012) Role of 5-Hydroxytryptamine$_{2C}$ Receptors in Marble-Burying Behavior in Mice. Biol Pharm Bull 35:376–379.

Ellegood J, Pacey LK, Hampson DR, Lerch JP, Henkelman RM (2010) Anatomical phenotyping in a mouse model of fragile X syndrome with magnetic resonance imaging. Neuroimage 53:1023–1029.

Ermentrout GB, Cowan JD (1979) A mathematical theory of visual hallucination patterns. Biol Cybern 34:137–150.

Fadiman J, Grob C, Bravo G, Agar A, Walsh R (2003) Psychedelic research revisited. Journal of Transpersonal Psychology 35:111–126.

Fantegrossi WE, Harrington AW, Kiessel CL, Eckler JR, Rabin RA, Winter JC, Coop A, Rice KC, Woods JH (2006) Hallucinogen-like actions of 5-methoxy-N, N-diisopropyltryptamine in mice and rats. Pharmacol Biochem Behav 83:122–129.

Fantegrossi WE, Murnane KS, Reissig CJ (2008a) The behavioral pharmacology of hallucinogens. Biochem Pharmacol 75:17–33.

Fantegrossi WE, Reissig CJ, Katz EB, Yarosh HL, Rice KC, Winter JC (2008b) Hallucinogen-like effects of N, N-dipropyltryptamine (DPT): possible mediation by serotonin 5-HT1A and 5-HT2A receptors in rodents. Pharmacol Biochem Behav 88:358–365.

Fantegrossi WE, Simoneau J, Cohen MS, Zimmerman SM, Henson CM, Rice KC, Woods JH (2010) Interaction of 5-HT2A and 5-HT2C receptors in R (−)-2, 5-dimethoxy-4-iodoamphetamine-elicited head twitch behavior in mice. Journal of Pharmacology and Experimental Therapeutics 335:728–734.

Fantegrossi WE, Woods JH, Winger G (2004) Transient reinforcing effects of phenylisopropylamine and indolealkylamine hallucinogens in rhesus monkeys. Behavioural pharmacology 15:149–157.

Feltenstein MW, See RE (2008) The neurocircuitry of addiction: an overview. Br J Pharmacol 154:261–274.

Ferguson SM, Thomas MJ, Robinson TE (2004) Morphine-induced c-fos mRNA expression in striatofugal circuits: modulation by dose, environmental context, and drug history. Neuropsychopharmacology 29:1664–1674.

Ferrario CR, Gorny G, Crombag HS, Li Y, Kolb B, Robinson TE (2005) Neural and Behavioral Plasticity Associated with the Transition from Controlled to Escalated Cocaine Use. Biol Psychiatry 58:751–759.

Figee M, Pattij T, Willuhn I, Luigjes J, van den Brink W, Goudriaan A, Potenza MN, Robbins TW, Denys D (2016) Compulsivity in obsessive–compulsive disorder and addictions. European Neuropsychopharmacology 26:856–868.

Fink G, Sumner B, Rosie R, Wilson H, McQueen J (1999) Androgen actions on central serotonin neurotransmission: relevance for mood, mental state and memory. Behavioural brain research 105:53–68.

Fitzgerald PJ (2012) Whose side are you on: Does serotonin preferentially activate the right hemisphere and norepinephrine the left? Med Hypotheses 79:250–254.

Fox MA, French HT, LaPorte JL, Blackler AR, Murphy DL (2010) The serotonin 5-HT 2A receptor agonist TCB-2: a behavioral and neurophysiological analysis. Psychopharmacology (Berl) 212:13–23.

Frank MJ, Seeberger LC, O'reilly RC (2004) By carrot or by stick: cognitive reinforcement learning in parkinsonism. Science (1979) 306:1940–1943.

Frankel PS, Cunningham KA (2002) The hallucinogen d-lysergic acid diethylamide (d-LSD) induces the immediate-early gene c-Fos in rat forebrain. Brain Res 958:251–260.

Frankfurt M, McKittrick CR, Mendelson SD, McEwen BS (1994) Effect of 5, 7-dihydroxytryptamine, ovariectomy and gonadal steroids on serotonin receptor binding in rat brain. Neuroendocrinology 59:245–250.

Freund J, Brandmaier AM, Lewejohann L, Kirste I, Kritzler M, Krüger A, Sachser N, Lindenberger U, Kempermann G (2013) Emergence of individuality in genetically identical mice. Science (1979) 340:756–759.

Freund J, Brandmaier AM, Lewejohann L, Kirste I, Kritzler M, Krüger A, Sachser N, Lindenberger U, Kempermann G (2015) Association between exploratory activity and social individuality in genetically identical mice living in the same enriched environment. Neuroscience 309:140–152.

Friard O, Gamba M (2016) BORIS: a free, versatile open-source event-logging software for video/audio coding and live observations. Methods Ecol Evol 7:1325–1330.

Friedel M, van Eede MC, Pipitone J, Chakravarty MM, Lerch JP (2014) Pydpiper: a flexible toolkit for constructing novel registration pipelines. Front Neuroinform 8:67.

Frodl T, Jäger M, Smajstrlova I, Born C, Bottlender R, Palladino T, Reiser M, Möller H-J, Meisenzahl EM (2008) Effect of hippocampal and amygdala volumes on clinical outcomes in major depression: a 3-year prospective magnetic resonance imaging study. Journal of Psychiatry and Neuroscience 33:423–430.

Fu CHY, Williams SCR, Cleare AJ, Brammer MJ, Walsh ND, Kim J, Andrew CM, Pich EM, Williams PM, Reed LJ, Mitterschiffthaler MT, Suckling J, Bullmore ET (2004) Attenuation of the Neural Response to Sad Faces in Major Depressionby

Antidepressant Treatment: A Prospective, Event-Related Functional Magnetic Resonance ImagingStudy. Arch Gen Psychiatry 61:877–889.

Furr A, Lapiz-Bluhm MD, Morilak DA (2012) 5-HT2A receptors in the orbitofrontal cortex facilitate reversal learning and contribute to the beneficial cognitive effects of chronic citalopram treatment in rats. Int J Neuropsychopharmacol 15:1295–1305.

Gage FH (2019) Adult neurogenesis in mammals. Science (1979) 364:827–828.

Garcia-Garcia AL, Newman-Tancredi A, Leonardo ED (2014) 5-HT1A receptors in mood and anxiety: recent insights into autoreceptor versus heteroreceptor function. Psychopharmacology (Berl) 231:623–636.

Garcia-Romeu A, Richards WA (2018) Current perspectives on psychedelic therapy: use of serotonergic hallucinogens in clinical interventions. International Review of Psychiatry 30:291–316.

Genauck A, Quester S, Wüstenberg T, Mörsen C, Heinz A, Romanczuk-Seiferth N (2017) Reduced loss aversion in pathological gambling and alcohol dependence is associated with differential alterations in amygdala and prefrontal functioning. Sci Rep 7:1–11.

Genet JJ, Siemer M (2011) Flexible control in processing affective and non-affective material predicts individual differences in trait resilience. Cogn Emot 25:380–388.

Gewirtz JC, Chen AC, Terwilliger R, Duman RC, Marek GJ (2002) Modulation of DOI-induced increases in cortical BDNF expression by group II mGlu receptors. Pharmacol Biochem Behav 73:317–326.

Geyer MA, Light RK (1979) LSD-induced alterations of investigatory responding in rats. Psychopharmacology (Berl) 65:41–47.

Gillan CM, Kosinski M, Whelan R, Phelps EA, Daw ND (2016) Characterizing a psychiatric symptom dimension related to deficits in goal-directed control. Elife 5:e11305.

Glennon RA, Titeler M, McKenney JD (1984) Evidence for 5-HT2 involvement in the mechanism of action of hallucinogenic agents. Life Sci 35:2505–2511.

Goldberger L (1966) Cognitive test performance under LSD-25, placebo and isolation. Journal of Nervous and Mental Disease.

Golub Y, Kaltwasser SF, Mauch CP, Herrmann L, Schmidt U, Holsboer F, Czisch M, Wotjak CT (2011) Reduced hippocampus volume in the mouse model of Posttraumatic Stress Disorder. J Psychiatr Res 45:650–659.

González-Maeso J, Weisstaub N V, Zhou M, Chan P, Ivic L, Ang R, Lira A, Bradley-Moore M, Ge Y, Zhou Q (2007) Hallucinogens recruit specific cortical 5-HT2A receptor-mediated signaling pathways to affect behavior. Neuron 53:439–452.

Goodwin GM, Aaronson ST, Alvarez O, Arden PC, Baker A, Bennett JC, Bird C, Blom RE, Brennan C, Brusch D (2022) Single-dose psilocybin for a treatment-resistant episode of major depression. New England Journal of Medicine 387:1637–1648.

Gouzoulis-Mayfrank E, Schreckenberger M, Sabri O, Arning C, Thelen B, Spitzer M, Kovar K-A, Hermle L, Büll U, Sass H (1999) Neurometabolic effects of psilocybin, 3, 4-methylenedioxyethylamphetamine (MDE) and d-methamphetamine in healthy volunteers: a double-blind, placebo-controlled PET study with [18F] FDG. Neuropsychopharmacology 20:565–581.

Grandjean J, Buehlmann D, Buerge M, Sigrist H, Seifritz E, Vollenweider FX, Pryce CR, Rudin M (2021) Psilocybin exerts distinct effects on resting state networks associated with serotonin and dopamine in mice. Neuroimage 225:117456.

Griebeii G, Belzungz C, Misslin R, Vogel E (1993) The free-exploratory paradigm: an effective method for measuring neophobic behaviour in mice. Behavioural pharmacology 4:637.

Griffiths RR, Johnson MW, Carducci MA, Umbricht A, Richards WA, Richards BD, Cosimano MP, Klinedinst MA (2016) Psilocybin produces substantial and sustained decreases in depression and anxiety in patients with life-threatening cancer: A randomized double-blind trial. J Psychopharmacol 30:1181–1197.

Griffiths RR, Richards WA, McCann U, Jesse R (2006) Psilocybin can occasion mystical-type experiences having substantial and sustained personal meaning and spiritual significance. Psychopharmacology (Berl) 187:268–283.

Grob CS, Danforth AL, Chopra GS, Hagerty M, McKay CR, Halberstadt AL, Greer GR (2011) Pilot study of psilocybin treatment for anxiety in patients with advanced-stage cancer. Arch Gen Psychiatry 68:71–78.

Grogan JP, Tsivos D, Smith L, Knight BE, Bogacz R, Whone A, Coulthard EJ (2017) Effects of dopamine on reinforcement learning and consolidation in Parkinson's disease. Elife 6:e26801.

Gromer D, Kiser DP, Pauli P (2021) Thigmotaxis in a virtual human open field test. Sci Rep 11:1–13.

Guilfoyle DN, Hrabe J (2006) Interleaved snapshot echo planar imaging of mouse brain at 7.0 T. NMR in Biomedicine: An International Journal Devoted to the Development and Application of Magnetic Resonance In vivo 19:108–115.

Gulyaeva N v (2017) Molecular mechanisms of neuroplasticity: an expanding universe. Biochemistry (Moscow) 82:237–242.

Halberstadt AL, Chatha M, Klein AK, Wallach J, Brandt SD (2020) Correlation between the potency of hallucinogens in the mouse head-twitch response assay and their behavioral and subjective effects in other species. Neuropharmacology 167:107933.

Halberstadt AL, Geyer MA (2011) Multiple receptors contribute to the behavioral effects of indoleamine hallucinogens. Neuropharmacology 61:364–381.

Halberstadt AL, Geyer MA (2013) Characterization of the head-twitch response induced by hallucinogens in mice: detection of the behavior based on the dynamics of head movement. Psychopharmacology (Berl) 227:727–739.

Halberstadt AL, Koedood L, Powell SB, Geyer MA (2011) Differential contributions of serotonin receptors to the behavioral effects of indoleamine hallucinogens in mice. Journal of psychopharmacology 25:1548–1561.

Halberstadt AL, van der Heijden I, Ruderman MA, Risbrough VB, Gingrich JA, Geyer MA, Powell SB (2009) 5-HT 2A and 5-HT 2C receptors exert opposing effects on locomotor activity in mice. Neuropsychopharmacology 34:1958–1967.

Haleem DJ, Kennett GA, Curzon G (1990) Hippocampal 5-hydroxytryptamine synthesis is greater in female rats than in males and more decreased by the 5-HT 1A agonist 8-OH-DPAT. Journal of Neural Transmission/General Section JNT 79:93–101.

Hamada S, Senzaki K, Hamaguchi-Hamada K, Tabuchi K, Yamamoto H, Yamamoto T, Yoshikawa S, Okano H, Okado N (1998) Localization of 5-HT2A Receptor in rat cerebral cortex and olfactory system revealed by immunohistochemistry using two antibodies raised in rabbit and chicken. Molecular Brain Research 54:199–211.

Handa RJ, Cross MK, George M, Gordon BH, Burgess LH, Cabrera TM, Hata N, Campbell DB, Lorens SA (1993) Neuroendocrine and neurochemical responses to novelty stress in young and old male F344 rats: effects of d-fenfluramine treatment. Pharmacol Biochem Behav 46:101–109.

Hanks JB, González-Maeso J (2013) Animal models of serotonergic psychedelics. ACS Chem Neurosci 4:33–42.

Hartogsohn I (2016) Set and setting, psychedelics and the placebo response: An extra-pharmacological perspective on psychopharmacology. Journal of Psychopharmacology 30:1259–1267.

Hartogsohn I (2017) Constructing drug effects: A history of set and setting. Drug Sci Policy Law 3.

Harvey JA (2003) Role of the serotonin 5-HT2A receptor in learning. Learning & Memory 10:355–362.

Hattori R, Danskin B, Babic Z, Mlynaryk N, Komiyama T (2019) Area-specificity and plasticity of history-dependent value coding during learning. Cell 177:1858–1872.

Hayashi T, Su TP (2004) σ-1 receptor ligands: Potential in the treatment of neuropsychiatric disorders. CNS Drugs 18:269–284.

Heal DJ, Gosden J, Smith SL (2018) Evaluating the abuse potential of psychedelic drugs as part of the safety pharmacology assessment for medical use in humans. Neuropharmacology 142:89–115.

Heller AS, Ezie CEC, Otto AR, Timpano KR (2018) Model-based learning and individual differences in depression: The moderating role of stress. Behaviour research and therapy 111:19–26.

Hermle L, Fünfgeld M, Oepen G, Botsch H, Borchardt D, Gouzoulis E, Fehrenbach RA, Spitzer M (1992) Mescaline-induced psychopathological, neuropsychological, and neurometabolic effects in normal subjects: experimental psychosis as a tool for psychiatric research. Biol Psychiatry 32:976–991.

Hesselgrave N, Troppoli TA, Wulff AB, Cole AB, Thompson SM (2021) Harnessing psilocybin: antidepressant-like behavioral and synaptic actions of psilocybin are independent of 5-HT2R activation in mice. Proceedings of the National Academy of Sciences 118:e2022489118.

Heyser CJ, Chemero A (2012) Novel object exploration in mice: not all objects are created equal. Behavioural processes 89:232–238.

Hibicke M, Landry AN, Kramer HM, Talman ZK, Nichols CD (2020) Psychedelics, but Not Ketamine, Produce Persistent Antidepressant-like Effects in a Rodent Experimental System for the Study of Depression. ACS Chem Neurosci 11:864–871.

Hofmann A (1980) LSD: my problem child. Psychedelic Reflections.

Holahan MR, Honegger KS, Tabatadze N, Routtenberg A (2007) GAP-43 gene expression regulates information storage. Learning & memory 14:407–415.

Holloway T, Moreno JL, Umali A, Rayannavar V, Hodes GE, Russo SJ, González-Maeso J (2013) Prenatal stress induces schizophrenia-like alterations of serotonin 2A and metabotropic glutamate 2 receptors in the adult offspring: role of maternal immune system. Journal of Neuroscience 33:1088–1098.

Holmes HE et al. (2017) Comparison of In Vivo and Ex Vivo MRI for the Detection of Structural Abnormalities in a Mouse Model of Tauopathy. Front Neuroinform 11:20.

Holze F, Ley L, Müller F, Becker AM, Straumann I, Vizeli P, Kuehne SS, Roder MA, Duthaler U, Kolaczynska KE (2022) Direct comparison of the acute effects of lysergic acid diethylamide and psilocybin in a double-blind placebo-controlled study in healthy subjects. Neuropsychopharmacology 47:1180–1187.

Horvitz JC (2000) Mesolimbocortical and nigrostriatal dopamine responses to salient non-reward events. Neuroscience 96:651–656.

Hsu KJ, Beard C, Rifkin L, Dillon DG, Pizzagalli DA, Björgvinsson T (2015) Transdiagnostic mechanisms in depression and anxiety: The role of rumination and attentional control. J Affect Disord 188:22–27.

Hubel DH, Wiesel TN (1970) The period of susceptibility to the physiological effects of unilateral eye closure in kittens. J Physiol 206:419–436.

Hughes RN (2007) Neotic preferences in laboratory rodents: Issues, assessment and substrates. Neurosci Biobehav Rev 31:441–464.

Hutten NRPW, Mason NL, Dolder PC, Theunissen EL, Holze F, Liechti ME, Varghese N, Eckert A, Feilding A, Ramaekers JG (2020) Low doses of LSD acutely increase BDNF blood plasma levels in healthy volunteers. ACS Pharmacol Transl Sci 4:461–466.

Huys QJM, Daw ND, Dayan P (2015) Depression: a decision-theoretic analysis. Annu Rev Neurosci 38:1–23.

Hyde KL, Lerch J, Norton A, Forgeard M, Winner E, Evans AC, Schlaug G (2009) Musical training shapes structural brain development. Journal of Neuroscience 29:3019–3025.

Hyde RW (1960) Psychological and social determinants of drug action. The dynamics of psychiatric drug therapy SpringfieldIL: Thomas:297–315.

Izquierdo A, Brigman JL, Radke AK, Rudebeck PH, Holmes A (2017) The neural basis of reversal learning: an updated perspective. Neuroscience 345:12–26.

Jaster AM, de la Fuente Revenga M, González-Maeso J (2022a) Molecular targets of psychedelic-induced plasticity. J Neurochem 162:80–88.

Jaster AM, Younkin J, Cuddy T, de la Fuente Revenga M, Poklis JL, Dozmorov MG, González-Maeso J (2022b) Differences across sexes on head-twitch behavior and 5-HT2A receptor signaling in C57BL/6J mice. Neurosci Lett:136836.

Jefsen O, Højgaard K, Christiansen SL, Elfving B, Nutt DJ, Wegener G, Müller HK (2019) Psilocybin lacks antidepressant-like effect in the Flinders Sensitive Line rat. Acta Neuropsychiatr 31:213–219.

Jha S, Rajendran R, Fernandes KA, Vaidya VA (2008) 5-HT2A/2C receptor blockade regulates progenitor cell proliferation in the adult rat hippocampus. Neurosci Lett 441:210–214.

Johnson CM, Peckler H, Tai L-H, Wilbrecht L (2016) Rule learning enhances structural plasticity of long-range axons in frontal cortex. Nat Commun 7:1–14.

Johnson GA, Cofer GP, Gewalt SL, Hedlund LW (2002) Morphologic Phenotyping with MR Microscopy: The Visible Mouse. Radiology 222:789–793.

Johnson MW, Garcia-Romeu A, Griffiths RR (2017) Long-term follow-up of psilocybin-facilitated smoking cessation. Am J Drug Alcohol Abuse 43:55–60.

Johnson MW, Richards WA, Griffiths RR (2008) Human hallucinogen research: guidelines for safety. Journal of psychopharmacology 22:603–620.

Jovanovic H, Lundberg J, Karlsson P, Cerin Å, Saijo T, Varrone A, Halldin C, Nordström A-L (2008) Sex differences in the serotonin 1A receptor and serotonin

transporter binding in the human brain measured by PET. Neuroimage 39:1408–1419.

Kaiser RH, Andrews-Hanna JR, Wager TD, Pizzagalli DA (2015) Large-Scale Network Dysfunction in Major Depressive Disorder: A Meta-analysis of Resting-State Functional Connectivity. JAMA Psychiatry 72:603–611.

Kanen JW, Luo Q, Kandroodi MR, Cardinal RN, Robbins TW, Carhart-Harris RL, den Ouden HEM (2021) Effect of lysergic acid diethylamide (LSD) on reinforcement learning in humans. bioRxiv:2020.12.04.412189.

Kaplan AL et al. (2022) Bespoke library docking for 5-HT2A receptor agonists with antidepressant activity. Nature 610:582–591.

Karpova NN, Pickenhagen A, Lindholm J, Tiraboschi E, Kulesskaya N, Ágústsdóttir A, Antila H, Popova D, Akamine Y, Sullivan R, Hen R, Drew LJ, Castrén E (2011) Fear Erasure in Mice Requires Synergy Between Antidepressant Drugs and Extinction Training. Science (1979) 334:1731–1734.

Kassem MS, Lagopoulos J, Stait-Gardner T, Price WS, Chohan TW, Arnold JC, Hatton SN, Bennett MR (2013) Stress-induced grey matter loss determined by MRI is primarily due to loss of dendrites and their synapses. Mol Neurobiol 47:645–661.

Keifer OP, Hurt RC, Gutman DA, Keilholz SD, Gourley SL, Ressler KJ (2015) Voxel-based morphometry predicts shifts in dendritic spine density and morphology with auditory fear conditioning. Nat Commun 6:1–12.

Keller DL, Umbreit WW (1956) Permanent alteration of behavior in mice by chemical and psychological Means. Science (1979) 124:723–724.

Kesby JP, Eyles DW, McGrath JJ, Scott JG (2018) Dopamine, psychosis and schizophrenia: the widening gap between basic and clinical neuroscience. Transl Psychiatry 8:30.

Kettner H, Rosas FE, Timmermann C, Kärtner L, Carhart-Harris RL, Roseman L (2021) Psychedelic Communitas: Intersubjective Experience During Psychedelic Group Sessions Predicts Enduring Changes in Psychological Wellbeing and Social Connectedness. Front Pharmacol 12:234.

Kim JH, Budde MD, Liang H-F, Klein RS, Russell JH, Cross AH, Song S-K (2006) Detecting axon damage in spinal cord from a mouse model of multiple sclerosis. Neurobiol Dis 21:626–632.

King AR, Martin IL, Melville KA (1974) Reversal learning enhanced by lysergic acid diethylamide (LSD): concomitant rise in brain 5-hydroxytryptamine levels. Br J Pharmacol 52:419.

Kometer M, Schmidt A, Jäncke L, Vollenweider FX (2013) Activation of Serotonin 2A Receptors Underlies the Psilocybin-Induced Effects on α Oscillations, N170 Visual-Evoked Potentials, and Visual Hallucinations. The Journal of Neuroscience 33:10544–10551.

Konstandi M (2013) Psychophysiological stress: a significant parameter in drug pharmacokinetics. Expert Opin Drug Metab Toxicol 9:1317–1334.

Koolschijn PCMP, van Haren NEM, Lensvelt-Mulders GJLM, Hulshoff Pol HE, Kahn RS (2009) Brain volume abnormalities in major depressive disorder: A meta-analysis of magnetic resonance imaging studies. Hum Brain Mapp 30:3719–3735.

Korn C, Akam T, Jensen K, Vagnoni C, Huber A, Tunbridge E, Walton M (2021) Distinct roles for dopamine clearance mechanisms in regulating behavioral flexibility. Mol Psychiatry 26.

Kronenberger J-P, Médioni J (1985) Food neophobia in wild and laboratory mice (Mus musculus domesticus). Behavioural Processes 11:53–59.

Krubitzer L (1995) The organization of neocortex in mammals: are species differences really so different? Trends Neurosci 18:408–417.

Kuypers KPC, Riba J, de La Fuente Revenga M, Barker S, Theunissen EL, Ramaekers JG (2016) Ayahuasca enhances creative divergent thinking while decreasing conventional convergent thinking. Psychopharmacology (Berl) 233:3395–3403.

Laaris N, Le Poul E, Laporte AM, Hamon M, Lanfumey L (1999) Differential effects of stress on presynaptic and postsynaptic 5-hydroxytryptamine-1A receptors in the rat brain: an in vitro electrophysiological study. Neuroscience 91:947–958.

Landis C, Hunt W (1939) The startle pattern. Farrar & Rinehart.

Landry M, Di Paolo T (2003) Effect of chronic estradiol, tamoxifen or raloxifene treatment on serotonin 5-HT1A receptor. Molecular brain research 112:82–89.

Lau JC, Lerch JP, Sled JG, Henkelman RM, Evans AC, Bedell BJ (2008) Longitudinal neuroanatomical changes determined by deformation-based morphometry in a mouse model of Alzheimer's disease. Neuroimage 42:19–27.

Le Saux M, Di Paolo T (2005) Changes in 5-HT1A receptor binding and G-protein activation in the rat brain after estrogen treatment: comparison with tamoxifen and raloxifene. Journal of Psychiatry and Neuroscience 30:110.

Leary T, Litwin GH, Metzner R (1963) Reactions to psilocybin administered in a supportive environment. Journal of Nervous and Mental Disease.

Lebedev A v, Kaelen M, Lövdén M, Nilsson J, Feilding A, Nutt DJ, Carhart-Harris RL (2016) LSD-induced entropic brain activity predicts subsequent personality change. Hum Brain Mapp 37:3203–3213.

Leber AB, Turk-Browne NB, Chun MM (2008) Neural predictors of moment-to-moment fluctuations in cognitive flexibility. Proceedings of the National Academy of Sciences 105:13592–13597.

Lee EE, della Selva MP, Liu A, Himelhoch S (2015) Ketamine as a novel treatment for major depressive disorder and bipolar depression: a systematic review and quantitative meta-analysis. Gen Hosp Psychiatry 37:178–184.

Lees AJ, Bannister R (1981) The use of lisuride in the treatment of multiple system atrophy with autonomic failure (Shy-Drager syndrome). J Neurol Neurosurg Psychiatry 44:347–351.

Leptourgos P, Fortier-Davy M, Carhart-Harris R, Corlett PR, Dupuis D, Halberstadt AL, Kometer M, Kozakova E, LarØi F, Noorani TN, Preller KH, Waters F, Zaytseva Y, Jardri R (2020) Hallucinations Under Psychedelics and in the Schizophrenia Spectrum: An Interdisciplinary and Multiscale Comparison. Schizophr Bull 46:1396–1408.

Lerch J (2014) Voxel-wise morphometry using RMINC.

Lerch JP, Carroll JB, Spring S, Bertram LN, Schwab C, Hayden MR, Henkelman RM (2008) Automated deformation analysis in the YAC128 Huntington disease mouse model. Neuroimage 39:32–39.

Lerch JP, Gazdzinski L, Germann J, Sled JG, Henkelman RM, Nieman BJ (2012) Wanted dead or alive? The tradeoff between in-vivo versus ex-vivo MR brain imaging in the mouse. Front Neuroinform 6:6.

Lerch JP, Yiu AP, Martinez-Canabal A, Pekar T, Bohbot VD, Frankland PW, Henkelman RM, Josselyn SA, Sled JG (2011) Maze training in mice induces MRI-detectable brain shape changes specific to the type of learning. Neuroimage 54:2086–2095.

Leussis MP, Bolivar VJ (2006) Habituation in rodents: A review of behavior, neurobiology, and genetics. Neurosci Biobehav Rev 30:1045–1064.

Leysen JE, Niemegeers CJE, van Nueten JM, Laduron PM (1982) [3H] Ketanserin (R 41 468), a selective 3H-ligand for serotonin2 receptor binding sites: Binding properties, brain distribution, and functional role.

Li N, Lee B, Liu R-J, Banasr M, Dwyer JM, Iwata M, Li X-Y, Aghajanian G, Duman RS (2010) mTOR-dependent synapse formation underlies the rapid antidepressant effects of NMDA antagonists. Science (1979) 329:959–964.

Li Y, Acerbo MJ, Robinson TE (2004) The induction of behavioural sensitization is associated with cocaine-induced structural plasticity in the core (but not shell) of the nucleus accumbens. European Journal of Neuroscience 20:1647–1654.

Lombardi G, Gandolfi O, Dall'Olio R, Pellegrini-Giampietro DE, Beni M, Carla V, Consolazione A, Moroni F (1987) Lesioning and recovery of the serotoninergic projections to the hippocampus. Brain Res 411:275–281.

Lord L-D, Expert P, Atasoy S, Roseman L, Rapuano K, Lambiotte R, Nutt DJ, Deco G, Carhart-Harris RL, Kringelbach ML, Cabral J (2019) Dynamical exploration of

the repertoire of brain networks at rest is modulated by psilocybin. Neuroimage 199:127–142.

Lord LD, Stevner AB, Deco G, Kringelbach ML (2017) Understanding principles of integration and segregation using whole-brain computational connectomics: implications for neuropsychiatric disorders. Philosophical Transactions of the Royal Society A: Mathematical, Physical and Engineering Sciences 375.

Lu J, Tjia M, Mullen B, Cao B, Lukasiewicz K, Shah-Morales S, Weiser S, Cameron LP, Olson DE, Chen L (2021) An analog of psychedelics restores functional neural circuits disrupted by unpredictable stress. Mol Psychiatry 26:6237–6252.

Lucantonio F, Stalnaker TA, Shaham Y, Niv Y, Schoenbaum G (2012) The impact of orbitofrontal dysfunction on cocaine addiction. Nat Neurosci 15:358–366.

Ly C, Greb AC, Cameron LP, Wong JM, Barragan E v, Wilson PC, Burbach KF, Soltanzadeh Zarandi S, Sood A, Paddy MR, Duim WC, Dennis MY, McAllister AK, Ori-McKenney KM, Gray JA, Olson DE (2018) Psychedelics Promote Structural and Functional Neural Plasticity. Cell Rep 23:3170–3182.

Ly C, Greb AC, Vargas M v, Duim WC, Grodzki AC, Lein PJ, Olson DE (2020) Transient Stimulation with Psychoplastogens is Sufficient to Initiate Neuronal Growth. ACS Pharmacol Transl Sci 4:452–460.

MacLean KA, Johnson MW, Griffiths RR (2011) Mystical experiences occasioned by the hallucinogen psilocybin lead to increases in the personality domain of openness. Journal of Psychopharmacology 25:1453–1461.

Madsen MK, Fisher PM, Burmester D, Dyssegaard A, Stenbæk DS, Kristiansen S, Johansen SS, Lehel S, Linnet K, Svarer C (2019) Psychedelic effects of psilocybin

correlate with serotonin 2A receptor occupancy and plasma psilocin levels. Neuropsychopharmacology 44:1328–1334.

Maguire E (2001) The retrosplenial contribution to human navigation: a review of lesion and neuroimaging findings. Scand J Psychol 42:225–238.

Maguire EA, Gadian DG, Johnsrude IS, Good CD, Ashburner J, Frackowiak RSJ, Frith CD (2000) Navigation-related structural change in the hippocampi of taxi drivers. Proceedings of the National Academy of Sciences 97:4398–4403.

Malkova N v, Gallagher JJ, Collin ZY, Jacobs RE, Patterson PH (2014) Manganese-enhanced magnetic resonance imaging reveals increased DOI-induced brain activity in a mouse model of schizophrenia. Proceedings of the National Academy of Sciences 111:E2492–E2500.

Marek GJ (2017) Interactions of hallucinogens with the glutamatergic system: permissive network effects mediated through cortical layer V pyramidal neurons. Behavioral Neurobiology of Psychedelic Drugs:107–135.

Marie N, Canestrelli C, Noble F (2012) Transfer of neuroplasticity from nucleus accumbens core to shell is required for cocaine reward. PLoS One 7:e30241.

Markham JA, Greenough WT (2004) Experience-driven brain plasticity: beyond the synapse. Neuron Glia Biol 1:351–363.

Martinotti G, Santacroce R, Pettorruso M, Montemitro C, Spano MC, Lorusso M, di Giannantonio M, Lerner AG (2018) Hallucinogen Persisting Perception Disorder: Etiology, Clinical Features, and Therapeutic Perspectives. Brain Sciences 2018, Vol 8, Page 47 8:47.

Mason NL, Dolder PC, Kuypers KPC (2020a) Reported effects of psychedelic use on those with low well-being given various emotional states and social contexts. Drug Sci Policy Law 6.

Mason NL, Kuypers KPC, Müller F, Reckweg J, Tse DHY, Toennes SW, Hutten N, Jansen JFA, Stiers P, Feilding A (2020b) Me, myself, bye: regional alterations in glutamate and the experience of ego dissolution with psilocybin. Neuropsychopharmacology 45:2003–2011.

Mathis A, Mamidanna P, Cury KM, Abe T, Murthy VN, Mathis MW, Bethge M (2018) DeepLabCut: markerless pose estimation of user-defined body parts with deep learning. Nat Neurosci 21:1281–1289.

Matias S, Lottem E, Dugué GP, Mainen ZF (2017) Activity patterns of serotonin neurons underlying cognitive flexibility. Elife 6:e20552.

Matsushima Y, Shirota O, Kikura-Hanajiri R, Goda Y, Eguchi F (2009) Effects of Psilocybe argentipes on marble-burying behavior in mice. Biosci Biotechnol Biochem 73:1866–1868.

Mattson MP, Maudsley S, Martin B (2004) BDNF and 5-HT: a dynamic duo in age-related neuronal plasticity and neurodegenerative disorders. Trends Neurosci 27:589–594.

McCulloch DEW, Knudsen GM, Barrett FS, Doss MK, Carhart-Harris RL, Rosas FE, Deco G, Kringelbach ML, Preller KH, Ramaekers JG, Mason NL, Müller F, Fisher PMD (2022) Psychedelic resting-state neuroimaging: A review and perspective on balancing replication and novel analyses. Neurosci Biobehav Rev 138:104689.

McEwen BS, Nasca C, Gray JD (2016) Stress effects on neuronal structure: hippocampus, amygdala, and prefrontal cortex. Neuropsychopharmacology 41:3–23.

McKenzie IA, Ohayon D, Li H, de Faria JP, Emery B, Tohyama K, Richardson WD (2014) Motor skill learning requires active central myelination. Science (1979) 346:318–322.

McKinnon MC, Yucel K, Nazarov A, MacQueen GM (2009) A meta-analysis examining clinical predictors of hippocampal volume in patients with major depressive disorder. Journal of Psychiatry and Neuroscience 34:41–54.

Meehan SM, Schechter MD (1998) LSD produces conditioned place preference in male but not female fawn hooded rats. Pharmacol Biochem Behav 59:105–108.

Menon V (2011) Large-scale brain networks and psychopathology: a unifying triple network model. Trends Cogn Sci 15:483–506.

Michaiel AM, Parker PRL, Niell CM (2019) A hallucinogenic serotonin-2A receptor agonist reduces visual response gain and alters temporal dynamics in mouse V1. Cell Rep 26:3475–3483.

Milczarek MM, Vann SD, Sengpiel F (2018) Spatial memory engram in the mouse retrosplenial cortex. Current Biology 28:1975–1980.

Miliano C, Marti M, Pintori N, Castelli MP, Tirri M, Arfè R, De Luca MA (2019) Neurochemical and behavioral profiling in male and female rats of the psychedelic agent 25I-NBOMe. Front Pharmacol 10:1406.

Miller WR (2004) The phenomenon of quantum change. J Clin Psychol 60:453–460.

Minassian H, Huang S (1979) Effect of sodium azide on the ultrastructural preservation of tissues. J Microsc 117:243–253.

Mithoefer MC, Wagner MT, Mithoefer AT, Jerome L, Doblin R (2011) The safety and efficacy of±3, 4-methylenedioxymethamphetamine-assisted psychotherapy in subjects with chronic, treatment-resistant posttraumatic stress disorder: the first randomized controlled pilot study. Journal of Psychopharmacology 25:439–452.

Mithoefer MC, Wagner MT, Mithoefer AT, Jerome L, Martin SF, Yazar-Klosinski B, Michel Y, Brewerton TD, Doblin R (2013) Durability of improvement in post-traumatic stress disorder symptoms and absence of harmful effects or drug dependency after 3, 4-methylenedioxymethamphetamine-assisted psychotherapy: a prospective long-term follow-up study. Journal of Psychopharmacology 27:28–39.

Mittman SM, Geyer MA (1991) Dissociation of multiple effects of acute LSD on exploratory behavior in rats by ritanserin and propranolol. Psychopharmacology (Berl) 105:69–76.

Miura H, Qiao H, Ohta T (2002) Attenuating effects of the isolated rearing condition on increased brain serotonin and dopamine turnover elicited by novelty stress. Brain Res 926:10–17.

Miyata S, Hirano S, Kamei J (2004) Diabetes inhibits the DOI-induced head-twitch response in mice. Psychopharmacology (Berl) 177:224–229.

Moda-Sava RN, Murdock MH, Parekh PK, Fetcho RN, Huang BS, Huynh TN, Witztum J, Shaver DC, Rosenthal DL, Alway EJ (2019) Sustained rescue of prefrontal circuit dysfunction by antidepressant-induced spine formation. Science (1979) 364.

Mollinedo-Gajate I, Song C, Sintes-Rodriguez M, Whelan T, Soula A, Selimbeyoglu A, Hurley S, Knöpfel T (2020) Psilocybin rescues sociability deficits in an animal model of autism. bioRxiv.

Monko ME, Heilbronner SR (2021) Retrosplenial Cortical Connectivity with Frontal Basal Ganglia Networks. J Cogn Neurosci 33:1096–1105.

Morales-Garcia JA, Calleja-Conde J, Lopez-Moreno JA, Alonso-Gil S, Sanz-SanCristobal M, Riba J, Perez-Castillo A (2020) N,N-dimethyltryptamine compound found in the hallucinogenic tea ayahuasca, regulates adult neurogenesis in vitro and in vivo. Translational Psychiatry 2020 10:1 10:1–14.

Moreno FA, Wiegand CB, Taitano EK, Delgado PL (2006) Safety, tolerability, and efficacy of psilocybin in 9 patients with obsessive-compulsive disorder. Journal of clinical Psychiatry 67:1735–1740.

Morey RD, Rouder JN (2015) Package "bayesfactor." Available at: https://richarddmorey.github.io/BayesFactor/ [Accessed December 2, 2022].

Motulsky HJ, Brown RE (2006) Detecting outliers when fitting data with nonlinear regression–a new method based on robust nonlinear regression and the false discovery rate. BMC Bioinformatics 7:1–20.

Muir JJ, Pfister HP (1987) Time course of the corticosterone and prolactin response following predictable and unpredictable novelty stress in Rattus norvegicus. Physiol Behav 40:103–107.

Muñoz-Cuevas FJ, Athilingam J, Piscopo D, Wilbrecht L (2013) Cocaine-induced structural plasticity in frontal cortex correlates with conditioned place preference. Nat Neurosci 16:1367–1369.

Murphy-Beiner A, Soar K (2020) Ayahuasca's 'afterglow': improved mindfulness and cognitive flexibility in ayahuasca drinkers. Psychopharmacology (Berl) 237:1161–1169.

Muthukumaraswamy SD, Forsyth A, Lumley T (2021) Blinding and expectancy confounds in psychedelic randomized controlled trials. Expert Rev Clin Pharmacol.

Nair G, Duong TQ (2004) Echo-planar BOLD fMRI of mice on a narrow-bore 9.4 T magnet. Magnetic Resonance in Medicine: An Official Journal of the International Society for Magnetic Resonance in Medicine 52:430–434.

Namgung U, Routtenberg A (2000) Transcriptional and post-transcriptional regulation of a brain growth protein: regional differentiation and regeneration induction of GAP-43. European Journal of Neuroscience 12:3124–3136.

Nardou R, Lewis EM, Rothhaas R, Xu R, Yang A, Boyden E, Dölen G (2019) Oxytocin-dependent reopening of a social reward learning critical period with MDMA. Nature 569:116–120.

Nayak S, Bari BA, Yaden DB, Spriggs MJ, Rosas F, Peill JM, Giribaldi B, Erritzoe D, Nutt DJ, Carhart-Harris R (2022) A Bayesian Reanalysis of a Trial of Psilocybin versus Escitalopram for Depression.

Newman JP (1998) Psychopathic behavior: An information processing perspective. In: Psychopathy: Theory, research and implications for society, pp 81–104. Springer.

Nibuya M, Morinobu S, Duman RS (1995) Regulation of BDNF and trkB mRNA in rat brain by chronic electroconvulsive seizure and antidepressant drug treatments. Journal of Neuroscience 15:7539–7547.

Nichols DE (2012) Structure–activity relationships of serotonin 5-HT2A agonists. Wiley Interdiscip Rev Membr Transp Signal 1:559–579.

Nichols DE (2016) Psychedelics. Pharmacol Rev 68:264–355.

Nichols DE, Johnson MW, Nichols CD (2017) Psychedelics as medicines: an emerging new paradigm. Clin Pharmacol Ther 101:209–219.

Niitsu Y, Hatnada S, Hamaguchi K, Mikuni M, Okado N (1995) Regulation of synapse density by 5-HT2A receptor agonist and antagonist in the spinal cord of chicken embryo. Neurosci Lett 195:159–162.

Njung'e K, Handley SL (1991) Effects of 5-HT uptake inhibitors, agonists and antagonists on the burying of harmless objects by mice; a putative test for anxiolytic agents. Br J Pharmacol 104:105–112.

Odland AU, Jessen L, Kristensen JL, Fitzpatrick CM, Andreasen JT (2019) The 5-hydroxytryptamine 2A receptor agonists DOI and 25CN-NBOH decrease marble burying and reverse 8-OH-DPAT-induced deficit in spontaneous alternation. Neuropharmacology:107838 Available at: http://www.sciencedirect.com/science/article/pii/S0028390819304046.

Odland AU, Kristensen JL, Andreasen JT (2021) The selective 5-HT2A receptor agonist 25CN-NBOH does not affect reversal learning in mice. Behavioural Pharmacology 32:448–452.

O'Donnell LJ, Westin C-F (2011) An introduction to diffusion tensor image analysis. Neurosurgery Clinics 22:185–196.

Oliverio A, Eleftheriou BE, Bailey DW (1973) A gene influencing active avoidance performance in mice. Physiol Behav 11:497–501.

Olson DE (2018) Psychoplastogens: a promising class of plasticity-promoting neurotherapeutics. J Exp Neurosci 12.

Olson DE (2020) The subjective effects of psychedelics may not be necessary for their enduring therapeutic effects. ACS Pharmacol Transl Sci 4:563–567.

Osório F de L, Sanches RF, Macedo LR, dos Santos RG, Maia-de-Oliveira JP, Wichert-Ana L, de Araujo DB, Riba J, Crippa JA, Hallak JE (2015) Antidepressant effects of a single dose of ayahuasca in patients with recurrent depression: a preliminary report. Brazilian Journal of Psychiatry 37:13–20.

Österlund MK, Overstreet DH, Hurd YL (1999) The flinders sensitive line rats, a genetic model of depression, show abnormal serotonin receptor mRNA expression in the brain that is reversed by 17β-estradiol. Molecular brain research 74:158–166.

Ostrander MM, Badiani A, Day HEW, Norton CS, Watson SJ, Akil H, Robinson TE (2003) Environmental context and drug history modulate amphetamine-induced c-fos mRNA expression in the basal ganglia, central extended amygdala, and associated limbic forebrain. Neuroscience 120:551–571.

Páleníček T, Hliňák Z, Bubeníková-Valešová V, Novák T, Horáček J (2010) Sex differences in the effects of N, N-diethyllysergamide (LSD) on behavioural activity and prepulse inhibition. Prog Neuropsychopharmacol Biol Psychiatry 34:588–596.

Palhano-Fontes F, Barreto D, Onias H, Andrade KC, Novaes MM, Pessoa JA, Mota-Rolim SA, Osório FL, Sanches R, dos Santos RG (2019) Rapid antidepressant effects of the psychedelic ayahuasca in treatment-resistant depression: a randomized placebo-controlled trial. Psychol Med 49:655–663.

Pan S, Mayoral SR, Choi HS, Chan JR, Kheirbek MA (2020) Preservation of a remote fear memory requires new myelin formation. Nat Neurosci 23:487–499.

Park H-J, Friston K (2013) Structural and functional brain networks: from connections to cognition. Science (1979) 342.

Paulus MP, Geyer MA (1993) Quantitative assessment of the microstructure of rat behavior: If (d), The extension of the scaling hypothesis. Psychopharmacology (Berl) 113:177–186.

Pędzich BD, Rubens S, Sekssaoui M, Pierre A, van Schuerbeek A, Marin P, Bockaert J, Valjent E, Bécamel C, de Bundel D (2022) Effects of a psychedelic 5-HT2A receptor agonist on anxiety-related behavior and fear processing in mice. Neuropsychopharmacology 47:1304–1314.

Peeler DF, Nowakowski RS (1987) Genetic factors and the measurement of exploratory activity. Behav Neural Biol 48:90–103.

Peričić D (2003) Swim stress inhibits 5-HT 2A receptor-mediated head twitch behaviour in mice. Psychopharmacology (Berl) 167:373–379.

Pernía-Andrade AJ, Wenger N, Esposito MS, Tovote P (2021) Circuits for state-dependent modulation of locomotion. Front Hum Neurosci 15:745689.

Peters J, Dieppa-Perea LM, Melendez LM, Quirk GJ (2010) Induction of fear extinction with hippocampal-Infralimbic BDNF. Science (1979) 328:1288–1290.

Petri G, Expert P, Turkheimer F, Carhart-Harris R, Nutt D, Hellyer PJ, Vaccarino F (2014) Homological scaffolds of brain functional networks. J R Soc Interface 11.

Player MJ, Taylor JL, Weickert CS, Alonzo A, Sachdev P, Martin D, Mitchell PB, Loo CK (2013) Neuroplasticity in depressed individuals compared with healthy controls. Neuropsychopharmacology 38:2101–2108.

Pompeiano M, Palacios JM, Mengod G (1994) Distribution of the serotonin 5-HT2 receptor family mRNAs: comparison between 5-HT2A and 5-HT2C receptors. Molecular Brain Research 23:163–178.

Preece MA, Taylor MJ, Raley J, Blamire A, Sharp T, Sibson NR (2009) Evidence that increased 5-HT release evokes region-specific effects on blood-oxygenation level-dependent functional magnetic resonance imaging responses in the rat brain. Neuroscience 159:751–759.

Price RB, Duman R (2019) Neuroplasticity in cognitive and psychological mechanisms of depression: An integrative model. Mol Psychiatry:1–14.

Qiu LR, Fernandes DJ, Szulc-Lerch KU, Dazai J, Nieman BJ, Turnbull DH, Foster JA, Palmert MR, Lerch JP (2018) Mouse MRI shows brain areas relatively larger in males emerge before those larger in females. Nat Commun 9:1–15.

Rae CD (2014) A guide to the metabolic pathways and function of metabolites observed in human brain 1H magnetic resonance spectra. Neurochem Res 39:1–36.

Rambousek L, Palenicek T, Vales K, Stuchlik A (2014) The effect of psilocin on memory acquisition, retrieval, and consolidation in the rat. Front Behav Neurosci 8:180.

Raval NR, Johansen A, Donovan LL, Ros NF, Ozenne B, Hansen HD, Knudsen GM (2021) A single dose of psilocybin increases synaptic density and decreases 5-HT2A receptor density in the pig brain. Int J Mol Sci 22:835.

Reissig CJ, Rabin RA, Winter JC, Dlugos CA (2008) d-LSD-induced c-Fos expression occurs in a population of oligodendrocytes in rat prefrontal cortex. Eur J Pharmacol 583:40–47.

Roberts MHT, Bradley PB (1967) Studies on the effects of drugs on performance of a delayed discrimination. Physiol Behav 2:389–397.

Robinson MJF, Robinson TE, Berridge KC (2013) Incentive salience and the transition to addiction. Biological research on addiction 2:391–399.

Roseman L, Demetriou L, Wall MB, Nutt DJ, Carhart-Harris RL (2018a) Increased amygdala responses to emotional faces after psilocybin for treatment-resistant depression. Neuropharmacology 142:263–269.

Roseman L, Leech R, Feilding A, Nutt DJ, Carhart-Harris RL (2014) The effects of psilocybin and MDMA on between-network resting state functional connectivity in healthy volunteers. Front Hum Neurosci 8:204 Available at: https://www.frontiersin.org/article/10.3389/fnhum.2014.00204.

Roseman L, Nutt DJ, Carhart-Harris RL (2018b) Quality of acute psychedelic experience predicts therapeutic efficacy of psilocybin for treatment-resistant depression. Front Pharmacol 8:974.

Ross S, Bossis A, Guss J, Agin-Liebes G, Malone T, Cohen B, Mennenga SE, Belser A, Kalliontzi K, Babb J (2016) Rapid and sustained symptom reduction following psilocybin treatment for anxiety and depression in patients with life-threatening cancer: a randomized controlled trial. Journal of psychopharmacology 30:1165–1180.

Roth BL, Lopez E, Patel S, Kroeze WK (2000) The multiplicity of serotonin receptors: uselessly diverse molecules or an embarrassment of riches? The Neuroscientist 6:252–262.

Rouder JN, Speckman PL, Sun D, Morey RD, Iverson G (2009) Bayesian t tests for accepting and rejecting the null hypothesis. Psychon Bull Rev 16:225–237.

Rubinow DR, Schmidt PJ (2019) Sex differences and the neurobiology of affective disorders. Neuropsychopharmacology 44:111–128.

Sagi Y, Tavor I, Hofstetter S, Tzur-Moryosef S, Blumenfeld-Katzir T, Assaf Y (2012) Learning in the fast lane: new insights into neuroplasticity. Neuron 73:1195–1203.

Sairanen M, Lucas G, Ernfors P, Castrén M, Castrén E (2005) Brain-derived neurotrophic factor and antidepressant drugs have different but coordinated effects on neuronal turnover, proliferation, and survival in the adult dentate gyrus. Journal of Neuroscience 25:1089–1094.

Sakaue M, Ago Y, Sowa C, Sakamoto Y, Nishihara B, Koyama Y, Baba A, Matsuda T (2002) Modulation by 5-HT2A receptors of aggressive behavior in isolated mice. Jpn J Pharmacol 89:89–92.

Sampaio-Baptista C, Johansen-Berg H (2017) White matter plasticity in the adult brain. Neuron 96:1239–1251.

Sampedro F, de la Fuente Revenga M, Valle M, Roberto N, Domínguez-Clavé E, Elices M, Luna LE, Crippa JAS, Hallak JEC, de Araujo DB (2017) Assessing the psychedelic “after-glow” in ayahuasca users: post-acute neurometabolic and functional connectivity changes are associated with enhanced mindfulness capacities. International Journal of Neuropsychopharmacology 20:698–711.

Sanches RF, de Lima Osório F, dos Santos RG, Macedo LRH, Maia-de-Oliveira JP, Wichert-Ana L, de Araujo DB, Riba J, Crippa JAS, Hallak JEC (2016) Antidepressant effects of a single dose of ayahuasca in patients with recurrent depression: a SPECT study. J Clin Psychopharmacol 36:77–81.

Sansone RA, Sansone LA (2010) SSRI-induced indifference. Psychiatry (Edgmont) 7:14.

Sawyer E (2022) Psychedelics reopen the critical period for social reward learning. Unpublished work.

Schmack K, Bosc M, Ott T, Sturgill JF, Kepecs A (2021) Striatal dopamine mediates hallucination-like perception in mice. Science (1979) 372:eabf4740.

Schmid Y, Liechti ME (2018) Long-lasting subjective effects of LSD in normal subjects. Psychopharmacology (Berl) 235:535–545.

Schobel SA, Chaudhury NH, Khan UA, Paniagua B, Styner MA, Asllani I, Inbar BP, Corcoran CM, Lieberman JA, Moore H (2013) Imaging patients with psychosis and a mouse model establishes a spreading pattern of hippocampal dysfunction and implicates glutamate as a driver. Neuron 78:81–93.

Scholz J, Allemang-Grand R, Dazai J, Lerch JP (2015) Environmental enrichment is associated with rapid volumetric brain changes in adult mice. Neuroimage 109:190–198.

Scholz J, Klein MC, Behrens TEJ, Johansen-Berg H (2009) Training induces changes in white-matter architecture. Nat Neurosci 12:1370–1371.

Schreiber R, Brocco M, Audinot V, Gobert A, Veiga S, Millan MJ (1995) (1-(2, 5-dimethoxy-4 iodophenyl)-2-aminopropane)-induced head-twitches in the rat are mediated by 5-hydroxytryptamine (5-HT) 2A receptors: modulation by novel 5-

HT2A/2C antagonists, D1 antagonists and 5-HT1A agonists. Journal of Pharmacology and Experimental Therapeutics 273:101–112.

Scott WA (1962) Cognitive complexity and cognitive flexibility. Sociometry:405–414.

Sebold M, Deserno L, Nebe S, Schad DJ, Garbusow M, Hägele C, Keller J, Jünger E, Kathmann N, Smolka M (2014) Model-based and model-free decisions in alcohol dependence. Neuropsychobiology 70:122–131.

Shao L-X, Liao C, Gregg I, Davoudian PA, Savalia NK, Delagarza K, Kwan AC (2021) Psilocybin induces rapid and persistent growth of dendritic spines in frontal cortex in vivo. Neuron 109:2535–2544.

Sharp T, Barnes NM (2020) Central 5-HT receptors and their function; present and future. Neuropharmacology:108155.

Shulgin AT, Shulgin A (1995) PIHKAL: a chemical love story. Transform Press Berkeley.

Siegel RK (1984) LSD-induced effects in elephants: Comparisons with musth behavior. Bull Psychon Soc 22:53–56.

Singleton SP, Luppi AI, Carhart-Harris RL, Cruzat J, Roseman L, Nutt DJ, Deco G, Kringelbach ML, Stamatakis EA, Kuceyeski A (2022) Receptor-informed network control theory links LSD and psilocybin to a flattening of the brain's control energy landscape. Nature Communications 2022 13:1 13:1–13.

Smith RL, Barrett RJ, Sanders-Bush E (1990) Adaptation of brain 5HT2 receptors after mianserin treatment: receptor sensitivity, not receptor binding, more accurately correlates with behavior. Journal of Pharmacology and Experimental Therapeutics 254:484–488.

Soler J, Elices M, Franquesa A, Barker S, Friedlander P, Feilding A, Pascual JC, Riba J (2016) Exploring the therapeutic potential of Ayahuasca: acute intake increases mindfulness-related capacities. Psychopharmacology (Berl) 233:823–829.

Spain A, Howarth C, Khrapitchev AA, Sharp T, Sibson NR, Martin C (2015) Neurovascular and neuroimaging effects of the hallucinogenic serotonin receptor agonist psilocin in the rat brain. Neuropharmacology 99:210–220.

Sparks DW, Tian MK, Sargin D, Venkatesan S, Intson K, Lambe EK (2018) Opposing cholinergic and serotonergic modulation of layer 6 in prefrontal cortex. Front Neural Circuits 11:107.

Spring S, Lerch JP, Henkelman RM (2007) Sexual dimorphism revealed in the structure of the mouse brain using three-dimensional magnetic resonance imaging. Neuroimage 35:1424–1433.

Spring S, Lerch JP, Wetzel MK, Evans AC, Henkelman RM (2010) Cerebral asymmetries in 12-week-old C57Bl/6J mice measured by magnetic resonance imaging. Neuroimage 50:409–415.

Stahl SM (2013) Stahl's Essential Psychopharmacology : Neuroscientific Basis and Practical Applications, 4th ed. Cambridge: Cambridge University Press.

Steadman PE, Xia F, Ahmed M, Mocle AJ, Penning ARA, Geraghty AC, Steenland HW, Monje M, Josselyn SA, Frankland PW (2020) Disruption of oligodendrogenesis impairs memory consolidation in adult mice. Neuron 105:150–164.

Streitbürger D-P, Möller HE, Tittgemeyer M, Hund-Georgiadis M, Schroeter ML, Mueller K (2012) Investigating structural brain changes of dehydration using voxel-based morphometry.

Studerus E, Gamma A, Kometer M, Vollenweider FX (2012) Prediction of psilocybin response in healthy volunteers. PLoS One 7:e30800.

Studerus E, Kometer M, Hasler F, Vollenweider FX (2011) Acute, subacute and long-term subjective effects of psilocybin in healthy humans: a pooled analysis of experimental studies. Journal of psychopharmacology 25:1434–1452.

Sumner BEH, Fink G (1995) Estrogen increases the density of 5-hydroxytryptamine2A receptors in cerebral cortex and nucleus accumbens in the female rat. J Steroid Biochem Mol Biol 54:15–20.

Sutton RS, Barto AG (1998) Introduction to reinforcement learning. MIT press Cambridge.

Szabo A (2015) Psychedelics and immunomodulation: novel approaches and therapeutic opportunities. Front Immunol 6:358.

Taubert M, Draganski B, Anwander A, Müller K, Horstmann A, Villringer A, Ragert P (2010) Dynamic properties of human brain structure: learning-related changes in cortical areas and associated fiber connections. Journal of Neuroscience 30:11670–11677.

Terracciano A, Löckenhoff CE, Crum RM, Bienvenu OJ, Costa PT (2008) Five-Factor Model personality profiles of drug users. BMC Psychiatry 8:1–10.

Thavarajah R, Mudimbaimannar VK, Elizabeth J, Rao UK, Ranganathan K (2012) Chemical and physical basics of routine formaldehyde fixation. J Oral Maxillofac Pathol 16:400.

Timmermann C, Spriggs MJ, Kaelen M, Leech R, Nutt DJ, Moran RJ, Carhart-Harris RL, Muthukumaraswamy SD (2018) LSD modulates effective connectivity and

neural adaptation mechanisms in an auditory oddball paradigm. Neuropharmacology 142:251–262.

Toga AW, Thompson PM (2003) Mapping brain asymmetry. Nat Rev Neurosci 4:37–48.

Tolman EC (1948) Cognitive maps in rats and men. Psychol Rev 55:189.

Toth LA, Gardiner TW (2000) Food and water restriction protocols: physiological and behavioral considerations. Journal of the American Association for Laboratory Animal Science 39:9–17.

Trefler A, Sadeghi N, Thomas AG, Pierpaoli C, Baker CI, Thomas C (2016) Impact of time-of-day on brain morphometric measures derived from T1-weighted magnetic resonance imaging. Neuroimage 133:41–52.

Treit D, Fundytus M (1988) Thigmotaxis as a test for anxiolytic activity in rats. Pharmacol Biochem Behav 31:959–962.

Turner P V, Pekow C, Vasbinder MA, Brabb T (2011) Administration of substances to laboratory animals: equipment considerations, vehicle selection, and solute preparation. Journal of the American Association for Laboratory Animal Science 50:614–627.

Tylš F, Páleníček T, Kadeřábek L, Lipski M, Kubešová A, Horáček J (2016) Sex differences and serotonergic mechanisms in the behavioural effects of psilocin. Behavioural Pharmacology 27:309–320.

Uslaner J, Badiani A, Day HEW, Watson SJ, Akil H, Robinson TE (2001) Environmental context modulates the ability of cocaine and amphetamine to induce c-fos mRNA expression in the neocortex, caudate nucleus, and nucleus accumbens. Brain Res 920:106–116.

Uthaug M v., van Oorsouw K, Kuypers KPC, van Boxtel M, Broers NJ, Mason NL, Toennes SW, Riba J, Ramaekers JG (2018) Sub-acute and long-term effects of ayahuasca on affect and cognitive thinking style and their association with ego dissolution. Psychopharmacology (Berl) 235:2979–2989.

Vaidya VA, Marek GJ, Aghajanian GK, Duman RS (1997) 5-HT2A receptor-mediated regulation of brain-derived neurotrophic factor mRNA in the hippocampus and the neocortex. Journal of Neuroscience 17:2785–2795.

van den Heuvel MP, Pol HEH (2010) Exploring the brain network: a review on resting-state fMRI functional connectivity. European neuropsychopharmacology 20:519–534.

van Doorn J, van den Bergh D, Böhm U, Dablander F, Derks K, Draws T, Etz A, Evans NJ, Gronau QF, Haaf JM (2021) The JASP guidelines for conducting and reporting a Bayesian analysis. Psychon Bull Rev 28:813–826.

van Praag HM (1998) Anxiety and increased aggression as pacemakers of depression. Acta Psychiatr Scand 98:81–88.

Verma P, Thakur AS, Deshmukh K, Jha AK, Verma S (2010) Routes of drug administration. International Journal of Pharmaceutical Studies and Research 1:54–59.

Vetencourt JFM, Sale A, Viegi A, Baroncelli L, de Pasquale R, F. O'Leary O, Castrén E, Maffei L (2008) The antidepressant fluoxetine restores plasticity in the adult visual cortex. Science (1979) 320:385–388.

Vetencourt JFM, Tiraboschi E, Spolidoro M, Castrén E, Maffei L (2011) Serotonin triggers a transient epigenetic mechanism that reinstates adult visual cortex plasticity in rats. European Journal of Neuroscience 33:49–57.

Vickers SP, Easton N, Malcolm CS, Allen NH, Porter RH, Bickerdike MJ, Kennett GA (2001) Modulation of 5-HT2A receptor-mediated head-twitch behaviour in the rat by 5-HT2C receptor agonists. Pharmacol Biochem Behav 69:643–652.

Vives M, López-Navarro E, García-Campayo J, Gili M (2015) Cognitive impairments and depression: a critical review. Actas Esp Psiquiatr 43:187–193.

Vollenweider FX, Geyer MA (2001) A systems model of altered consciousness: integrating natural and drug-induced psychoses. Brain Res Bull 56:495–507.

Vollenweider FX, Kometer M (2010) The neurobiology of psychedelic drugs: implications for the treatment of mood disorders. Nat Rev Neurosci 11:642–651.

Vollenweider FX, Leenders KL, Scharfetter C, Maguire P, Stadelmann O, Angst J (1997) Positron emission tomography and fluorodeoxyglucose studies of metabolic hyperfrontality and psychopathology in the psilocybin model of psychosis. Neuropsychopharmacology 16:357–372.

Vollenweider FX, Vollenweider-Scherpenhuyzen MFI, Bäbler A, Vogel H, Hell D (1998) Psilocybin induces schizophrenia-like psychosis in humans via a serotonin-2 agonist action. Neuroreport 9:3897–3902.

Voon V, Derbyshire K, Rück C, Irvine MA, Worbe Y, Enander J, Schreiber LRN, Gillan C, Fineberg NA, Sahakian BJ (2015) Disorders of compulsivity: a common bias towards learning habits. Mol Psychiatry 20:345–352.

Vousden DA, Friesen A, Wen X, Qiu LR, O'Toole N, Darwin BC, Noakes LS, Grand RA, Diorio J, Frankland PW (2018) Genetic and behavioural requirements for structural brain plasticity. bioRxiv.

Wagner S, Doering B, Helmreich I, Lieb K, Tadić A (2012) A meta-analysis of executive dysfunctions in unipolar major depressive disorder without psychotic symptoms

and their changes during antidepressant treatment. Acta Psychiatr Scand 125:281–292.

Warraich Z, Kleim JA (2010) Neural Plasticity: The Biological Substrate For Neurorehabilitation. PM&R 2:S208–S219.

Weisholtz DS, Sullivan JF, Nelson AP, Daffner KR, Silbersweig DA (2017) Cognitive, Emotional, and Behavioral Inflexibility and Perseveration in Neuropsychiatric Illness. In: Executive Functions in Health and Disease (Goldberg EBT-EF in H and D, ed), pp 219–248. San Diego: Academic Press.

Weiskopf N, Edwards LJ, Helms G, Mohammadi S, Kirilina E (2021) Quantitative magnetic resonance imaging of brain anatomy and in vivo histology. Nature Reviews Physics 3:570–588.

Wheeler AL, Lerch JP, Chakravarty MM, Friedel M, Sled JG, Fletcher PJ, Josselyn SA, Frankland PW (2013) Adolescent cocaine exposure causes enduring macroscale changes in mouse brain structure. Journal of Neuroscience 33:1797–1803.

Wieland S, Kreider MS, McGonigle P, Lucki I (1990) Destruction of the nucleus raphe obscurus and potentiation of serotonin-mediated behaviors following administration of the neurotoxin 3-acetylpyridine. Brain Res 520:291–302.

Wießner I, Olivieri R, Falchi M, Palhano-Fontes F, Maia LO, Feilding A, Araujo DB, Ribeiro S, Tófoli LF (2022) LSD, afterglow and hangover: Increased episodic memory and verbal fluency, decreased cognitive flexibility. European Neuropsychopharmacology 58:7–19.

Wilkinson ST, Sanacora G, Bloch MH (2017) Hippocampal volume changes following electroconvulsive therapy: a systematic review and meta-analysis. Biol Psychiatry Cogn Neurosci Neuroimaging 2:327–335.

Wing LL, Tapson GS, Geyer MA (1990) 5HT-2 mediation of acute behavioral effects of hallucinogens in rats. Psychopharmacology (Berl) 100:417–425.

Wojtas A, Bysiek A, Wawrzczak-Bargiela A, Szych Z, Majcher-Maślanka I, Herian M, Maćkowiak M, Gołembiowska K (2022) Effect of psilocybin and ketamine on brain neurotransmitters, glutamate receptors, DNA and rat behavior. Int J Mol Sci 23:6713.

Wu H, Wang X, Gao Y, Lin F, Song T, Zou Y, Xu L, Lei H (2016) NMDA receptor antagonism by repetitive MK801 administration induces schizophrenia-like structural changes in the rat brain as revealed by voxel-based morphometry and diffusion tensor imaging. Neuroscience 322:221–233.

Wyckmans F, Otto AR, Sebold M, Daw N, Bechara A, Saeremans M, Kornreich C, Chatard A, Jaafari N, Noël X (2019) Reduced model-based decision-making in gambling disorder. Sci Rep 9:1–10.

Xin W, Chan JR (2020) Myelin plasticity: sculpting circuits in learning and memory. Nature Reviews Neuroscience 2020 21:12 21:682–694.

Xu J (2018) New insights into GFAP negative astrocytes in calbindin D28k immunoreactive astrocytes. Brain Sci 8:143.

Xue R, Sawada M, Goto S, Hurn PD, Traystman RJ, van Zijl PCM, Mori S (2001) Rapid three-dimensional diffusion MRI facilitates the study of acute stroke in mice. Magnetic Resonance in Medicine: An Official Journal of the International Society for Magnetic Resonance in Medicine 46:183–188.

Yaden DB, Griffiths RR (2020) The subjective effects of psychedelics are necessary for their enduring therapeutic effects. ACS Pharmacol Transl Sci 4:568–572.

Yamada J, Sugimoto Y, Horisaka K (1995a) Serotonin2 (5-HT2) receptor agonist 1-(2, 5-dimethoxy-4-iodophenyl)-2-aminopropane (DOI) inhibits chlorpromazine- and haloperidol-induced hypothermia in mice. Biol Pharm Bull 18:1580–1583.

Yamada S, Watanabe A, Nankai M, Toru M (1995b) Acute immobilization stress reduces (±DOI)-induced 5-HT 2A receptor-mediated head shakes in rats. Psychopharmacology (Berl) 119:9–14.

Young MB, Andero R, Ressler KJ, Howell LL (2015) 3, 4-Methylenedioxymethamphetamine facilitates fear extinction learning. Transl Psychiatry 5:e634–e634.

Zamfir O, Broqua P, Baudrie V, Chaouloff F (1992) Effects of cold stress on some 5-HT1A, 5-HT1C and 5-HT2 receptor-mediated responses. Eur J Pharmacol 219:261–269.

Zeifman RJ, Spriggs MJ, Kettner H, Lyons T, Rosas F, Mediano PAM, Erritzoe D, Carhart-Harris R (2022) From Relaxed Beliefs Under Psychedelics (REBUS) to Revised Beliefs After Psychedelics (REBAS): Preliminary Development of the RElaxed Beliefs Questionnaire (REB-Q). PsyArXiv.

Zemmar A, Chen C-C, Weinmann O, Kast B, Vajda F, Bozeman J, Isaad N, Zuo Y, Schwab ME (2018) Oligodendrocyte-and neuron-specific Nogo-A restrict dendritic branching and spine density in the adult mouse motor cortex. Cerebral cortex 28:2109–2117.

Zhan Y, Paolicelli RC, Sforazzini F, Weinhard L, Bolasco G, Pagani F, Vyssotski AL, Bifone A, Gozzi A, Ragozzino D, Gross CT (2014) Deficient neuron-microglia

signaling results in impaired functional brain connectivity and social behavior. Nature Neuroscience 2014 17:3 17:400–406.

Zhang C, Marek GJ (2008) AMPA receptor involvement in 5-hydroxytryptamine2A receptor-mediated pre-frontal cortical excitatory synaptic currents and DOI-induced head shakes. Prog Neuropsychopharmacol Biol Psychiatry 32:62–71.

Zhang J, Peng Q, Li Q, Jahanshad N, Hou Z, Jiang M, Masuda N, Langbehn DR, Miller MI, Mori S (2010) Longitudinal characterization of brain atrophy of a Huntington's disease mouse model by automated morphological analyses of magnetic resonance images. Neuroimage 49:2340–2351.

Zhou W, Cunningham KA, Thomas ML (2002) Estrogen regulation of gene expression in the brain: a possible mechanism altering the response to psychostimulants in female rats. Molecular Brain Research 100:75–83.

Zilles K, Dabringhaus A, Geyer S, Amunts K, Qü M, Schleicher A, Gilissen E, Schlaug G, Steinmetz H (1996) Structural Asymmetries in the Human Forebrain and the Forebrain of Non-human Primates and Rats. Neurosci Biobehav Rev 20:593–605.

Zühlsdorff K, Dalley J, Robbins T, Morein S (2022) Cognitive flexibility: neurobehavioural correlates of changing one's mind. Cerebral Cortex.